SPECTRAL STUDIES OF THE COMPLEXATION OF LANTHANIDES WITH SELECTED AMINO ACIDS: EVALUATION OF THERMODYNAMIC PARAMETERS

by

CHUBAZENBA IMSONG

Registration No.: 808/2018

Submitted to

NAGALAND UNIVERSITY

In Partial Fulfillment of the Requirements for Award of the Degree

of

DOCTOR OF PHILOSOPHY IN CHEMISTRY

DEPARTMENT OF CHEMISTRY
NAGALAND UNIVERSITY
LUMAMI-798627
NAGALAND, INDIA
2023

Dedicated to my beloved mother and family

नागालैण्ड विश्वविद्यालय
NAGALAND UNIVERSITY
(केंद्रीय विश्वविद्यालय) / (A Central University)
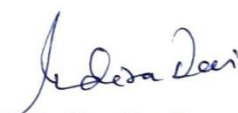मुख्यालय : लुमामी, जिला : जुन्हेबोटो (नागालैण्ड) – **798 627**
Hqrs: Lumami, Dist: Zunheboto, Nagaland – **798 627**

Department of Chemistry

CERTIFICATE

This is to certify that **Mr. Chubazenba Imsong**, a registered Research Scholar for Ph.D. degree in Chemistry under Nagaland University has carried out his research work under my guidance and supervision. His thesis entitled **"Spectral Studies of the Complexation of Lanthanides with Selected Amino Acids: Evaluation of Thermodynamic Parameters"** embodies the original research work and has fulfilled all the requirements according to the rules/regulations of Nagaland University.

Further, to the best of my knowledge, the research work has not been submitted to any university/ institution for the award of any degree or diploma.

(Prof. M. Indira Devi)
Professor
Supervisor Dept. of Chemistry
Nagaland University
Lumami-798627

DECLARATION

I, **Mr. Chubazenba Imsong** bearing Ph.D. Registration No. **808/2018** with effect from 30th **August 2016**, hereby declare that the subject matter of my Ph.D. thesis entitled **"Spectral Studies of the Complexation of Lanthanides with Selected Amino Acids: Evaluation of Thermodynamic Parameters"** is the record of original work done by me and the contents of this thesis did not comprise of the basis for the award of any previous degree/ diploma to me or to anybody else in any other University/Institute to the best of my knowledge.

This Ph.D. thesis is submitted in compliance with the UGC Regulation 2016 dated May 05, 2016 (Minimum Standard and Procedure for Award of M. Phil. /Ph.D. Degree) to the Nagaland University for the degree of Doctor of Philosophy in Chemistry.

(Chubazenba Imsong)

Head श्रिध्यक्ष / Head
Department of Chemistry
Nagaland University

23/02/'23
(Prof. M. Indira Devi)
Supervisor of Chemistry
Nagaland University
Lumami-798627

नागालैण्ड विश्वविद्यालय
NAGALAND UNIVERSITY
(केंद्रीय विश्वविद्यालय) / (A Central University)
मुख्यालय : लुमामी, जिला : जुन्हेबोटो (नागालैण्ड) – 798 627
Hqrs: Lumami, Dist: Zunheboto, Nagaland – 798 627

CERTIFICATE

This is to certify that **Mr. Chubazenba Imsong**, a registered Research Scholar for Ph.D. degree in Chemistry under Nagaland University, bearing Ph.D. Registration No. **808/2018,** has satisfactorily completed all the courses offered in the Pre-Ph.D. Course Work Programme in the Department of Chemistry, Nagaland University, Hqrs. Lumami.

The course includes:

CHEM-601 Research Methodology

CHEM-602 Advance in Chemistry

CHEM-603 Literature Review, Report Writing and Presentation.

Head
Department of Chemistry
Nagaland University

Sl. No. : 16- **59075**

NAGALAND UNIVERSITY

STATEMENT OF MARKS

Ph. D COURSE WORK EXAMINATION, 2017

DEPARTMENT OF ___CHEMISTRY___

The following are the marks secured by ___Chubazenba Imsong___

Roll No. ___02/16___ of Ph.D Course Work Examination held in ___2017___

Subject(s)/Paper(s)	Max. Marks	Minimun Qualifying Marks	Marks Secured
Paper No. Chem-601 Research Methodology	100	35	68
Paper No. Chem-602 (D) Advance in Chemistry	100	35	64
Paper No. Chem-603 Literature Review, Report Writing and Presentation	100	35	66
Total Aggregate Marks			198
Average Pass Mark – 55 %			

Result	Division	Percentage
Passed	**I Division**	**66 %**

Marks compared by

COE/Dy. Reg. AR (Exams)

NAGALAND UNIVERSITY

HEAD QUARTERS : LUMAMI

Ph. D COURSE WORK EXAMINATION

This is to certify that Mr/Ms. ___Chubazenba Imsong___

of Nagaland University bearing Roll No. ___2/16___ is qualified in the Ph.D Course Work Examination

in the Department of ___Chemistry___, Nagaland University held in the Year 20 ___17___

Head of Department
Head
Department of Chemistry
Nagaland University

Dean
School of Sciences
School of ___Sciences Nagaland University Hqs. Lumami Nagaland___

Acknowledgement

First, I would want to thank our Almighty God for providing me with good health and guidance over the course of my research.

I would like to express my heartfelt and profound gratitude to my Supervisor, Prof. M. Indira Devi, Department of Chemistry, Nagaland University, for her dedicated guidance, unwavering support, and insightful positive criticisms that allowed me to complete this work.

My sincere appreciation goes out to the teaching faculties of the Department of Chemistry, Nagaland University, especially Prof. Upasana Bora Sinha (HOD), Prof. Dipak Sinha, Dr. I. Tovishe Phucho, Dr. M. Prabhakar, Dr. Nurul Alam Choudhury, and Dr. Seram Dushila Devi, for all of their help and suggestions.

I am grateful to Nagaland University for providing all of the necessary facilities for my research.

I would like to express my deep gratitude to all of my lab mates in the Department of Chemistry, Nagaland University, including Mr. Mhasiriekho Ziekhrü, Ms. Zevivonü Thakro, Ms. Juliana Sanchu, Mr. Punazungba Imsong, and Ms. Sentienla Imsong, for the tremendous support and love they have shown me.

My sincere appreciation and thanks go out to the non-teaching staffs of the Department of Chemistry, Nagaland University, Mr.S. Bendangtemsu, Ms. Sunepjungla, Ms. Temsuienla Amer, Mr. Johnny Yanthan, and Mr. Phyobemo Patton for the immense help they provided me with over the course of my research.

I would also like to express my profound gratitude, to all the research scholar friends from other labs and departments for their wonderful friendship and encouragement.

My deepest appreciation goes out to my wife, children, and other family members for their unwavering moral support and care.

Last but not the least, I want to thank everyone who has influenced and contributed to the completion of this research endeavour, whether directly or indirectly.

(CHUBAZENBA IMSONG)

CONTENTS

Introduction

    1.1 General Features of Lanthanides

    1.2 Magnetic and Spectroscopic Properties of Lanthanides

    1.3 Selection Rules and Hypersensitivity

    1.4 Coordination Chemistry of Lanthanides

    1.5 Interaction of Lanthanides with Amino acids as Ligands

    1.6 General Properties and Structures of the Amino Acids (L-Glutamine,

       L-Threonine, L-Tryptophan and L-Isoleucine)

    1.7 Isomorphous Characteristics of Lanthanides with Alkaline Earth Metals

    1.8 Chemical Kinetics

       1.8.1 Factors affecting the rate of a reaction

       1.8.2 Concept of activation energy (E_a)

       1.8.3 Activation energy and the rate of the reaction

       1.8.4 Arrhenius Rate Equation

    1.9 Review on the coordination chemistry of lanthanides with biological ligands

    1.10 Scope and objectives of the present study

    References

Lists of Symbols and Abbreviations

A	Absorbance
E_a	Activation energy
$b^{\frac{1}{2}}$	Bonding parameter
δ	Covalency parameter
ΔS	Entropy change
ΔH	Enthalpy change
ΔG	Free energy change
T_λ	Intensity parameters (Judd – Ofelt parameter)
Ω_λ	Intensity parameter
ξ_{4f}	Lande spin orbit interaction parameter
ε	Molar absorptivity
β	Nephelauxetic parameter
ξ	Radial function
E^k	Rate constant
F_k	Slator-Condon parameter
λ	Wavelength
K	Racah Parameter
$U^{(\lambda)}$	Square reduced matrix element
RMS	Root mean square
DMF	Dimethylformamide
ACN/ CH_3CN	Acetonitrile
MeOH/ CH_3OH	Methanol
$C_4H_8O_2$	1,4-Dioxane
Ln	Lanthanide
Mg	Magnesium
Pr	Praseodymium
Nd	Neodymium
L-Glu	L-Glutamine
L-Thr	L-Threonine
L-Trp	L-Tryptophan
L-Ile	L-Isoleucine

List of Tables

List of Figures

Chapter 1

Introduction

1.1 General Features of Lanthanides

The lanthanoids (IUPAC) or lanthanides (commonly used) are a series of 15 elements from lanthanum (Z = 57) through lutetium (Z = 71) [1,2]. When scandium and yttrium are included, the series is referred to as 'rare earths' which is found in the Group 3 of the modern periodic table. The term '*earth*' in '*rare earths*' derives from the minerals from which they were extracted, which were unusual oxide minerals. However, these elements are neither rare nor earths (an obsolete term for water-insoluble strongly basic oxides of electropositive metals incapable of being smelted into metal using late 18th century technology). The term 'rare' in 'rare earths' refers more to the difficulty of isolating the different lanthanide elements than to the scarcity of any of them. In terms of abundance rather than scarcity, cerium is the 26th most abundant element in the earth's crust (refer table 1.1) and more abundant than copper [1], neodymium is more abundant than gold, and thulium is more abundant than iodine [3], bismuth, cadmium and mercury [4]. The first rare earth element, or rather its sesquioxide yttria, Y_2O_3, was discovered in 1794. It took a little more than 100 years to separate and characterize the other nonradioactive rare earths, with lutetium being the last one to be done in 1907. Radioactive promethium was synthesized in the year 1947 [5]. Victor Goldschmidt possibly coined "lanthanide" in 1925 [6], which derives from the Greek word '*lanthanein*' means '*to lie hidden*', it is a term that does not allude to their natural abundance but rather to the fact that they have the ability to "hide" behind one another in minerals. Due to their close chemical similarity, members of the lanthanide series were difficult to separate and purify. Along with the actinides, they are categorized as f block elements.

In general discussions of lanthanide chemistry, the symbol Ln is used to refer to any lanthanide. The lanthanides are characterized by the gradual filling up of the 4f energy levels and are generally referred to as 4f elements.

Exciting new developments in the 25 years have emerged in the field of 4f element coordination chemistry, including those dealing with macrocyclic ligands, new extraction methods, self-assembled supramolecular structures, heterometallic d-f compounds, ionic liquid coordination, lantanidomesogens, lanthanidofullerenes, nanoparticles, crystal-to-crystal reactions, coordination polymers (CPs), functionalized and host-guest hybrid materials. Simultaneously, physicochemical studies have shed light on the thermodynamic aspects of chemical bonding in f-element compounds, while theoretical modelling has made significant strides due to the recent availability of relativistic and contracted basis sets for the elements La–Lu that are optimized for density functional theory applications.

The general electronic configuration of the lanthanides is [Xe] $4f^{1-14} 5d^{0-1} 6s^2$. Electronic configurations for Ln^{3+} ions increase from $4f^0$ for La^{3+} to $4f^{14}$ for Lu^{3+}, which is the most remarkable characteristic. Lanthanides are highly electropositive elements and have a common stable oxidation state of +3, however, lanthanides also show +2 and +4 oxidation states which also show stability due to the presence of either half-filled or completely filled or empty 4f-subshell [6,7]. All lanthanide elements form trivalent cations, Ln^{3+}, whose chemistry is primarily governed by their decreasing ionic radius from lanthanum to lutetium. A significant characteristic of the lanthanide elements is the occurrence of the lanthanide contraction, in which the ionic radii of the lanthanides decreases gradually from lanthanum to lutetium. The fact that the stabilities of complexes with certain ligands increase from La^{3+} to Lu^{3+} is one of the consequences of the lanthanide contraction (refer table 1.1). The primary cause of lanthanide contraction is the electrostatic effect of increasing nuclear charge, which is very inadequately screened by inner sphere 4f- electrons.

In recent years, it has been determined that the lanthanide contraction is also caused by relativistic processes that impact the shielding properties of inner shell electrons [8]. Ionic radii are substantially influenced by coordination numbers: the gap between coordination numbers 6 and 12 is around 30 pm, making Ln(III) ions highly adaptable to a wide range of coordination settings.

Table 1.1: Electronic Configuration, Oxidation State and Ionic Radius of Lanthanides

Name of Element (Symbol)	Atomic Number	Electronic Configuration	Oxidation State	Abundance in Earth's crust[a] ppm	Ionic Radius[b] Ln^{+3} (Å)
Lanthanum (La)	57	[Xe] $4f^0 5d^1 6s^2$	+3	39	1.061
Cerium (Ce)	58	[Xe] $4f^1 5d^1 6s^2$	+3,+4	66.5	1.034
Praseodymium (Pr)	59	[Xe] $4f^3 6s^2$	+3,+4	9.2	1.013
Neodymium (Nd)	60	[Xe] $4f^4 6s^2$	+2,+3	41.5	0.995
Promethium (Pm)	61	[Xe] $4f^5 6s^2$	+2,+3	≈ 0	0.979
Samarium (Sm)	62	[Xe] $4f^6 6s^2$	+2,+3	7.1	0.964
Europium (Eu)	63	[Xe] $4f^7 6s^2$	+2,+3	2.0	0.950
Gadolinium (Gd)	64	[Xe] $4f^7 5d^1 6s^2$	+3	6.2	0.938
Terbium (Tb)	65	[Xe] $4f^9 6s^2$	+3,+4	1.2	0.923
Dysprosium (Dy)	66	[Xe] $4f^{10} 6s^2$	+3,+4	5.2	0.908
Holmium (Ho)	67	[Xe] $4f^{11} 6s^2$	+3	1.3	0.894
Erbium	68	[Xe] $4f^{12} 6s^2$	+3	3.5	0.881
Thulium (Tm)	69	[Xe] $4f^{13} 6s^2$	+2,+3	0.5	0.869
Ytterbium (Yb)	70	[Xe] $4f^{14} 6s^2$	+2,+3	3.2	0.858
Lutetium(Lu)	71	[Xe] $4f^{14} 5d^1 6s^2$	+3	0.8	0.848

[a] Abundances in earth's crust; values vary depending on sources; data from Handbook of Chemistry and Physics, CRC Press, Boca Raton, Fla., 2007.
[b] G.T. Seaborg

The behaviour of lanthanides is characteristic of hard acids, and the bonding sites are oriented in a way that gives bonding preference to fluorine and oxygen donor ligands. Complexes containing nitrogen, sulphur, and halogen (with the exception of F⁻) donors are not stable when present in the presence of water. If, on the other hand, these donor sites are a component of multidentate ligands, which are ligands that contain more than one donor group, then even these donor sites are implicated in strong complexation with lanthanides [9]. The lack of substantial interaction with the 4f- orbitals reduces the ligand field stabilization energies (LFSE). The absence of LFSE lowers overall stability, but gives

greater flexibility in geometry and co-ordination number, as LFSE is not lost when, for instance, an octahedral complex is converted into trigonal prismatic or square anti-prismatic geometry. In addition, the complexes are often unstable in solution.

1.2 Magnetic and Spectroscopic Properties of Lanthanides

The existence of unpaired 4f electrons in lanthanide ions causes them to exhibit paramagnetic characteristics; these electrons are well shielded by the filled outermost 5s and 5p orbitals. Except for lutetium, all of the trivalent lanthanide ions have unpaired 4f electrons. However the magnetic moment deviate considerably from the spin-only values because of strong spin-orbit coupling. Magnetic moments, however, show large deviations from the spin-only values due to the presence of substantial spin-orbit coupling. The intriguing magnetic behaviour of these elements arises because the magnetic effects of the various electrons in the incomplete 4f sub shell do not cancel each other out as they do in completed sub shell. It has been shown that Ln^{3+} ion behaviour is less sensitive to changes in the coordination environment than that of 3d transition series elements. All of the lanthanides, with the exception of lutetium, are paramagnetic at higher temperatures, and this paramagnetism typically demonstrates a significant anisotropy. The phenomenon of paramagnetism increases as the number of unpaired electrons increases. Many metals demonstrate a point below which they become antiferromagnetic when the temperature is reduced. The study of the magnetism of rare earth elements has had a significant impact on modern magnetism theories [10]. The paramagnetism of Ln(III) ions has applications in high coercivity magnet design ($CoSm_5$ and $Fe_{14}Nd_2B$), magnetic resonance imaging (Gd complexes as contrast agents), shift reagents for analysing nuclear magnetic resonance spectra, and magnetic refrigeration [11].

A plethora of electronic levels are produced by the $[Xe]4f^n$ electronic configurations of the Ln(III) ions. Because of the shielding of the 4f electrons, these levels

are clearly defined, with sharp absorption and emission bands. In addition, interactions with ligands are rather weak, which results in the splitting of electronic levels at just a few hundred cm^{-1} apart. This allows for an adequate description of electronic properties to be made within the framework of the ligand (crystal) field theory. Typically, the Russels–Saunders method for spin-orbit coupling is also assumed, such that the three quantum numbers S, L, and J define the electronic configurations [12]. However, further calculations must be performed within the framework of the intermediate spin-orbit coupling method. Some of the basic electronic properties of Ln (III) ions are summarized in table 1.2 and the electronic energy levels of some trivalent lanthanide ions are shown in figure 1.1 [13].

Table 1.2: Electronic Properties of Ln(III) Ions [12].

f^n		Multiplicity	No. of Terms	No. of levels	Ground level	
f^0	f^{14}	1	1	1	$^1S_0$	$^1S_0$
f^1	f^{13}	14	1	2	$^2F_{5/2}$	$^2F_{7/2}$
f^2	f^{12}	91	7	13	$^3H_4$	$^3H_6$
f^3	f^{11}	364	17	41	$^4I_{9/2}$	$^4I_{15/2}$
f^4	f^{10}	1001	47	107	$^5I_4$	$^5I_8$
f^5	f^9	2002	73	198	$^6H_{5/2}$	$^6H_{15/2}$
f^6	f^8	3003	119	295	$^7F_0$	$^7F_6$
f^7		3432	119	327	$^8S_{7/2}$	
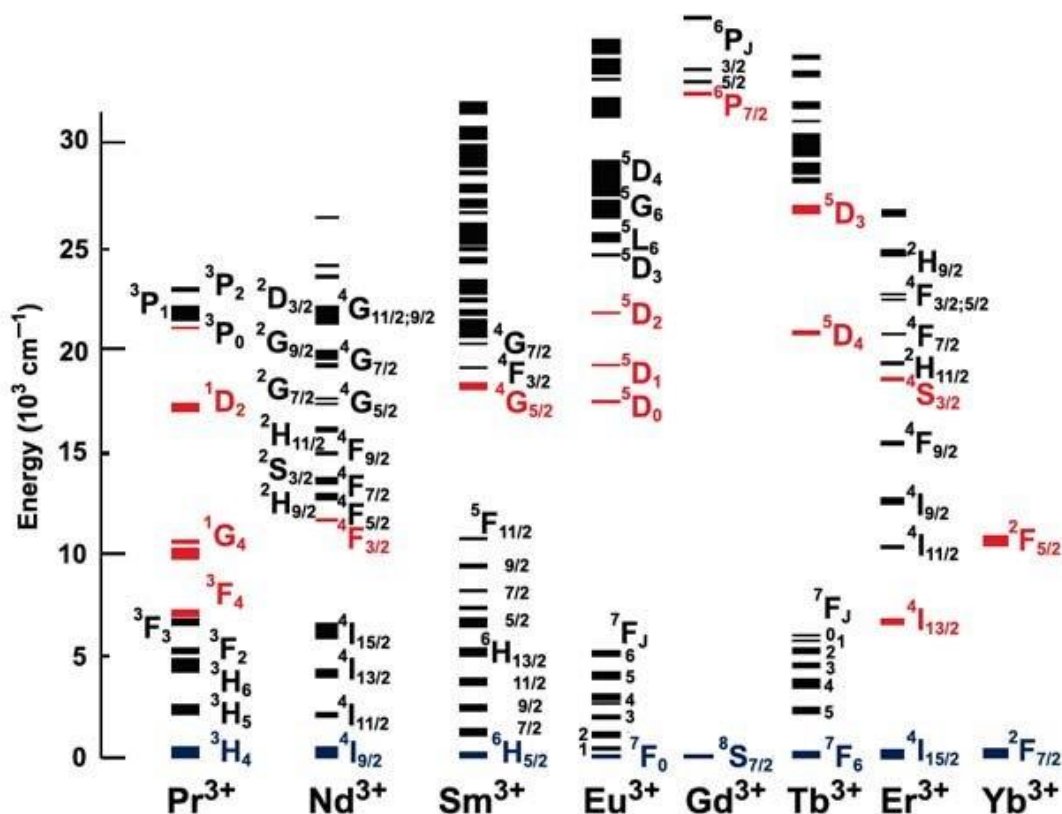
Fig. 1.1: Energy levels of some trivalent lanthanide ions.

(The ground levels and the main emissive levels are depicted in blue and red respectively).

The spectroscopic characteristics of the trivalent lanthanide ions are unique in nature. The shielding of the 4f orbitals by the filled $5s^2$ and $5p^6$ subshells is the main cause of the unique spectroscopic features shown by the Ln(III) cations. The trivalent lanthanide ions, with the exception of lanthanum and lutetium (which do not absorb light), show absorption with very sharp bands in the ultraviolet, visible, and infrared regions of the electromagnetic spectrum [14]. These bands are distinctive for each individual ion, and their wavelengths are same in the solid state and in the aqueous solution in which they are found. Their complexes have spectra that display significantly smaller and more prominent absorption bands, which are linked with a weak f-f transition. The 4f orbital is deeply embedded into the atom, and it is shielded by the 5s and 5p electrons that surround it. When compared to the broad bands caused by the d-d transition, the bands produced by the f-f transition are sharp.

Absorption and luminescence spectroscopy are essential to the study of the lanthanide system because they permit the determination of the natural frequencies of lanthanides. In solution or in glasses, the absorption spectra of a lanthanide-doped single crystal of lanthanide display a group of narrow lines; however, the lines within the group widen to form a single absorption band. It is necessary to attribute these bands to the electronic transition that takes place inside the 4f-shell. Each group or band corresponds to the transition between the levels of $^{2S+1}L_J$ free ions (or J-manifolds). They are called Intra-Configurational Transitions because they are not accompanied by a change in configuration. In order to describe the observed transitions [15], three mechanisms must be considered:

(i) Magnetic Dipole Transition

(ii) Induced Electric Dipole Transition

(iii) Electric Quadrupole Transition

(i) Magnetic Dipole Transition

The magnetic dipole transition is induced by the interaction of an active spectroscopic ion with the magnetic field component of the light passing through a magnetic dipole. Magnetic dipole radiation can alternatively be considered of as rotating charge displacement. A magnetic dipole transition has even parity because the sense of rotation is not reversed when inverted through a point (or inversion centre). As a result, a magnetic dipole operator has even transformation characteristics between states with equal parity (or intra-configurational transition).

(ii) Induced Electric Dipole Transition

The vast majority of optical transitions recorded in lanthanides are induced electric dipole transitions. These transitions are the result of an interaction between a spectroscopically active ion (the lanthanide ion) and the electric field vector through an electric dipole. The creations of electric dipole suppose a linear movement of charge, such transition has odd

parity. The electric dipole operator has therefore odd transformation properties under inversion with respect to an inversion centre. Intra configurational electric dipole transition is forbidden by the Laporte Selection Rules. Judd-Ofelt theory [16,17] provided a comprehensive account of the induced electric dipole transition.

(iii) Electric Quadrupole Transition

The electric quadrupole transition arises from the displacement that has a quadrupole nature. A quadrupole electric charge is made up of four point charges, all of which have zero dipole moment and no net charge. It may be thought of as an arrangement of two dipoles that cancel each other's dipole moment. An electric quadrupole has even parity. Electric quadrupole transitions are much weaker than magnetic dipole, which in turn are weaker than induced electric dipole transitions. However, hypersensitive transitions are regarded to be pseudoquadrupole transitions due to the fact that these transitions obey the selection rules of quadrupole transitions.

1.3 Selection Rules and Hypersensitivity

1.3.1 Selection Rules

Selection rules define the probable quantum level transitions caused by electromagnetic radiation absorption or emission. The chance of transitioning from one eigenstate to another is determined by the selection rules. The transition probability is the probability that a specific spectroscopic transition will occur. When an atom or molecule absorbs a photon, the probability that it will transit from one energy level to another relies on two factors: the nature of the atom's or molecule's initial and final state wavefunctions, and the strength of the photon's interaction with an eigenstate. Transition strengths are used to describe the likelihood of transitions. The application of selection rules determines whether a transition is permitted or not. A selection rule governs the occurrence of spectral transitions in atomic and molecular spectra. Under the Russell-Saunders Coupling Scheme, the multiplet terms of the Ln^{3+} ions are denoted by the notation $^{2S+1}L_J$, where S is the total

electron spin, L is the total orbital angular momentum, and J is the total momentum. The selection rules are only applicable under stringent conditions and might be relaxed under certain conditions. The selection rules for ΔL and ΔS are applicable only to the Russell-Saunders Coupling Scheme. The selection rules are relaxed in intermediate coupling scheme, since in this scheme L and S are not good numbers. The selection rules on ΔJ are more difficult to breakdown since J remains a good quantum number in the intermediate coupling scheme; it can be relaxed only by J-mixing, which is a weak effect. The selection rules on ΔM depend on point group symmetry of the rare earth site [18]. The selection rules for magnetic dipole and induced electric dipole transitions are given in Table 1.3

Table 1.3 Selection Rules for magnetic dipole and induced electric dipole transitions.

Magnetic Dipole Transitions (MD)	Induced Electric Dipole Transition(ED)
$\Delta J = \Delta S = \Delta L = 0$	$\Delta L = \pm 1, \Delta J = 0, \Delta S = 0, \|\Delta L\| \leq 6$
$\Delta J = 0, \pm 1$ but $0 \leftrightarrow 0$ is forbidden	$\|\Delta J\| \leq 6$; $\|\Delta L\| = 2, 4, 6$ if $J = 0$ and $J' = 0$
M' - M = -P, where P = ± 1	M' - M = - (q + p)

The selection rules for intraconfigurational optical transitions of lanthanide ions between $^{2S+1}L_J$ levels are $\Delta L = \pm 1$ or $\Delta J = \pm 1$. Among the $4f^n$-$4f^n$ electronic transitions, magnetic dipole and electric quadrupole transitions are allowed. Only the oscillating magnetic vector of the radiation interacts with the 4f electrons of Ln^{3+} ions in magnetic dipole intraconfigurational electronic transitions, not the oscillating electric vector. Though the oscillator strengths of these types of transitions are around 10^{-6} times lesser to that of a fully allowed transition, they can provide useful information for some of the lanthanides [19]. One of the well-known examples of the breakdown of selection rules of Judd-Ofelt theory is the occurrence of $^7F_0 \rightarrow {}^5D_0$ and $^5D_0 \rightarrow {}^7F_0$ transitions in some Eu(III) complexes [20–22]. The $^7F_0 \rightarrow {}^5D_0$ transitions are forbidden by the selection rules, as ΔJ ($0 \leftrightarrow 0$) is forbidden. The breakdown of closure approximation in Judd–Ofelt can be explained to this

exceptional behaviour was ascribed by Tanaka *et al.* [23,24]. Wybourne [25] has shown that the second order matrix element $U^{(0)}$ is zero so that no intensity can come from this mechanism. Wybourne proposed a mechanism in which spin selection rule is relaxed by scalar third order contribution involving spin-orbit interaction acting within higher lying perturbing states. This model was later developed by Burdick [26,27].

1.3.2 Hypensensitivity

In lanthanides, the intensities of the induced dipole transitions are not considerably impacted by the chemical environment in which they are found. The dipole strength of a given transition of the lanthanide (III) ion does not change by more than a factor of two or three regardless of the matrix in which it is occurring. However, there are a few transitions that are highly sensitive to the surrounding environment, and they are far more intense in the lanthanides complex than they are in the lanthanide (III) aquo ion complex [28–30]. Moeller et al. were the ones who made the initial investigation about the high sensitivity of spectral intensities for ligand environment as a general phenomenon [31,32] for β-diketonate and EDTA complexes of Nd^{3+}, Ho^{3+} and Er^{3+} much before the advent of Judd-Ofelt Theory. These kinds of transitions were referred to as "Hypersensitive" by Jorgensen and Judd, and these transitions obeyed the selection rules $|\Delta S|=0$; $|\Delta L|\leq2$; $|\Delta J|\leq2$ and these rules are the same as the selection rules for pure quadrupole transitions. However, studies have shown that the intensities also have a quadrupole character; for this reason, hypersensitive transitions are regarded to have a pseudoquadrupole character [33,34]. Nearly all Ln^{3+} ions exhibit hypersensitive transitions, as listed in Table 1.4. The observations of hypersensitive transitions have been made for virtually every Ln^{3+} ion. Inhomogeneities in the dielectric medium that surrounds the Ln^{3+} ion, as described by Jorgensen and Judd have the potential to increase the intensity of hypersensitive transitions.

Table 1.4: Identified Hypersensitive Transitions [18] of Ln^{3+} Ions (Wavelength are approximate).

Ln^{3+}	Transition	$\bar{\nu}(cm^{-1})$	$\lambda(nm)$
Pr^{3+} $(4f^2)$	$^3H_4 \rightarrow {}^3F_2$	5200	1920
Nd^{3+} $(4f^3)$	$^4I_{9/2} \rightarrow {}^4G_{5/2}$	17300	578
Sm^{3+} $(4f^5)$	$^6H_{5/2} \rightarrow {}^4F_{3/2},\ {}^4F_{1/2}$	6400	1560
Eu^{3+} $(4f^6)$	$^7F_1 \rightarrow {}^5D_1$	18700	535
	$^7F_0 \rightarrow {}^5D_2$	21500	465
	$^7F_2 \rightarrow {}^5D_0$	16300	613
Gd^{3+} $(4f7^2)$	$^8S_{7/2} \rightarrow {}^6P_{7/2},\ {}^6P_{5/2}$	32500	308
Tb	a	-	-
Dy^{3+} $(4f^9)$	$^6H_{15/2} \rightarrow {}^6F_{11/2}$	7700	1300
	$^6H_{15/2} \rightarrow {}^4I_{15/2},\ {}^4G_{11/2}$	23400	427
Ho^{3+} $(4f^{10})$	$^5I_8 \rightarrow {}^5G_6$	22100	452
	$^5I_8 \rightarrow {}^3H_6$	27700	361
Er^{3+} $(4f^{11})$	$^4I_{15/2} \rightarrow {}^2H_{11/2}$	19200	521
	$^4I_{15/2} \rightarrow {}^4G_{11/2}$	26400	379
Tm^{3+} $(4f^{12})$	$^3H_6 \rightarrow {}^3F_4$	5900	1695
	$^3H_6 \rightarrow {}^3H_4$	12700	787
	$^3H_6 \rightarrow {}^1G_4$	21300	469

^{a}None identified positively, but the $^5D_4 \rightarrow {}^7F_5$ transition sometimes display Ligand-induced pseudo-hypersensitivity.

Karraker [35] studied the hypersensitivity transitions of Nd^{3+}, Ho^{3+} and Er^{3+} and the absorption spectra of six, seven, and eight coordinated β-diketonates in non-aqueous mediums to examine the impact of coordination number on the intensity and fine structure of the spectra. The β-diketonate ligands were selected because each of them binds to lanthanides (III) in a bi-dentate way involving two oxygen donor atoms and produces a six-membered chelate ring. Therefore, the number of coordination and the geometric arrangement of the bonded ligands were the two most important factors. Solvents with low polarity were selected because of their ability to reduce the influence of the solvent on the crystal field splitting of the lanthanide ion.

Choppin [36] observed a significant relationship between the oscillator strength and the sum of the ligand's pKa value for the dibasic acid. Three broad statements were made by these researchers on the intensity of hypersensitive transitions:

i.   An increasing basic character of coordination ligand results in increasing ligand absorption intensity;

ii.   Decreasing metal ligand bond distance results in intensity enhancement; and

iii.   The greater is the number of more basic ligand greater is the degree if enhanced intensity.

It has been observed that the hypersensitive transition for praseodymium, Pr^{3+}, is the $^{3}H_4 \rightarrow {}^{3}F_2$ transition that occurs at about 5,200 cm^{-1}. On the other hand, the hypersensitive transition for neodymium, Nd^{3+}, is the $^{4}I_{9/2} \rightarrow {}^{4}G_{5/2}$ transition that takes place around 17,300 cm^{-1}. In presence of ligands, it has been found that the hypersensitivity can be extended to more transitions which do not exhibit hypersensitivity generally, such as $^{3}H_4 \rightarrow {}^{3}P_2, {}^{3}P_1, {}^{3}P_0$ and $^{1}D_2$ for Pr^{3+} and $^{4}I_{9/2} \rightarrow {}^{4}G_{7/2}, {}^{4}F_{7/2}, {}^{4}F_{5/2}$ and $^{4}F_{3/2}$ in case of Nd^{3+}. These transitions of Pr^{3+} and Nd^{3+} have been found to show high sensitivity towards even minor changes in the immediate coordination environment [37–39]. Further Peacock [40], observed hypersensitivity in the $^{4}I_{9/2} \rightarrow {}^{4}G_{5/2}$ transition of Nd^{3+} whereas Choppin et al. observed hypersensitivity in $^{4}G_{7/2} \rightarrow {}^{4}K_{13/1}$ in addition to $^{4}G_{5/2}$. In their series of investigations with Nd^{3+} complexes, Misra and co-workers [41–44] identified unique sensitivities in the $^{4}I_{9/2} \rightarrow {}^{4}F_{7/2}$ and $^{4}F_{5/2}$ transitions. These complexes demonstrated diverse binding properties respective of each ligand employed and were termed 'Ligand-Mediated Pseudohypersensitive Transitions'.

1.4 Coordination Chemistry of Lanthanides

Several books and reviews provide concise summaries of the information needed to understand the coordination chemistry of lanthanide inorganic compounds [45–48]. Polyoxometalates [49] and cluster compounds [50] are also considered to be members of this type of compounds. As was mentioned earlier, the majority of the organic molecules that are used to tailor Ln(III) complexes are polydentate ligands. Throughout the course of history, carboxylates and polyaminocarboxylates have played an important role, particularly with regard to the extraction and separation of lanthanides [51].

Table 1.5 provides some generalizations related to the topic[52]. The chemistry of lanthanide compounds in solution, in general, and in aqueous solution, in particular, has garnered a significant amount of interest over the course of the past several years. The coordination chemistry of lanthanides differs significantly from that of d-transition metals [53]. The majority of trivalent lanthanides form ionic salts. The mode of bonding between lanthanide ions and ligands can mostly be characterized as electrostatic. In a particular series, covalency is anticipated to increase as the central metal ion sizes (La-Lu) decrease. Ionicity is supported by a substantial data, both theoretical and experimental. Even in the most stable complexes, the bond strength is on the same order of magnitude as the Ln^{3+}-water dipole interaction, as pointed out by Moller et al. [54]. The extremely ionic character of lanthanide bonding has also been confirmed by bond distance measurements.

Table 1.5: Compilation of some general characteristics of Lanthanides [52].

- Highly electropositive elements – compounds are essentially ionic
- Ln (III) is the dominant oxidation state but others are known (Table 1.1)
- Ions are oxophilic and hard Lewis acids
- Large ion size and high charge in the main oxidation state lead to high coordination numbers; 8–10 common; 11,12 known
- Low coordination numbers (2–6) are possible with bulky ligands
- Complexes are generally labile, hence geometric isomers are rare
- The lanthanide contraction gives a higher charge/size ratio from La → Lu leading to increased stability in that sequence, but may cause a coordination number decrease
- Organometallics (Ln-C), organoamidometallics (Ln-N), or organooxometallics (Ln-O) are sensitive to air and water
- Ln^{3+} can replace Ca^{2+} in biological systems and act as a probe for Ca^{2+}

In both crystalline complexes and solutions, the coordination number of lanthanides ranges from 6 to 12, with C.N. 9 being the most prevalent. Coordination numbers below 6 are only seen with extremely bulky ligands, and coordination number 6 itself is rare; coordination numbers 7, 8 and 9 are more characteristic. The trivalent ions are hard acceptors, and the complexes they form with oxygen-donor ligands are more stable as a result. Water molecules are generally difficult to remove from the initial coordination sphere, making complexation with monodentate ligands weak. Because of the chelate effect, complexes generated with chelating ligands are stronger. The majority of lanthanide complexes are formed by chelation. Complexes formed by donor atoms in nonchelated structures are weaker than those formed by the identical donor atoms in chelates. Water is a very potent ligand for Ln^{3+} ions. The difficulty of competing ligands to remove water molecules from the coordination sphere significantly limits the ligand types with which Ln^{3+} ions can bind in aqueous solution. These ligands are expected based on the

categorization of lanthanides as hard acceptors; one feature of such acceptors is their high level of ionic bonding, and another is their preference for donor atoms in the sequence $O > N > S$ and $F > Cl$. Therefore, oxo donors such as O_2^-, OH^- and water predominate in the coordination chemistry of lanthanides, thus, making carboxylate complexes the most prevalent. Within the first coordination sphere, there is negligible stereochemical preference because Ln^{3+}-Ligand interactions have negligible or no directionality. For this reason, the ion-formation, donor atoms, sizes and number, as well as solvation effects, of the ligands play a crucial role in determining the coordination numbers and geometries. This means that the geometry of lanthanide compounds is flexible. In terms of the occupancy of biological Ca^{2+} binding sites, this geometrical flexibility is important. In addition, the poor polarizing ability of Ln^{3+} ions and the ionic character of their interactions demonstrate that they do not significantly alter the electronic charge distributions at their bonding sites.

The lanthanide ion has the ability to form complexes with many different types of organic molecules, including polyaminopolycarboxylic acids (such as EDTA and similar compounds), thiosemicarbazide, and amino acids. It is possible to generate extremely luminous lanthanide complexes if the ligands comprise organic chromophores that have the appropriate photophysical characteristics. Despite the fact that lanthanide complexes of $EDTA^{4-}$ have been the subject of a significant amount of research in the past [55,56], relatively little is known about the coordination chemistry of functionalized EDTA derivatives [57,58]. Some characteristics of the Ln^{3+} complexes, particularly their stability, are profoundly affected when two EDTA carboxylates are replaced with amide functionalities. In contrast to ethylenediamine, EDTA is a hexadentate rather than a bidentate ligand. The anticancer and antibacterial properties of metal complexes containing

sulfur ligands such as thiosemicarbazide and its derivatives [59] have received considerable attention.

1.5 Interaction of Lanthanides with Amino acids

Due to their varied donor atoms, many coordination modes and different protonated-deprotonated forms, the biologically significant amino acids exhibit rich coordination chemistry. Interest in employing trivalent lanthanide ions (Ln^{3+}) as structural probes in biological systems, especially those systems which contain Ca^{2+}, prompted the study of the chemical interaction between Ln^{3+} and amino acids or peptides [60,61]. Strong evidence suggests that the bonding between Ln^{3+} ions and amino acids occurs via the oxygen of the carboxylate group and that bonding via the nitrogen of the amino group is implausible at pH values up to 5.6 [62]. L-Cysteine is one of the 20 natural amino acids. It is the only one with sulphur besides methionine. Their sulfhydryl side-chain is efficient at binding to metals like zinc, which explains why cysteine (and other amino acids such as histidine) is prevalent in zinc-binding motifs. Several lanthanide compounds of mono-, di-, and tri-carboxylic acids are of biological interest. Acetate and lactate produce complexes in which at least three, if not four, acetate groups are linked to a single Ln^{3+} ion. The stability of complexes produced with chelators such as EDTA rises gradually with decreasing size of the Ln^{3+} ion, owing to the higher charge-to-volume ratio as one progresses from La^{3+} to Lu^{3+}, resulting in more electrostatic interaction. Nioboer (1975) proposed that the distinctive variation in complex stability that occurs over the lanthanide series would be of diagnostic utility when investigating the binding sites of the lanthanides. The stability of Ln^{3+} complexes formed with dicarboxylic acids is higher than that of Ln^{3+} complexes formed with monocarboxylic acids. Ln^{3+} ions have found more broad application as informative substituents to examine different structural and functional features of the Ca^{2+}-binding sites on proteins. This is because Ca^{2+} is a recalcitrant ion. In order to report

on the binding sites of other metal ions, such as Fe^{3+} in transferrin and ferrin or Mn^{2+} in pyruvate kinase and alkaline phosphatase, lanthanides have been used. In normal settings, it is believed that proteins such as lysozyme do not interact directly with Ca^{2+} or any other metal ion. Lanthanides have provided important information on these proteins. Additionally, chemical alteration of a protein can be employed to introduce particular, strong Ln^{3+} binding sites. Despite the fact that f-block elements, i.e., the lanthanide series, play no known vital function in life processes [63], they offer some of the most intriguing, challenging, and significant chemical and biological issues of all inorganic elements in the periodic table. This is because of the capabilities imparted by their outer electron configuration and related energy levels, as well as their minimal chemical toxicity. The unprotonated carbonyl groups found in amino acids form a coordination complex with lanthanides. Weak interaction with the hydroxyl oxygen of serine [62], which most likely also occurs with threonine and tyrosine. Both of amino and carbonyl components [64] of the amino acids contribute to complexing Ln^{3+} ions, and this is used as an explanation for why amino acids form stronger complexes with Ln^{3+} than monocarboxylic acids do. These claims are supported by the findings of spectroscopic investigations of the interaction of Pr^{3+} and Eu^{3+} with a variety of amino acids at pH 7 conducted by Katzin and Gulyas [65]. At pH 7, histidine may coordinate to Ln^{3+} via its imidazole nitrogen, as proposed by Sherry et al. [66] . NMR investigations of the interaction of Gd^{3+} with several small glycopeptides at pH 6-7 [65] provide evidence that the N-terminal amino groups of peptides also coordinate Ln^{3+} ions.

Nevertheless, according to Prados et al., the high pK_a values for the deprotonation of L-amino nitrogens ensure that Ln^{3+} ions are hydrolyzed prior to the formation of uncharged N-donors. Several studies have used pH values as low as permitted by the pK_a of the carboxyl group [67] in order to limit coordination to the amino nitrogen. However, this strategy might reduce the affinity of the Ln^{3+} ion for zwitterions due to the repulsive

effect of the protonated amino group. Acetylation, which was performed by other researchers, has been shown to covalently block the amino group. Evans (1990) has provided a comprehensive overview of the interactions that various lanthanides have with a very broad spectrum of proteins. The range of proteins that have been studied is extensive, including enzymes like trypsins, elastase, collagenase, amylase, nuclease, ATPase, phospholipase-A2 and acetylcholinesterase; the contractile proteins actin and myosin; and molecular oxygen carriers like haemocyanin. According to the results of these analyses, the carboxyl group serves as a major ligand for Lu^{3+} ions, with further coordination occurring via the carboxyl or hydroxylic oxygen groups. The lanthanides can often replace Ca^{2+} or any other metal. Proteins often have a greater affinity for Ln^{3+} ions than Ca^{2+} ions due to their larger charge to volume ratio. Although the affinities of the various lanthanides vary greatly, in general they grow when the hydration of the sequestered lanthanide ion decreases and the cationic charge of the binding site increases. Ln^{3+} binding to various types of biomolecules in vitro can reveal significant structural and other information, similar to what has been found with protein studies. Nucleic acids, phospholipids, phospholipid membranes, porphyrins, vitamin B12, and high density lipoproteins are some of the biomolecules. The pH of the medium is an extremely important factor in the chemistry of the Ln(III)/amino acid systems [68,69]. When the pH is low (below 5), some species are formed that have the COO^- covalently bonded to the central atom. Formation of $Ln(OH)_3$ and numerous polynuclear lanthanide/oxo/hydroxo complexes has been reported to take place at higher pH levels [70].

1.6 General Properties and Structures of the Amino Acids (L-Glutamine, L-Threonine, L-Tryptophan and L-Isoleucine)

Amino acids are molecules containing an amine group, a carboxylic group and a side chain that varies among different amino acids. The elements present in amino acids i.e. carbon, nitrogen and oxygen are particularly important in biochemistry, where the term alpha-

amino acids is used. An alpha-amino acid has the generic formula $H_2NCHRCOOH$, where the R is an organic substituent; the amino group is attached to the carbon atom immediately adjacent to the carboxylate group (the α-carbon).

Fig.1.2: General Structures of unionized and ionized form of α-amino acid.

The various alpha-amino acids differ in which side chain (R-group) is attached to their alpha carbon, and can vary in size from just one hydrogen atom in Glycine to a large heterocyclic group in Tryptophan. Amino acids can be linked together in varying sequences to form a vast variety of proteins. 22 amino acids are naturally incorporated into polypeptides and are called proteinogenic or standard amino acids. Out of these, 20 are encoded by the universal genetic code. 8 standard amino acids are called 'essential' for humans because they cannot be created from other compounds by the human body, and must be taken in external sources as food. Amino acids are usually classified by the properties of their side chains into four groups. The side chain can make an amino acid a weak acid or a weak base, and a hydrophile if the side chain is polar or a hydrophobe if it is non- polar [71].

Table 1.6: Essential and Non-essential Amino Acids.

Essential	Nonessential
Isoleucine	Alanine
Leucine	Asparagine
Lysine	Aspartic acid
Methionine	Cysteine[*]
Phenylalanine	Glutamic acid
Threonine	Glutamine[*]
Tryptophan	Glycine[*]
Valine	Selenocysteine[*]
Histidine	Serine[*]
	Tyrosine[*]
	Arginine[*]

*Conditionally essential
^ *Fürst.P,Stehle.P(2004);J.of Nutrit.**134**.Pg 1558S-1565S*
^ *Reeds PJ(2000),J.of Nutrit.,**130**(7).Pg1835S-40S.*

L-Glutamine (2*S*)-2,5-diamino-5-oxopentanoic acid

L-glutamine is an optically active form of glutamine having L-configuration. Glutamine (abbreviated as **Gln** or **Q**) is an α-amino acid that is used in the biosynthesis of proteins. It contains an α-amino group (which is in the protonated $-NH_3^+$ form under biological conditions), an α-carboxylic acid group (which is in the deprotonated $-COO^-$ form under biological conditions), and a side chain amide which replaces the side chain hydroxyl of glutamic acid with an amine functional group, classifying it as a charge neutral, polar (at physiological pH) amino acid. It is non-essential and conditionally essential in humans, meaning the body can usually synthesize sufficient amounts of it, but in some instances of stress, the body's demand for glutamine increases and glutamine must be obtained from the diet.

Table 1.7: Properties of L-Glutamine.

Chemical formula	$C_5H_{10}N_2O_3$
Molar mass	146.15 g·mol^{-1}
Melting point	decomposes around 185°C
Solubility in water	soluble
Acidity (pK_a)	2.2 (carboxyl), 9.1 (amino)

^*Weast, Robert C., ed. (1981). CRC Handbook of Chemistry and Physics (62nd ed.). Boca Raton, FL: CRC Press. p. C-311*
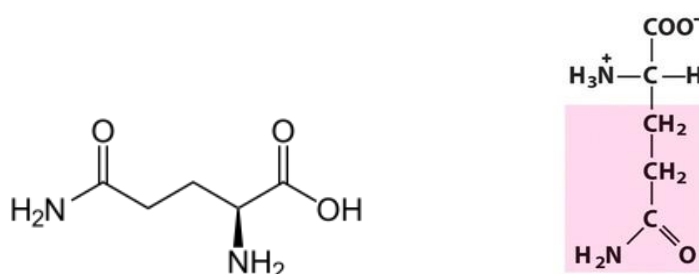
Fig.1.3: Structural Representation of L-Glutamine.

In human blood, glutamine is the most abundant free amino acid. Glutamine plays a role in a variety of biochemical functions- Protein synthesis, lipid synthesis, regulation of acid-base balance in the kidney by producing ammonium, cellular energy (as a source, next to glucose), nitrogen donation for many anabolic processes, carbon donation (as a source,

refilling the citric acid cycle), nontoxic transporter of ammonia in the blood circulation and precursor to the neurotransmitter glutamate. L-glutamine use has been found to be of great importance in the treatment of trauma and surgery patients, and has been shown to decrease the incidence of infection in these patients [72].

L-Threonine (2*S*,3*R*)-2-amino-3-hydroxybutanoic acid

L-threonine is an optically active form of threonine having L-configuration. **Threonine** (symbol **Thr** or **T**) is an amino acid that is used in the biosynthesis of proteins. Threonine is an essential amino acid in humans (meaning the human body cannot synthesize it and it must be obtained from the diet). It contains an α-amino group (which is in the protonated –NH_3^+ form under biological conditions), a carboxyl group (which is in the deprotonated –COO^- form under biological conditions), and a side chain containing a hydroxyl group, making it a polar, uncharged amino acid.

Table 1.8: Properties of L-Threonine.

Chemical formula	$C_4H_9NO_3$
Molar mass	119.12 g·mol^{-1}
Melting point	decomposes around 256°C
Solubility in water	97000 mg/L (at 25 °C)
Acidity (pK_a)	2.63 (carboxyl), 10.43 (amino)
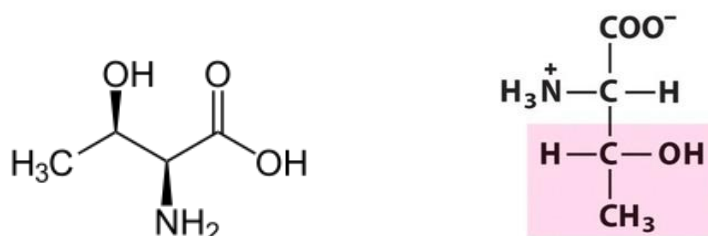
Fig.1.4: Structural Representation of L-Threonine.

L-Threonine has a role as a nutraceutical, a micronutrient, a plant metabolite, an Escherichia coli metabolite, a human metabolite, an algal metabolite and a mouse metabolite. It is an important amino acid for the nervous system; threonine also plays an important role in porphyrin and fat metabolism and prevents fat build-up in the liver.

Useful with intestinal disorders and indigestion, threonine has also been used to alleviate anxiety and mild depression [73,74].

L-Tryptophan (2*S*)-2-amino-3-(1*H*-indol-3-yl)propanoic acid

L-Tryptophan is an essential amino acid and the least plentiful of all 22 amino acids in the human body. **Tryptophan** (symbol **Trp** or **W**) is an α-amino acid which is used in the biosynthesis of proteins. Tryptophan contains an α-amino group, an α-carboxylic acid group, and a side chain indole, making it a polar molecule with a non-polar aromatic beta carbon substituent. It is essential in humans, meaning that the body cannot synthesize it and it must be obtained from the diet. Like other amino acids, tryptophan is a zwitterion at physiological pH where the amino group is protonated and the carboxylic acid is deprotonated. For all amino acids, including *L*-tryptophan, only the *L* isomer is used in protein synthesis and can pass across the blood-brain barrier [75].

Table 1.9: Properties of L-Tryptophan

Chemical formula	$C_{11}H_{12}N_2O_2$
Molar mass	204.229 g·mol^{-1}
Melting point	decomposes around 290°C
Solubility in water	11.4 g/L at 25 °C
Acidity (pK_a)	2.38 (carboxyl), 9.39 (amino)
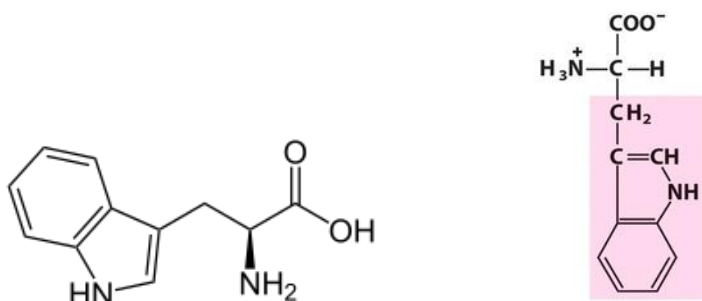
Fig.1.5: Structural Representation of L-Tryptophan.

Tryptophan is among the less common amino acids found in proteins, but it plays important structural or functional roles whenever it occurs.

Tryptophan functions as a biochemical precursor for the following compounds [76]:

- Serotonin (a neurotransmitter)

- Melatonin (a neurohormone)

- Kynurenine, to which tryptophan is mainly (more than 95%) metabolized.

- Niacin, also known as vitamin B_3, is synthesized from tryptophan via kynurenine and quinolinic acids.

- Auxins (a class of phytohormones)

L-Isoleucine (2*S*,3*S*)-2-amino-3-methylpentanoic acid

L-Isoleucine is one of nine essential amino acids in humans (present in dietary proteins).

Isoleucine (symbol **Ile** or **I**) is an α-amino acid that is used in the biosynthesis of proteins. It contains an α-amino group, an α-carboxylic acid group and a hydrocarbon side chain with a branch (a central carbon atom bound to three other carbon atoms). It is classified as a non-polar, uncharged (at physiological pH), branched-chain, aliphatic amino acid.

Isoleucine has diverse physiological functions, such as assisting wound healing, detoxification of nitrogenous wastes, stimulating immune function, and promoting secretion of several hormones. Necessary for haemoglobin formation and regulating blood sugar and energy levels, isoleucine is concentrated in muscle tissues in humans.

Beside its biological role as a nutrient, Isoleucine also has been shown to participate in regulation of glucose metabolism [77].

Table 1.10: Properties of L-Isoleucine.

Chemical formula	$C_6H_{13}NO_2$
Molar mass	$131.175 \text{ g·mol}^{-1}$
Melting point	decomposes around 285°C
Solubility in water	34400 mg/L (at 25 °C)
Acidity (pK_a)	2.36 (carboxyl), 9.68 (amino)
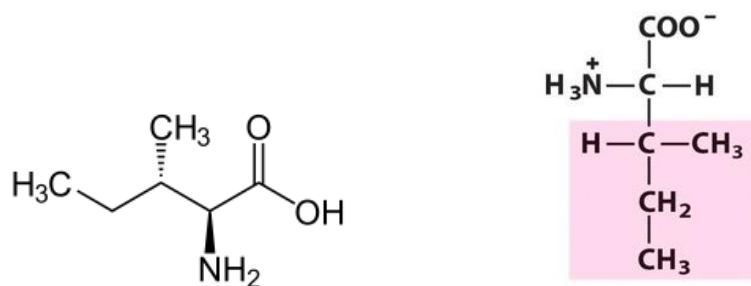
Fig.1.6: Structural Representation of L-Isoleucine.

1.7 Isomorphous Characteristics of Lanthanides and Alkaline Earth Metals

The potential of the Ln^{3+} ion to specifically and frequently substitute Ca^{2+} in an isomorphous manner is a big attraction for those interested in lanthanide biochemistry. In order to learn more about the structural and functional characteristics of Ca^{2+} binding sites on proteins, Ln^{3+} ions have been used extensively as an informative substituent for Ca^{2+}. Proteins like lysozyme have been studied using lanthanides despite the fact that they do not interact with Ca^{2+} or any other metal ion under physiological conditions. The differences between Ln^{3+} and Ca^{2+} in terms of their characteristics are interesting enough to encourage further investigation. Levine and Williams [78] and Einspahr and Bug [79] have both offered comprehensive reviews of the biologically significant chemical characteristics of Ca^{2+}. The structural chemistry of calcium and the lanthanides has been well studied by Martin [80].

In table 1.11, the characteristics of Ca(II) and Ln(III) that are most relevant to biochemistry are compared. These ions are quite comparable to one another in terms of their sizes, bonding, the geometry of their coordination, and their preferred donor atoms. These commonalities are what make it possible for the Ln(III) ion to replace Ca(II) in such a specific manner. Many Ca(II) binding sites have been specifically designed by nature to exclude competing metal ions, particularly Mg^{2+}. This is of utmost significance intracellularly, since certain proteins may selectively bind Ca^{2+}, which is present in submicromolar concentrations, while being submerged in fluids that contain millimolar

concentrations of Mg^{2+}. Studies on t-RNA have shown without a doubt that Ln^{3+} can also occupy Mg^{2+} sites. Ln^{3+} ions can occupy Mg^{2+} sites in enzymes, as shown by many reactions [81,82].

Table 1.11: Ca^{2+} and Ln^{3+} Ion Characteristics Comparison.

Property	Ca (II)	Ln(II)
Co-ordination number	6–12 reported 6 or 7 favoured	6 – 12 reported 8 or 9 observed
Co- ordination geometry	Highly flexible	Highly flexible
Preference for donor sites	O >> N > S	O >> N > S
Ionic radii (Å)	1.00 – 1.18 (C.N. 6 - 9)	0.86 – 1.22 (C.N. 6 – 9)
Type of bonding	Electrostatic	Electrostatic
Hydration number	Six	8 or 9
Water exchange rate constant (s^{-1})	$\sim 5 \times 10^8$	$\sim 5 \times 107$
Crystal field stabilization	None	Negligible

The most notable chemical difference between Ca(II) and Ln(III) ions is the former's spectroscopic silence and the latter's plethora of spectroscopic signals. From a scientific standpoint, it is quite unfortunate that one of the least informative metals is also one of the most biologically significant. In contrast, members of the lanthanides series are coloured, strongly paramagnetic, and luminous. Ca(II) is colourless, diamagnetic, and non-luminescent. Indeed, apart from its x-ray absorption features, Ca(II) is spectrally inert. Even within the lanthanide series, the biological responses of the different lanthanides are influenced by their unique ionic radii. Changes in the lanthanide series from La^{3+} to Lu^{3+} occur gradually and quantitatively, with a simple relation existing between ionic radius and activity. The influence of various ions on the activation of –amylase increases from La^{3+} to Lu^{3+} [83], although this order is reversed in the inhibition of Ca^{2+}/Mg^{2+} ATPase of skeletal muscle sarcoplasmic reticulum [84]. Exploring the rich and diverse spectrum properties of lanthanide ions and the isomorphous substitution of these metal ions by lanthanide ions are both helpful in obtaining information on the structural geometries, reactivities, and binding

aspects of Ca(II) and Mg(II) biochemistry. As revealed by the structural and functional experiments, the replacement does not alter the characteristics of the ligating molecules in any significant way. Therefore, replacing the Ca(II) ion with the Ln(III) ion is an extremely helpful technique to investigate the ligand interaction.

1.8 Chemical Kinetics

The study of chemical kinetics, which is one of the oldest branches of physical chemistry, deals with the rate of chemical reactions and is inextricably linked to the understanding of their mechanisms [85]. The rate of a reaction is a positive quantity that represents how the concentration of a reactant or product varies with time when the reaction is taking place. This may be thought of as an expression of how quickly the concentration of a reactant or product changes. When a reaction is allowed to continue, the concentration of the reactants will gradually decrease, while the concentration of the products will gradually increase as the time period advances.

1.8.1 Factors affecting the rate of a reaction

The following factors influence the rate of a reaction:

i. Concentration of the reactants.

   Concentration of reactants is directly proportional to the rate of a chemical reaction. The effective collision rate of the molecules is increased when there is a higher concentration of the reactants in a given volume. A higher rate of reaction is produced as a direct consequence of a higher frequency of collision.

ii. Temperature

   If the temperature of a reaction is lowered or raised, a dramatic shift in the reaction rate is noticed. For every factor of 10° increase in temperature, the rate of a reaction is found to increase by a factor of two to three. Because the effective number of collisions increases with temperature, more and more molecules are able to overcome the threshold energy (E_T) [86].

iii. Presence of catalyst

A catalyst is a material that alters the rate of a chemical reaction without itself experiencing a chemical change. It has been found that the presence of a certain catalyst causes a number of reactions to happen at a faster rate than they would have otherwise. This is because the magnitude of activation energy, shown by E_a, is reduced when a catalyst is present in the reaction.

iv. Nature of the reactants

With the exception of proton-transfer reactions, reactions involving polar and ionic substances typically proceed at a relatively high rate. Bond rearrangement and electron transfer reactions, on the other hand, are quite slow. Oxidation-reduction reactions that involve the transport of electrons are also slower than ionic reactions.

v. Surface area of the reactants

For heterogeneous reactions, the rate of a reaction is proportional to the surface area of the reactants and products. The rate of the reaction increases with an increase in surface area (that is, a decrease in the particle size of the reactants).

vi. Exposure to radiation

The use of particular radiations can, in certain circumstances, result in a substantial acceleration of the rate at which a chemical reaction occurs. These radiations have frequencies (v), and their photons have sufficient energy ($E = hv$) to break particular bonds in reactants.

1.8.2 Concept of activation energy (E_a)

In the year 1897, a Swedish scientist named Svante Arrhenius, introduced the concept of activation energy (E_a) According to Arrhenius, the process of converting reactants into products does not follow a "down the slope" trajectory (process taking place of its own). Instead, in order for the interacting molecules to be transformed into products, they have to first cross through an energy barrier. The energy barrier is an imaginary high-energy state

that exists between the reactants and the products of the reaction. The name given to the amount of energy that corresponds to the peak of the energy barrier is "threshold energy" (E_T). It is the minimum amount of energy that the reacting molecules need to have in order for the reaction to take place. The molecules that react and have an energy that is more than or equal to the threshold energy are referred to as activated molecules. This occurs at the top of the energy barrier. Every molecule contains a minimal quantity of energy. The energy might exist as either kinetic or potential energy. The kinetic energy of colliding molecules can be utilised to stretch, bend, and ultimately break bonds, resulting in chemical reactions. If molecules move too slowly or have insufficient kinetic energy, or if they collide with the wrong orientation, they do not respond and simply bounce off one another. However, if the molecules are moving fast enough with the correct collision orientation so that the kinetic energy upon impact exceeds the minimum energy barrier, then a reaction occurs. The minimal amount of energy required for a chemical reaction to occur is known as the activation energy (E_a). Thus,

Activation energy = Threshold energy – Average energy of the reactant molecules

$$\text{Or, } E_a = E_T - E_R$$

Where E_a represents the activation energy of the reaction, E_T represents the threshold energy, and E_R represents the average energy of the reactant molecules.

1.8.3 Activation energy and the rate of the reaction

Depending on the magnitude of the activation energy, there are three possible outcomes:

i.   If the activation energy (Ea) is small, the rate of the reaction is fast.

ii. If the activation energy (Ea) is large, the reaction will proceed slowly.

iii. When the activation energy (Ea) is zero, the reaction is instantaneous or extremely fast.

1.8.4 Arrhenius Rate Equation

Arrhenius described the temperature dependence of the rate constant (k) using the concept

of activation energy, by the equation

$$k = Ae^{\frac{-E_a}{RT}} \tag{1.1}$$

Where

k is the rate constant

T is the absolute temperature (in Kelvin)

E_a is the activation energy for the reaction

R is the universal gas constant

A is the frequency factor The factor exp(-E$_a$/RT) is a measure of the

probability for the occurrence of a molecule in the activated state.

The above equation (1.1) is known as the Arrhenius equation and can written as

$$\ln k = \ln A - \frac{E_a}{RT}$$

or $\qquad 2.303 \log k = 2.303 \log k - \dfrac{E_a}{RT}$

or $\qquad \log k = \log A - \dfrac{E_a}{2.303}\dfrac{1}{RT} \tag{1.2}$
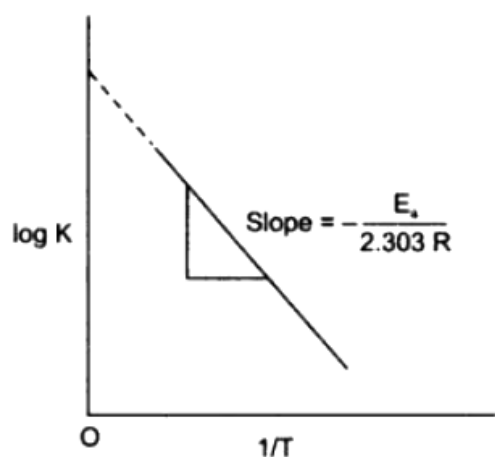
Fig. 1.7: Plot of logk against 1/T to find out activation energy.

Thus, a plot of logk against 1/T should give a straight line with negative slope, in which

$$\text{Slope} = -\frac{E_a}{2.303R} \quad \text{and intercept} = \log A \tag{1.3}$$

1.9 Review on the coordination chemistry of lanthanides with biological ligands

Rare earth (RE) elements, which include the lanthanides, yttrium, and scandium, are vital components for a wide variety of cutting-edge technologies. These technologies range from the permanent magnets found in wind turbines and electric car batteries to lasers, phosphors, and medical imaging agents. The spectral and magnetic characteristics of lanthanide coordination chemistry have increased dramatically as a result of these ions' many advantageous physical qualities. With the increasing use of lanthanide probes in a variety of biological activities involving Ca^{+2} and Mg^{+2} ions [87,88], lanthanide coordination chemistry in aqueous and non-aqueous solutions enters a new era.

Judd [16] reported on the optical absorption intensities of rare-earth ions and observed that electric dipole transitions within the 4f – shell of a rare-earth ion are allowed if its nucleus is not located at a centre of inversion.

Carnall, Fields, and Rajnak [89] correlated experimentally determined band intensities in trivalent lanthanide solution spectra with a theoretical expression deduced by Judd. The spectra were taken in a single medium dilute acid solution and ranged from 6000 to 50,000 cm^{-1} in most cases. They had also discovered how the intensity parameters varied.

Bukietynka and Mondry [90] studied the spectral properties of Nd^{3+}-EDTA solutions at various Nd^{3+} and EDTA concentrations over a wide pH range. The oscillator strength values of the hypersensitive $^{4}G_{7/2}$, $^{4}G_{5/2} \leftarrow ^{4}I_{9/2}$ transitions, as well as the Judd-Ofelt intensity parameter, were analysed to investigate the formation and type of bonding in the Nd^{3+}-EDTA species. The correlation of these results with NMR and kinetic data suggested a relatively complete model of the Nd-EDTA co-ordination.

Misra et al. [91] proposed a modified method for evaluating spectral parameters of 4f -4f transitions in Pr(III) and Nd(III) complexes (i.e., energy interaction, bonding, nephelauxetic, oscillator strength, and Judd-Ofelt parameters).

Misra and Somerer [39] investigated the ligand-mediated pseudohypersensitivity of the Pr(III) transitions $^3H_4 \rightarrow {}^3P_2$, $^3H_4 \rightarrow {}^3P_1$, $^3H_4 \rightarrow {}^3P_0$, and $^3H_4 \rightarrow {}^1D_2$ in solution media. They reported that using absorption difference, comparative absorption spectrophotometry, and quantitative analysis of 4f-4f spectra of Pr(III) complexes with ligands with varying structural features and binding capabilities, such transitions exhibit significant intensification as well as wide variation in oscillator strength. Because they do not adhere to the selection rule, these transitions cannot be considered hypersensitive. They had also examined the solution spectra of 173 species and reported the high sensitivity of the Pr(III) species transitions, which they had termed 'Ligand Mediated Pseudohypersensitivity'. Peacock [92] analysed the sensitivities of computed Judd-Ofelt parameters to the particular transition employed, concluding that a separate value of T_2 must be associated with each hypersensitive transition.

Jerrico et al. [93] examined the behaviour of the phenomenological 4f-4f intensity parameters in compounds of the Nd^{3+} ion with Amino acids (glycine, L-Aspartic acid, L-glutamic acid, L-histidine, DL-malic acid, and Aspartame) in aqueous solution, as a function of the pk values and partial charges on the oxygen of the carboxylate groups of these molecules. They discovered that the intensity of the hypersensitive $^4I_{9/2} \rightarrow {}^4G_{5/2}$, $^4G_{7/2}$ transitions rises with increasing pH values up to about 5.4.

Debecca et al. [94] reported on the absorption spectral analysis of 4f-4f transitions for the interaction of Pr(III) with DL-valine, L-leucine, L-hydroxyproline, DL-alanine, L(+) arginine, and β-alanine in aqueous and aqueous and aquated organic solvent. The addition of ligand causes a red shift in all energy bands, but the intensity data undergoes substantial changes.

Indira et al. [95] investigated 4f-4f transitions for the interaction of Nd(III) with various diols (butane 1, 4-diol, butene 1, 4-diol, and butyne 1, 4-diol) using intensity difference and comparative absorption spectrophotometric technique in DMF and

Methanol, as well as in equimolar mixtures of DMF + CH_3CN, DMF + CH_3OH. The correlations between oscillator strength (Pobs) and T_λ parameters demonstrate the involvement of π-electron density in the complexation of diols with Nd(III). The existence of single, double, and triple bonds in diols affects the energies and oscillator intensity of these 4f-4f absorption spectral bands of Nd(III) diols in DMF solvent. It has been discovered that the complexation sequence of the three diols is butanediol < butenediol < butynediol.

Mehta et al. [96] examined heterobimetallic complexation of lysozyme (HEW) with hard metal ions Pr(III)/Nd(III) and soft metal ion Zn(II) using absorption difference and comparative absorption spectroscopy involving 4f-4f transitions in aquated organic solvents. They recorded the comparative absorption spectra of Pr(III) /Nd(III) in aqueous and organic solvents at pH 0.6, 1.4, 2.0, 4.0, and 6.0, and computed intensity parameters from the observed 4f-4f bands using partial and multiple regression analysis.

Khan and Iftikhar [97] investigated the absorption spectra for the mixed-ligand complexes of Pr^{3+}, Nd^{3+}, Ho^{3+}, and Er^{3+} containing ligands having nitrogen donors in different solvents (pyridine, DMSO, DMF and methanol) In terms of ligand (solvent) structures and ligand co-ordination properties, they rationalised changes in oscillator strength and band shapes with regard to solvent type. Pyridine has been determined to be the most effective solvent for enhancing 4f-4f intensity and is the strongest ligand in a Nephelauxetic sense.

Z.M. Wang et al. [98] also reported spectroscopic investigation of lanthanide (III) complexes with aliphatic dicarboxylic acids.

Binnemans et al [99] studied the spectroscopic behaviour of lanthanide(III) coordination compounds with Schiff base (substituted salicyaldimines). Nd(III), Ho(III), and Er(III) complex absorption spectra were observed in chloroform. The transitions between states of the complexes were notably hypersensitive. The enhancement of

intensity has been linked to the highly polarizable ligands and the low symmetry site around lanthanide ions.

Mehta and Shah [100] investigated the absorption difference spectroscopy of lysozyme with Nd(III) in the presence of Zn(II), Cd(II), Ca(II), and Mg(II) involving the 4f transition at varied pH(2,4,6) and in different solvents methanol, dimethylformanide, acetonitrile, and t-butanol. It has been determined that the binding capacity of lysozyme is greater at pH 2 than at pH 4 and 6, because lysozyme is known to have biological activities in a moderately acidic media, but the higher pH range does not contribute significantly to binding.

Gagnani et al. [101] investigated the kinetics of the complexation of Zn^{2+} with $Er_2(GSH)_2(H_2O)_4$ (GSH = reduced glutathione) complexes by using comparative absorption spectroscopy including 4f-4f transitions. Following five 4f-4f sensitive transitions of Er^{3+}, $^4I_{15/2} \rightarrow ^4G_{11/2}, ^4F_{7/2}, ^2H_{11/2}, ^4F_{9/2}$, and $^4I_{11/2}$ in water and equimolar mixture of DMF and water, they conducted a kinetic investigation at 30^oC. On the basis of kinetic studies conducted by tracking the changes in the intensity absorbance (molar absorptivity) and intensity parameters (oscillator strength P and Judd-Ofelt T_λ parameter), it was determined that the performance of the five bands was adequately sensitive. The rate of $Er_2(GSH)_2Zn(H_2O)_6$ production was dependent on the concentrations of Zn^{2+} and the complex to the first order.

Ranjana et al. [102] examined the Pr(III)/Nd(III) complex with Gly-Gly by absorption spectroscopy and potentiometric titrations and reported that the complexation reaction has a favourable entropy change with high stability at a Metal-Ligand stoichiometric ratio of 1:1.

Ch. Victory and Rajmuhon Singh [103] employed comparative absorption spectroscopy using 4f-4f transitions to investigate the kinetics and thermodynamic characteristics of simultaneous coordination of uracil with Nd(III) and Zn(II). They

showed that the complexation reaction rate increases with temperature and that simultaneous coordination is an endothermic process.

Bendangsenla et al. [104] studied the interactions of Pr(III) with Adenosine and Adenosinetriphosphate (ATP) in various organic solvents (CH$_3$CN, CH$_3$OH, DMF, and 1,4-dioxane) by means of absorption spectral analyses, measuring the energy interaction and intensity parameters. It was reported that the intensity of absorption bands in the absorption spectra of praseodymium complexes exhibited substantial variations. The intensification of the bands was interpreted as a result of an increase in the interaction between 4f-orbitals and ligand orbitals. They found that DMF is the favoured solvent, while methanol is the least preferred.

Moaienla et al.[105,106] conducted solution absorption spectral investigation of the interaction of Pr(III)/Nd(III) with L-phenylalanine, L-glycine, L-alanine, and L-aspartic acid in organic solvents with and without Ca(II). For the examination of the interactions between the lanthanide metal and the ligands, spectral characteristics including energy interaction and intensity parameters were assessed. Analysis of the spectral parameters could reveal the binding properties of Ln(III) with various ligands. Ca(II) is also implicated in the multimetal complexation of Pr(III)/Nd(III) with the various amino acids, according to their research. Additional thermodynamic and kinetic investigation of the complexation of Nd(III):glycine with Ca(II) ion revealed that the complexation rate increased with time and temperature. The reaction is shown to be endothermic and favourable in solution.

Bendangsenla et al.[107] calculated spectral parameters for the interaction of Ln(III) with nucleic acid by employing 4f-4f transition spectra as a probe in various solvents. They analysed the structural conformations, chemical kinetics, and thermodynamic behaviour of the lanthanide complex using the computed parameters. Their research revealed that ligands bind to Ln(III) in solution form. The metal-ligand bond was found to be covalent. The absorbance and intensity increased with time and temperature,

according to studies of kinetics. It was observed that the complexation process is endothermic and entropy-driven. The complexation's Gibbs free energy suggested that the reaction is spontaneous and favourable in solution.

Ramananda et al. [108] analysed the absorption spectra of the interaction between Pr(III) and L-tryptophan system exhibiting 4f–4f transitions in the presence and absence of Zn(II) using different aquated organic solvents such as methanol, dioxane, acetonitrile, and N,N-dimethylformamide (DMF), and the same were also analysed for the equimolar mixtures (1:1) They found that DMF was the most effective solvent for increasing the 4f–4f electric dipole intensity.

1.10 Scope and objectives of the present study

Understanding the behaviours of lanthanide ions in biological systems has become ever more essential as a result of the widespread use of lanthanide elements in a variety of fields bimolecular reactions. Consequently, the purpose of this study is to investigate the potential of these interesting lanthanides as spectral and structural probes in biochemical reactions that are vital to human metabolism. Since solution spectral studies involving lanthanide complexes (lanthanide metallo-organic compounds, lanthanide based molecular organic precursors, lanthanide complexes as catalysts in a number of synthetic processes, and lanthanide complexes with biological molecules) are extremely important due to the fact that spectral monitoring can provide extremely relevant information about the mechanism and reaction pathways. Consequently, quantitative absorption spectrum analysis of lanthanide compounds becomes incredibly important. Even if the absolute values of certain spectral parameters may not be precise, the trends of their variation during the processes provide valuable information.

Praseodymium and Neodymium were selected from the lanthanides based on their isomorphous properties with the Group II elements of the periodic table of elements (Ca^{2+},

Mg^{2+} and Zn^{2+}); their ions have optimal radii for effective isomorphic substitution in biomolecules containing the elements of Group II (for the present study Mg^{2+} was selected), simulating the interaction between the metabolites and Mg^{2+} that occurs in vivo intracellularly. However, Mg^{2+}, being diamagnetic, are undetectable to optical and magnetic spectroscopy techniques. Since Ln^{3+} are paramagnetic and spectroscopically active, the isomorphous substitution of Mg^{2+} by Ln^{3+} can be a very valuable addition for understanding the interaction of amino acids with Mg^{2+}.

Although Solution Absorption Spectral Analysis involving 4f-4f transition provides less accurate information than that obtained by Crystal Absorption Spectral Analysis, due to the fact that in solution, a number of processes such as dissociation, association, isomerization, etc., are of common occurrence, and as a result, more than one species can occur, resulting in an absorption spectrum that is an average spectrum of all the species that are present in equilibrium. However, the Linear Curve Analyses and the Individual Absorption Band Gaussian Curve Analysis greatly refine the spectral data that was obtained. The solution system is employed in studying biochemical reactions, as well as in the monitoring of the behaviour of contrast enhancing biological drugs and in following the kinetics of the simultaneous complexation of two or three chemically distinct metal ions to biomolecular polydentate ligands. This has resulted in an expansion of the investigation into these fields. Even though the solution spectral analysis may not give very distinguishable quantitative data, it does provide useful data for structural determination, mechanistic studies, and for creating the optimal experimental condition required for product formation of some desired pre-determined configurations with advanced technology adopting much better resolution of solution spectral 4f-4f bands. Quantitative absorption spectroscopy has the potential to be an effective tool for investigations including mechanistic processes, diagnostic procedures, and condensation. Since less is known about the spectra of the 4f-4f transition than the d-d transition, theoretical analysis

of the 4f-4f transition spectra has become one of the focus areas. Absorption spectrophotometry has shown to be an exceptionally effective technique for researching lanthanide chemistry, especially in solutions both in aqueous and non-aqueous environments, due to the presence of quite detailed internal f-electron transition spectra in most of the lanthanides. The strength of the Ln^{3+} ligand interaction, geometry of the coordination polyhedron, ligand structure, and chelate-solvent interactions can all be determined from the absorption spectra for the 4f-4f transitions of the Ln^{3+} ions. Absorption spectra containing 4f-4f in lanthanides are rarely used to follow the kinetics of a chemical reaction. Because of this, kinetic studies, including thermodynamic parameters, will be conducted in an effort to comprehend the rate of reaction of the simultaneous complexation of Pr^{3+} ion involving amino acids. The main scheme will be as follows:

- to calculate intensity parameters [oscillator strength(P) and Judd-Ofelt electric dipole intensity (T_λ, $\lambda=2,4,6$) parameters] and the energy interaction parameters [Slater-Condon (F^k), Lande spin orbit coupling constant (ξ_{4f}), Racah energy (E^k, k = 2,4,6), Nephelauxetic ratio (β), bonding parameter ($b^{1/2}$) and percentage covalency (δ)] of Pr^{3+}/Nd^{3+} complexes with selected amino acids in presence and absence of Mg^{2+} in different aquated organic solvents like dimethyl formamide, acetonitrile, 1,4-Dioxane and methanol at 298K.

- to calculate the intensity parameters and the energy interaction parameters for the complexation of Pr^{3+}/Nd^{3+} with selected amino acids in presence and absence of Mg^{2+} at different pH (pH = 2, 4 and 6) in aquated dimethylformamide solvent at 298 K.

- to study the kinetics for the complexation of Pr^{3+} with selected amino acids in presence of Mg^{2+} in DMF medium at different temperatures: 298K, 303K, 308K, 313K and 318K.

- to determine the rate of reaction from the changes in the intensity of hypersensitive transitions of Pr^{3+}, to calculate the activation energy (E_a) and thermodynamic parameters like ΔH^o, ΔS^o and ΔG^o for the complexation of Pr^{3+} with selected amino acids in presence of Mg^{2+}.

References

[1]   T. Gray, The Elements: A Visual Exploration of Every Known Atom in the Universe, New York: Black Dog & Leventhal Publishers, New York, 2009.

[2]   T. Coplen, N.E. Holden, The Periodic Table of the Elements, *Chem. Int.* **26** (2004) 8–9. https://doi.org/doi:10.1515/ci.2004.26.1.8.

[3]   H.C. Aspinall, Chemistry of the f-Block Elements, 1st ed., Routledge, London, 2018. https://doi.org/10.1201/9781315139258.

[4]   S.T. Liddle, D.P. Mills, L.S. Natranjan, The Lanthanides And Actinides: Synthesis, Reactivity, Properties And Applications, World Scientific Publishing Europe Ltd., London, 2022.

[5]   J.C.G. Bünzli, Review: Lanthanide coordination chemistry: From old concepts to coordination polymers, *J. Coord. Chem.* **67** (2014) 3706–3733. https://doi.org/10.1080/00958972.2014.957201.

[6]   R.W. Hakala, Letters, *J. Chem. Educ.* **29** (1952) 581. https://doi.org/10.1021/ed029p581.2.

[7]   N.N. Greenwood, A. Earnshaw, Chemistry of the Elements, 2nd ed., Butterworth-Heinemann, Oxford, 2001.

[8]   K.S. Pitzer, Relativistic Effects on Chemical Properties, *Acc. Chem. Res.* **12** (1979) 271–276. https://doi.org/10.1021/ar50140a001.

[9]   H. Schmidbaur, Comprehensive Coordination Chemistry. The Synthesis, Reactions, Properties and Applications of Coordination Compounds, Pergamon Press, Oxford, 1989. https://doi.org/10.1002/ange.19891010642.

[10]   J.D. Lee, A new Concise Inorganic Chemistry, 3rd ed., Chapman & Hall, UK, 1977.

[11]   S. V. Eliseeva, J.C.G. Bünzli, Rare earths: Jewels for functional materials of the future, *New J. Chem.* **35** (2011) 1165–1176. https://doi.org/10.1039/c0nj00969e.

[12]   R.E. Kirk, D.F. Othmer, C.A. Mann, Encyclopedia of Chemical Technology. Vol. II, *J. Phys. Colloid Chem.* **53** (2000) 591. https://doi.org/10.1021/j150469a016.

[13]   G.H. Dieke, H.M. Crosswhite, The Spectra of the Doubly and Triply Ionized Rare Earths, *Appl. Opt.* **2** (1963) 675–686. https://doi.org/10.1364/ao.2.000675.

[14]   T. Moeller, J.C. Brantley, Rare Earths, *Anal. Chem.* **22** (1950) 433–441. https://doi.org/10.1021/ac60039a014.

[15]   J.-C.G. Bünzli, S. V. Eliseeva, Basics of Lanthanide Photophysics, in: P. Hänninen, H. Härmä (Eds.), Lanthan. Lumin., Springer Berlin, Heidelberg, 2010: pp. 1–45. https://doi.org/10.1007/4243_2010_3.

[16] B.R. Judd, Optical absorption intensities of rare-earth ions, *Phys. Rev.* **127** (1962) 750–761. https://doi.org/10.1103/PhysRev.127.750.

[17] G.S. Ofelt, Intensities of Crystal Spectra of Rare-Earth Ions, *J. Chem. Phys.* **37** (1962) 511–520. https://doi.org/10.1063/1.1701366.

[18] C. Görller-Walrand, K. Binnemans, Chapter 167 Spectral intensities of f-f transitions, *Handb. Phys. Chem. Rare Earths.* **25** (1998) 101–264. https://doi.org/10.1016/S0168-1273(98)25006-9.

[19] P.A. Tanner, Spectra, Energy Levels and Energy Transfer in High Symmetry Lanthanide Compounds, in: Top. Curr. Chem., Springer, Berlin, 2012: pp. 167–278. https://doi.org/10.1007/b96863.

[20] G. Blasse, The influence of charge-transfer and rydberg states on the luminescence properties of lanthanides and actinides, *Spectra Chem. Interact.* **26** (1976) 43. https://doi.org/10.1007/bfb0116577.

[21] G. Blasse, Vibronic transitions in rare earth spectroscopy, *Int. Rev. Phys. Chem.* **11** (1992) 71–100. https://doi.org/10.1080/01442359209353266.

[22] G. Blasse, B.C. Grabmaier, A General Introduction to Luminescent Materials, in: Lumin. Mater., Springer, Berlin, 1994: pp. 1–9. https://doi.org/10.1007/978-3-642-79017-1_1.

[23] M. Tanaka, G. Nishimura, T. Kushida, Contribution of J mixing to the 5D0-7F0 transition of Eu3+ ions in several host matrices, *Phys. Rev. B.* **49** (1994) 16917. https://doi.org/10.1103/PhysRevB.49.16917.

[24] M. Tanaka, T. Kushida, J-mixing effect on the vibronic spectra of Eu3+ ions, *J. Alloys Compd.* **93** (1993) 183–185. https://doi.org/10.1016/0925-8388(93)90343-L.

[25] B.G. Wybourne, Optical Properties of Ions in Crystals, in: H.M. Crosswhite, H.M. Moos (Eds.), Wiley Interscience, New York, 1996.

[26] M.C. Downer, G.W. Burdick, D.K. Sardar, A new contribution to spin-forbidden rare earth optical transition intensities: Gd3+ and Eu3+, *J. Chem. Phys.* **89** (1988) 1787. https://doi.org/10.1063/1.455125.

[27] G.W. Burdick, M.F. Reid, Burdick and Reid reply, *Phys. Rev. Lett.* **71** (1993) 3892. https://doi.org/10.1103/PhysRevLett.71.3892.

[28] D.M. Gruen, C.W. Dekock, Absorption spectra of gaseous NdBr3 and NdI3, *J. Chem. Phys.* **45** (1966) 455. https://doi.org/10.1063/1.1727588.

[29] D.M. Gruen, C.W. DeKock, R.L. McBeth, Electronic Spectra of Lanthanide Compounds in the Vapor Phase, in: P.R. Fields, T. Moeller (Eds.), Lanthanide/Actinide Chem., 1st ed., American Chemical Society, Washington, 1967: pp. 102–121. https://doi.org/10.1021/ba-1967-0071.ch008.

[30] L.I. Katzin, Absorption and circular dichroic spectral studies of europium(III) complexes with sugar acids and amino acids, with remarks on "hypersensitivity," *Inorg. Chem.* **8** (1969) 1649–1654. https://doi.org/10.1021/ic50078a015.

[31] T. Moeller, J.C. Brantley, Observations on the Rare Earths. LVIII. Reaction between Neodymium and Ethylenediaminetetraacetate Ions in Aqueous Solution, *J. Am. Chem. Soc.* **72** (1950) 5447–5451. https://doi.org/10.1021/ja01168a022.

[32] T. Moeller, D.E. Jackson, Rare Earths. Separation Extraction of Certain Rare Earth Elements as 5,7-Dichloro-8-quinolinol Chelates, *Anal. Chem.* **22** (1950) 1393–1397. https://doi.org/10.1021/ac60047a012.

[33] J. Chrysochoos, A. Evers, Effect of the primary and secondary solvation spheres of Eu3+ upon the electric-quadrupole transitions ($\Delta J = 2$), *Chem. Phys. Lett.* **18** (1973) 115–119. https://doi.org/10.1016/0009-2614(73)80353-7.

[34] J. Chrysochoos, Dependence of the intensity of the absorption bands of Eu3+ in solution upon the anions present, *J. Chem. Phys.* **60** (1974) 1110. https://doi.org/10.1063/1.1681121.

[35] D.G. Karraker, Hypersensitive transitions of six-, seven-, and eight-coordinate neodymium, holmium, and erbium chelates, *Inorg. Chem.* **6** (1967) 1863–1868. https://doi.org/10.1021/ic50056a022.

[36] G.R. Choppin, Speciation of trivalent f elements in natural waters, *J. Less-Common Met.* **126** (1986) 307. https://doi.org/10.1016/0022-5088(86)90315-2.

[37] M.T. Devlin, E.M. Stephens, M.F. Reid, F.S. Richardson, Model Calculations for the Intensity Parameters of Nine-Coordinate Erbium(III) Complexes of Trigonal Symmetry, *Inorg. Chem.* **26** (1987) 1208–1211. https://doi.org/10.1021/ic00255a007.

[38] M.T. Devlin, E.M. Stephens, F.S. Richardson, Comparison of Electric-Dipole Intensity Parameters for a Series of Structurally Related Neodymium, Holmium, and Erbium Complexes in Aqueous Solution. Theory and Experiment, *Inorg. Chem.* **27** (1988) 1517–1524. https://doi.org/10.1021/ic00282a003.

[39] S.N. Misra, S.O. Sommerer, Absorption Spectra of Lanthanide Complexes in Solution, *Appl. Spectrosc. Rev.* **26** (1991) 151–202. https://doi.org/https://doi.org/10.1080/05704929108050880.

[40] R.D. Peacock, Structure and Bonding, Springer, New York, 1975.

[41] S.N. Misra, S.B. Mehta, Ligand-Mediated Pseudohypersensitivity of Some 4f–4f Transitions in Neodymium(III) Interaction with Fluorinated Nucleic Acid Components, *Bull. Chem. Soc. Jpn.* **64** (1991) 3653–3658. https://doi.org/10.1246/bcsj.64.3653.

[42] S. Misra, Lanthanoid (III) ions as structural probe in biochemical reactions, *Proc. Indian Natn. Sci. Acad.* **60** (1994) 637–637.

[43] S.N. Misra, Energy interaction parameters and intensity analysis of praseodymium and neodymium complexes, *J. Sci. Ind. Res. (India).* **44** (1985) 366–375.

[44] S.N. Misra, M. Indira Devi, C.M. Suveerkumar, K.M. Suma, Electric dipole intensity parameters for a series of structurally related praseodymium(III) and neodymium(III) complexes and unusual sensitivities of some 4f-4f transitions, *Rev. Inorg. Chem.* **14** (1994) 347–362. https://doi.org/10.1515/REVIC.1994.14.5.347.

[45] C. Huang, Rare Earth Coordination Chemistry, Fundamentals and Applications, John Wiley & Sons, Ltd, Singapore, 2010.

[46] V.S. Sastri, J.C. Bünzli, V.R. Rao, G.V.S. Rayudu, J.R. Perumareddi, Modern Aspects of Rare Earths and Their Complexes, 1st ed., Elsevier Science, Amsterdam, 2003. https://doi.org/10.1016/B978-0-444-51010-5.X5014-7.

[47] K.B. P. Thyssen, Handbook on the Physics and Chemistry of Rare Earths, 41st ed., Elsevier Science B.V., Amsterdam, 2011.

[48] Z. Zheng, R. Wang, Rare Earth Coordination Chemistry, Fundamentals and Applications, John Wiley & Sons, Ltd, Singapore, 2010.

[49] T. Yamase, Handbook on the Physics and Chemistry of Rare Earths, Elsevier B.V., Amsterdam, 2009.

[50] K.A. Gschneidner Jr., J.-C.G. Bünzli, V.K. Pecharsky, eds., Handbook on the Physics and Chemistry of Rare Earths, in: Z. Zheng, Elsevier B.V., Amsterdam, 2010: pp. 297–356.

[51] R. Wang, Z. Zheng, Rare Earth Coordination Chemistry, Fundamentals and Applications, John Wiley & Sons, Ltd, Singapore, 2010.

[52] Behrsing, Thomas, G.B. Deacon, P.C. Junk, The chemistry of rare earth metals, compounds, and corrosion inhibitors, in: Rare Earth-Based Corros. Inhib., Woodhead Publishing, 2014: pp. 1–37.

[53] F. Arnaud-Neu, Solution chemistry of lanthanide macrocyclic complexes, *Chem. Soc. Rev.* **23** (1994) 235–241. https://doi.org/10.1039/CS9942300235.

[54] T. Moeller, D.F. Martin, L.C. Thompson, R. Ferrus, G.R. Feistel, W.J. Randall, The Coordination Chemistry of Yttrium and the Rare Earth Metal Ions, *Chem. Rev.* **65** (1965) 1–50. https://doi.org/10.1021/cr60233a001.

[55] C.M. Dobson, R.J.P. Williams, A. V. Xavier, Ethylenediaminetetra-acetato-lanthanate(III), -praesodimate(III), -europate(III), and -gadolinate(III) complexes as nuclear magnetic resonance probes of the molecular conformations of adenosine 5′-monophosphate and cytidine 5′-monophosphate in solution, *J. Chem. Soc. Dalt. Trans.* (1974) 1762–1764. https://doi.org/10.1039/DT9740001762.

[56] A.D. Sherry, P.P. Yang, L.O. Morgan, ChemInform Abstract: Separation of contact and pseudocontact contributions to carbon-13 lanthanide induced shifts in non-axially-symmetric lanthanide ethylenediaminetetraacetate chelates, *Chem. Informationsd.* **102** (1980) 5755–5759. https://doi.org/10.1002/chin.198047061.

[57] P. Caravan, P. Mehrkhodavandi, C. Orvig, Cationic Lanthanide Complexes of N,N′-Bis(2-pyridylmethyl)ethylenediamine-N,N′-diacetic Acid (H2bped), *Inorg. Chem.* **36** (1997) 1316–1321. https://doi.org/10.1021/ic9613016.

[58] Y.M. Wang, Y.J. Wang, Y.L. Wu, Synthesis, stability and nuclear magnetic resonance studies for the complexation of trivalent lanthanides, Ca2, Cu2 and Zn2 by N,N′-bis (amide) derivatives of ethylenedinitrilotetraacetic acid, *Polyhedron.* **18** (1998) 109–117. https://doi.org/10.1016/S0277-5387(98)00273-3.

[59] B. Singh, U. Srivastava, 4-(2-Thiazolyl)-1-(2-Hydroxybenzaldehyde)Thiosemicarbazone as a Chelating Ligand: Complexes with Oxovanadium(IV), Cobalt(II), Nickel(II), Copper(II), Cadmium(II) and Mercury(II), *Synth. React. Inorg. Met. Chem.* **19** (1989) 279–291. https://doi.org/10.1080/00945718908048069.

[60] E. Nieboer, The lanthanide ions as structural probes in biological and model systems, in: Rare Earths, Springer, Berlin, 2007. https://doi.org/10.1007/bfb0116554.

[61] R.B. Martin, F.S. Richardson, Lanthanides as probes for calcium in biological systems, *Q. Rev. Biophys.* **12** (1979) 181–209. https://doi.org/10.1017/S0033583500002754.

[62] R. Prados, L.G. Stadtherr, H. Donato, R.B. Martin, Lanthanide complexes of amino acids, *J. Inorg. Nucl. Chem.* **36** (1974) 689–693. https://doi.org/10.1016/0022-1902(74)80135-1.

[63] D. R. Williams, Biographic Pharmacy: Metal Complexation and Metal Side Effects in Drug Design in Principles of Drug Design, Butterworth, London, 1988.

[64] S.P. Sinha, Complexes of the rare earths, Pergamon Press, London, 1996.

[65] L.I. Katzin, E. Gulyas, Absorption and Circular Dichroism Spectral Studies of Chelate Complexes of Praseodymium(III) with α-Amino Acids, *Inorg. Chem.* **7** (1968) 2442–2446. https://doi.org/10.1021/ic50069a051.

[66] A.D. Sherry, C. Yoshida, E.R. Birnbaum, D.W. Darnall, NMR-untersuchung der wechselwirkung von neodym (iii) mit aminosaeuren und carbonsaeuren, ein verschiebungsreagenz, *Chem. Informationsd.* **4** (1973) no-no.

[67] S.P. Tanner, G.R. Choppin, Lanthanide and Actinide Complexes of Glycine. Determination of Stability Constants and Thermodynamic Parameters by a Solvent Extraction Method, *Inorg. Chem.* **7** (1968) 2046–2048. https://doi.org/10.1021/ic50068a017.

[68] R. Wang, H. Liu, M.D. Carducci, T. Jin, C. Zheng, Z. Zheng, Lanthanide coordination with α-amino acids under near physiological pH conditions: Polymetallic complexes containing the cubane-like [Ln4(μ3-OH)4]8+ cluster core, *Inorg. Chem.* **40** (2001) 2743–2750. https://doi.org/10.1021/ic001469y.

[69] A.E. Martell, R.D. Hancock, Metal Complexes in Aqueous Solutions, Plenum Press, New York, 1996.

[70] Z. Zheng, Ligand-controlled self-assembly of polynuclear lanthanide—oxo/hydroxo complexes: From synthetic serendipity to rational supramolecular design, *Chem. Commun.* (2001) 2521–2529. https://doi.org/10.1039/b107971a.

[71] D. Elmore, G.. Barrett, Amino Acids and Peptides, Cambridge University Press, UK, 1998.

[72] P.E. Wischmeyer, Clinical Applications of L-Glutamine: Past, Present, and Future, *Nutr. Clin. Pract.* **18** (2003) 377–385. https://doi.org/10.1177/0115426503018005377.

[73] M. Adeva-Andany, G. Souto-Adeva, E. Ameneiros-Rodríguez, C. Fernández-Fernández, C. Donapetry-García, A. Domínguez-Montero, Insulin resistance and glycine metabolism in humans, *Amino Acids*. **50** (2018) 11–27. https://doi.org/10.1007/s00726-017-2508-0.

[74] R. Dalangin, A. Kim, R.E. Campbell, The role of amino acids in neurotransmission and fluorescent tools for their detection, *Int. J. Mol. Sci.* **21** (2020) 6197. https://doi.org/10.3390/ijms21176197.

[75] W.M. Pardridge, W.H. Oldendorf, Kinetic analysis of blood-brain barrier transport of amino acids, *BBA - Biomembr.* **40** (1975) 128–136. https://doi.org/10.1016/0005-2736(75)90347-8.

[76] A. Slominski, I. Semak, A. Pisarchik, T. Sweatman, A. Szczesniewski, J. Wortsman, Conversion of L-tryptophan to serotonin and melatonin in human melanoma cells, *FEBS Lett.* **511** (2002) 1873–3468. https://doi.org/10.1016/S0014-5793(01)03319-1.

[77] F. Yoshizawa, Effects of Leucine and Isoleucine on Glucose Metabolism, in: Branched Chain Amin. Acids Clin. Nutr., 2015: pp. 63–73. https://doi.org/10.1007/978-1-4939-1923-9_6.

[78] B.A Levine, R.J.. William, The chemistry of calcium ion and its biological relevance, in the role of calcium in Biological System, CRC Press, Boca Raton, 1982.

[79] H Einspahr, C.. Bugg, Crystal structure studies of calcium complexes and implications for biological system, in metal ions in biological system, Marcel Dekker, New York, 1984.

[80] R.B Martin, Structural chemistry of calcium: lanthanides as probes, in calcium Biology, Wiley, New York, 1983.

[81] Z. Fishelson, H.J. Müller-Eberhard, The C3/C5 convertase of the alternative pathway of complement: Stabilization and restriction of control by lanthanide ions, *Mol. Immunol.* **20** (1983) 309–315. https://doi.org/10.1016/0161-5890(83)90070-6.

[82] J.M. Brewer, Specificity and mechanism of action of metal ions in yeast enolase, *FEBS Lett.* **182** (1985) 8–14. https://doi.org/10.1016/0014-5793(85)81143-1.

[83] G.E. Smolka, E.R. Birnbaum, D.W. Darnall, Rare Earth Metal Ions as Substitutes for the Calcium Ion in Bacillus subtilis α-Amylase, *Biochemistry*. **10** (1971) 4556–4561. https://doi.org/10.1021/bi00800a033.

[84] C.G. Dos Remedios, J.A. Barden, Effects of Gd(III) on G-actin: Inhibition of polymerization of G-actin and activation of myosin ATPase activity by Gd-G-actin, *Biochem. Biophys. Res. Commun.* **77** (1977) 1339–1346. https://doi.org/10.1016/S0006-291X(77)80126-5.

[85] A. Frost, R. Pearson, Kinetics and Mechanism, Second Edition, *J. Phys. Chem.* **65** (1961) 384. https://doi.org/10.1021/j100820a601.

[86] Keith J. Laidler, Chemical Kinetics, 3rd ed., Anand Sons, Delhi, 2005.

[87] J. GLASEL, Lanthanide ions as nuclear magnetic resonance chemical shift probes in biological systems, *Curr. Res. Top. Bioinorg. Chem. Vol. 18*. **18** (2009) 383.

[88] S.N. Misra, G. Ramchandriah, M.A. Gagnani, R.S. Shukla, M.I. Devi, Absorption spectral studies involving 4f-4f transitions as structural probe in chemical and biochemical reactions and compositional dependence of intensity parameters, *Appl. Spectrosc. Rev.* **38** (2003) 433–493. https://doi.org/10.1081/ASR-120026330.

[89] W.T. Carnall, P.R. Fields, K. Rajnak, Electronic Energy Levels of the Trivalent Lanthanide Aquo Ions. II. Gd^{3+}, *J. Chem. Phys.* **49** (1968) 4443–4446. https://doi.org/10.1063/1.1669894.

[90] K. Bukietyńska, A. Mondry, Spectroscopy and structure of neodymium complexes with EDTA, *Inorganica Chim. Acta*. **110** (1985) 1–5.

[91] S.N. Misra, Interaction of some fluorinated nucleic acid components with praseodymium: An absorption spectral approach, *Indian J. Biochem. Biophys.* (1990).

[92] R.D. Peacock, The sensitivity of computed Judd-Ofelt parameters to the particular transitions used, *Chem. Phys. Lett.* **16** (1972) 590–592.

[93] S. Jericó, C.R. Carubelli, A.M.G. Massabni, E.B. Stucchi, S.R.D.A. Leite, O. Malta, Spectroscopic study of the interaction of Nd3+ with amino acids: Phenomenological 4f-4f intensity parameters, *J. Braz. Chem. Soc.* **9** (1998) 487–493. https://doi.org/10.1590/S0103-50531998000500014.

[94] H.D. Devi, C. Sumitra, T.D. Singh, N. Yaiphaba, N.M. Singh, N.R. Singh, Calculation and Comparison of Energy Interaction and Intensity Parameters for the Interaction of Nd(III) with DL-Valine, DL-Alanine and β-Alanine in Presence and Absence of Ca2+/Zn2+ in Aqueous and Different Aquated Organic Solvents Using 4f-4f Transitio, *Int. J. Spectrosc.* **2009** (2009) 784305.

[95] M.I. Devi, Electric-dipole intensity of nona-coordinated complexes of Nd(III) with diols in non-aqueous solution: Evidence of participation of π-electron density of diols with Nd(III), *Indian J. Chem. - Sect. A Inorganic, Phys. Theor. Anal. Chem.* **43A** (2004) 1692–1695.

[96] J.P. Mehta, P.N. Bhatt, S.N. Misra, An absorption spectral study of Nd(III) with glutathione (reduced), GSH in aqueous and aquated organic solvent in presence and absence of Zn(II), *J. Solid State Chem.* **171** (2003) 175–182. https://doi.org/10.1016/S0022-4596(02)00205-0.

[97] A.A. Khan, K. Iftikhar, Mixed-ligand lanthanide complexes - XI. Absorption spectra and hypersensitivity in the complexes of PrIII, NdIII, HoIII and ErIII in non-aqueous solutions, *Polyhedron.* **16** (1997) 4153–4161. https://doi.org/10.1016/S0277-5387(97)00138-1.

[98] Z.M. Wang, Van de Burgt,; LJ; Choppin, GR, *Inorg. Chim. Acta.* **310** (2000) 248.

[99] K. Binnemans, R. Van Deun, C. Görller-Walrand, S.R. Collinson, F. Martin, D.W. Bruce, C. Wickleder, Spectroscopic behaviour of lanthanide(III) coordination compounds with Schiff base ligands, *Phys. Chem. Chem. Phys.* **2** (2000) 3753–3757.

[100] S.B. Mehta, M.K. Shah, Absorption difference spectroscopy of lysozyme with Nd (III) in presence of Zn(II), Cd(II), Ca(II) and Mg(II) involving 4f-4f transition, *Asian J. Chem.* **14** (2002) 236–242.

[101] M.A. Gagnani, S.K. Hari, S.N. Misra, Comparative absorption spectroscopy involving 4f-4f transitions to complex & compositional dependence of intensity parameters, *J. Solid State Chem.* **4** (2003) 374–383.

[102] N.R. Devi, B. Huidrom, N.R. Singh, Studies on the complexation of Pr(III) and Nd (III) with glycyl–glycine (gly–gly) using spectral analysis of 4f–4f transitions and potentiometric titrations, *Spectrochim. Acta Part A Mol. Biomol. Spectrosc.* **96** (2012) 370–379.

[103] C.V. Devi, N.R. Singh, Comparative absorption spectroscopy involving 4f–4f transitions to explore the kinetics of simultaneous coordination of uracil with Nd (III) and Zn(II) and its associated thermodynamics, *Spectrochim. Acta Part A Mol. Biomol. Spectrosc.* **81** (2011) 296–303.

[104] N. Bendangsenla, M.I. Devi, T. Moaienla, T.D. Singh, Comarative 4f-4f Absorption Spectral Approach to Study the Complexation of Pr(III) with Guanosine and Guanosine Tri Phosphate (GTP) in the Presence and Absence of Ca(II), *Int. J. Basic Appl. Chem. Sci.* **3** (2013) 19–30.

[105] T. Moaienla, T.D. Singh, N.R. Singh, M.I. Devi, Computation of energy interaction parameters as well as electric dipole intensity parameters for the absorption spectral study of the interaction of Pr(III) with l-phenylalanine, l-glycine, l-alanine and l-aspartic acid in the presence and absence of Ca2+, *Spectrochim. Acta - Part A Mol. Biomol. Spectrosc.* **74** (2009) 434–440. https://doi.org/10.1016/j.saa.2009.06.039.

[106] T. Moaienla, N. Bendangsenla, T. David, C. Sumitra, N.R. Singh, M.I. Devi, Spectrochimica Acta Part A : Molecular and Biomolecular Spectroscopy Comparative 4f – 4f absorption spectral study for the interactions of Nd(III) with some amino acids : Preliminary thermodynamics and kinetic studies of interaction of Nd(III): glycine , *Spectrochim. Acta Part A Mol. Biomol. Spectrosc.* **87** (2012) 142–150. https://doi.org/10.1016/j.saa.2011.11.028.

[107] N. Bendangsenla, Computation of Energy, Intensity and Thermodynamic Parameters for the Interaction of Ln(III) with Nucleic Acid: Analysis of Structural Conformations, Chemical Kinetics and Thermodynamic Behaviour through 4f-4f Transition Spectra as Probe, *J. Mater. Sci. Chem. Eng.* **6** (2018) 169.

[108] R. Singh, N. Naorem, P. Singh, N. Mohondas, 4f – 4f Spectral Analysis and Solvent Effect for the Interaction of Pr(III) with l-Tryptophan Using Different Aquated Solvents in the Presence and Absence of Zn (II), *Chem. Africa*. **3** (2020) 171–180. https://doi.org/10.1007/s42250-019-00111-9.

Chapter 2

Absorption spectral analysis for the complexation of Pr(III) with L-Glutamine, L-Threonine, L-Tryptophan and L-Isoleucine in the presence/absence of Mg(II) in different aquated organic solvents and pH using 4f-4f transition spectra as probe

2.1 Introduction

Over the years, lanthanides have become indispensable for several applications ranging from optical technologies, biosciences, modern devices like lasers, displays, telecommunications and nanotechnology owing to their special chemical, optical and magnetic features [1–4]. The use of lanthanides in biological and medical applications has increasingly grown over the years. The basis for such applications mainly stems from their similarities to calcium ions [5]. Historically, most of the research on lanthanides in the field of therapeutics took off since lanthanides resemble Ca^{2+} due to which lanthanide ions have a high affinity for Ca^{2+} sites that are present in biomolecules [6]. This allows Ln(III) ions to act as inhibitors or probes of Ca^{2+}. For this reason as well as the spectroscopic features of lanthanide ions, they have long been used as probes for the binding sites of Ca^{2+} in biomolecules [7–10]. The coordination chemistry of lanthanides plays an emerging role in the understanding of biomolecular reactions. Several studies on the calculation of spectral energy and intensity (Judd-Ofelt intensity, T_{λ} (λ=2, 4, 6) and oscillator strength) parameters have been carried out [10–13]. The semiempirical theory known as the Judd-Ofelt theory has long been used to investigate the oscillator strengths of f-f transitions. The Judd-Ofelt theory says that odd parity force fields cause the oscillator strengths of f-f transitions. Both theoretical and experimental studies of the intensities of Ln(III)

systems have been conducted and explained using the Judd-Ofelt theory [14]. Apart from the conventional method, several new modified approaches of the Judd-Ofelt theory have also been used to successfully evaluate the said parameters of lanthanide systems [15–18].

The following four amino acids were chosen as ligands for the present study: L-Glutamine (L-Gln), L-Threonine (L-Thr), L-Tryptophan (L-Trp), and L-Isoleucine (L-Ile). Out of these four amino acids with the exception of L-glutamine which is non-essential, the remaining three are essential amino acids. L-Glutamine and L-Threonine are hydrophilic, polar, uncharged amino acids whereas L-Tryptophan and L-Isoleucine are hydrophobic, non-polar amino acids. From the selected four amino acids, only L-Tryptophan is aromatic in nature, the other three amino acids are aliphatic. In humans, L-glutamine is both non-essential and conditionally essential, which means that the body can usually produce sufficient amounts of it on its own; however, in certain instances of stress, the body's demand for glutamine increases, and glutamine must be obtained from the diet in order to meet the increased demand.

The chemical structure of all these four amino acids consists of two functional groups i.e., an amino group and a carboxylic group which serve as potential binding sites. In addition to the main metabolic activity (that is biosynthesis of proteins) all these four selected amino acids play vital roles in a wide range of other metabolic processes.

Additionally, we have also incorporated magnesium ions in our study. Magnesium is an endogenous metal ion that is essential for human metabolism as well as other biological functions. Mg(II) on the other hand is diamagnetic and does not emit any spectroscopic signals. As such, the use of Pr(III) which is spectroscopically active to substitute Mg(II) could provide valuable information on the binding nature of Mg(II) with biological molecules.

Most of the intensities of the f-f transitions of Ln(III) are only slightly affected by their surrounding environment. Some of the 4f transitions of Ln(III) ions are however particularly sensitive toward their local environment and exhibit a significant change in oscillator strength values. Compared to independent Ln(III) ions, they are usually found to be more intense. Such types of transitions are known as hypersensitive transitions and have been observed for nearly all Ln(III) ions [19,20]. Hypersensitive transitions obey the Laporte selection rules ($|\Delta S| = 0$, $|\Delta L| \leq 2$, $|\Delta J| \leq 2$). The hypersensitive transition of Pr(III), $^3H_4 \rightarrow {}^3F_2$ obeys the selection rules, but it is found beyond the UV-visible range while the ligand-mediated pseudohypersensitive transitions $^3H_4 \rightarrow {}^3P_2$, $^3P_1$, $^3P_0$ and $^1D_2$ do not. These pseudohypersensitive transitions, which are non-hypersensitive transitions of lanthanide ions that do not follow the selection rules, also exhibit enhanced sensitivity of its intensity and energies when subjected to changes in their surrounding environment. Such transitions whose intensity and energies are influenced by the surrounding ligand are called pseudohypersensitive transitions [21–23].

In this chapter, we report the interaction of Pr(III) with the amino acids, L-Glutamine, L-Threonine, L-Tryptophan and L-Isoleucine with Mg(II) in different organic/aqueous (v/v 50%) solvents and pH levels (2, 4, 6). The Pr(III) interaction with the selected amino acids and Mg(II) has been analysed by evaluating the intensity [oscillator strength and the Judd Ofelt parameter, T_λ (λ=2, 4, 6)] and energy interaction parameters: Slater-Condon (F_k), Racah (E^k), Lande (ξ_{4f}), nephelauxetic ratio (β), bonding ($b^{1/2}$), percent covalency (δ) of the 4f-4f absorption spectra of Pr(III). From the computed parameters, the mode of complexation between Pr(III) and the amino acids ligands in the presence and absence of Mg(II) was studied.

2.2 Experimental: Materials and Method

For the analysis, the chemicals- Praseodymium nitrate hexahydrate (99.99%) was procured from Sigma-Aldrich and L-Glutamine, L-Threonine, L-Tryptophan, L-Isoleucine, and magnesium nitrate hexahydrate (≥98.0%) were procured from HiMedia. The solvents-Dimethylformamide (C_3H_7NO), Dioxane ($C_4H_8O_2$), acetonitrile (CH_3CN), and methanol (CH_3OH) were purchased from HiMedia and used for the analysis.

5 mmol solutions of Pr(III), Pr(III):Ligand (L-Glutamine, L-Threonine, L-Tryptophan and L-Isoleucine), and Pr(III):Ligand:Mg(II) were prepared in various organic/aquated solvents (v/v 50%) using acetonitrile, DMF, dioxane and methanol. For pH studies, the pH level of the prepared solutions was maintained at 2, 4 and 6 using fresh solutions of NaOH and HCl. The UV-Vis absorption spectra of the prepared solutions were recorded in the 400-650 nm range using a PerkinElmer Lambda 365 UV/Vis spectrophotometer.

2.3 Theoretical: Energy Interaction Parameters and Electric Dipole Intensity Parameters

The energy of the spin-orbit interaction, E_{so} for the 4f-4f electronic transitions can be expressed as

$$E_{so} = A_{so}\, \xi_{4f} \tag{1}$$

ξ_{4f} represents the Lande spin-orbit coupling parameter and A_{so} denotes the angular component of the spin-orbit interaction. Wong, using first order approximation presented the following relation for E_j (jth level energy) [24]

$$E_j(F_k,\, \xi_{4f}) = E_{oj}(F_k^0,\, \xi_{4f}) + \frac{\partial E_j}{\partial F_k}\Delta F_K + \frac{\partial E_j}{\partial \xi 4f}\Delta\,\xi_{4f} \tag{2}$$

Here, E_{oj} denotes zero-order energy of the jth level.

The Lande (ξ_{4f}) and Slator-Condon (F_k) parameter values can be obtained from Eq.(3) as

$$\xi_{4f} = \xi_{4f}^0 + \Delta\xi_{4f} \text{ and } F_K = F_k^0 + \Delta F_k \tag{3}$$

ΔEj represents the difference between the values of the observed and zero-order energy. ΔEj is given by,

$$\Delta E_j \; = \Sigma_{k=2,4,6} \; \frac{\partial E_j}{\partial F_k} \Delta F_k + \; \frac{\partial E_j}{\partial \xi_{4f}} \; \Delta \xi_{4f} \tag{4}$$

By using the zero order energy and partial derivatives of Pr(III) ion given by Wong (Table 2.1), the above equation (4.5) can be solved by least square fit technique and the values of $\Delta \xi_{4f}$ and ΔF_k can be found out by using equation (3).

Table 2.1: The zero-order energies and partial derivatives with respect to F_k and ξ_{4f} parameters for Pr(III) [24].

Level	$E_{oj}^{(a)}$	$\dfrac{\delta E_j}{\delta F_2}$	$\dfrac{\delta E_j}{\delta F_4}$	$\dfrac{\delta E_j}{\delta F_6}$	$\dfrac{\delta E_j}{\delta \xi_{4f}}$
$^1D_2$	16972	45.97	-37.63	510	2.906
$^3P_0$	20412	70.17	81.17	-1253	1.905
$^3P_1$	20990	70.07	80.66	-1278	3.974
$^3P_2$	22220	67.56	68.42	-1077	5.029

(a) F_2^0=305.000 cm^{-1} F_4^0= 51.880 cm^{-1}

F_6^0=5.321 cm^{-1} ξ_{4f}^0=730.50 cm^{-1}

The crystal field effect removes the degeneracy and brings about a shift in the barycenter of the lanthanide ion's $^{2S+J}L_J$ electronic state. This phenomenon is denoted as the nephelauxetic effect [25] which is an effect of covalency in the Ln(III) and the ligand [26]. The nephelauxetic effect results in the delocalization of the electrons over the ligands away from the metal which separates them and hence reduces repulsion.

The Slater-Condon and Racah parameters can be used to interpret the nephelauxetic ratio as follows[7]:

$$\beta = \frac{F_k^C}{F_k^f} \text{ or } \frac{E_C^k}{E_f^k} \tag{5}$$

Where F_k^C, F_k^f and E_C^k, E_f^k denote the Slater-Condon and Racah parameters for the complex and free ion respectively. The values of the percent covalency (δ)[27] and bonding parameter ($b^{1/2}$) are correlated to the nephelauxetic ratio and are shown below:

$$\delta = \left[\frac{1-\beta}{\beta}\right] \times 100 \tag{6}$$

$$b^{1/2} = \left[\frac{1-\beta}{2}\right]^{1/2} \tag{7}$$

E_0, which represents the electrostatic energy term, can be stated as a function of the Slater-Condon parameter (F_k) as

$$E_0 = \sum_{k=0}^{k=6} K^k F_k \tag{8}$$

F_k which is a decreasing function of k can be represented as follows

$$F_i^k = \int_0^\infty \int_0^\infty \frac{r_<^k}{r_>^{k+1}} R_i^2(r_i) R_j^2(r_j) r_i^2 r_j^2 dr_i dr_j \tag{9}$$

Here, $r_<$ and $r_>$ denotes the electrons' minimum and maximum radii, R denotes the 4f-radial wave function whereas the ith and jth electrons under consideration are indicated by i and j.

The F^k integrals have been reconfigured as follows by Condon and Shortley [28] with respect to the reduced integral F_k:

$$F_k = \frac{F^k}{D_k} \tag{10}$$

The reduced Slater-Condon integral can be reproduced from a combination of Equations (9) and (10) as follows:

$$F_k = \frac{1}{D_k} \int_0^\infty \int_0^\infty r_<^k r_>^{k+1} R_i^2(r_i) R_j^2(r_j) r_i^2 r_j^2 dr_i dr_j \tag{11}$$

Where the angular component of the interaction is represented by the coefficient of the linear combination, F_k and D_k represent the denominator. The Racah parameter E^{ki} is obtained by a linear combination of F_k as follows:

$$E^1 = \frac{70F_2 + 231F_4 + 20.02F_6}{9}$$

$$E^2 = \frac{F_2 - 3F_4 + 7F_6}{9} \tag{12}$$

$$E^3 = \frac{5F_2 + 6F_4 - 9F_6}{3}$$

Equation 4 can be solved using the least square method and applying the partial derivatives

of Pr(III) ion and zero-order energy given by Wong [24] and the values of ΔF_k and $\Delta \xi_{4f}$ can

be determined. Using the values of these two parameters, other values of different

parameters ξ_{4f} and F_2, F_4, F_6 are found out from equation (3) [29].

The f-f absorption band intensities are calculated using the Judd and Ofelt theory [30,31].

Intraconfigurational transitions like the f-f transitions are not allowed by the Laporte rule

and hence forbidden by the electric dipole mechanism. Judd and Ofelt demonstrated that

mixing of opposite parity electronic states may occur in the presence of a ligand field,

thereby, enabling f-f transitions. These types of transitions are denoted as induced electric

dipole transitions [32]. Accordingly, for an induced electric dipole transition $\psi J \rightarrow \psi' J'$

bearing $\bar{\upsilon}$ energy, its oscillator strength (P_{cal}) can be expressed as

$$P_{cal} = \sum_{\lambda=2,4,6} T_\lambda \sigma (f^n \psi J \| U^\lambda \| f^n \psi' J')^2 \tag{13}$$

In this case, U^λ (λ = 2, 4, 6) represents the Carnall matrix elements [33] for the

praseodymium ion which connects the states $f^n \psi J$ to $f^n \psi' J'$ through T_λ. T_λ (λ= 2, 4, 6)

represent the Judd-Ofelt parameters and are associated with the $4f^n$ wave function. The

Judd-Ofelt parameters provide information on the environment of the Ln(III) ion as well as

the interaction between Ln(III) and ligand. The Judd-Ofelt parameters are very sensitive to

small variations in complex symmetry and coordination around the Ln(III) ion.

The experimental oscillator strength (P_{obs}) value is used for measuring the absorption band intensity. Gaussian-curve analysis is used to determine P_{obs}, which is equivalent to the area underneath the absorption curve as

$$P_{obs} = 4.6 \text{ x } 10^{-9} \times \mathcal{E}_{max} \times \Delta \nu_{1/2} \tag{14}$$

$\Delta \nu_{1/2}$ denotes the half-band width while $\mathcal{E}_{max}$ represents the molar extinction coefficient. The following relation is used to compute T_2, T_4 and T_6 values

$$\frac{P_{obs}}{\nu} = [U^2]^2 . \text{T}_2 + [U^4]^2 . \text{T}_4 + [U^6]^2 . \text{T}_6 \tag{15}$$

Whereby the values of $[U^2]^2$, $[U^4]^2$ and $[U^6]^2$ from Carnell's [32] matrix elements were used in order to solve T_2, T_4 and T_6. The matrix elements for Pr(III) ion are given in Table 2.2.

Table 2.2: Matrix elements $U^{(\lambda)}$ for Pr(III) aquo [34].

Levels	$[U^{(2)}]^2$	$[U^{(4)}]^2$	$[U^{(6)}]^2$
$^1D_2$	0.0026	0.0170	0.0520
$^3P_0$	0	0.1728	0
$^3P_1$	0	0.1707	0
$^3P_2$	0	0.0362	0.1355

2.4 Results and discussion

In the spectral range of 400-620 nm, four transitions ($^3H_4 \rightarrow {}^3P_2$, $^3H_4 \rightarrow {}^3P_1$, $^3H_4 \rightarrow {}^3P_0$ and $^3H_4 \rightarrow {}^1D_2$) have been detected in Pr(III) complexes with amino acids. These transitions are the pseudohypersensitive transitions of Pr(III) ion and have been employed in the spectral study of Pr(III) complexation with different amino acid ligands in the presence and absence of Mg(II).

Figure 2.5, 2.10, 2.15 and 2.20 depicts the UV-visible spectra of Pr(III), Pr(III):Ligands (L) (L-Glutamine, L-Threonine, L-Tryptophan and L-Isoleucine) in the

presence and absence of Mg(II) in DMF: water (50% v/v) solvent. The figures clearly show that adding L-Glutamine, L-Threonine, L-Tryptophan and L-Isoleucine to Pr(III) increases the intensities of its 4f-4f transitions spectra. This is most likely caused by the Pr(III):Ligand complex formation. The intensities of the transition bands are further enhanced when Mg(II) is incorporated into the complex [Pr(III):Ligand(L)] indicating the possible interaction of the ligand orbital with the lanthanide metal orbital as a result of which a heterobimetallic complex Pr(III):L:Mg(II) may be formed. Energy interaction as well as intensity parameters were used to determine the difference in magnitude of the different Ln(III) systems. Introduction of Mg(II) into the binary system of Pr(III):L causes significant changes in oscillator strengths as well as the magnitude of Judd-Ofelt (T_λ) intensity parameters in the same way when the Ligands are added to Pr(III). This result could demonstrate the possibility of an interaction of Pr(III):Ligand with Mg(II) in the solution. In addition, the degree of mixing of Ln(III) and ligand orbitals will have a significant impact on the T_λ parameters. Table 2.11 to 2.14 gives the oscillator strength and computed values of Judd-Ofelt intensity parameters (T_2, T_4 and T_6). From the computed intensity parameter values it is observed that the oscillator strength and Judd-Ofelt parameters increases on the addition of the Ligands (amino acids) to the Pr(III) ion. It is clearly seen that T_λ are significantly affected in the presence of Mg(II), indicating a change in the immediate coordination environment of Pr(III). These changes may be the evidence for involvement of Mg(II) in coordination with Pr(III) ion [23,29,35]. The computed values of the energy interaction parameters like the Slater-Condon (F_k), Racah parameters (E^k), Lande (ξ_{4f}), nephelauxetic ratio (β), bonding ($b^{1/2}$), and covalency (δ) parameters for the complexation of Pr(III) and Pr(III):Ligands in the presence and absence of Mg(II) in different solvents are given in Table 2.3 to 2.6. These tables further show that on introducing Mg(II) and the amino acid ligands to Pr(III) could make changes to the energy parameter values. It is observed that the values of the Slater-Condon (F_k), Racah (E^k) and

Lande spin-orbit interaction (ξ_{4f}) parameter decreases when Pr(III):L and Pr(III):L:Mg(II) complexes were formed in which the interelectronic repulsion between the metal and ligand orbitals decreases because of the expansion of the central metal orbital causing the bond distance between the ligand and the metal to shorten. The decrease in F_k, E^k, and ξ_{4f} parameter values subsequently causes the nephelauxetic effect which leads to an increase in bonding and percent covalency parameter values, thereby indicating a possibility of stronger bonding in the Pr(III) complexes with the amino acids and Mg(II) as well as the covalent character of the complexes.

A similar trend is observed for the praseodymium complex systems at different pH (2, 4 and 6). The UV-visible spectra of Pr(III), Pr(III):L and Pr(III):L:Mg(II) at pH levels 2, 4, and 6 are shown in Figure 2.22 to 2.37. The F_k, E^k, and ξ_{4f} parameter values decrease with an increase in $b^{1/2}$ and δ values as the pH increase from 2 to 4 and to 6 which suggest that the binding is stronger at the higher pH. Lanthanides are hard metal ions and prefer hard donor sites such as oxygen. At a lower pH, the carboxylate group of amino acids is likely deprotonated creating a binding site for the metal ion while at a higher pH the amino group deprotonates which allows for more binding possibilities resulting in a stronger complex formation. Tables 2.7 to 2.10 gives the computed and observed values of energies for the various bands and root mean square (RMS) deviation values. The RMS value is a measure of the accuracy of the evaluated energy parameters.

The observed and computed oscillator strengths (P) and Judd-Ofelt (T$_\lambda$) parameter values for Pr(III), Pr(III):L, and Pr(III):L:Mg(II) in DMF solvent at different pH levels are given in Table 2.23 to 2.26. The values show that the oscillator strengths are substantially enhanced when the ligands are added and increase further with the addition of Mg(II), which suggests that the amino acid ligands and magnesium are involved in the complex formation. From the computed intensity parameter values, the values of T$_2$ are found to be negative and hold no meaning. The values of T$_4$ and T$_6$ on the other hand undergo

substantial changes which could be indicative of symmetry changes in the formation of lanthanide complexes. Such distinct changes strongly suggest the formation of inner-sphere coordination of the amino acids ligands complex with Pr(III). The increase in the degree of inner-sphere coordination is believed to be due to the substantial increase in the values of oscillator strength and Judd-Ofelt intensity parameters.

The pH of the medium influences the degree of protonation and deprotonation of coordinating sites in the ligands. As a result, it has a considerable effect on the binding of Pr(III) with the ligand in the presence and absence of Mg(II). This is evident from the significant enhancement in the oscillator strength (P) and T_λ parameters. Figures 2.25, 2.29, 2.33 and 2.37 shows the comparative absorption spectra of Pr(III):L-Gln, Pr(III):L-Thr, Pr(III):L-Trp and Pr(III):L-Ile in aquated DMF at various pH levels (pH 2, pH 4, and pH 6). Based on the figures and tables, we can deduce that the complexation is most suited in pH 6.

Thus, the information gathered from the energy interaction parameters is well substantiated by the evaluated values of the intensity parameters viz., oscillator strength (P) and Judd-Ofelt (T_λ). Figure 2.1 shows the possible structures of Pr(III):L-Ile as nona-coordinated complex.
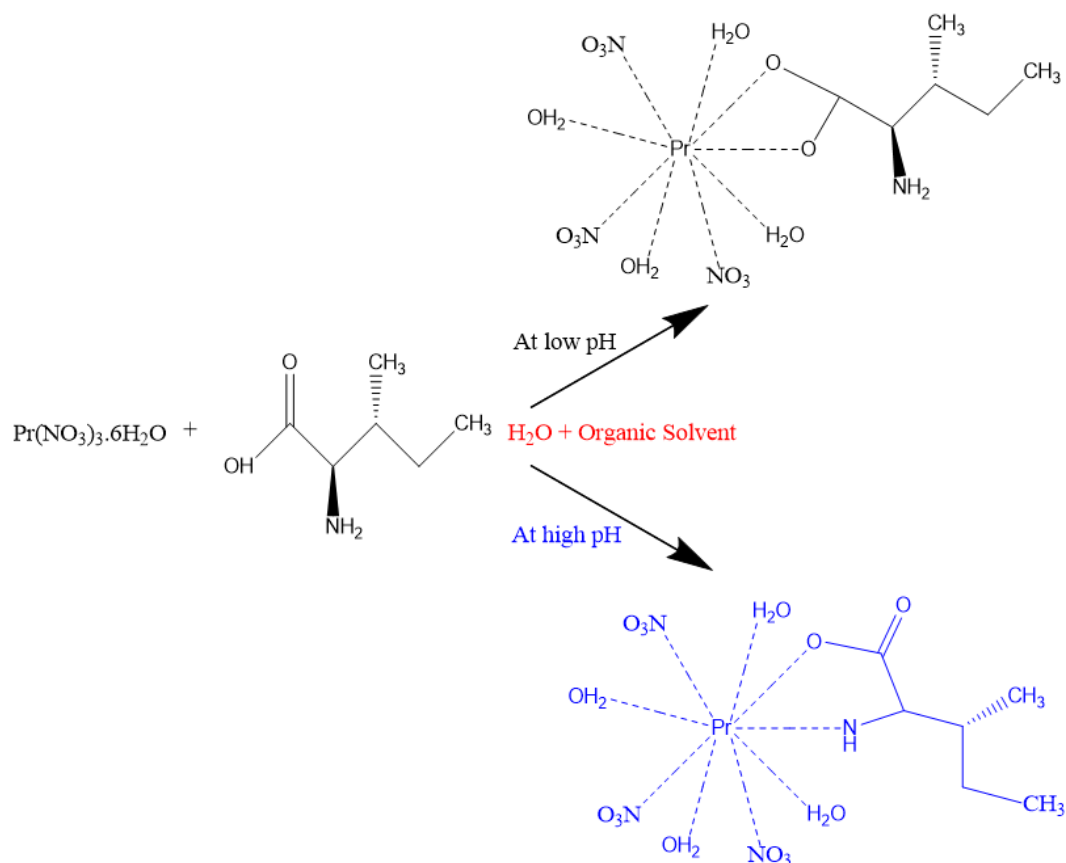
Fig. 2.1: Possible nona-coordinated structures of Pr(III):L-Ile at low pH and high pH.

Figure 2.6, 2.11, 2.16 and 2.21 shows a comparative UV-visible spectra of Pr(III):L-Gln, Pr(III):L-Thr, Pr(III):L-Trp and Pr(III):L-Ile in different aquated organic solvents (methanol, dioxane, acetonitrile and dimethylformamide). From the computed values of intensity and energy parameters in different solvents, it is evident that the largest intensification was observed in DMF solvent (Tables 2.3 to 2.6 and 2.11 to 2.14). This suggests that DMF has the greatest effect out of the four solvents in promoting Pr(III) ion complexation with the ligands. The sensitivity of the band intensities of the four solvents follows the order dimethylformamide>acetonitrile>dioxane>methanol.

References

[1]   Y. Ning, G.Q. Jin, M.X. Wang, S. Gao, J.L. Zhang, Recent progress in metal-based molecular probes for optical bioimaging and biosensing, *Curr. Opin. Chem. Biol.* **66** (2022) 102097. https://doi.org/10.1016/j.cbpa.2021.102097.

[2]   H. Li, X. Wang, T.Y. Ohulchanskyy, G. Chen, Lanthanide-Doped Near-Infrared Nanoparticles for Biophotonics, *Adv. Mater.* **33** (2021) 2000678. https://doi.org/10.1002/adma.202000678.

[3]   P. Li, H. Li, Recent progress in the lanthanide-complexes based luminescent hybrid materials, *Coord. Chem. Rev.* **441** (2021) 213988. https://doi.org/10.1016/j.ccr.2021.213988.

[4]   J.G. Bünzli, Lanthanide Photonics : Shaping the Nanoworld, *Trends Chem.* **1** (2019) 751–762. https://doi.org/10.1016/j.trechm.2019.05.012.

[5]   S.N. Misra, G. Ramchandriah, M.A. Gagnani, R.S. Shukla, M.I. Devi, Absorption spectral studies involving 4f-4f transitions as structural probe in chemical and biochemical reactions and compositional dependence of intensity parameters, *Appl. Spectrosc. Rev.* **38** (2003) 433–493. https://doi.org/10.1081/ASR-120026330.

[6]   S.P. Fricker, The therapeutic application of lanthanides, *Chem. Soc. Rev.* **35** (2006) 524–533. https://doi.org/10.1039/b509608c.

[7]   S.N. Misra, S.O. Sommerer, Absorption Spectra of Lanthanide Complexes in Solution, *Appl. Spectrosc. Rev.* **26** (1991) 151–202. https://doi.org/https://doi.org/10.1080/05704929108050880.

[8]   W.H. William De, D.R. Sudnick, Lanthanide Ion Probes of Structure in Biology. Laser-Induced Luminescence Decay Constants Provide a Direct Measure of the Number of Metal-Coordinated Water Molecules, *J. Am. Chem. Soc.* **101** (1979) 334–340. https://doi.org/10.1021/ja00496a010.

[9]   P. Mulqueen, J.M. Tingey, W.D.W. Horrocks, Characterization of Lanthanide(III) Ion Binding to Calmodulin Using Luminescence Spectroscopy, *Biochemistry.* **24** (1985) 6639–6645. https://doi.org/10.1021/bi00344a051.

[10]   T. Moaienla, N. Bendangsenla, T. David, C. Sumitra, N.R. Singh, M.I. Devi, Spectrochimica Acta Part A : Molecular and Biomolecular Spectroscopy Comparative 4f – 4f absorption spectral study for the interactions of Nd(III) with some amino acids : Preliminary thermodynamics and kinetic studies of interaction of Nd(III): glycine , *Spectrochim. Acta Part A Mol. Biomol. Spectrosc.* **87** (2012) 142–150. https://doi.org/10.1016/j.saa.2011.11.028.

[11] A. Dalal, K. Nehra, A. Hooda, D. Singh, S. Kumar, R.S. Malik, Synthesis, photophysical characteristics and geometry optimization of Tris(2-benzoylacetophenonate)europium complexes with 2, 2′-Bipyridine derivatives, *J. Lumin.* **247** (2022) 118873. https://doi.org/10.1016/J.JLUMIN.2022.118873.

[12] L. Blois, A.N.C. Neto, R.L. Longo, I.F. Costa, T.B. Paolini, H.F. Brito, O.L. Malta, On the Experimental Determination of 4f–4f Intensity Parameters from the Emission Spectra of Europium (III) Compounds, *Opt. Spectrosc.* **130** (2022) 10–17. https://doi.org/10.1134/S0030400X2201009X.

[13] B. Huidrom, N. Ranjana Devi, T.D. Singh, N.R. Singh, Studies on the complexation of neodymium(III) ion with 1,2,4-1H-triazole and 1,2,3-benzotriazole in absence and presence of calcium(II) ion in aqueous and some selected different aquated organic solvents by an absorption spectroscopy involving 4f-4f trans, *Spectrochim. Acta - Part A Mol. Biomol. Spectrosc.* **85** (2012) 127–133. https://doi.org/10.1016/j.saa.2011.09.045.

[14] A.A. Kornienko, A.A. Kaminskii, E.B. Dunina, Dependence of the Line Strength of f–f Transitions on the Manifold Energy. II. Analysis of Pr3+ in KPrP4O12, *Phys. Status Solidi.* **157** (1990) 267–273. https://doi.org/10.1002/pssb.2221570127.

[15] W. Luo, J. Liao, R. Li, X. Chen, Determination of Judd-Ofelt intensity parameters from the excitation spectra for rare-earth doped luminescent materials, *Phys. Chem. Chem. Phys.* **12** (2010) 3276–3282. https://doi.org/10.1039/b921581f.

[16] Y. Tian, B. Chen, R. Hua, J. Sun, L. Cheng, H. Zhong, X. Li, J. Zhang, Y. Zheng, T. Yu, L. Huang, H. Yu, Optical transition, electron-phonon coupling and fluorescent quenching of La2(MoO4)3:Eu3+ phosphor, *J. Appl. Phys.* **109** (2011) 053511. https://doi.org/10.1063/1.3551584.

[17] Y. Zhang, B. Chen, S. Xu, X. Li, J. Zhang, J. Sun, X. Zhang, H. Xia, R. Hua, A universal approach for calculating the Judd-Ofelt parameters of RE3+ in powdered phosphors and its application for the β-NaYF4:Er3+/Yb3+ phosphor derived from auto-combustion-assisted fluoridation, *Phys. Chem. Chem. Phys.* **20** (2018) 15876–15883. https://doi.org/10.1039/c8cp02317d.

[18] M. Luo, B. Chen, X. Li, J. Zhang, S. Xu, X. Zhang, Y. Cao, J. Sun, Y. Zhang, X. Wang, Y. Zhang, D. Gao, L. Wang, Fluorescence decay route of optical transition calculation for trivalent rare earth ions and its application for Er3+-doped NaYF4phosphor, *Phys. Chem. Chem. Phys.* **22** (2020) 25177–25183. https://doi.org/10.1039/d0cp04379f.

[19] J.-C.G. Bünzli, S. V. Eliseeva, Basics of Lanthanide Photophysics, in: P. Hänninen, H. Härmä (Eds.), Lanthan. Lumin., Springer Berlin, Heidelberg, 2010: pp. 1–45. https://doi.org/10.1007/4243_2010_3.

[20] D.G. Karraker, Hypersensitive transitions of six-, seven-, and eight-coordinate neodymium, holmium, and erbium chelates, *Inorg. Chem.* **6** (1967) 1863–1868. https://doi.org/10.1021/ic50056a022.

[21] C. Görller-Walrand, K. Binnemans, Chapter 167 Spectral intensities of f-f transitions, *Handb. Phys. Chem. Rare Earths.* **25** (1998) 101–264. https://doi.org/10.1016/S0168-1273(98)25006-9.

[22] T.D. Singh, C. Sumitra, N. Rajmuhon Singh, M. Indira Devi, Spectral study of the complexation of Nd(III) with glutathione reduced (GSH) in the presence and absence of Zn(II) in aquated organic solvents, *J. Chem. Sci.* **116** (2004) 303–309. https://doi.org/10.1007/BF02711430.

[23] M. Ziekhrü, Z. Thakro, C. Imsong, J. Sanchu, M. Indira Devi, Computation of energy interaction and intensity parameters for the complexation of Pr(III) with glutathione at different pH in the presence/absence of Mg2+: 4f-4f transition spectra as a probe, *Polyhedron.* **200** (2021) 115099. https://doi.org/10.1016/j.poly.2021.115099.

[24] E.Y. Wong, Configuration interaction of the Pr3+ ion, *J. Chem. Phys.* **38** (1963) 976–978. https://doi.org/10.1063/1.1733794.

[25] C.K. Jorgensen, Electron Transfer Spectra, *Progr. Inorg. Chem.* **12** (1970) 101. https://doi.org/10.1002/9780470166130.ch2.

[26] R. Reisfeld, C.K. Jorgensen, Lasers and Excited States of Rare Earths, 1st ed., Springer-Verlag Berlin, Heidelberg, 1977.

[27] S.P. Sinha, Spectroscopic investigations of some neodymium complexes, *Spectrochim. Acta.* **22** (1966) 57–62. https://doi.org/10.1016/0371-1951(66)80008-5.

[28] E.U. Condon, G.H. Shortley, The Theory of Atomic Spectra, Cambridge: University Press, Cambridge, 1963.

[29] S.N. Misra, G. Ramchandriah, M.A. Gagnani, R.S. Shukla, M.I. Devi, Absorption spectral studies involving 4f-4f transitions as structural probe in chemical and biochemical reactions and compositional dependence of intensity parameters, *Appl. Spectrosc. Rev.* **38** (2003) 433–493. https://doi.org/10.1081/ASR-120026330.

[30] G.S. Ofelt, Intensities of Crystal Spectra of Rare-Earth Ions, *J. Chem. Phys.* **37** (1962) 511–520. https://doi.org/10.1063/1.1701366.

[31] B.R. Judd, Optical absorption intensities of rare-earth ions, *Phys. Rev.* **127** (1962) 750–761. https://doi.org/10.1103/PhysRev.127.750.

[32] M. Hatanaka, S. Yabushita, Theoretical study on the f-f transition intensities of lanthanide trihalide systems, *J. Phys. Chem. A*. **113** (2009) 12615–12625. https://doi.org/10.1021/jp9049507.

[33] W.T. Carnall, P.R. Fields, B.G. Wybourne, Spectral intensities of the trivalent lanthanides and actinides in solution. I. Pr3+, Nd3+, Er3+, Tm3+, and Yb3+, *J. Chem. Phys.* **42** (1965) 3797–3806. https://doi.org/10.1063/1.1695840.

[34] W.T. Carnall, P.R. Fields, K. Rajnak, Electronic Energy Levels in the Trivalent Lanthanide Aquo Ions. I. Pr3+, Nd3+, Pm3+, Sm3+, Dy3+, Ho3+, Er3+, and Tm3+, *J. Chem. Phys.* **49** (1968) 4424. https://doi.org/https://doi.org/10.1063/1.1669896.

[35] J.P. Mehta, P.N. Bhatt, S.N. Misra, An absorption spectral study of Nd (III) with glutathione (reduced), GSH in aqueous and aquated organic solvent in presence and absence of Zn (II), *J. Solid State Chem.* **171** (2003) 175–182. https://doi.org/10.1016/S0022-4596(02)00205-0.

Table 2.3: Computed values of the energy interaction parameters: Slater-Condon factor F_k (cm^{-1}), Lande's Spin-orbit interactions ξ_{4f} (cm^{-1}), Racah parameters (E^k), Nephelauxetic ratio (β), Bonding ($b^{1/2}$) and Percent covalency (δ) of Pr(III) with L-Glutamine in absence and presence of Mg(II) in 50% (v/v) aquated solvents (Methanol, 1,4-Dioxane, Acetonitrile and Dimethylformamide)

System	F_2	F_4	F_6	ξ_{4f}	E^1	E^2	E^3	β	$b^{1/2}$	δ
Solvent: Methanol (CH$_3$OH:H$_2$O)										
Pr(III)	309.3749	42.7092	4.6716	722.3264	3512.8436	23.7720	615.0579	0.9470	0.1628	5.5975
Pr(III):L-Gln	309.3254	42.7024	4.6708	722.1663	3512.2814	23.7682	614.9595	0.9468	0.1631	5.6178
Pr(III): L-Gln:Mg(II)	309.2359	42.6900	4.6695	721.7541	3511.2658	23.7613	614.7816	0.9464	0.1637	5.6638
Solvent: 1,4-Dioxane (C$_4$H$_8$O$_2$:H$_2$O)										
Pr(III)	309.3721	42.7088	4.6715	721.8506	3512.8125	23.7718	615.0525	0.9467	0.1633	5.6342
Pr(III):L-Gln	309.2455	42.6913	4.6696	721.8006	3511.3740	23.7621	614.8006	0.9464	0.1636	5.6587
Pr(III): L-Gln:Mg(II)	309.1636	42.6800	4.6684	721.4918	3510.4450	23.7558	614.6379	0.9461	0.1641	5.6957
Solvent: Acetonitrile (CH$_3$CN:H$_2$O)										
Pr(III)	309.3838	42.7104	4.6717	721.7487	3512.9443	23.7727	615.0755	0.9466	0.1634	5.6401
Pr(III):L-Gln	309.2128	42.6868	4.6691	720.9187	3511.0034	23.7596	614.7357	0.9458	0.1646	5.7315
Pr(III): L-Gln:Mg(II)	309.1440	42.6773	4.6681	720.4162	3510.2225	23.7543	614.5990	0.9453	0.1653	5.7812
Solvent: DMF (C$_3$H$_7$NO:H$_2$O)										
Pr(III)	308.9360	42.6486	4.6649	719.4690	3507.8601	23.7383	614.1854	0.9443	0.1668	5.8956
Pr(III):L-Gln	308.8349	42.6347	4.6634	719.4297	3506.7118	23.7305	613.9843	0.9442	0.1670	5.9075
Pr(III): L-Gln:Mg(II)	308.7792	42.6270	4.6626	719.3659	3506.0793	23.7262	613.8736	0.9441	0.1672	5.9216

Table 2.4: Computed values of the energy interaction parameters: Slater-Condon factor F_k (cm^{-1}), Lande's Spin-orbit interactions ξ_{4f} (cm^{-1}), Racah parameters (E^k), Nephelauxetic ratio (β), Bonding ($b^{1/2}$) and Percent covalency (δ) of Pr(III) with L-Threonine in absence and presence of Mg(II) in 50% (v/v) aquated solvents (Methanol, 1,4-Dioxane, Acetonitrile and Dimethylformamide)

System	F_2	F_4	F_6	ξ_{4f}	E^1	E^2	E^3	β	$b^{1/2}$	δ
Solvent: Methanol (CH₃OH:H₂O)										
Pr(III)	309.3540	42.7063	4.6712	722.3768	3512.6060	23.7704	615.0163	0.9470	0.1628	5.5970
Pr(III):L-Thr	309.2794	42.6960	4.6701	722.3809	3511.7599	23.7647	614.8682	0.9469	0.1630	5.6089
Pr(III): L-Thr:Mg(II)	309.2122	42.6867	4.6691	722.3199	3510.9968	23.7595	614.7345	0.9468	0.1632	5.6245
Solvent: 1,4-Dioxane (C₄H₈O₂:H₂O)										
Pr(III)	309.3725	42.7089	4.6715	721.8144	3512.8161	23.7718	615.0531	0.9466	0.1633	5.6369
Pr(III):L-Thr	309.2914	42.6977	4.6703	721.6395	3511.8953	23.7656	614.8919	0.9464	0.1637	5.6635
Pr(III): L-Thr:Mg(II)	309.1904	42.6837	4.6688	721.6074	3510.7485	23.7578	614.6911	0.9462	0.1640	5.6825
Solvent: Acetonitrile (CH₃CN:H₂O)										
Pr(III)	309.3345	42.7036	4.6710	721.3926	3512.3847	23.7689	614.9776	0.9463	0.1639	5.6754
Pr(III):L-Thr	309.2427	42.6910	4.6696	721.0749	3511.3424	23.7619	614.7951	0.9459	0.1644	5.7147
Pr(III): L-Thr:Mg(II)	309.1994	42.6850	4.6689	720.9586	3510.8509	23.7585	614.7090	0.9458	0.1646	5.7306
Solvent: DMF (C₃H₇NO:H₂O)										
Pr(III)	308.9367	42.6487	4.6649	719.5496	3507.8687	23.7384	614.1868	0.9445	0.1667	5.8816
Pr(III):L-Thr	308.8674	42.6391	4.6639	719.4735	3507.0812	23.7330	614.0490	0.9443	0.1669	5.8988
Pr(III): L-Thr:Mg(II)	308.8026	42.6302	4.6629	719.4602	3506.3454	23.7280	613.9201	0.9442	0.1670	5.9105

Table 2.5: Computed values of the energy interaction parameters: Slater-Condon factor F_k (cm^{-1}), Lande's Spin-orbit interactions ξ_{4f} (cm^{-1}), Racah parameters (E^k), Nephelauxetic ratio (β), Bonding ($b^{1/2}$) and Percent covalency (δ) of Pr(III) with L-Tryptophan in absence and presence of Mg(II) in 50% (v/v) aquated solvents (Methanol, 1,4-Dioxane, Acetonitrile and Dimethylformamide)

System	F_2	F_4	F_6	ξ_{4f}	E^1	E^2	E^3	β	$b^{1/2}$	δ
Solvent: Methanol (CH$_3$OH:H$_2$O)										
Pr(III)	309.3532	42.7062	4.6712	722.4992	3512.5978	23.7704	615.0149	0.9471	0.1627	5.5878
Pr(III):L-Trp	309.2367	42.6901	4.6695	722.1690	3511.2751	23.7614	614.7833	0.9467	0.1633	5.6320
Pr(III): L-Trp:Mg(II)	309.1942	42.6843	4.6688	722.1020	3510.7915	23.7581	614.6986	0.9466	0.1634	5.6441
Solvent: 1,4-Dioxane (C$_4$H$_8$O$_2$:H$_2$O)										
Pr(III)	309.3716	42.7088	4.6715	721.8560	3512.8067	23.7718	615.0514	0.9467	0.1633	5.6339
Pr(III):L-Trp	309.3019	42.6991	4.6705	721.7628	3512.0146	23.7664	614.9127	0.9465	0.1636	5.6524
Pr(III): L-Trp:Mg(II)	309.2355	42.6900	4.6695	721.4652	3511.2608	23.7613	614.7808	0.9462	0.1640	5.6860
Solvent: Acetonitrile (CH$_3$CN:H$_2$O)										
Pr(III)	309.3605	42.7072	4.6713	721.8061	3512.6800	23.7709	615.0293	0.9466	0.1634	5.6395
Pr(III):L-Trp	309.2947	42.6981	4.6704	721.7350	3511.9336	23.7659	614.8986	0.9465	0.1636	5.6557
Pr(III): L-Trp:Mg(II)	309.2543	42.6926	4.6697	721.3351	3511.4744	23.7628	614.8182	0.9461	0.1641	5.6929
Solvent: DMF (C$_3$H$_7$NO:H$_2$O)										
Pr(III)	308.9378	42.6489	4.6650	719.5850	3507.8804	23.7384	614.1889	0.9445	0.1666	5.8787
Pr(III):L-Trp	308.8665	42.6390	4.6639	719.5095	3507.0711	23.7330	614.0472	0.9443	0.1669	5.8962
Pr(III): L-Trp:Mg(II)	308.7989	42.6297	4.6629	719.4186	3506.3032	23.7278	613.9127	0.9442	0.1671	5.9143

Table 2.6: Computed values of the energy interaction parameters: Slater-Condon factor F_k (cm^{-1}), Lande's Spin-orbit interactions ξ_{4f} (cm^{-1}), Racah parameters (E^k), Nephelauxetic ratio (β), Bonding ($b^{1/2}$) and Percent covalency (δ) of Pr(III) with L-Isoleucine in absence and presence of Mg(II) in 50% (v/v) aquated solvents (Methanol, 1,4-Dioxane, Acetonitrile and Dimethylformamide)

System	F_2	F_4	F_6	ξ_{4f}	E^1	E^2	E^3	β	$b^{1/2}$	δ
Solvent: Methanol (CH$_3$OH:H$_2$O)										
Pr(III)	309.3647	42.7078	4.6714	721.7662	3512.7285	23.7712	615.0377	0.9466	0.1634	5.6419
Pr(III):L-Ile	309.3010	42.6990	4.6704	721.4749	3512.0043	23.7663	614.9109	0.9463	0.1639	5.6746
Pr(III): L-Ile:Mg(II)	309.2384	42.6904	4.6695	721.1828	3511.2938	23.7615	614.7865	0.9460	0.1643	5.7071
Solvent: 1,4-Dioxane (C$_4$H$_8$O$_2$:H$_2$O)										
Pr(III)	309.3715	42.7087	4.6715	721.8728	3512.8057	23.7718	615.0513	0.9467	0.1633	5.6326
Pr(III):L-Ile	309.3136	42.7007	4.6706	721.6836	3512.1473	23.7673	614.9360	0.9465	0.1636	5.6565
Pr(III): L-Ile:Mg(II)	309.1983	42.6848	4.6689	721.1135	3510.8389	23.7585	614.7069	0.9459	0.1645	5.7190
Solvent: Acetonitrile (CH$_3$CN:H$_2$O)										
Pr(III)	309.3426	42.7047	4.6711	722.3644	3512.4773	23.7695	614.9938	0.9470	0.1628	5.5998
Pr(III):L-Ile	309.2499	42.6919	4.6697	722.2890	3511.4241	23.7624	614.8094	0.9468	0.1631	5.6207
Pr(III): L-Ile:Mg(II)	309.1876	42.6833	4.6687	722.2948	3510.7171	23.7576	614.6856	0.9467	0.1633	5.6304
Solvent: DMF (C$_3$H$_7$NO:H$_2$O)										
Pr(III)	308.9331	42.6482	4.6649	719.5285	3507.8271	23.7381	614.1796	0.9444	0.1667	5.8838
Pr(III):L-Ile	308.8807	42.6410	4.6641	719.4279	3507.2327	23.7341	614.0755	0.9443	0.1669	5.9002
Pr(III): L-Ile:Mg(II)	308.8038	42.6304	4.6629	719.4543	3506.3596	23.7281	613.9226	0.9442	0.1670	5.9107

Table 2.7: Observed and computed values of energies (cm^{-1}) and R.M.S values of Pr(III) with L-Glutamine in absence and presence of Mg(II) systems in 50% (v/v) aquated solvents (Methanol, 1,4-Dioxane, Acetonitrile and Dimethylformamide)

System	$^3H_4 \rightarrow {}^3P_2$		$^3H_4 \rightarrow {}^3P_1$		$^3H_4 \rightarrow {}^3P_0$		$^3H_4 \rightarrow {}^1D_2$		R.M.S
	E_{obs}	E_{cal}	E_{obs}	E_{cal}	E_{obs}	E_{cal}	E_{obs}	E_{cal}	
Solvent: Methanol (CH$_3$OH:H$_2$O)									
Pr(III)	22514.99	22472.47	21346.93	21261.96	20757.42	20701.22	16975.56	17147.99	102.37
Pr(III):L-Gln	22507.15	22465.83	21339.67	21255.16	20751.27	20694.57	16971.33	17143.51	102.11
Pr(III): L-Gln:Mg(II)	22502.30	22461.65	21335.39	21250.82	20746.84	20690.21	16968.95	17140.66	101.85
Solvent: 1,4-Dioxane(C$_4$H$_8$O$_2$:H$_2$O)									
Pr(III)	22510.25	22470.96	21340.84	21261.13	20762.17	20701.64	16973.94	17147.27	101.98
Pr(III):L-Gln	22506.53	22465.19	21337.94	21255.50	20759.18	20696.61	16963.85	17143.49	105.70
Pr(III): L-Gln:Mg(II)	22504.67	22459.49	21336.11	21249.96	20756.33	20691.66	16952.00	17139.76	110.57
Solvent: Acetonitrile(CH$_3$CN:H$_2$O)									
Pr(III)	22527.50	22471.96	21342.56	21262.03	20762.75	20702.32	16964.71	17147.89	108.14
Pr(III):L-Gln	22522.93	22467.09	21339.70	21257.21	20759.60	20697.89	16957.94	17144.67	110.23
Pr(III): L-Gln:Mg(II)	22511.13	22456.43	21333.98	21246.88	20754.25	20688.72	16942.46	17137.72	115.11
Solvent: DMF (C$_3$H$_7$NO:H$_2$O)									
Pr(III)	22497.13	22430.54	21297.24	21221.99	20744.89	20667.08	16908.72	17120.92	123.67
Pr(III):L-Gln	22491.62	22426.50	21293.70	21217.92	20741.66	20663.22	16905.53	17118.22	123.87
Pr(III): L-Gln:Mg(II)	22486.43	22421.45	21288.10	21212.66	20736.18	20657.90	16902.64	17114.78	123.53

Table 2.8: Observed and computed values of energies (cm^{-1}) and R.M.S values of Pr(III) with L-Threonine in absence and presence of Mg(II) systems in 50% (v/v) aquated solvents (Methanol, 1,4-Dioxane, Acetonitrile and Dimethylformamide)

System	$^3H_4 \rightarrow {}^3P_2$		$^3H_4 \rightarrow {}^3P_1$		$^3H_4 \rightarrow {}^3P_0$		$^3H_4 \rightarrow {}^1D_2$		R.M.S
	E_{obs}	E_{cal}	E_{obs}	E_{cal}	E_{obs}	E_{cal}	E_{obs}	E_{cal}	
Solvent: Methanol (CH₃OH:H₂O)									
Pr(III)	22515.61	22473.30	21347.02	21262.80	20758.17	20702.04	16976.89	17148.55	101.85
Pr(III):L-Thr	22510.31	22468.29	21342.34	21257.60	20752.89	20696.82	16973.35	17145.13	101.98
Pr(III): L-Thr:Mg(II)	22504.73	22463.44	21337.64	21252.64	20748.45	20691.99	16969.73	17141.87	102.16
Solvent: 1,4-Dioxane (C₄H₈O₂:H₂O)									
Pr(III)	22510.30	22471.72	21340.96	21261.86	20762.45	20702.27	16975.82	17147.76	101.15
Pr(III):L-Thr	22504.38	22465.37	21335.65	21255.48	20757.65	20696.25	16968.69	17143.53	102.82
Pr(III): L-Thr:Mg(II)	22501.41	22458.38	21328.87	21248.28	20750.88	20689.10	16960.74	17138.79	104.72
Solvent: Acetonitrile (CH₃CN:H₂O)									
Pr(III)	22518.47	22467.04	21339.01	21257.52	20762.44	20698.80	16958.40	17144.79	109.63
Pr(III):L-Thr	22516.16	22459.24	21335.76	21249.83	20757.70	20691.75	16943.32	17139.65	115.67
Pr(III): L-Thr:Mg(II)	22512.97	22455.73	21332.03	21246.33	20755.29	20688.49	16939.68	17137.32	116.35
Solvent: DMF (C₃H₇NO:H₂O)									
Pr(III)	22497.15	22430.90	21297.29	21222.33	20745.04	20667.38	16909.60	17121.15	123.28
Pr(III):L-Thr	22492.15	22425.83	21292.44	21217.17	20740.56	20662.37	16905.10	17117.74	123.89
Pr(III): L-Thr:Mg(II)	22487.02	22421.38	21287.14	21212.58	20736.08	20657.80	16902.85	17114.72	123.37

Table 2.9: Observed and computed values of energies (cm^{-1}) and R.M.S values of Pr(III) with L-Tryptophan in absence and presence of Mg(II) systems in 50% (v/v) aquated solvents (Methanol, 1,4-Dioxane, Acetonitrile and Dimethylformamide)

System	$^3H_4\rightarrow {}^3P_2$		$^3H_4\rightarrow {}^3P_1$		$^3H_4\rightarrow {}^3P_0$		$^3H_4\rightarrow {}^1D_2$		R.M.S
	E_{obs}	E_{cal}	E_{obs}	E_{cal}	E_{obs}	E_{cal}	E_{obs}	E_{cal}	
Solvent: Methanol (CH$_3$OH:H$_2$O)									
Pr(III)	22517.78	22473.87	21347.22	21263.24	20757.56	20702.22	16977.67	17148.87	101.68
Pr(III):L-Trp	22508.37	22464.34	21335.15	21253.76	20751.22	20693.42	16969.42	17142.55	102.32
Pr(III): L-Trp:Mg(II)	22504.22	22461.12	21332.32	21250.51	20748.52	20690.31	16966.87	17140.40	102.53
Solvent: 1,4-Dioxane (C$_4$H$_8$O$_2$:H$_2$O)									
Pr(III)	22510.20	22471.88	21340.88	21261.97	20762.17	20702.29	16976.65	17147.84	100.74
Pr(III):L-Trp	22505.01	22466.70	21336.73	21256.71	20757.72	20697.22	16971.43	17144.37	101.78
Pr(III): L-Trp:Mg(II)	22502.33	22460.71	21335.06	21250.88	20754.58	20691.99	16959.37	17140.45	106.69
Solvent: Acetonitrile (CH$_3$CN:H$_2$O)									
Pr(III)	22523.45	22470.87	21343.13	21260.99	20762.13	20701.41	16964.12	17147.19	108.06
Pr(III):L-Trp	22518.58	22466.07	21336.85	21256.10	20757.94	20696.66	16961.10	17143.96	107.79
Pr(III): L-Trp:Mg(II)	22510.15	22461.33	21335.50	21251.68	20756.90	20693.07	16954.05	17140.94	110.01
Solvent: DMF (C$_3$H$_7$NO:H$_2$O)									
Pr(III)	22497.17	22431.14	21297.26	21222.54	20744.92	20667.52	16910.43	17121.30	122.88
Pr(III):L-Trp	22492.30	22425.95	21292.21	21217.25	20740.32	20662.38	16905.75	17117.80	123.55
Pr(III): L-Trp:Mg(II)	22486.96	22420.92	21287.43	21212.15	20736.02	20657.46	16901.37	17114.43	124.09

Table 2.10: Observed and computed values of energies (cm^{-1}) and R.M.S values of Pr(III) with L-Isoleucine in absence and presence of Mg(II) systems in 50% (v/v) aquated solvents (Methanol, 1,4-Dioxane, Acetonitrile and Dimethylformamide)

System	$^3H_4 \rightarrow {}^3P_2$		$^3H_4 \rightarrow {}^3P_1$		$^3H_4 \rightarrow {}^3P_0$		$^3H_4 \rightarrow {}^1D_2$		R.M.S
	E_{obs}	E_{cal}	E_{obs}	E_{cal}	E_{obs}	E_{cal}	E_{obs}	E_{cal}	
Solvent: Methanol (CH$_3$OH:H$_2$O)									
Pr(III)	22510.25	22470.96	21340.84	21261.13	20762.17	20701.64	16973.94	17147.27	101.98
Pr(III):L-Ile	22506.53	22465.19	21337.94	21255.50	20759.18	20696.61	16963.85	17143.49	105.70
Pr(III): L-Ile:Mg(II)	22504.67	22459.49	21336.11	21249.96	20756.33	20691.66	16952.00	17139.76	110.57
Solvent: 1,4-Dioxane (C$_4$H$_8$O$_2$:H$_2$O)									
Pr(III)	22527.50	22471.96	21342.56	21262.03	20762.75	20702.32	16964.71	17147.89	108.14
Pr(III):L-Ile	22522.93	22467.09	21339.70	21257.21	20759.60	20697.89	16957.94	17144.67	110.23
Pr(III): L-Ile:Mg(II)	22511.13	22456.43	21333.98	21246.88	20754.25	20688.72	16942.46	17137.72	115.11
Solvent: Acetonitrile (CH$_3$CN:H$_2$O)									
Pr(III)	22514.99	22472.47	21346.93	21261.96	20757.42	20701.22	16975.56	17147.99	102.37
Pr(III):L-Ile	22507.15	22465.83	21339.67	21255.16	20751.27	20694.57	16971.33	17143.51	102.11
Pr(III): L-Ile:Mg(II)	22502.30	22461.65	21335.39	21250.82	20746.84	20690.21	16968.95	17140.66	101.85
Solvent: DMF (C$_3$H$_7$NO:H$_2$O)									
Pr(III)	22497.13	22430.54	21297.24	21221.99	20744.89	20667.08	16908.72	17120.92	123.67
Pr(III):L-Ile	22491.62	22426.50	21293.70	21217.92	20741.66	20663.22	16905.53	17118.22	123.87
Pr(III): L-Ile:Mg(II)	22486.43	22421.45	21288.10	21212.66	20736.18	20657.90	16902.64	17114.78	123.53

Table 2.11: Observed and computed values of Oscillator Strength (P x 10^6) and Judd-Ofelt (T$_\lambda$ x 10^{10}) parameters of the different Pr(III) systems with L-Glutamine in absence and presence of Mg(II) in 50% (v/v) aquated solvents (Methanol, 1,4-Dioxane, Acetonitrile and Dimethylformamide)

System	$^3H_4 \rightarrow {}^3P_2$		$^3H4 \rightarrow {}^3P_1$		$^3H_4 \rightarrow {}^3P_0$		$^3H_4 \rightarrow {}^1D_2$		T$_2$	T$_4$	T$_6$
	Pobs	Pcal	Pobs	Pcal	Pobs	Pcal	Pobs	Pcal			
Solvent: Methanol											
Pr(III)	4.2786	4.2786	1.8109	1.2347	0.6484	1.2159	1.3432	1.3432	20.157	3.389	13.112
Pr(III):L-Gln	4.5169	4.5169	1.8061	1.2570	0.6971	1.2379	1.7043	1.7043	86.518	3.451	13.890
Pr(III): L-Gln:Mg(II)	4.5761	4.5761	2.0029	1.3819	0.7497	1.3614	1.8822	1.8822	122.698	3.796	13.997
Solvent:1,4-Dioxane											
Pr(III)	5.7027	5.7027	1.9262	1.3767	0.8146	1.3558	1.3543	1.3543	-71.4617	3.7790	17.6824
Pr(III):L-Gln	5.7999	5.7999	2.0559	1.4572	0.8455	1.4351	1.5452	1.5452	-34.8680	4.0016	17.9495
Pr(III): L-Gln:Mg(II)	5.9165	5.9165	2.1966	1.5589	0.9071	1.5352	1.7804	1.7804	10.5206	4.2816	18.2653
Solvent: Acetonitrile											
Pr(III)	5.9400	5.9400	2.2267	1.5668	0.8928	1.5425	1.6625	1.6625	-17.861	4.300	18.319
Pr(III):L-Gln	6.1216	6.1216	2.4206	1.7099	0.9839	1.6836	2.0522	2.0522	58.138	4.694	18.811
Pr(III): L-Gln:Mg(II)	6.7873	6.7873	2.8905	2.0366	1.1644	2.0051	2.5784	2.5784	133.039	5.591	20.760
Solvent: DMF											
Pr(III)	8.2261	8.2261	3.2501	2.3220	1.3745	2.2898	2.3095	2.3095	-21.868	6.387	25.277
Pr(III):L-Gln	8.3564	8.3564	3.4577	2.4385	1.3996	2.4046	2.5921	2.5921	33.298	6.710	25.630
Pr(III): L-Gln:Mg(II)	8.5792	8.5792	3.5410	2.5540	1.5452	2.5184	2.9330	2.9330	95.888	7.029	26.283

Table 2.12: Observed and computed values of Oscillator Strength (P x 10^6) and Judd-Ofelt (T$_\lambda$ x 10^{10}) parameters of the different Pr(III) systems with L-Threonine in absence and presence of Mg(II) in 50% (v/v) aquated solvents (Methanol, 1,4-Dioxane, Acetonitrile and Dimethylformamide)

System	$^3H_4 \rightarrow ^3P_2$		$^3H4 \rightarrow ^3P_1$		$^3H_4 \rightarrow ^3P_0$		$^3H_4 \rightarrow ^1D_2$		T$_2$	T$_4$	T$_6$
	Pobs	Pcal	Pobs	Pcal	Pobs	Pcal	Pobs	Pcal			
Solvent: Methanol											
Pr(III)	3.9543	3.9543	1.7538	1.1872	0.6114	1.1694	1.3072	1.3072	33.377	3.259	12.089
Pr(III):L-Thr	3.9956	3.9956	1.7337	1.2085	0.6731	1.1903	1.6262	1.6262	103.246	3.318	12.210
Pr(III): L-Thr:Mg(II)	4.3719	4.3719	1.9030	1.3155	0.7170	1.2957	1.6940	1.6940	93.676	3.613	13.366
Solvent: 1,4-Dioxane											
Pr(III)	5.2287	5.2287	2.0106	1.3936	0.7648	1.3725	1.4687	1.4687	-14.655	3.825	16.121
Pr(III):L-Thr	5.4231	5.4231	2.0417	1.4180	0.7823	1.3965	1.6229	1.6229	7.497	3.893	16.744
Pr(III): L-Thr:Mg(II)	5.7166	5.7166	2.2490	1.5715	0.8806	1.5478	1.6305	1.6305	-10.409	4.316	17.596
Solvent: Acetonitrile											
Pr(III)	5.8092	5.8092	2.2034	1.5396	0.8621	1.5155	1.7207	1.7207	3.960	4.225	17.912
Pr(III):L-Thr	5.8266	5.8266	2.4500	1.6972	0.9296	1.6706	2.0101	2.0101	67.856	4.659	17.858
Pr(III): L-Thr:Mg(II)	6.2492	6.2492	2.5598	1.8135	1.0505	1.7851	2.3639	2.3639	119.951	4.979	19.163
Solvent: DMF											
Pr(III)	8.0078	8.0078	3.1546	2.2478	1.3224	2.2165	2.3395	2.3395	-0.637	6.183	24.617
Pr(III):L-Thr	8.3319	8.3319	3.3783	2.4148	1.4311	2.3811	2.6267	2.6267	42.909	6.644	25.563
Pr(III): L-Thr:Mg(II)	8.3505	8.3505	3.5133	2.4722	1.4111	2.4378	2.8402	2.8402	90.018	6.803	25.588

Table 2.13: Observed and computed values of Oscillator Strength (P x 10^6) and Judd-Ofelt (T_λ x 10^{10}) parameters of the different Pr(III) systems with L-Tryptophan in absence and presence of Mg(II) in 50% (v/v) aquated solvents (Methanol, 1,4-Dioxane, Acetonitrile and Dimethylformamide)

System	$^3H_4 \rightarrow {}^3P_2$		$^3H4 \rightarrow {}^3P_1$		$^3H_4 \rightarrow {}^3P_0$		$^3H_4 \rightarrow {}^1D_2$		T_2	T_4	T_6
	Pobs	Pcal	Pobs	Pcal	Pobs	Pcal	Pobs	Pcal			
Solvent: Methanol											
Pr(III)	4.1215	4.1215	1.7158	1.1927	0.6593	1.1745	1.3745	1.3745	37.636	3.274	12.630
Pr(III):L-Trp	4.1890	4.1890	1.8162	1.2510	0.6755	1.2321	1.5161	1.5161	65.108	3.435	12.811
Pr(III): L-Trp:Mg(II)	4.7161	4.7161	1.9270	1.3301	0.7221	1.3099	1.5485	1.5485	37.693	3.652	14.486
Solvent: 1,4-Dioxane											
Pr(III)	5.2886	5.2886	2.0604	1.4312	0.7899	1.4096	1.5278	1.5278	-5.354	3.929	16.289
Pr(III):L-Trp	5.7704	5.7704	2.2433	1.5686	0.8803	1.5448	1.6296	1.6296	-14.298	4.307	17.772
Pr(III): L-Trp:Mg(II)	5.8420	5.8420	2.4662	1.6974	0.9145	1.6715	1.7284	1.7284	3.209	4.661	17.915
Solvent: Acetonitrile											
Pr(III)	5.9808	5.9808	2.1306	1.5129	0.8813	1.4892	1.6562	1.6562	-21.792	4.152	18.493
Pr(III):L-Trp	7.0290	7.0290	2.6333	1.8467	1.0438	1.8183	2.2560	2.2560	44.333	5.071	21.692
Pr(III): L-Trp:Mg(II)	7.3839	7.3839	2.6517	1.9237	1.1772	1.8941	2.3120	2.3120	33.486	5.283	22.804
Solvent: DMF											
Pr(III)	8.0855	8.0855	3.1959	2.2625	1.3105	2.2309	2.3738	2.3738	1.994	6.223	24.861
Pr(III):L-Trp	8.1407	8.1407	3.2893	2.3524	1.3957	2.3196	2.6099	2.6099	51.815	6.472	24.982
Pr(III): L-Trp:Mg(II)	8.3493	8.3493	3.4333	2.4659	1.4776	2.4316	2.7906	2.7906	78.887	6.786	25.589

Table 2.14: Observed and computed values of Oscillator Strength (P x 10^6) and Judd-Ofelt (T$_\lambda$ x 10^{10}) parameters of the different Pr(III) systems with L-Isoleucine in absence and presence of Mg(II) in 50% (v/v) aquated solvents (Methanol, 1,4-Dioxane, Acetonitrile and Dimethylformamide)

System	$^3H_4 \rightarrow ^3P_2$		$^3H4 \rightarrow ^3P_1$		$^3H_4 \rightarrow ^3P_0$		$^3H_4 \rightarrow ^1D_2$		T$_2$	T$_4$	T$_6$
	Pobs	Pcal	Pobs	Pcal	Pobs	Pcal	Pobs	Pcal			
Solvent: Methanol											
Pr(III)	4.2573	4.2573	1.6525	1.1450	0.6277	1.1276	1.4370	1.4370	43.042	3.143	13.110
Pr(III):L-Ile	4.1921	4.1921	1.8719	1.2970	0.7111	1.2773	1.7353	1.7353	114.593	3.561	12.785
Pr(III): L-Ile:Mg(II)	4.6933	4.6933	1.9273	1.3428	0.7468	1.3224	1.9895	1.9895	139.496	3.687	14.401
Solvent: 1,4-Dioxane											
Pr(III)	5.1932	5.1932	2.1007	1.4522	0.7915	1.4302	1.5670	1.5670	9.7805	3.9863	15.9612
Pr(III):L-Ile	5.7569	5.7569	2.3236	1.6325	0.9272	1.6078	1.9126	1.9126	50.7292	4.4820	17.6798
Pr(III): L-Ile:Mg(II)	5.9704	5.9704	2.5081	1.7053	0.8888	1.6794	2.0303	2.0303	63.4669	4.6822	18.3280
Solvent: Acetonitrile											
Pr(III)	5.7753	5.7753	2.2842	1.5935	0.8886	1.5685	2.0261	2.0261	75.207	4.373	17.762
Pr(III):L-Ile	6.1538	6.1538	2.4792	1.7468	0.9987	1.7196	1.8551	1.8551	11.107	4.795	18.897
Pr(III): L-Ile:Mg(II)	6.4053	6.4053	2.8194	2.0008	1.1637	1.9695	2.4553	2.4553	129.792	5.494	19.540
Solvent: DMF											
Pr(III)	8.0719	8.0719	3.1503	2.2747	1.3795	2.2430	2.3328	2.3328	-6.439	6.257	24.808
Pr(III):L-Ile	8.6848	8.6848	3.8986	2.8168	1.7108	2.7775	2.8904	2.8904	78.378	7.749	26.427
Pr(III): L-Ile:Mg(II)	9.5563	9.5563	3.9545	2.8955	1.8108	2.8551	3.5827	3.5827	178.421	7.968	29.235

<u>Comparative UV-Vis. absorption spectra of Pr(III) with the selected amino acids in different aquated solvents</u>

1. **L-Glutamine**
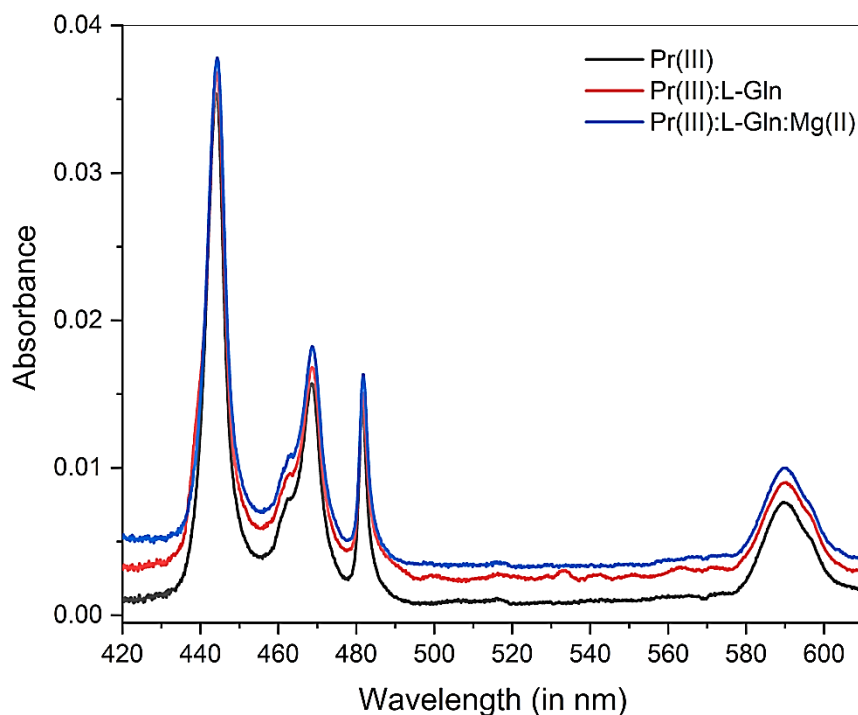
Fig. 2.2: Comparative UV-Vis. absorption spectra of Pr(III), Pr(III):L-Gln and Pr(III):L-Gln:Mg(II) in methanol: water (50% v/v) solvent
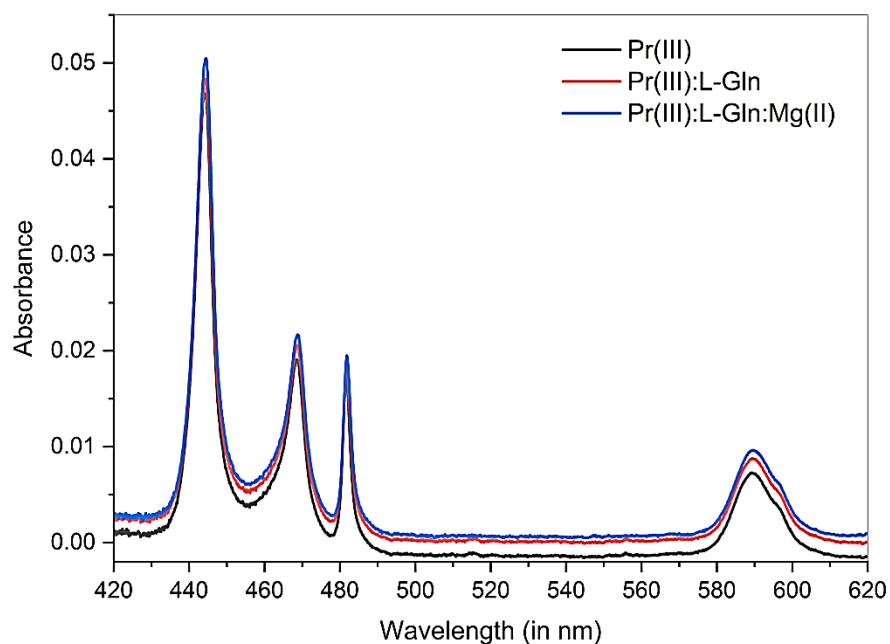
Fig. 2.3: Comparative UV-Vis. absorption spectra of Pr(III), Pr(III):L-Gln and Pr(III):L-Gln:Mg(II) in 1,4-dioxane: water (50% v/v) solvent
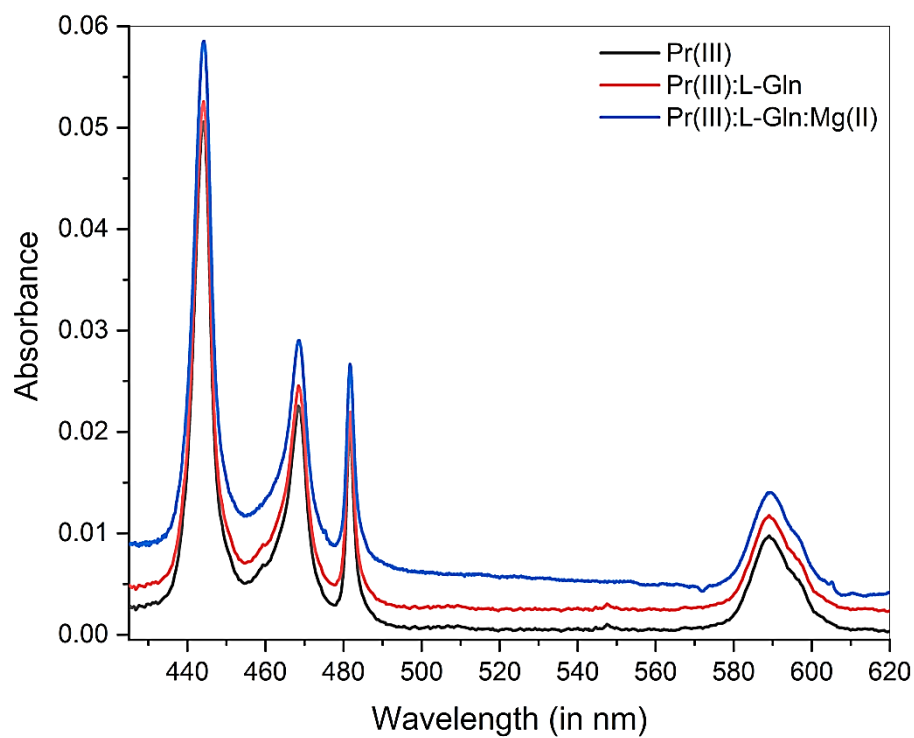
Fig. 2.4: Comparative UV-Vis. absorption spectra of Pr(III), Pr(III):L-Gln and Pr(III):L-Gln:Mg(II) in acetonitrile: water (50% v/v) solvent
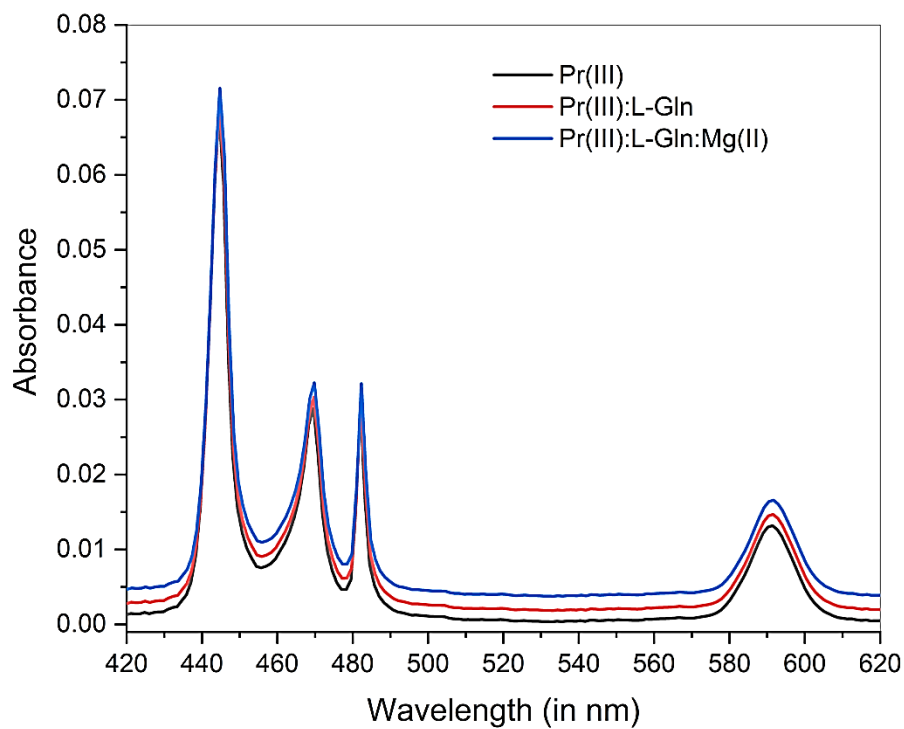
Fig. 2.5: Comparative UV-Vis. absorption spectra of Pr(III), Pr(III):L-Gln and Pr(III):L-Gln:Mg(II) in DMF: water (50% v/v) solvent
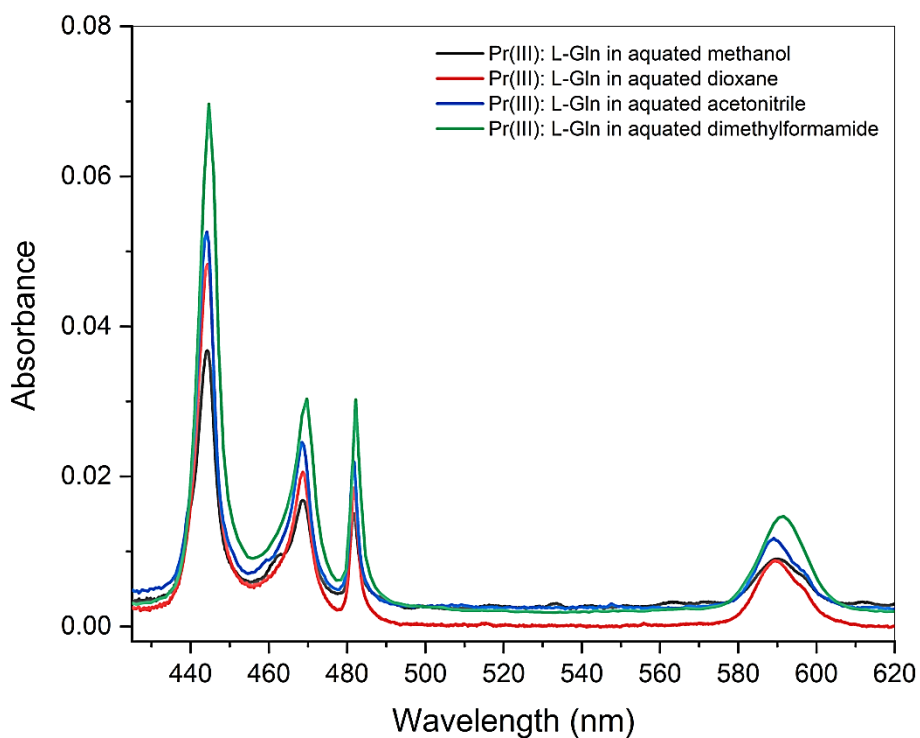
Fig. 2.6: Comparative UV-Vis. absorption spectra of Pr(III):L-Gln
in different aquated solvents

2. L-Threonine
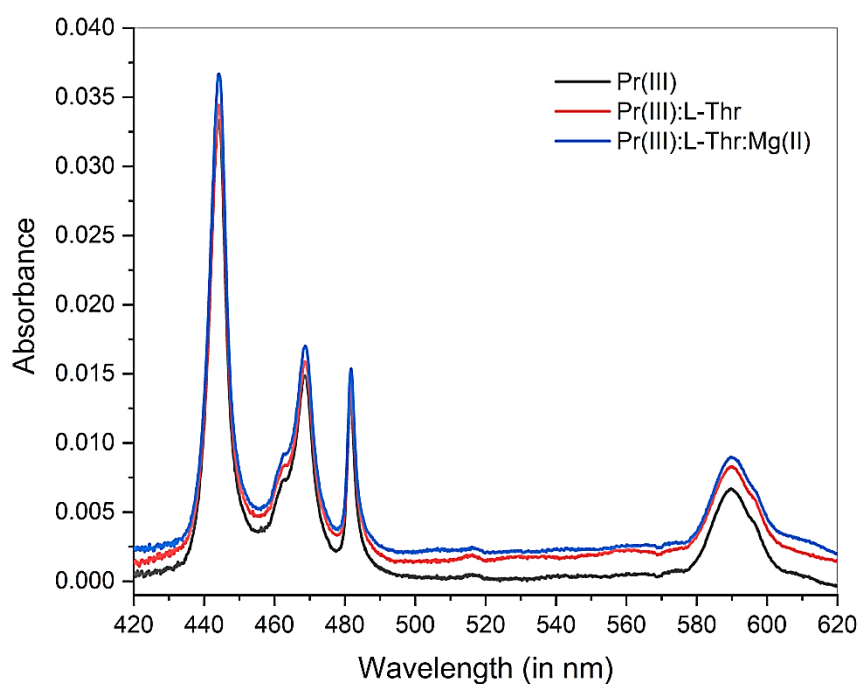
Fig. 2.7: Comparative UV-Vis. absorption spectra of Pr(III), Pr(III):L-Thr and
Pr(III):L-Thr:Mg(II) in methanol: water (50% v/v) solvent
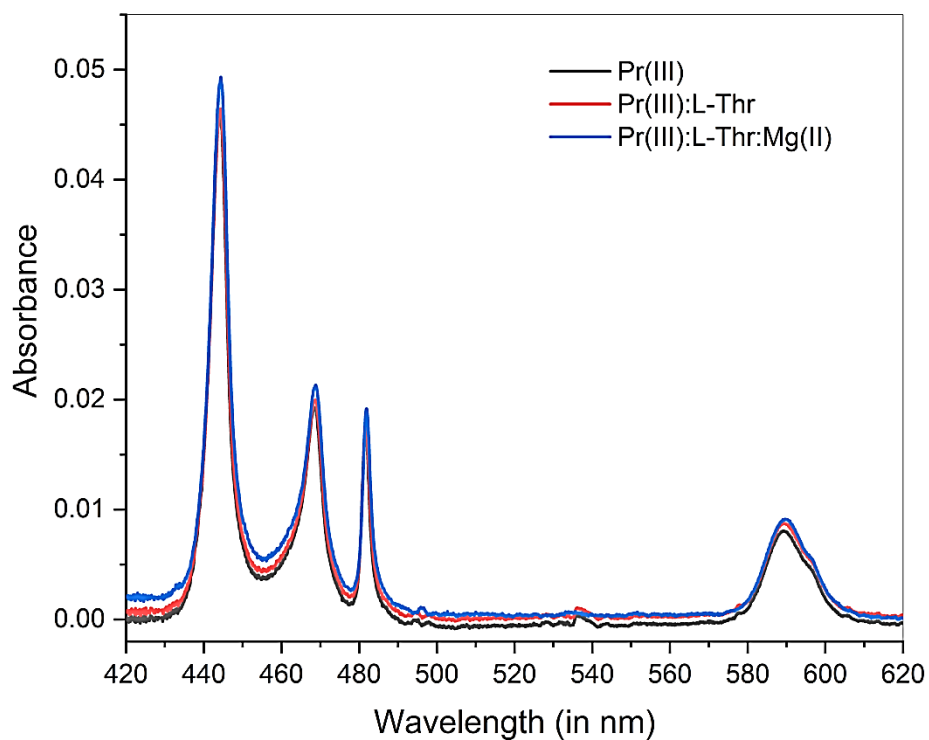
Fig. 2.8: Comparative UV-Vis. absorption spectra of Pr(III), Pr(III):L-Thr and Pr(III):L-Thr:Mg(II) in 1,4-dioxane: water (50% v/v) solvent
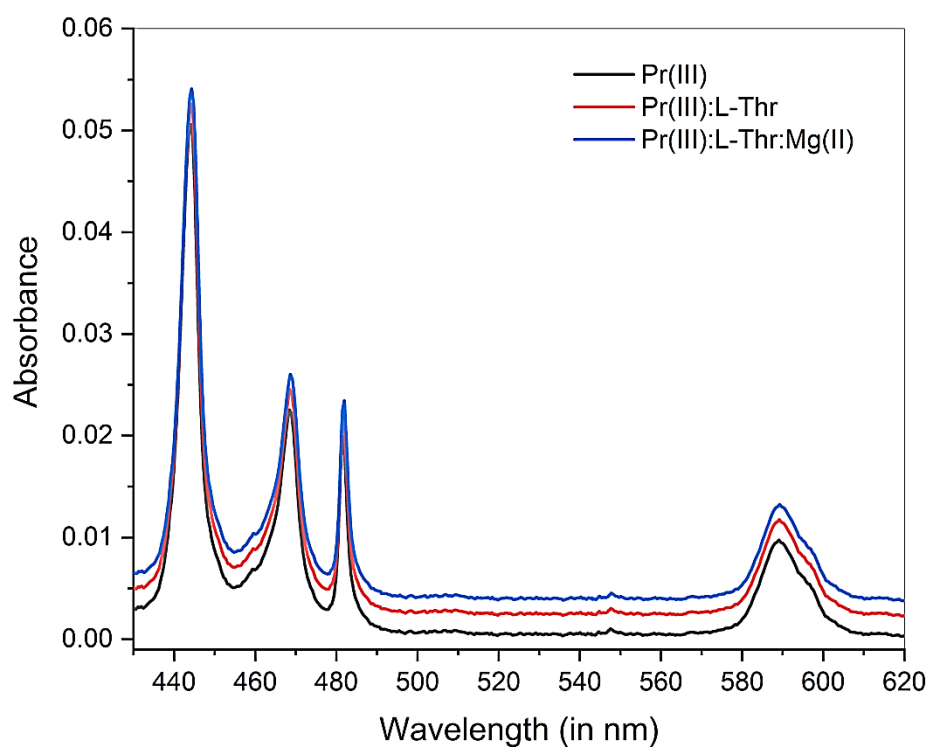
Fig. 2.9: Comparative UV-Vis. absorption spectra of Pr(III), Pr(III):L-Thr and Pr(III):L-Thr:Mg(II) in acetonitrile: water (50% v/v) solvent
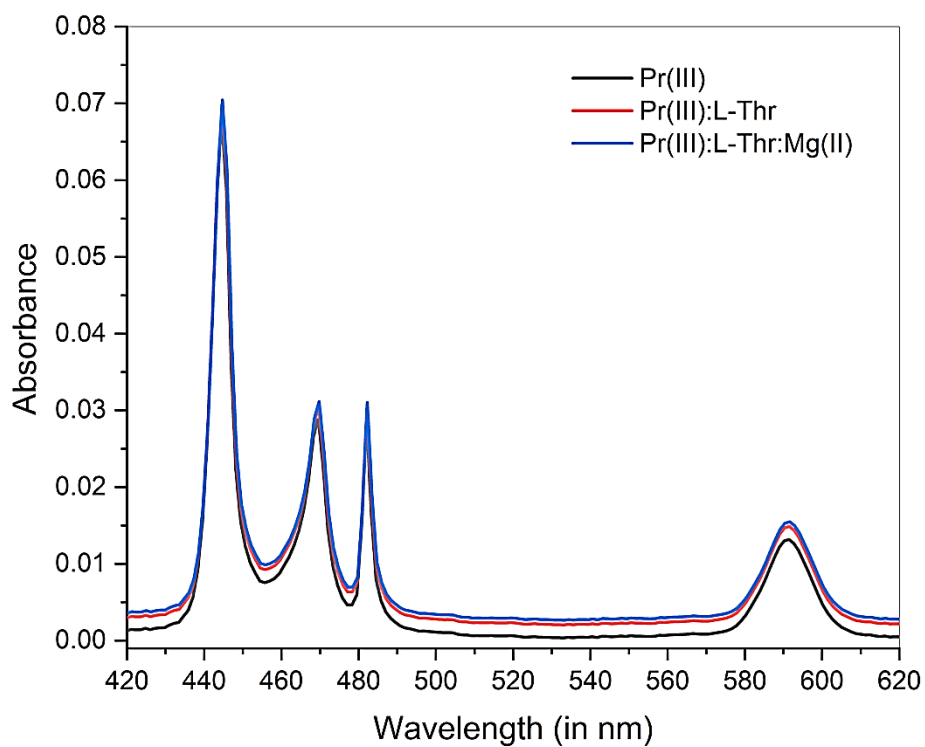
Fig. 2.10: Comparative UV-Vis. absorption spectra of Pr(III), Pr(III):L-Thr and Pr(III):L-Thr:Mg(II) in DMF: water (50% v/v) solvent
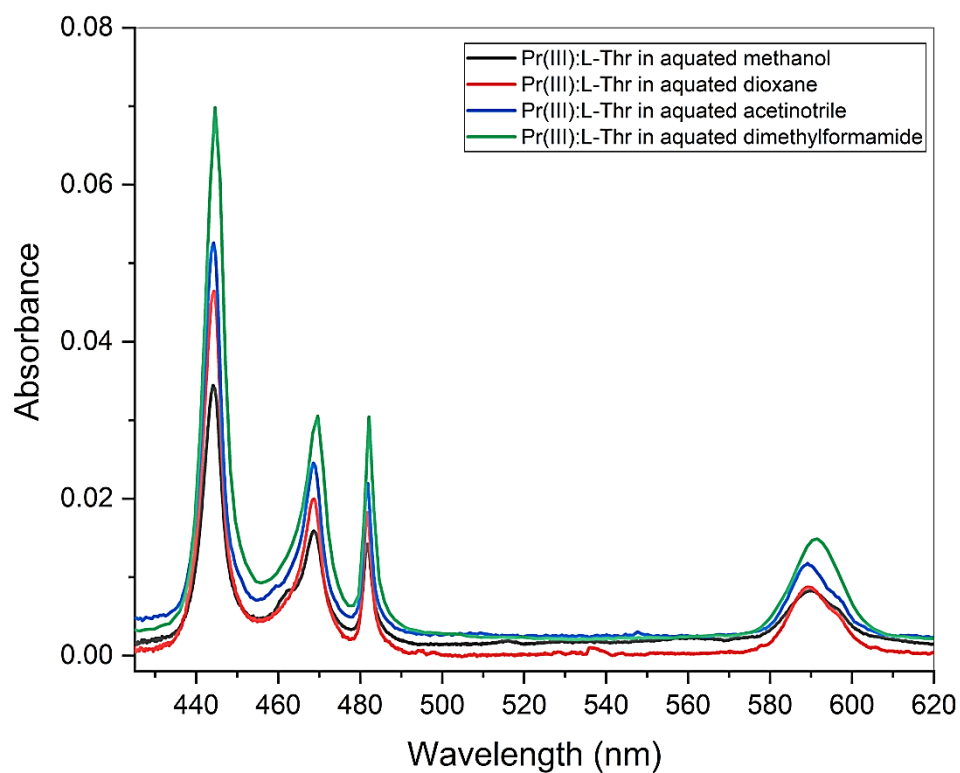
Fig. 2.11: Comparative UV-Vis. absorption spectra of Pr(III):L-Thr in different aquated solvents

3. L-Tryptophan
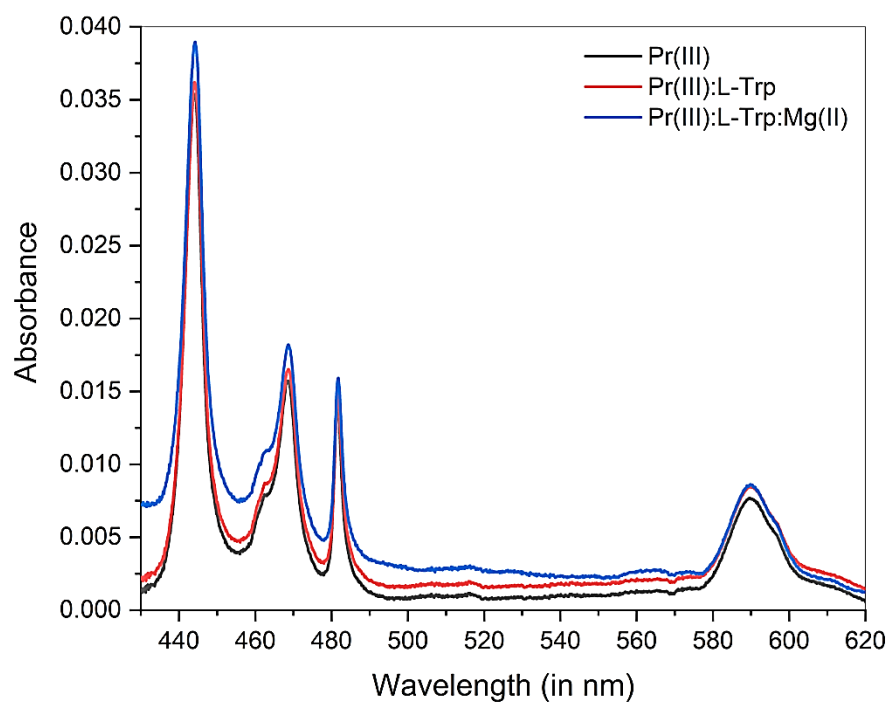
Fig. 2.12: Comparative UV-Vis. absorption spectra of Pr(III), Pr(III):L-Trp and Pr(III):L-Trp:Mg(II) in methanol: water (50% v/v) solvent
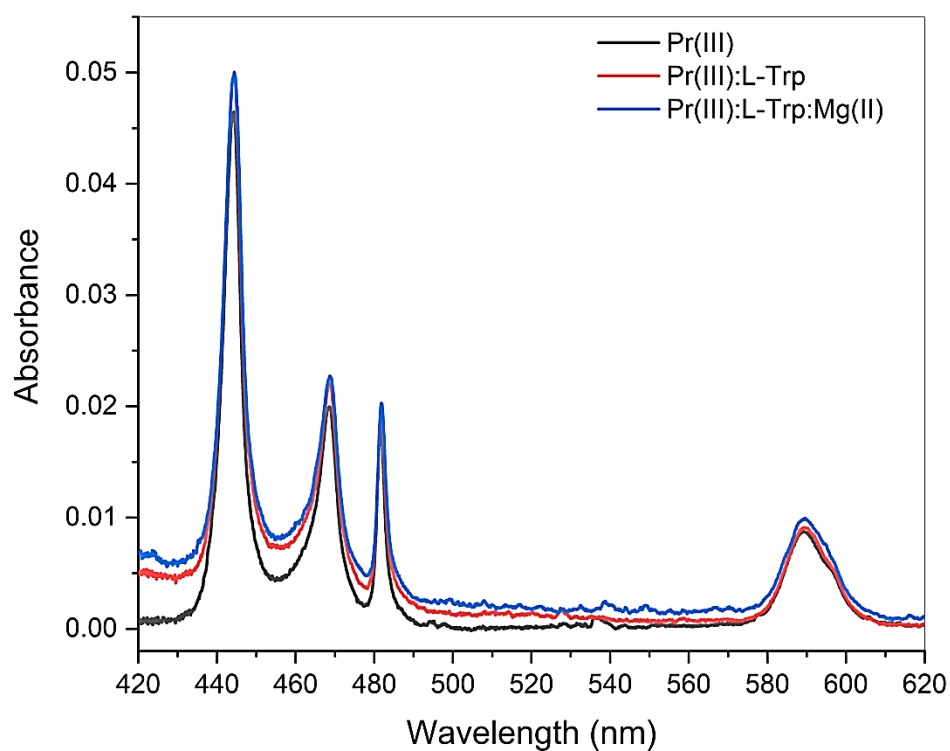
Fig. 2.13: Comparative UV-Vis. absorption spectra of Pr(III), Pr(III):L-Trp and Pr(III):L-Trp:Mg(II) in 1,4-dioxane: water (50% v/v) solvent
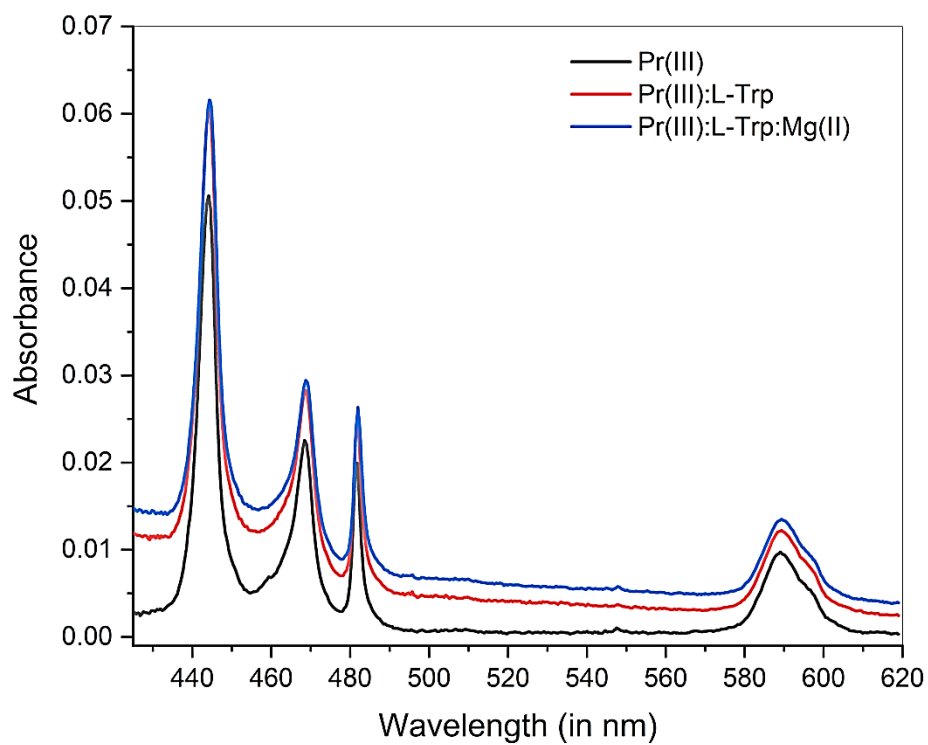
Fig. 2.14: Comparative UV-Vis. absorption spectra of Pr(III), Pr(III):L-Trp and Pr(III):L-Trp:Mg(II) in acetonitrile: water (50% v/v) solvent
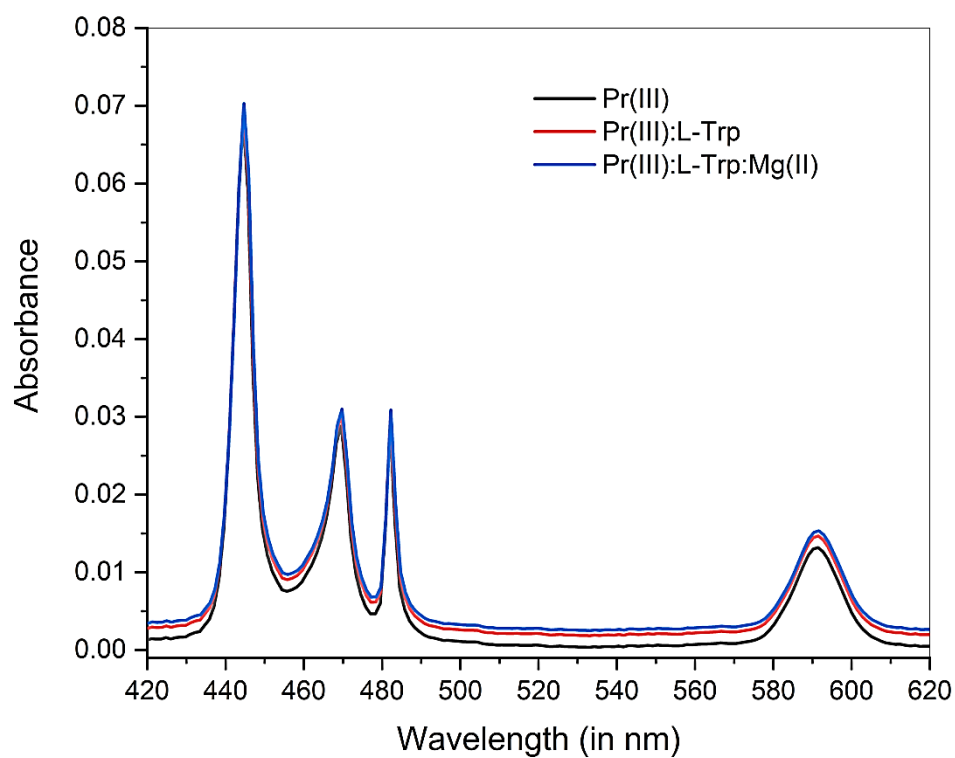
Fig. 2.15: Comparative UV-Vis. absorption spectra of Pr(III), Pr(III):L-Trp and Pr(III):L-Trp:Mg(II) in DMF: water (50% v/v) solvent
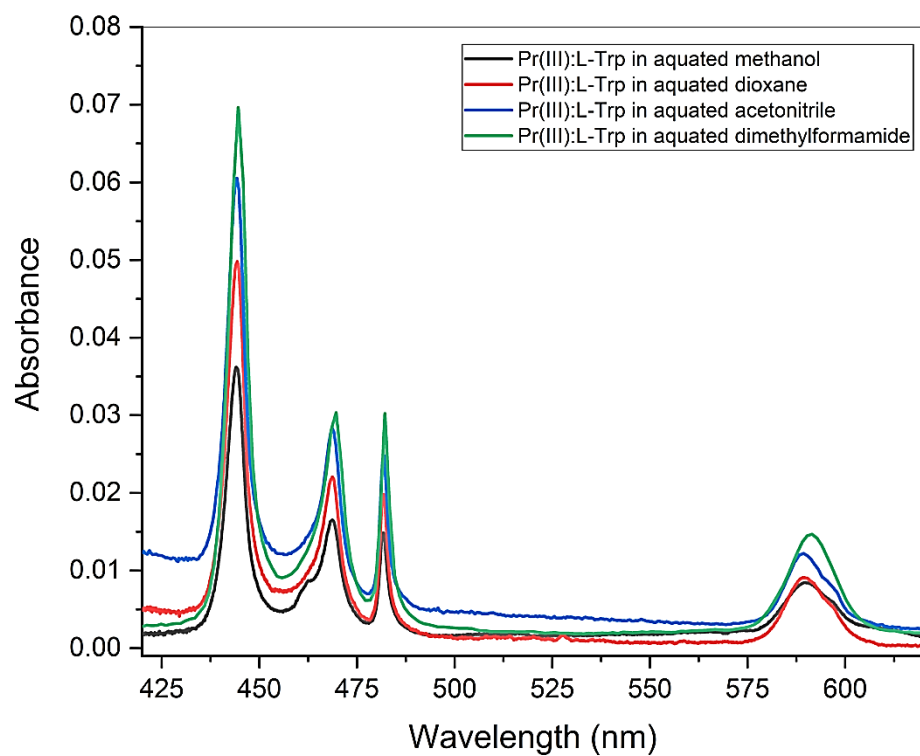
Fig. 2.16: Comparative UV-Vis. absorption spectra of Pr(III):L-Trp
in different aquated solvents

4. L-Isoleucine
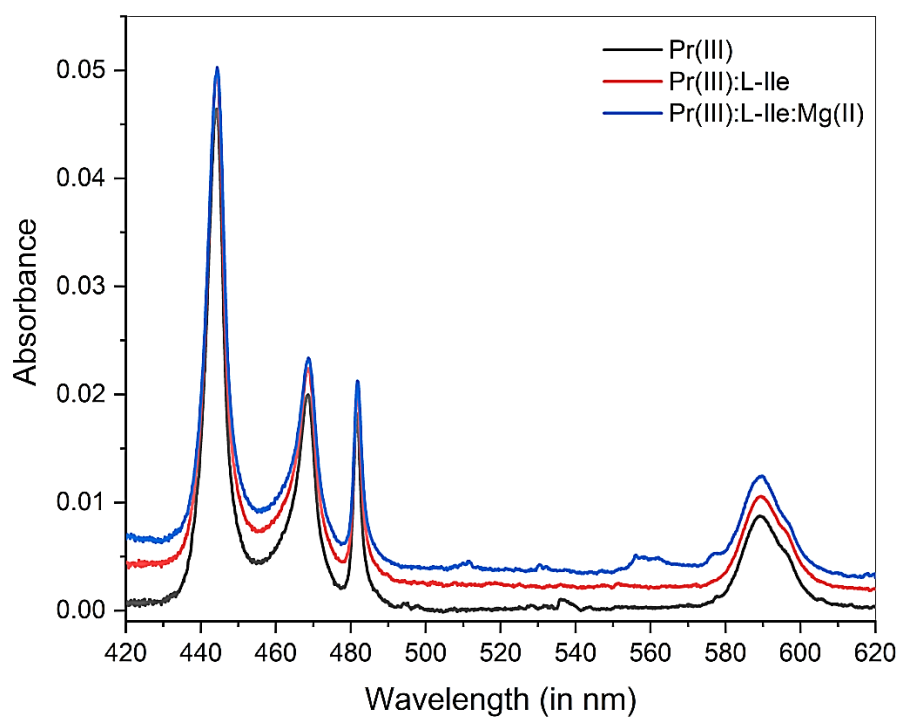
Fig. 2.17: Comparative UV-Vis. absorption spectra of Pr(III), Pr(III):L-Ile and
Pr(III):L-Ile:Mg(II) in methanol: water (50% v/v) solvent
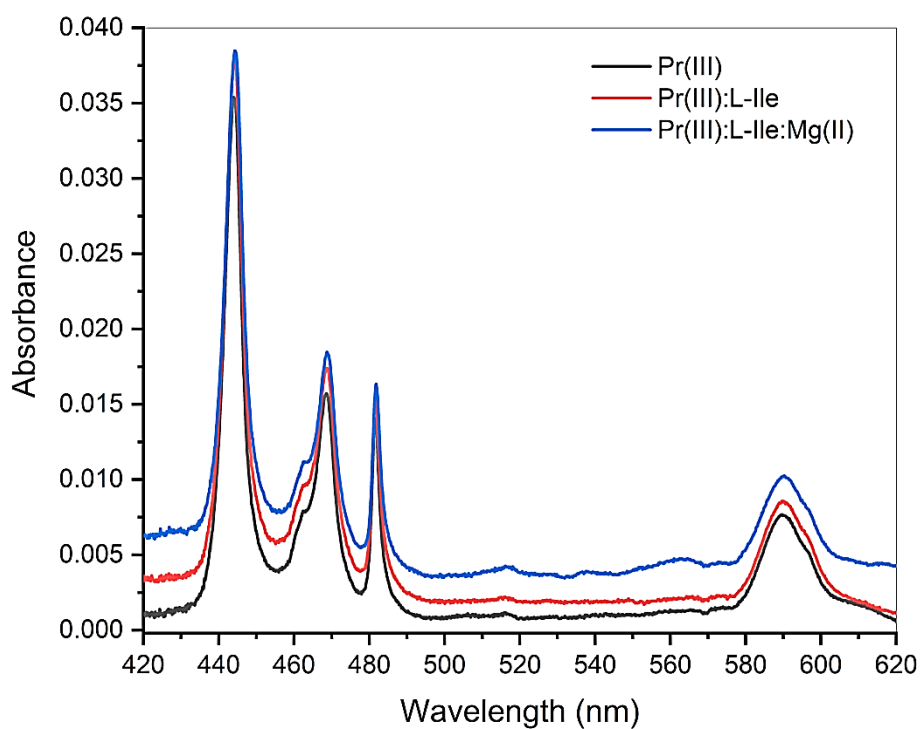
Fig. 2.18: Comparative UV-Vis. absorption spectra of Pr(III), Pr(III):L-Ile and Pr(III):L-Ile:Mg(II) in 1,4-dioxane: water (50% v/v) solvent
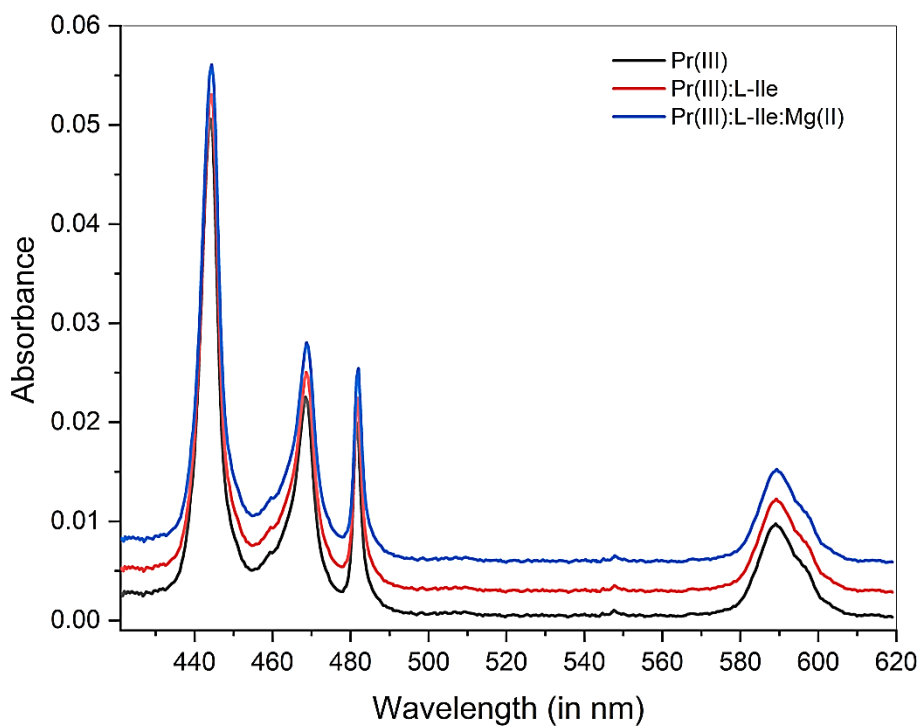
Fig. 2.19: Comparative UV-Vis. absorption spectra of Pr(III), Pr(III):L-Ile and Pr(III):L-Ile:Mg(II) in acetonitrile: water (50% v/v) solvent
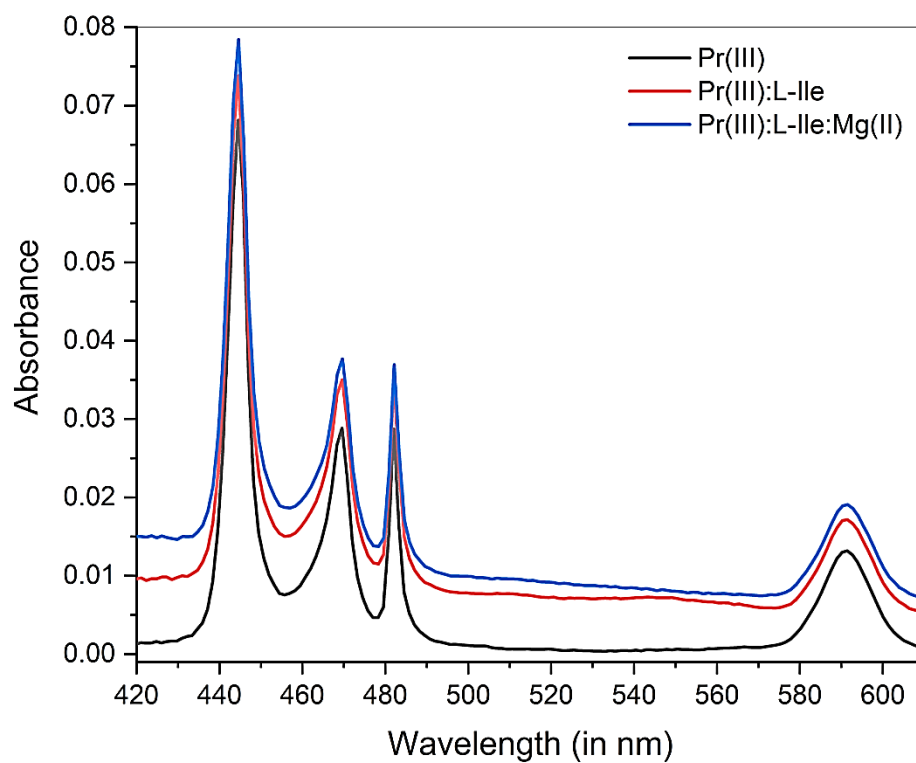
Fig. 2.20: Comparative UV-Vis. absorption spectra of Pr(III), Pr(III):L-Ile and Pr(III):L-Ile:Mg(II) in DMF: water (50% v/v) solvent
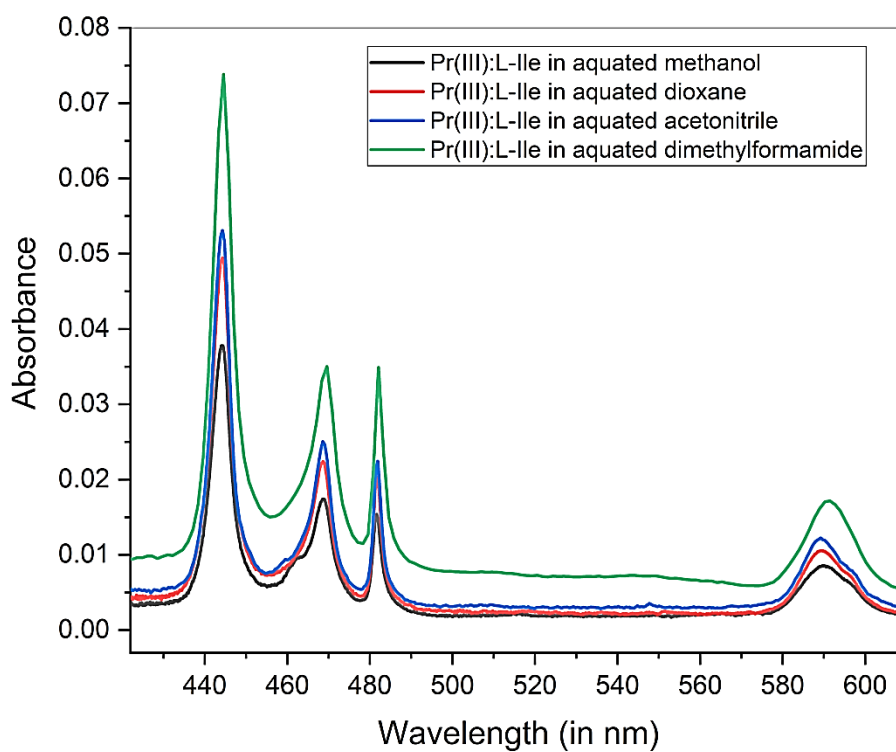
Fig. 2.21: Comparative UV-Vis. absorption spectra of Pr(III):L-Ile in different aquated solvents

Table 2.15: Computed values of the energy interaction parameters: Slater-Condon factor F_k (cm^{-1}), Lande's Spin-orbit interactions ξ_{4f} (cm^{-1}), Racah (E^k), Nephelauxetic ratio (β), Bonding ($b^{1/2}$) and Percent covalency (δ) for the different Pr(III) systems with L-Glutamine in absence and presence of Mg(II) in 50% (v/v) aquated DMF solvent at pH 2, 4 and 6

System	F_2	F_4	F_6	ξ_{4f}	E^1	E^2	E^3	β	$b^{1/2}$	δ
Solvent: DMF: H$_2$O	At pH = 2									
Pr(III)	308.9767	42.6542	4.6655	720.3942	3508.3229	23.7414	614.2664	0.9451	0.1657	5.8103
Pr(III):L-Gln	308.9314	42.6480	4.6649	719.9795	3507.8084	23.7379	614.1763	0.9447	0.1662	5.8495
Pr(III): L-Gln:Mg(II)	308.8924	42.6426	4.6643	719.8854	3507.3653	23.7349	614.0987	0.9446	0.1664	5.8631
	At pH = 4									
Pr(III)	309.0063	42.6583	4.6660	720.1138	3508.6581	23.7437	614.3251	0.9449	0.1659	5.8270
Pr(III):L-Gln	308.9123	42.6453	4.6646	719.8204	3507.5911	23.7365	614.1382	0.9446	0.1664	5.8649
Pr(III): L-Gln:Mg(II)	308.8365	42.6349	4.6634	719.6094	3506.7304	23.7307	613.9875	0.9443	0.1678	5.8935
	At pH = 6									
Pr(III)	309.1282	42.6752	4.6678	719.1340	3510.0429	23.7531	614.5675	0.9444	0.1665	5.8721
Pr(III):L-Gln	309.0048	42.6581	4.6660	719.0932	3508.6418	23.7436	614.3222	0.9443	0.1667	5.8935
Pr(III): L-Gln:Mg(II)	308.9154	42.6458	4.6646	719.0869	3507.6267	23.7367	614.1445	0.9442	0.1669	5.8976

Table 2.16: Computed values of the energy interaction parameters: Slater-Condon factor F_k (cm^{-1}), Lande's Spin-orbit interactions ξ_{4f} (cm^{-1}), Racah (E^k), Nephelauxetic ratio (β), Bonding ($b^{1/2}$) and Percent covalency (δ) for the different Pr(III) systems with L-Threonine in absence and presence of Mg(II) in 50% (v/v) aquated DMF solvent at pH 2, 4 and 6

System	F_2	F_4	F_6	ξ_{4f}	E^1	E^2	E^3	β	$b^{1/2}$	δ
Solvent-DMF:H$_2$O	At pH = 2									
Pr(III)	308.9429	42.6496	4.6650	720.2109	3507.9386	23.7388	614.1991	0.9449	0.1660	5.8299
Pr(III):L-Thr	308.9227	42.6468	4.6647	719.9360	3507.7092	23.7373	614.1589	0.9447	0.1663	5.8543
Pr(III): L-Thr:Mg(II)	308.8307	42.6341	4.6633	719.9030	3506.6649	23.7302	613.9761	0.9445	0.1665	5.8719
	At pH = 4									
Pr(III)	309.0804	42.6686	4.6671	719.9390	3509.5004	23.7494	614.4725	0.9449	0.1659	5.8282
Pr(III):L-Thr	308.9333	42.6482	4.6649	719.9015	3507.8291	23.7381	614.1799	0.9447	0.1663	5.8552
Pr(III): L-Thr:Mg(II)	308.8740	42.6401	4.6640	719.8456	3507.1564	23.7335	614.0621	0.9446	0.1665	5.8692
	At pH = 6									
Pr(III)	309.1371	42.6764	4.6680	718.9111	3510.1435	23.7538	614.5851	0.9443	0.1669	5.8978
Pr(III):L-Thr	309.0669	42.6667	4.6669	718.8052	3509.3468	23.7484	614.4456	0.9441	0.1671	5.9174
Pr(III): L-Thr:Mg(II)	308.9924	42.6564	4.6658	718.8068	3508.5003	23.7426	614.2974	0.9440	0.1673	5.9295

Table 2.17: Computed values of the energy interaction parameters: Slater-Condon factor F_k (cm^{-1}), Lande's Spin-orbit interactions ξ_{4f} (cm^{-1}), Racah (E^k), Nephelauxetic ratio (β), Bonding ($b^{1/2}$) and Percent covalency (δ) for the different Pr(III) systems with L-Tryptophan in absence and presence of Mg(II) in 50% (v/v) aquated DMF solvent at pH 2, 4 and 6

System	F_2	F_4	F_6	ξ_{4f}	E^1	E^2	E^3	β	$b^{1/2}$	δ
Solvent-DMF: H$_2$O	At pH = 2									
Pr(III)	308.9324	42.6481	4.6649	720.0905	3507.8194	23.7380	614.1782	0.9448	0.1661	5.8408
Pr(III):L-Trp	308.8844	42.6415	4.6642	720.0376	3507.2748	23.7343	614.0829	0.9447	0.1663	5.8528
Pr(III): L-Trp:Mg(II)	308.7357	42.6210	4.6619	719.8002	3505.5861	23.7229	613.7872	0.9443	0.1668	5.8954
	At pH = 4									
Pr(III)	309.0132	42.6593	4.6661	719.9405	3508.7363	23.7442	614.3387	0.9448	0.1661	5.8391
Pr(III):L-Trp	308.8655	42.6389	4.6639	719.6328	3507.0600	23.7329	614.0453	0.9444	0.1667	5.8869
Pr(III): L-Trp:Mg(II)	308.8217	42.6328	4.6632	719.5243	3506.5620	23.7295	613.9581	0.9443	0.1669	5.9024
	At pH = 6									
Pr(III)	309.1186	42.6738	4.6677	719.0303	3509.9333	23.7523	614.5483	0.9444	0.1668	5.8916
Pr(III):L-Trp	308.9556	42.6513	4.6652	719.1784	3508.0829	23.7398	614.2243	0.9442	0.1670	5.9010
Pr(III): L-Trp:Mg(II)	308.8314	42.6342	4.6634	719.4864	3506.6726	23.7303	613.9774	0.9443	0.1670	5.9137

Table 2.18: Computed values of the energy interaction parameters: Slater-Condon factor F_k (cm^{-1}), Lande's Spin-orbit interactions ξ_{4f} (cm^{-1}), Racah (E^k), Nephelauxetic ratio (β), Bonding ($b^{1/2}$) and Percent covalency (δ) for the different Pr(III) systems with L-Isoleucine in absence and presence of Mg(II) in 50% (v/v) aquated DMF solvent at pH 2, 4 and 6

System	F_2	F_4	F_6	ξ_{4f}	E^1	E^2	E^3	β	$b^{1/2}$	δ
Solvent-DMF: H$_2$O	At pH = 2									
Pr(III)	308.9767	42.6542	4.6655	720.3942	3508.3229	23.7414	614.2664	0.9451	0.1657	5.8103
Pr(III):L-Ile	308.9314	42.6480	4.6649	719.9795	3507.8084	23.7379	614.1763	0.9447	0.1662	5.8495
Pr(III): L-Ile:Mg(II)	308.8924	42.6426	4.6643	719.8854	3507.3653	23.7349	614.0987	0.9446	0.1664	5.8631
	At pH = 4									
Pr(III)	309.0063	42.6583	4.6660	720.1138	3508.6581	23.7437	614.3251	0.9449	0.1659	5.8270
Pr(III):L-Ile	308.9123	42.6453	4.6646	719.8204	3507.5911	23.7365	614.1382	0.9446	0.1664	5.8649
Pr(III): L-Ile:Mg(II)	308.8365	42.6349	4.6634	719.6094	3506.7304	23.7307	613.9875	0.9443	0.1668	5.8935
	At pH = 6									
Pr(III)	309.1282	42.6752	4.6678	719.1340	3510.0429	23.7531	614.5675	0.9444	0.1665	5.8821
Pr(III):L-Ile	309.0048	42.6581	4.6660	719.0932	3508.6418	23.7436	614.3222	0.9443	0.1667	5.8835
Pr(III): L-Ile:Mg(II)	308.9154	42.6458	4.6646	719.0869	3507.6267	23.7367	614.1445	0.9442	0.1669	5.8976

Table 2.19: Observed and computed values of energies (cm^{-1}) and R.M.S values of Pr(III) with L-Glutamine in absence and presence of Mg(II) systems in 50% (v/v) aquated DMF solvent at pH = 2, 4 and 6

System	$^3H_4 \rightarrow {}^3P_2$		$^3H_4 \rightarrow {}^3P_1$		$^3H_4 \rightarrow {}^3P_0$		$^3H_4 \rightarrow {}^1D_2$		R.M.S
	E_{obs}	E_{cal}	E_{obs}	E_{cal}	E_{obs}	E_{cal}	E_{obs}	E_{cal}	
				At pH = 2					
Pr(III)	22489.8	22437.85	21313.57	21228.49	20742.41	20671.8	16925.49	17125.44	117.16
Pr(III):L-Gln	22485.17	22432.7	21308.73	21223.67	20741.41	20667.83	16917.38	17122.16	119.73
Pr(III): L-Gln:Mg(II)	22480.54	22429.59	21307.46	21220.56	20739.02	20664.91	16914.04	17120.09	120.52
				At pH = 4					
Pr(III)	22484.5	22438.43	21318.07	21229.44	20745.54	20673.33	16924.41	17125.99	118.14
Pr(III):L-Gln	22476.89	22430.61	21312.13	21221.69	20740.41	20666.18	16914.71	17120.81	120.74
Pr(III): L-Gln:Mg(II)	22471.92	22424.42	21307.68	21215.54	20736.17	20660.46	16906.4	17116.72	123.20
				At pH = 6					
Pr(III)	22496.5	22441.74	21313.19	21234.1	20759.97	20680.03	16917.31	17128.74	122.83
Pr(III):L-Gln	22487.39	22434.71	21310.99	21226.48	20749.65	20671.86	16912.92	17123.83	122.93
Pr(III): L-Gln:Mg(II)	22479.87	22428.64	21307.46	21220.19	20743.23	20665.58	16907.81	17119.7	123.66

Table 2.20: Observed and computed values of energies (cm^{-1}) and R.M.S values of Pr(III) with L-Threonine in absence and presence of Mg(II) systems in 50% (v/v) aquated DMF solvent at pH = 2, 4 and 6

System	$^3H_4 \rightarrow {}^3P_2$		$^3H_4 \rightarrow {}^3P_1$		$^3H_4 \rightarrow {}^3P_0$		$^3H_4 \rightarrow {}^1D_2$		R.M.S
	E_{obs}	E_{cal}	E_{obs}	E_{cal}	E_{obs}	E_{cal}	E_{obs}	E_{cal}	
				At pH = 2					
Pr(III)	22485.14	22434.64	21309.05	21225.39	20740.99	20669.07	16923.3	17123.36	116.99
Pr(III):L-Thr	22483.44	22431.89	21307.98	21222.88	20740.99	20667.13	16916.95	17121.63	119.63
Pr(III): L-Thr:Mg(II)	22477.57	22425.51	21305.33	21216.31	20734.56	20660.61	16909.32	17117.3	121.82
				At pH = 4					
Pr(III)	22490.77	22442.56	21324.67	21233.95	20751.66	20678.21	16922.63	17128.89	120.93
Pr(III):L-Thr	22482.07	22432.43	21315.55	21223.49	20741.54	20667.81	16913.54	17122.01	122.31
Pr(III): L-Thr:Mg(II)	22481.53	22428.15	21308.88	21219.11	20737.93	20663.54	16909.16	17119.13	123.01
				At pH = 6					
Pr(III)	22497.14	22441.22	21308.4	21233.83	20761.99	20680.22	16916.92	17128.5	122.62
Pr(III):L-Thr	22492.08	22435.95	21303.65	21228.49	20757.61	20675.1	16911.71	17124.97	123.58
Pr(III): L-Thr:Mg(II)	22487.17	22430.92	21298.37	21223.28	20752.37	20669.87	16908.27	17121.55	123.59

Table 2.21: Observed and computed values of energies (cm^{-1}) and R.M.S values of Pr(III) with L-Tryptophan in absence and presence of Mg(II) systems in 50% (v/v) aquated DMF solvent at pH = 2, 4 and 6

System	$^3H_4 \rightarrow {}^3P_2$		$^3H_4 \rightarrow {}^3P_1$		$^3H_4 \rightarrow {}^3P_0$		$^3H_4 \rightarrow {}^1D_2$		R.M.S
	E_{obs}	E_{cal}	E_{obs}	E_{cal}	E_{obs}	E_{cal}	E_{obs}	E_{cal}	
	At pH = 2								
Pr(III)	22480.85	22433.32	21308.89	21224.18	20740.71	20668.11	16922.36	17122.52	117.02
Pr(III):L-Trp	22477.05	22429.82	21304.65	21220.61	20737.63	20664.64	16920.06	17120.16	118.90
Pr(III): L-Trp:Mg(II)	22468.53	22418.58	21298.72	21209.24	20728.32	20653.75	16904.58	17112.64	121.81
	At pH = 4								
Pr(III)	22484.99	22438.02	21319.88	21229.24	20746.88	20673.49	16920.41	17125.8	120.41
Pr(III):L-Trp	22477.16	22426.5	21302.31	21217.67	20738.54	20662.54	16911.03	17118.12	120.82
Pr(III): L-Trp:Mg(II)	22473.45	22423	21298.01	21214.17	20736.05	20659.26	16908.18	17115.79	121.01
	At pH = 6								
Pr(III)	22496.72	22440.57	21309.52	21233.01	20760	20679.15	16916.26	17128	120.86
Pr(III):L-Trp	22474.42	22430.3	21307.49	21222.18	20746.91	20668	16912.68	17120.94	121.27
Pr(III): L-Trp:Mg(II)	22471.03	22423.46	21304.17	21214.7	20736.57	20659.87	16906.2	17116.12	122.70

Table 2.22: Observed and computed values of energies (cm^{-1}) and R.M.S values of Pr(III) with L-Isoleucine in absence and presence of Mg(II) systems in 50% (v/v) aquated DMF solvent at pH = 2, 4 and 6

System	$^3H_4 \rightarrow {}^3P_2$		$^3H_4 \rightarrow {}^3P_1$		$^3H_4 \rightarrow {}^3P_0$		$^3H_4 \rightarrow {}^1D_2$		R.M.S
	E_{obs}	E_{cal}	E_{obs}	E_{cal}	E_{obs}	E_{cal}	E_{obs}	E_{cal}	
				At pH = 2					
Pr(III)	22489.8	22437.85	21313.57	21228.49	20742.41	20671.8	16925.49	17125.44	117.16
Pr(III):L-Ile	22485.17	22432.7	21308.73	21223.67	20741.41	20667.83	16917.38	17122.16	119.73
Pr(III): L-Ile:Mg(II)	22480.54	22429.59	21307.46	21220.56	20739.02	20664.91	16914.04	17120.09	120.52
				At pH = 4					
Pr(III)	22484.5	22438.43	21318.07	21229.44	20745.54	20673.33	16924.41	17125.99	118.14
Pr(III):L-Ile	22476.89	22430.61	21312.13	21221.69	20740.41	20666.18	16914.71	17120.81	120.74
Pr(III): L-Ile:Mg(II)	22471.92	22424.42	21307.68	21215.54	20736.17	20660.46	16906.4	17116.72	123.20
				At pH = 6					
Pr(III)	22496.5	22441.74	21313.19	21234.1	20759.97	20680.03	16917.31	17128.74	122.83
Pr(III):L-Ile	22487.39	22434.71	21310.99	21226.48	20749.65	20671.86	16912.92	17123.83	122.93
Pr(III): L-Ile:Mg(II)	22479.87	22428.64	21307.46	21220.19	20743.23	20665.58	16907.81	17119.7	123.66

Table 2.23: Observed and computed values of Oscillator Strength (P x 10^6) and Judd-Ofelt (T$_\lambda$ x 10^{10}) parameters of the different Pr(III) systems with L-Glutamine in absence and presence of Mg(II) in 50% (v/v) aquated DMF solvent at pH = 2, 4 and 6

System	$^3H_4 \rightarrow ^3P_2$		$^3H_4 \rightarrow ^3P_1$		$^3H_4 \rightarrow ^3P_0$		$^3H_4 \rightarrow ^1D_2$		T$_2$	T$_4$	T$_6$
	Pobs	Pcal	Pobs	Pcal	Pobs	Pcal	Pobs	Pcal			
	At pH = 2										
Pr(III)	5.9745	5.9745	2.2907	1.6511	0.9966	1.6266	1.6673	1.6673	-18.649	4.538	18.393
Pr(III):L-Gln	5.9882	5.9882	2.4266	1.7232	1.0047	1.6979	1.9579	1.9579	46.377	4.737	18.389
Pr(III): L-Gln:Mg(II)	6.6619	6.6619	2.7021	1.9328	1.1463	1.9043	1.9840	1.9840	7.397	5.314	20.451
	At pH = 4										
Pr(III)	5.8041	5.8041	2.2250	1.5964	0.9534	1.5727	1.7320	1.7320	7.358	4.387	17.879
Pr(III):L-Gln	6.8129	6.8129	2.5247	1.8353	1.1288	1.8080	1.9880	1.9880	-1.370	5.045	21.022
Pr(III): L-Gln:Mg(II)	7.1552	7.1552	2.9225	2.0826	1.2242	2.0517	2.3385	2.3385	55.191	5.726	21.969
	At pH = 6										
Pr(III)	6.7547	6.7547	2.6525	1.8992	1.1300	1.8727	2.0807	2.0807	23.623	5.220	20.764
Pr(III):L-Gln	7.6220	7.6220	2.5836	1.8775	1.1546	1.8505	2.1057	2.1057	-27.610	5.161	23.636
Pr(III): L-Gln:Mg(II)	8.4627	8.4627	2.7985	2.0215	1.2265	1.9922	2.1864	2.1864	-64.947	5.558	26.298

Table 2.24: Observed and computed values of Oscillator Strength (P x 10^6) and Judd-Ofelt (T$_\lambda$ x 10^{10}) parameters of the different Pr(III) systems with L-Threonine in absence and presence of Mg(II) in 50% (v/v) aquated DMF solvent at pH = 2, 4 and 6

System	$^3H_4 \rightarrow ^3P_2$		$^3H_4 \rightarrow ^3P_1$		$^3H_4 \rightarrow ^3P_0$		$^3H_4 \rightarrow ^1D_2$		T$_2$	T$_4$	T$_6$
	Pobs	Pcal	Pobs	Pcal	Pobs	Pcal	Pobs	Pcal			
At pH = 2											
Pr(III)	6.2401	6.2401	2.4173	1.7640	1.0945	1.7381	1.8136	1.8136	-3.243	4.850	19.185
Pr(III):L-Thr	6.3002	6.3002	2.3820	1.7462	1.0942	1.7207	1.7948	1.7948	-11.284	4.801	19.397
Pr(III): L-Thr:Mg(II)	6.7398	6.7398	2.5678	1.8597	1.1346	1.8322	1.9002	1.9002	-16.484	5.114	20.763
At pH = 4											
Pr(III)	6.6025	6.6025	2.5698	1.8537	1.1220	1.8284	2.0805	2.0805	33.727	5.096	20.298
Pr(III):L-Thr	6.9915	6.9915	2.7993	2.0236	1.2309	1.9960	2.4040	2.4040	81.268	5.565	21.454
Pr(III): L-Thr:Mg(II)	7.3311	7.3311	2.9959	2.1633	1.3126	2.1338	2.6296	2.6296	109.853	5.950	22.470
At pH = 6											
Pr(III)	6.9463	6.9463	2.6180	1.8639	1.0934	1.8362	1.9286	1.9286	-23.668	5.121	21.425
Pr(III):L-Thr	7.0439	7.0439	2.8320	2.0280	1.2056	1.9976	2.1988	2.1988	30.885	5.574	21.634
Pr(III): L-Thr:Mg(II)	7.5521	7.5521	3.0209	2.1611	1.2820	2.1291	2.3475	2.3475	31.029	5.941	23.204

Table 2.25: Observed and computed values of Oscillator Strength (P x 10^6) and Judd-Ofelt (T_λ x 10^{10}) parameters of the different Pr(III) systems with L-Tryptophan in absence and presence of Mg(II) in 50% (v/v) aquated DMF solvent at pH = 2, 4 and 6

System	$^3H_4 \rightarrow ^3P_2$		$^3H_4 \rightarrow ^3P_1$		$^3H_4 \rightarrow ^3P_0$		$^3H_4 \rightarrow ^1D_2$		T_2	T_4	T_6
	Pobs	Pcal	Pobs	Pcal	Pobs	Pcal	Pobs	Pcal			
At pH = 2											
Pr(III)	6.2558	6.2558	2.5246	1.8106	1.0806	1.7840	1.8411	1.8411	1.772	4.978	19.207
Pr(III):L-Trp	6.6906	6.6906	2.5694	1.8500	1.1141	1.8229	2.0078	2.0078	10.961	5.087	20.609
Pr(III): L-Trp:Mg(II)	7.3647	7.3647	2.6880	1.9755	1.2444	1.9463	1.8715	1.8715	-64.499	5.434	22.738
At pH = 4											
Pr(III)	6.8828	6.8828	2.5116	1.8655	1.2012	1.8377	2.1424	2.1424	29.054	5.126	21.221
Pr(III):L-Trp	7.2110	7.2110	2.8589	2.0773	1.2770	2.0472	2.1135	2.1135	0.330	5.713	22.150
Pr(III): L-Trp:Mg(II)	7.4293	7.4293	2.9634	2.1481	1.3137	2.1172	2.3330	2.3330	35.698	5.909	22.819
At pH = 6											
Pr(III)	6.6268	6.6268	2.5673	1.8794	1.1752	1.8535	2.0551	2.0551	26.290	5.167	20.359
Pr(III):L-Trp	7.8479	7.8479	2.7102	1.9584	1.1893	1.9303	2.0793	2.0793	-48.980	5.384	24.332
Pr(III): L-Trp:Mg(II)	8.1922	8.1922	2.7289	2.1279	1.5045	2.0966	2.4144	2.4144	4.172	5.851	25.342

Table 2.26: Observed and computed values of Oscillator Strength (P x 10^6) and Judd-Ofelt (T$_\lambda$ x 10^{10}) parameters of the different Pr(III) systems with L-Isoleucine in absence and presence of Mg(II) in 50% (v/v) aquated DMF solvent at pH = 2, 4 and 6

System	$^3H_4 \rightarrow {}^3P_2$		$^3H_4 \rightarrow {}^3P_1$		$^3H_4 \rightarrow {}^3P_0$		$^3H_4 \rightarrow {}^1D_2$		T_2	T_4	T_6
	Pobs	Pcal	Pobs	Pcal	Pobs	Pcal	Pobs	Pcal			
At pH = 2											
Pr(III)	5.9745	5.9745	2.2907	1.6511	0.9966	1.6266	1.6673	1.6673	-18.649	4.538	18.393
Pr(III):L-Ile	5.9882	5.9882	2.4266	1.7232	1.0047	1.6979	1.9579	1.9579	46.377	4.737	18.389
Pr(III): L-Ile:Mg(II)	6.6619	6.6619	2.7021	1.9328	1.1463	1.9043	1.9840	1.9840	7.397	5.314	20.451
At pH = 4											
Pr(III)	5.8041	5.8041	2.2250	1.5964	0.9534	1.5727	1.7320	1.7320	7.358	4.387	17.879
Pr(III):L-Ile	6.8129	6.8129	2.5247	1.8353	1.1288	1.8080	1.9880	1.9880	-1.370	5.045	21.022
Pr(III): L-Ile:Mg(II)	7.1552	7.1552	2.9225	2.0826	1.2242	2.0517	2.3385	2.3385	55.191	5.726	21.969
At pH = 6											
Pr(III)	6.7547	6.7547	2.6525	1.8992	1.1300	1.8727	2.0807	2.0807	23.623	5.220	20.764
Pr(III):L-Ile	7.6220	7.6220	2.5836	1.8775	1.1546	1.8505	2.1057	2.1057	-27.610	5.161	23.636
Pr(III): L-Ile:Mg(II)	8.4627	8.4627	2.7985	2.0215	1.2265	1.9922	2.1864	2.1864	-64.947	5.558	26.298

Comparative UV-Vis. absorption spectra of Pr(III) with the selected amino acids at different pH levels in aquated DMF solvent

1. **L-Glutamine**
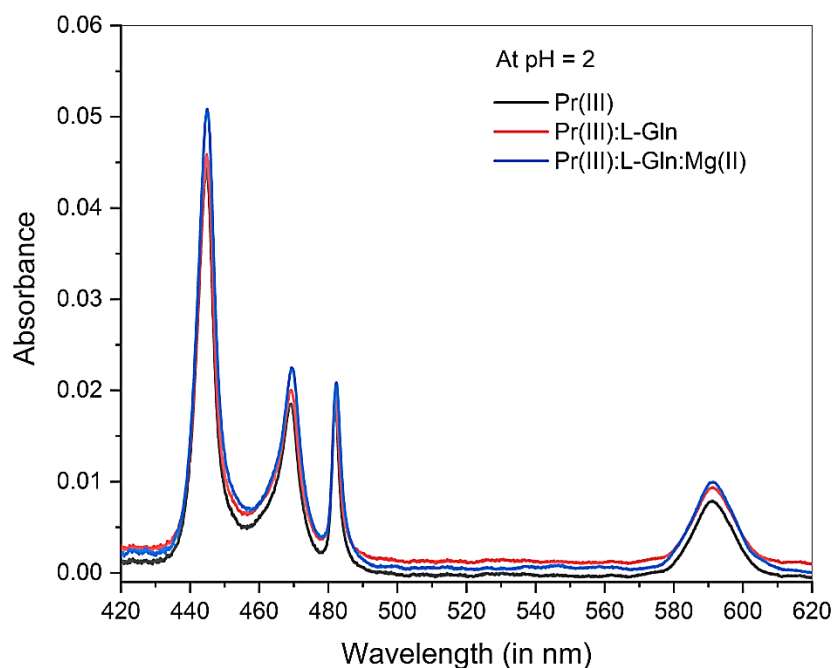
Fig. 2.22: Comparative UV-Vis. absorption spectra of Pr(III), Pr(III):L-Gln and Pr(III):L-Gln:Mg(II) at pH = 2 in DMF: water (50% v/v) solvent
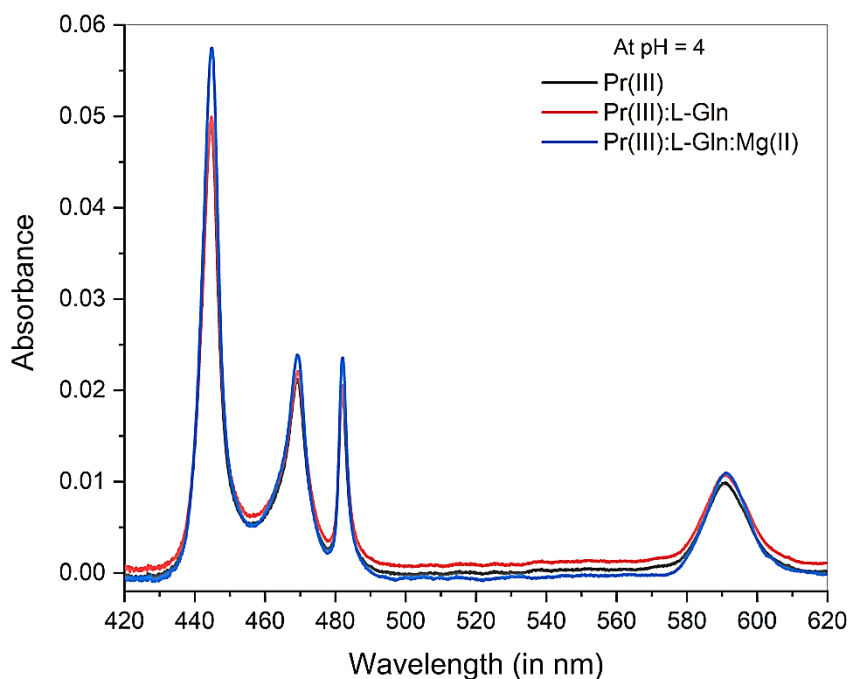
Fig. 2.23: Comparative UV-Vis. absorption spectra of Pr(III), Pr(III):L-Gln and Pr(III):L-Gln:Mg(II) at pH = 4 in DMF: water (50% v/v) solvent
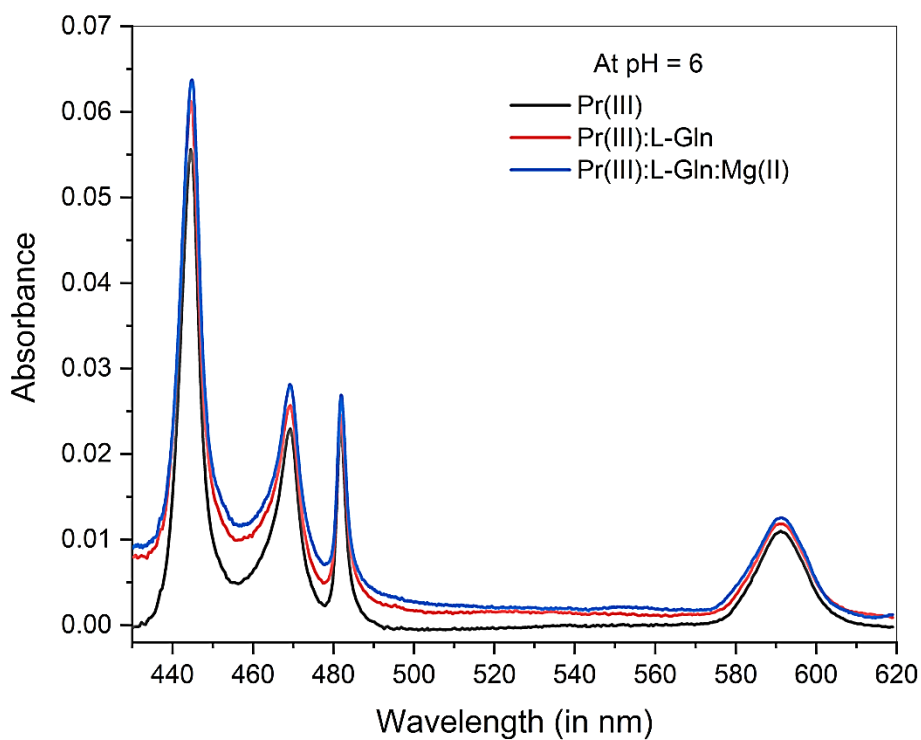
Fig. 2.24: Comparative UV-Vis. absorption spectra of Pr(III), Pr(III):L-Gln and Pr(III):L-Gln:Mg(II) at pH = 6 in DMF: water (50% v/v) solvent
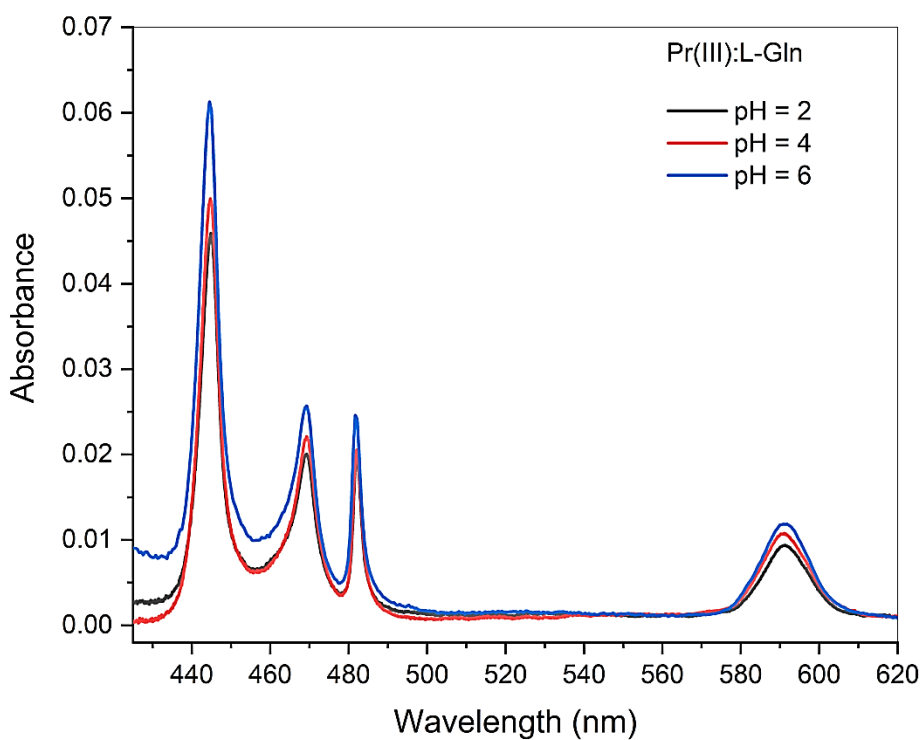
Fig. 2.25: Comparative UV-Vis. absorption spectra of Pr(III):L-Gln at pH = 2, 4 and 6 in DMF: water (50% v/v) solvent

2. L-Threonine
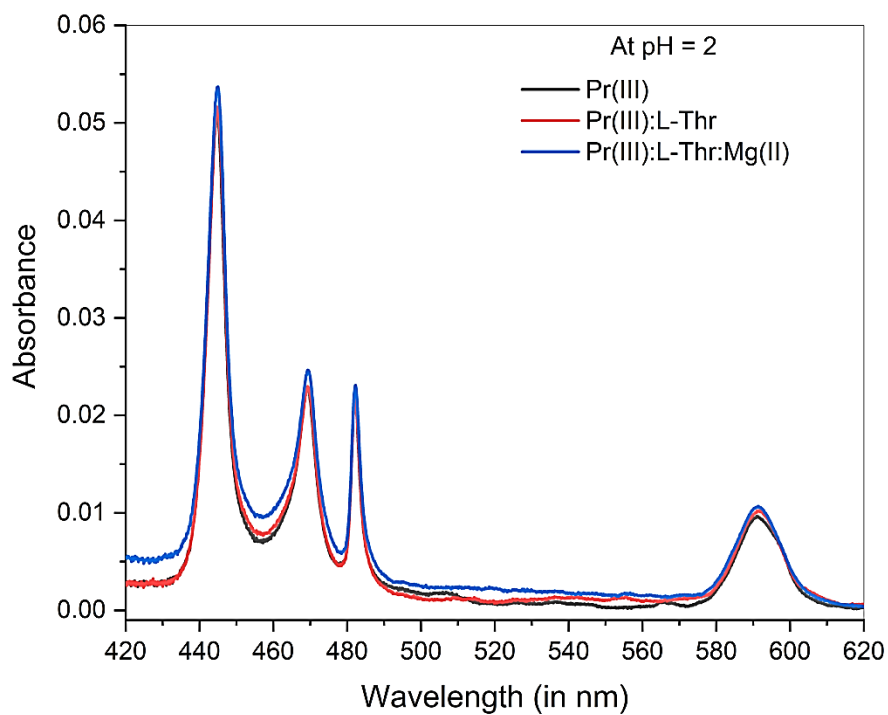
Fig. 2.26: Comparative UV-Vis. absorption spectra of Pr(III), Pr(III):L-Thr and Pr(III):L-Thr:Mg(II) at pH = 2 in DMF: water (50% v/v) solvent
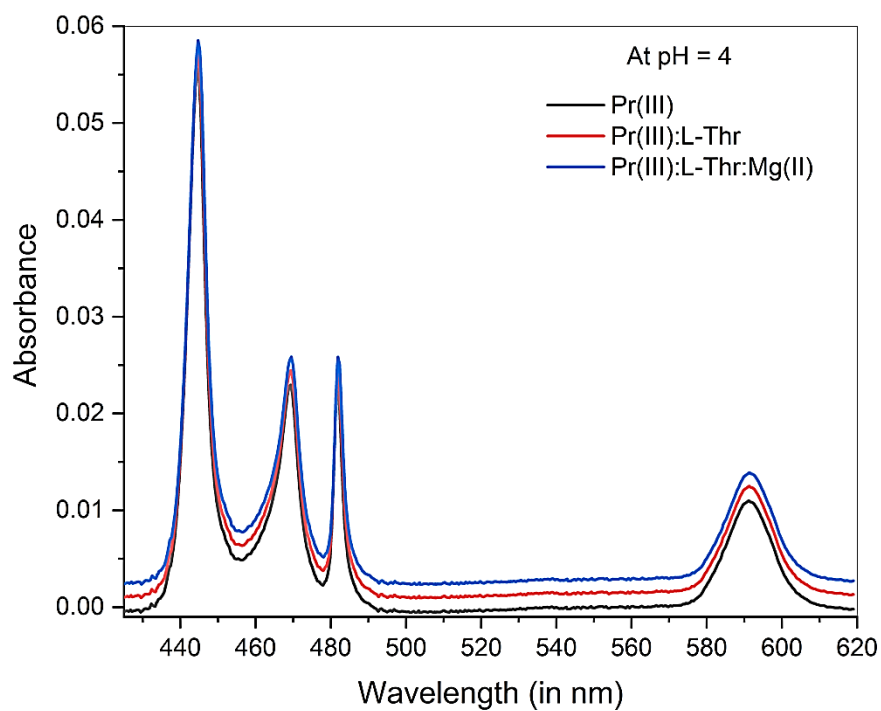
Fig. 2.27: Comparative UV-Vis. absorption spectra of Pr(III), Pr(III):L-Thr and Pr(III):L-Thr:Mg(II) at pH = 4 in DMF: water (50% v/v) solvent
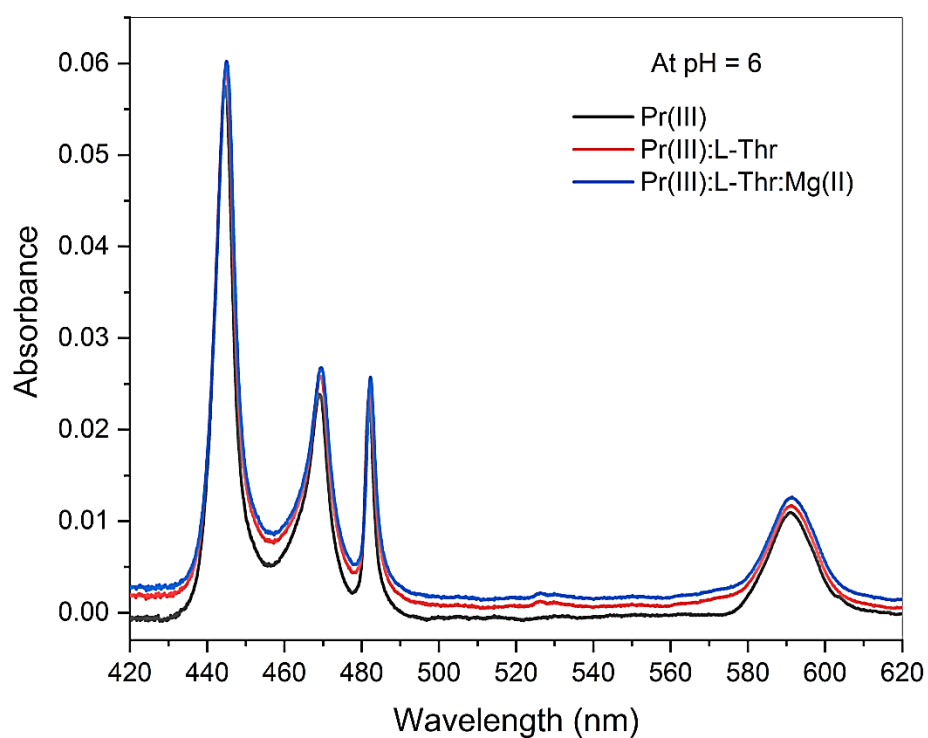
Fig. 2.28: Comparative UV-Vis. absorption spectra of Pr(III), Pr(III):L-Thr and Pr(III):L-Thr:Mg(II) at pH = 6 in DMF: water (50% v/v) solvent
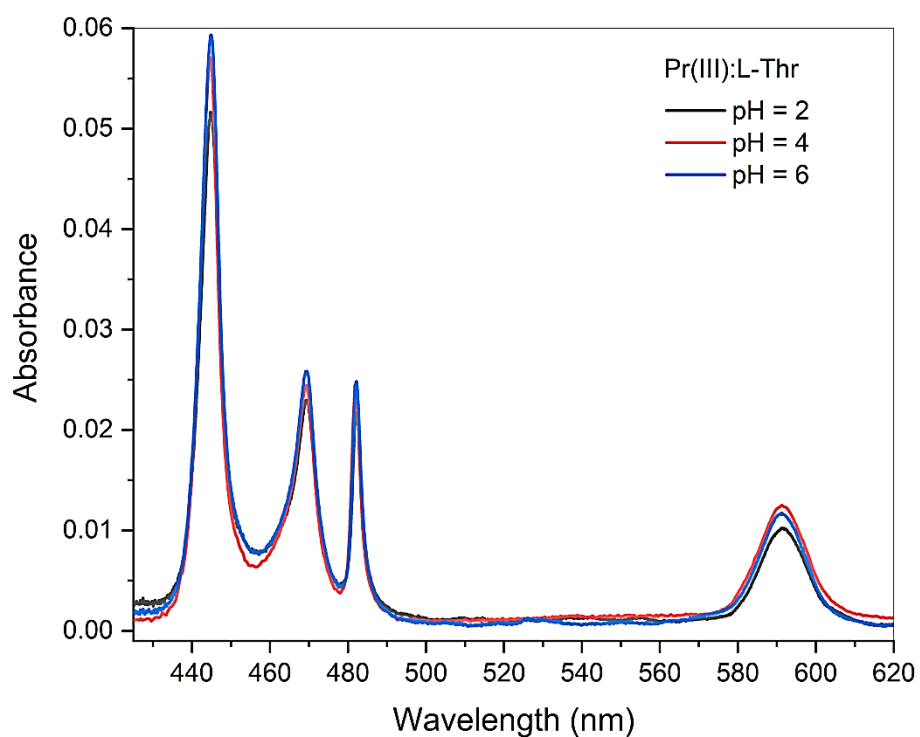
Fig. 2.29: Comparative UV-Vis. absorption spectra of Pr(III):L-Thr at pH = 2, 4 and 6 in DMF: water (50% v/v) solvent

3. L-Tryptophan
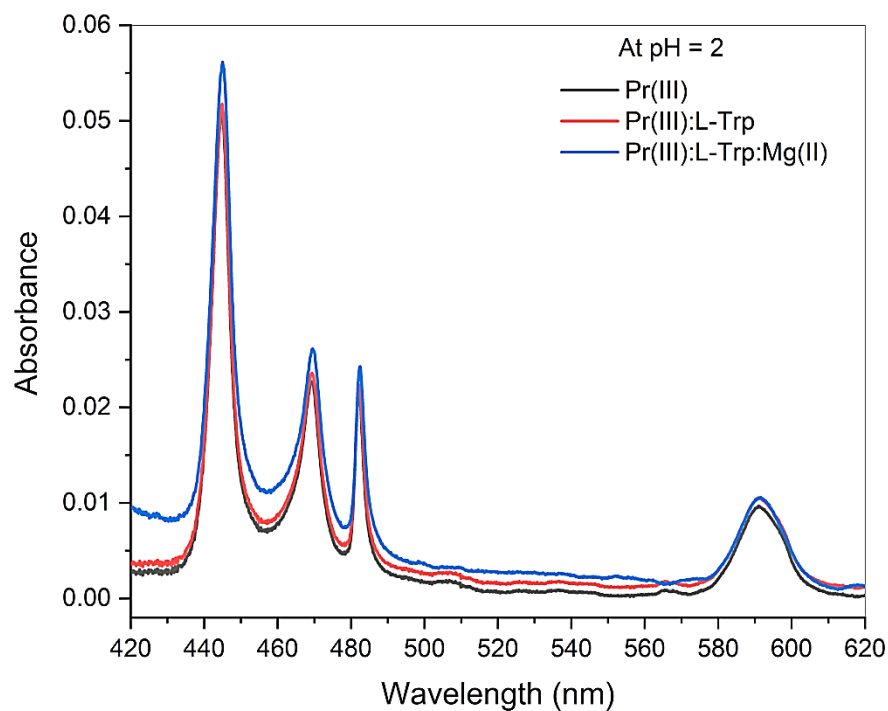
Fig. 2.30: Comparative UV-Vis. absorption spectra of Pr(III), Pr(III):L-Trp and Pr(III):L-Trp:Mg(II) at pH = 2 in DMF: water (50% v/v) solvent
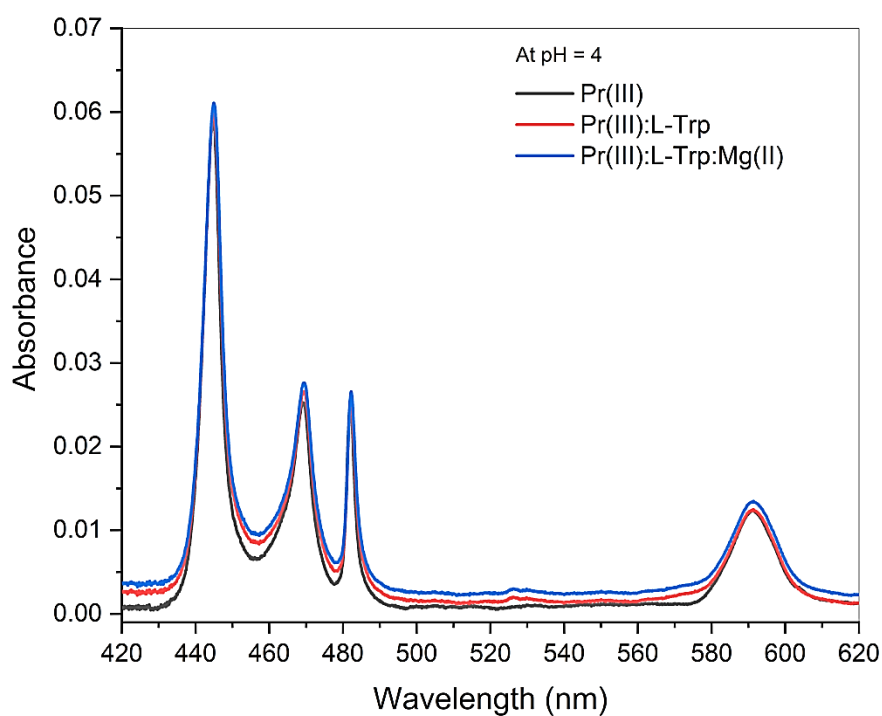
Fig. 2.31: Comparative UV-Vis. absorption spectra of Pr(III), Pr(III):L-Trp and Pr(III):L-Trp:Mg(II) at pH = 4 in DMF: water (50% v/v) solvent
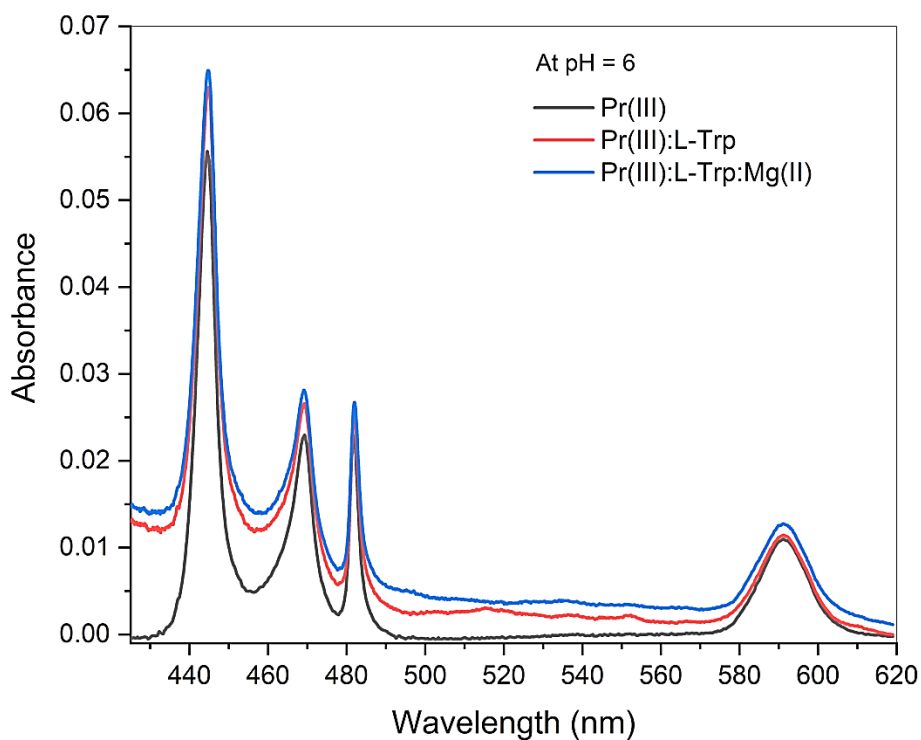
Fig. 2.32: Comparative UV-Vis. absorption spectra of Pr(III), Pr(III):L-Trp and Pr(III):L-Trp:Mg(II) at pH = 6 in DMF: water (50% v/v) solvent
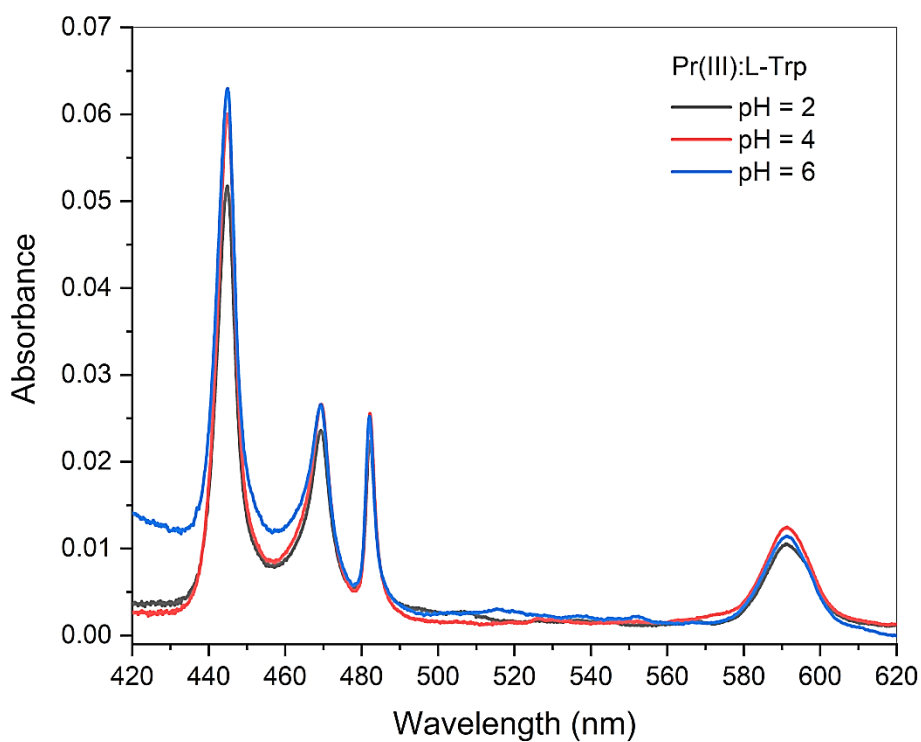
Fig. 2.33: Comparative UV-Vis. absorption spectra of Pr(III):L-Trp at pH = 2, 4 and 6 in DMF: water (50% v/v) solvent

4. L-Isoleucine
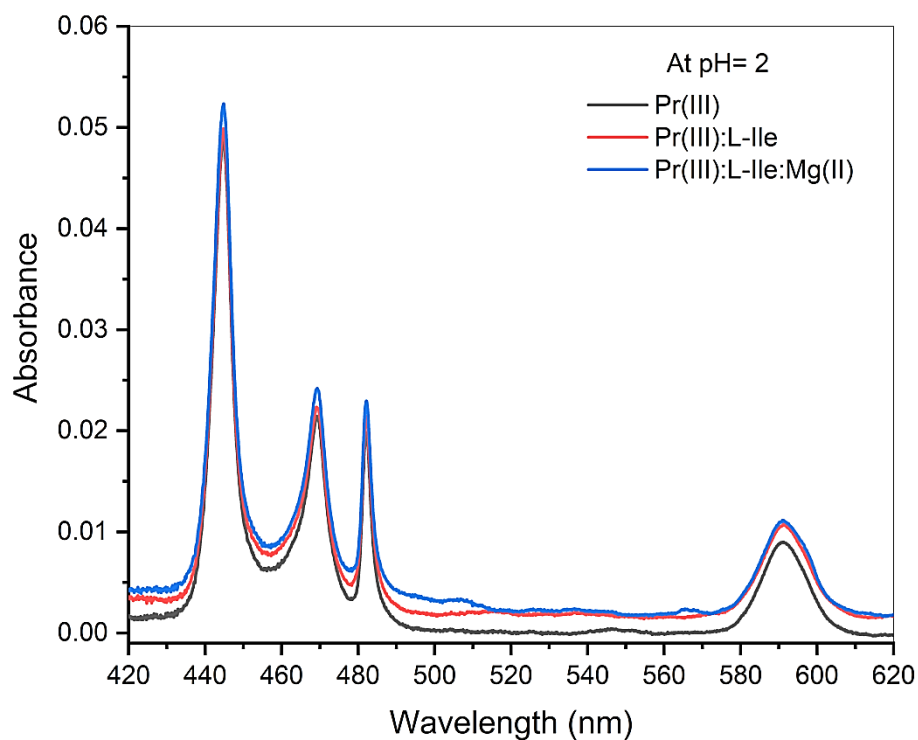
Fig. 2.34: Comparative UV-Vis. absorption spectra of Pr(III), Pr(III):L-Ile and Pr(III):L-Ile:Mg(II) at pH = 2 in DMF: water (50% v/v) solvent
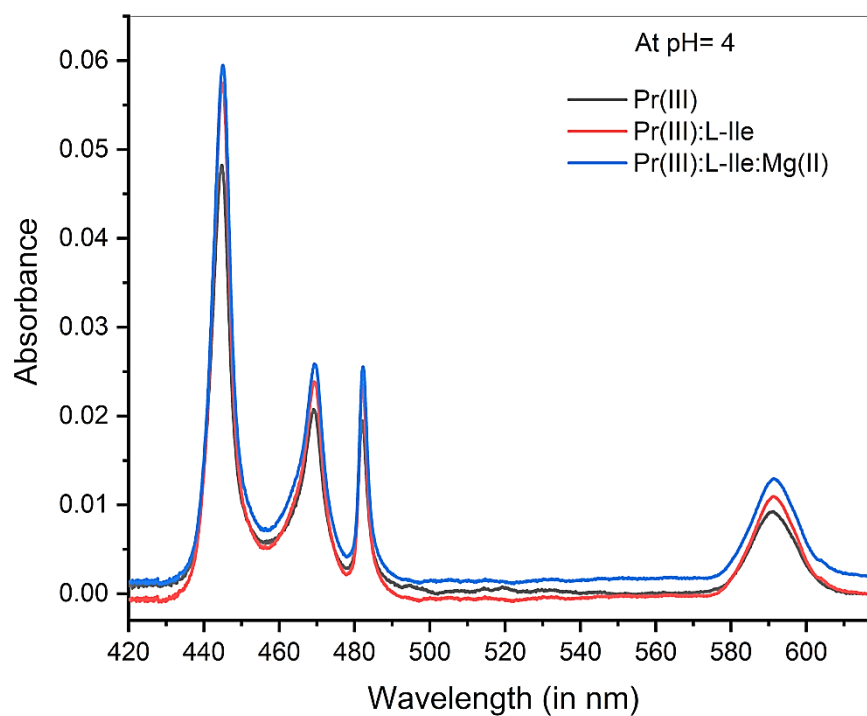
Fig. 2.35: Comparative UV-Vis. absorption spectra of Pr(III), Pr(III):L-Ile and Pr(III):L-Ile:Mg(II) at pH = 4 in DMF: water (50% v/v) solvent
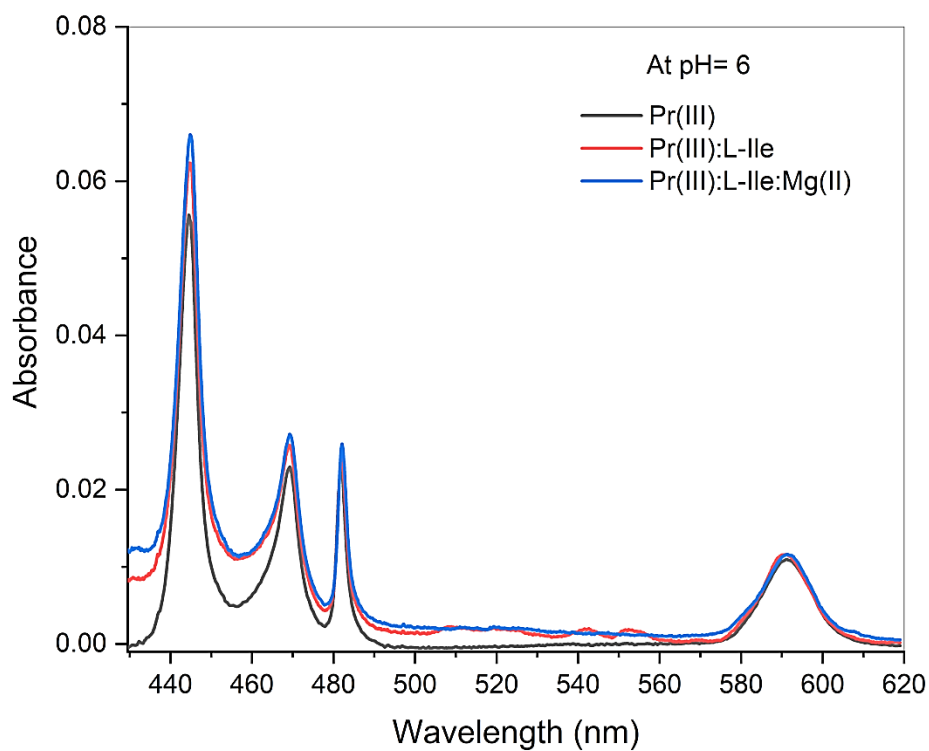
Fig. 2.36: Comparative UV-Vis. absorption spectra of Pr(III), Pr(III):L-Ile and Pr(III):L-Ile:Mg(II) at pH = 6 in DMF: water (50% v/v) solvent
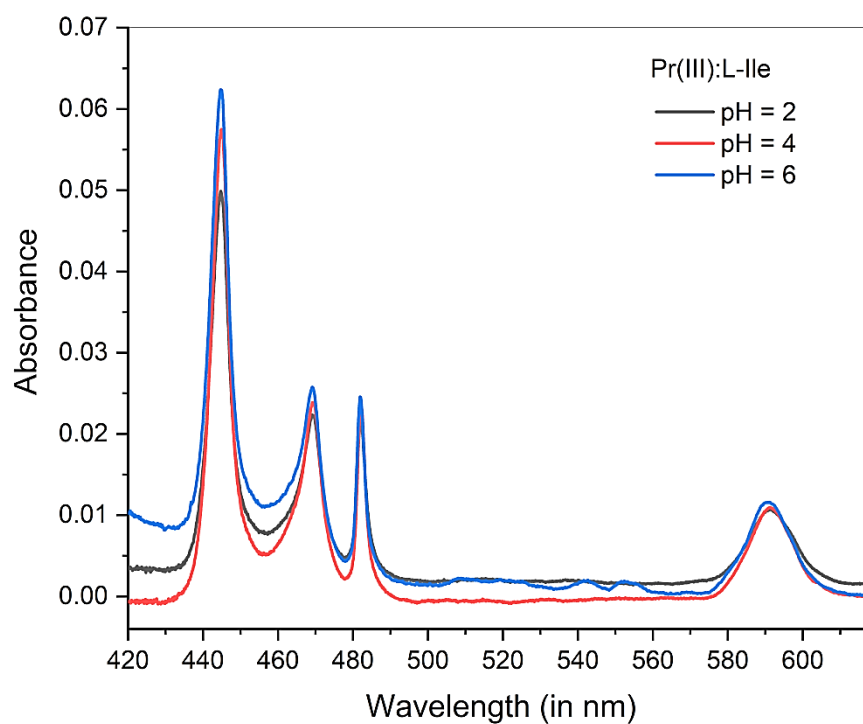
Fig. 2.37: Comparative UV-Vis. absorption spectra of Pr(III):L-Ile at pH = 2, 4 and 6 in DMF: water (50% v/v) solvent

Chapter 3

Absorption spectral analysis of 4f-4f transition for the complexation of Nd(III) with in the presence/absence of Mg(II) in different aquated organic solvents and at different pH medium

3.1 Introduction

Lanthanides are characterized by their 4f electronic configuration. The partially filled 4f shell of lanthanides is well-shielded by their outer filled 5s, 5p and 6s electrons which resulted in their unique spectroscopic properties. Accordingly, they are also known as 4f elements. Lanthanides are gaining a lot of attention, due to their distinct magnetic, optical and chemical properties. The chemistry of lanthanides' coordination is an interesting and well-studied subject, which is rapidly emerging as a result of having prospective applications of lanthanides in pharmaceutical, biochemical, biomedical, bioinorganic, and pharmaceutics fields. Numerous investigations on solution-based lanthanide complexes and their coordination chemistry have been published. In particular, the solution coordination chemistry of lanthanides is very important in the exploration of its biological functions. The ability of the lanthanide ions to be utilised as structural probes has sparked the curiosity of researchers within the realm of biological chemistry [1,2]. Comparative absorption spectroscopy investigations can aid in understanding the bioactivity of biological molecules when they interact with lanthanides [3].

We have selected four amino acids for this study, namely L-Glutamine, L-Threonine, L-Tryptophan and L-Isoleucine as the ligands. We have also chosen magnesium because of its biological importance. Mg(II) functions as a catalyst or stimulant for many bio-molecular reactions [4]. Mg(II) is diamagnetic in nature and is

spectroscopically silent to optical and magnetic spectral studies. Ln(III) on the other hand are paramagnetic in nature and spectroscopically active hence, the isomorphous substitution of Mg(II) with Ln(III) could provide important information regarding its interactions with different amino acids [5].

The energy interaction parameters for the complex formation between Nd(III) ion and the ligands L-Glutamine, L-Threonine, L-Tryptophan and L-Isoleucine, in the absence/presence of Mg(II) in different aquated organic solvents, and also at pH levels 2, 4, 6 (only in aquated DMF solvent) is theoretically discussed in the present chapter. The values of energy interaction parameters: Slater Condon (F_k), Racah (E^k) parameter, Lande (ξ_{4f}), nephelauxetic ratio (β), bonding ($b^{1/2}$) parameter, percent covalency (δ), were calculated in order to investigate the complexation mode.

3.2 Experimental: Materials and Method

For the present study, the chemicals: L-Glutamine, L-Threonine, L-Tryptophan, L-Isoleucine, magnesium nitrate hexahydrate ($\geq 98.0\%$) and neodymium nitrate hexahydrate (99.9%) were procured from HiMedia and Sigma-Aldrich. Dimethylformamide (DMF), acetonitrile, 1,4-Dioxane and methanol (99.5%) were purchased from HiMedia and used for the analysis. UV-Vis spectra in the region of 460-920 nm were recorded using a conventional 1cm path length quartz cuvette on a Lambda 365 UV/Vis Perkin Elmer spectrophotometer. The pH was measured using a digital pH metre- Eutech pH 700.

Nd(III), amino acid ligands and Mg(II) concentrations are kept constant at 0.005 M for absorption spectral studies. Standard solutions are added and the pH is kept stable with the help of hydrochloric acid and sodium hydroxide solution. For the formation of the complex in solution, the mixture is thoroughly stirred. The molar ratio for the

Nd(III):Amino acid complex study was set to 1:1, whereas the molar ratio for the Nd(III):Amino acid:Mg(II) multimetal complexation investigation was maintained at 1:1:1.

3.3 Theoretical: Energy Interaction Parameters

The spin-orbit interaction energy (E_{so}) of 4f-4f electronic transitions that result from magnetic interactions is made up of two components namely the spin-orbital and the electrostatic interactions.

$$E_{so} = A_{so}\ \xi_{4f} \tag{1}$$

where 'ξ_{4f}' is the Lande parameter representing the radial integral. 'A_{so}' is the angular component of spin-orbit interaction.

According to E.Wong [6], the energy E_j of the jth level by the first-order approximation, is represented as,

$$E_j(F_k,\ \xi_{4f}) = E_{oj}(F_k^0,\ \xi_{4f}) + \frac{\partial E_j}{\partial F_k}\Delta F_K + \frac{\partial E_j}{\partial \xi 4f}\Delta\ \xi_{4f} \tag{2}$$

Where E_{0j} is the zero-order energy of the jth level

The Slator-Condon (F_k) and Lande (ξ_{4f}) parameters' values can be determined from the following equations,

$$F_k = F_k^0 + \Delta F_k \tag{3}$$

$$\xi_{4f} = \xi^0_{4f} + \Delta\xi_{4f} \tag{4}$$

ΔE_j which is the difference between the observed Ej value and the zero-order values, is calculated by,

$$\Delta E_j = \sum_{k=2,4,6}\frac{\partial E_j}{\partial F_K}\Delta F_k + \frac{\partial E_j}{\partial\xi_{4f}}\Delta\xi_{4f} \tag{5}$$

By using the zero order energy and partial derivatives of Nd(III) ion given by Wong (Table 3.1), equation (5) can be solve by least square fit technique and F_k and ξ_{4f} values can be founout by solving equation (3) and (4).

Table 3.1: The zero-order energies and partial derivatives with respect to F_k and ξ_{4f} parameters for Nd(III) [7].

Level	$E_{oj}^{(a)}$	$\dfrac{\delta E_j}{\delta F_2}$	$\dfrac{\delta E_j}{\delta F_4}$	$\dfrac{\delta E_j}{\delta F_6}$	$\dfrac{\delta E_j}{\delta \xi_{4f}}$
$^4F_{3/2}$	11523.34	35.27	39.50	-588.9	1.02
$^4F_{5/2}$	12606.77	34.93	39.36	-631.4	2.58
$^4F_{7/2}$	13453.73	35.02	41.04	-602.5	3.24
$^4G_{5/2}$	17357.56	54.98	63.01	-991.2	1.29
$^4G_{7/2}$	19288.93	41.95	101.66	-620.8	4.13

(a) $F_2^0 = 331.567$ cm^{-1} $F_4^0 = 49.057$ cm^{-1}

   $F_6^0 = 5.170$ cm^{-1} $\xi_{4f}^0 = 906.00$ cm^{-1}

The covalency is determined using the Nephelauxetic ratio, which is the ratio of complex and free ions [8–13]. In terms of the relationship between Slater-Condon (F_k) and Racah parameters (E^k), it can be translated as follows:

$$\beta = \frac{F_k^C}{F_k^f} \ \ or \ \ \frac{E_C^k}{E_f^k} \tag{6}$$

where, $k = 2, 4,$ and 6 for the parameter F_k

          (f) and (c) refers to the free and complex ions

The magnitude of the nephelauxetic effect is expressed by the nephelauxetic ratio which reveals the metal-ligand interaction's covalent nature [10,11]. The covalent percentage ($b^{1/2}$) [12] and bonding parameters (δ) are calculated using the following equations.

$$b^{1/2} = \left[\frac{1-\beta}{2}\right]^{1/2} \tag{7}$$

$$\delta = \left[\frac{1-\beta}{\beta}\right] \times 100 \tag{8}$$

The electrostatic term E_0 is given by the product of the slater radial integral and the Slater-Condon parameter, F_k.

$$E_o = \sum_{k=0}^{k=6} K^k F_k \tag{9}$$

The Slater-Condon parameters are often referred to as direct-integral parameters which are a decreasing function of K as demonstrated by the relationship,

$$F_i^k = \int_0^\infty \int_0^\infty \frac{r_<^k}{r_>^{k+1}} R_i^2(r_i) R_j^2(r_j) r_i^2 r_j^2 dr_i dr_j \tag{10}$$

Where   R = radial wave function

                 $r_<$ = radius of the near electron

                 $r_>$ = radius of the more distant electron

                 i and j = the ith and jth electrons being considered

The F^k integrals are characterized by Condon and Shortley [14] in terms of reduced integral F_k whose relationship is as follows:

$$F_k = \frac{F^k}{D_k} \tag{11}$$

From equations (10) and (11), the reduced Slater-Condon integral can be obtained as:

$$F_k = \frac{1}{D_k} \int_0^\infty \int_0^\infty r_<^k r_>^{k+1} R_i^2(r_i) R_j^2(r_j) r_i^2 r_j^2 dr_i dr_j \tag{12}$$

Where F_k and D_k are coefficients of the linear combination that represents the angular part of the interaction, F_k is the expectation value of the scalar product $(C_1^{(k)} C_2^{(k)})$.

The Racah parameter E^k is linear combinations of F_k and represented as follows

$$E^1 = (70 \times F_2 + 231F_4 + 20.02F_6)/9$$

$$E^2 = (F_2 - 3F_4 + 7F_6)/9 \tag{13}$$

$$E^3 = (5F_2 + 6F_4 - 9F_6)/3$$

By employing the least square method, the zero-order energy and the partial derivatives, we can solve equation (5) to find the values of ΔF_2 and $\Delta \xi_{4f}$. From these and by utilizing the equations (3 and 4), the values of F_2 and ξ_{4f} are obtained. The estimated values of F_4 and F_6 are evaluated by the equations given below,

$$\frac{F_4}{F_2} = 0.1380 \; and \; \frac{F_6}{F_2} = 0.0150 \tag{14}$$

3.4 Results and discussion

The lanthanides show sharp absorption bands caused by transition between the levels of f^N configurations. In the neodymium complex, the following five transitions of Nd(III) viz., $^4I_{9/2} \rightarrow {}^4F_{3/2}$, $^4I_{9/2} \rightarrow {}^4F_{5/2}$, $^4I_{9/2} \rightarrow {}^4F_{7/2}$, $^4I_{9/2} \rightarrow {}^4G_{5/2}$ and $^4I_{9/2} \rightarrow {}^4G_{7/2}$ which originate from symmetry forbidden $^4I_{9/2}$ level, have been observed in the spectral region of 400–900 nm. In the complexation of Nd(III), its transition ($^4I_{9/2} \rightarrow {}^4G_{5/2}$) in all solvents has an unusually high sensitivity towards their surrounding chemical environment and show a relatively high-intensity transition, and is classified as 'hypersensitive' [15]. The remaining four transitions of Nd(III) are referred to as pseudo-hypersensitive transitions since they do not follow the selection rules for hypersensitive transitions but they demonstrate significant sensitivity in the complexation various ligands [16].

Figures 3.4 to 3.23 depict the comparative absorption spectra of Nd(III), Nd(III):Ligands (L) (L-Glutamine, L-Threonine, L-Tryptophan and L-Isoleucine) and Nd(III):L:Mg(II) in different aquated organic solvents. The figures distinctly demonstrate that addition of the amino acid ligands to Nd(III) boosts the 4f-4f transitions' intensities, which are possibly due to the interaction of neodymium with the four ligands, resulting in the possible formation of the Nd(III):L complexes. With the addition of Mg(II) to the Nd(III):L complex, the transition band intensities are further enhanced, showing that the metal orbital expands thereby decreasing the metal-ligand bond distances leading to the interaction of the metal with ligand, forming the heterobimetallic complexes. Thus, the

intensification of the 4f-4f transition bands demonstrates how the addition of ligands to the Nd(III) ion causes the energy bands to experience a red shift.

In all the systems, it can be seen from Tables 3.2 to 3.5, that there is a decrease in Slater–Condon (F_k), spin-orbit interaction (ξ_{4f}), Racah (E^k) and Nephelauxetic ratio (β). This indicates that when we add ligands to Nd(III), expansion of the central metal ion orbital occurs which decreases the bond length between the central metal ion and the ligand. The positive values of bonding ($b^{1/2}$) and covalency (δ) parameters substantiate the formation of Nd(III):L and Nd(III):L:Mg(II) with a stronger binding interaction in the Ln(III) complexes which is in line with earlier reports on the theory of f-f transitions [17,18].

Tables 3.6 to 3.9 display the calculated and observed transition energies as well as their RMS deviation values. We can learn about the accuracy of the energy parameters from the RMS deviation value. Figures 3.8, 3.13, 3.18 and 3.23 show the comparative absorption spectra of Nd(III):L-Gln, Nd(III):L-Thr, Nd(III):L-Trp and Nd(III):L-Ile in different aquated organic solvents. The band intensification may be due to the increased interaction between 4f-orbitals and ligand orbitals. As can be seen, the spectra of the complexes in the DMF solution have significantly intensified. The sensitivity of the band intensities in the four solvents follow the order dimethylformamide > acetonitrile > dioxane > methanol. In general, the order in which different donor atoms prefer to make bonding with lanthanide ions is O > N > S [19]. In the present study, it is found that acetonitrile binds through nitrogen while DMF typically binds through oxygen for coordinating with hard acids such as Ln(III). The better bonding ability of oxygen than that of nitrogen is also revealed by the higher intensification in the DMF medium.

A similar trend is observed for the neodymium complex systems at different pH (2, 4 and 6). Figures 3.24 to 3.39 show the comparative absorption spectra of Nd(III), Nd(III):L and Nd(III):L:Mg(II) respectively at different pH levels. On moving from pH 2

to 4 and from 4 to 6, it can be seen that the intensities of the 4f transition bands could show a sharp increase. From Tables 3.10 to 3.13, as the pH increases from 2 to 4 and 4 to 6, the F_k, E^k, and ξ_{4f} parameters decrease gradually whereas there is an increase in $b^{1/2}$ and δ values, which imply that at higher pH levels, the interaction of the metal with the ligand is stronger compared to that at lower pH level. The carboxylate group of the amino acids presumably creates a binding site for the metal ion at lower pH values, whereas the amino group of the aforementioned ligands deprotonate at higher pH values that allow more possibilities of binding between the Ln(III) and the ligands. Thus, at higher pH, the formation of a stronger complexation takes place. Figures 3.1 and 3.2 depict the possible nona-coordinated structures of the Nd(III) complexes with L-Isoleucine and L-Tryptophan respectively, with the corresponding 3D structures as shown in Fig. 3.3.
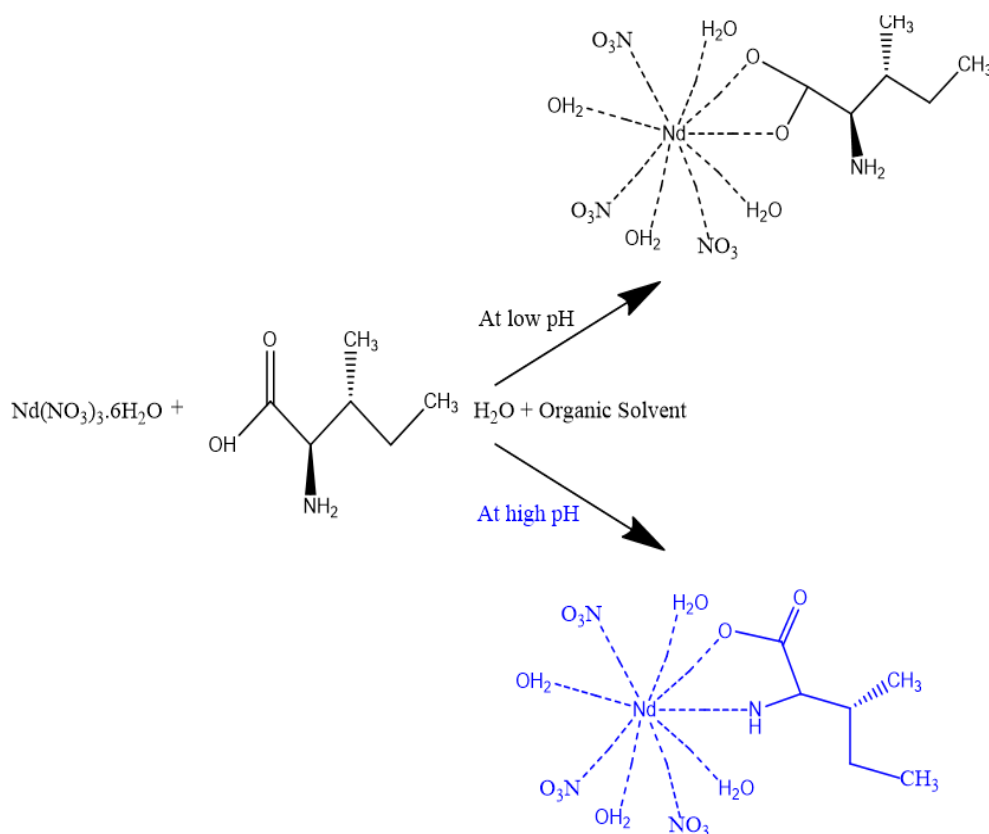
Fig 3.1: Probable structure of Nd(III):L-isoleucine at low and high pH
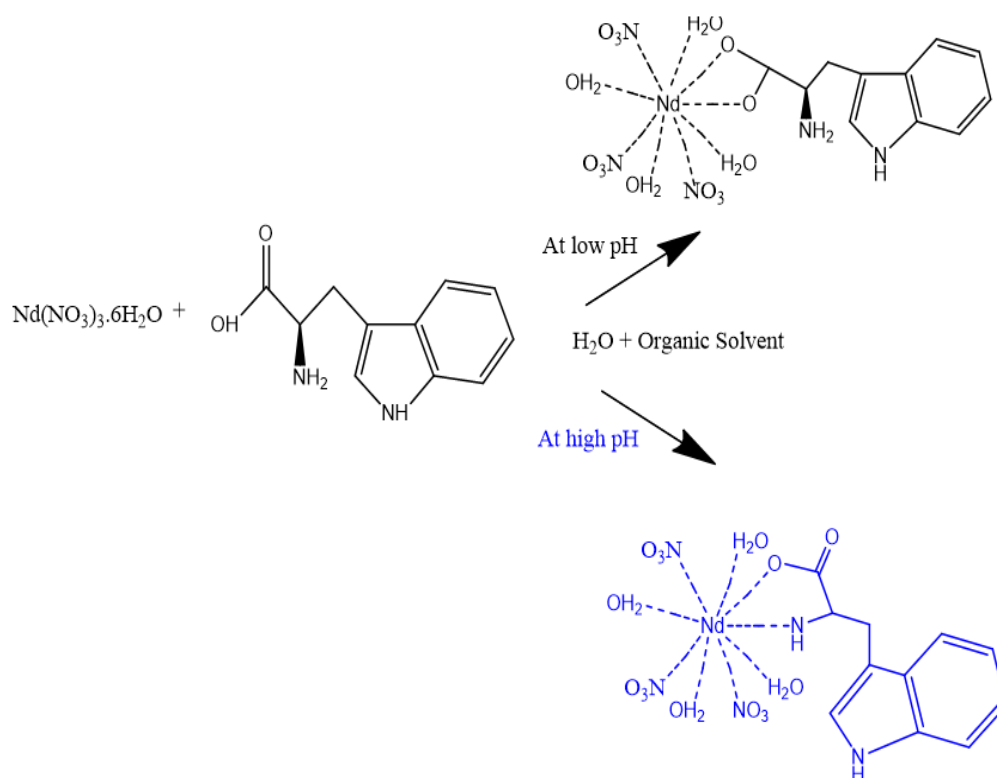
Fig 3.2: Probable structure of Nd(III):L-tryptophan at low and high pH

(a)   **(b)**
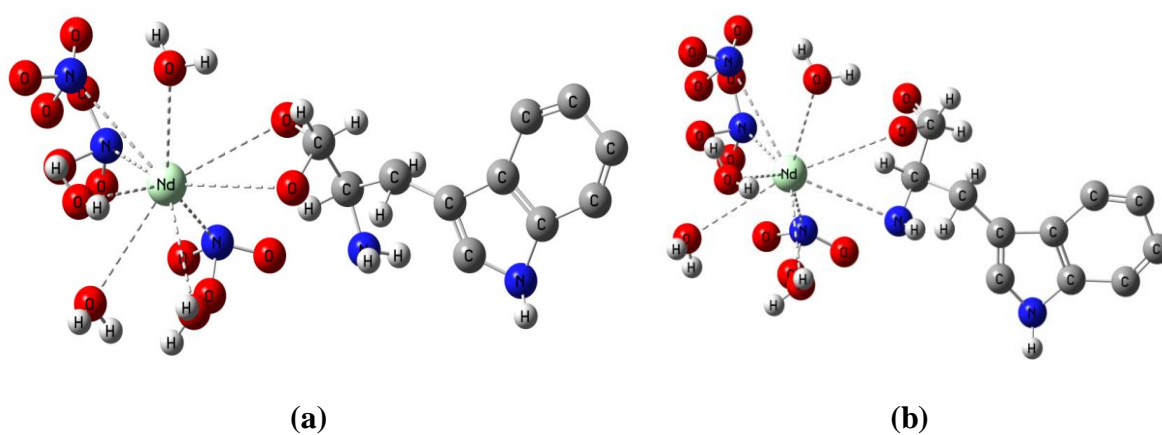
Fig. 3.3: Possible 3D Nona-coordinated structures of Nd(III):L-Trp at (a) at low pH and (b) at high pH

* Part of the work presented in this chapter has been communicated and is under review.

References

[1] A.-M. Măciucă, A.-C. Munteanu, V. Uivarosi, Quinolone Complexes with Lanthanide Ions: An Insight into their Analytical Applications and Biological Activity, *Molecules*. **25** (2020) 1347. https://doi.org/10.3390/molecules25061347.

[2] J.A. Cotruvo, The Chemistry of Lanthanides in Biology: Recent Discoveries, Emerging Principles, and Technological Applications, *ACS Cent. Sci.* **5** (2019) 1496–1506. https://doi.org/10.1021/acscentsci.9b00642.

[3] M.A. Gagnani, S.K. Hari, S.N. Misra, Comparative absorption spectroscopy involving 4f-4f transitions to complex & compositional dependence of intensity parameters, *J. Solid State Chem.* **4** (2003) 374–383.

[4] T. Moaienla, N. Bendangsenla, T. David Singh, C. Sumitra, N. Rajmuhon Singh, M. Indira Devi, Comparative 4f–4f absorption spectral study for the interactions of Nd(III) with some amino acids: Preliminary thermodynamics and kinetic studies of interaction of Nd(III):glycine with Ca(II), *Spectrochim. Acta Part A Mol. Biomol. Spectrosc.* **87** (2012) 142–150. https://doi.org/10.1016/J.SAA.2011.11.028.

[5] C.V. Devi, 4f-4f absorption spectral study for the interaction of Pr(III) and Nd(III) with uracil in presence and absence of Ca(II): A Model on the use of Ln(III) as probes at Ca(II) binding sites in biological systems., *Int. J. Chem. Biochem. Sci.* **7** (2015) 68–78.

[6] E.Y. Wong, Configuration Interaction of the Pr3+ Ion, *J. Chem. Phys.* **38** (1963) 976–978. https://doi.org/10.1063/1.1733794.

[7] E.Y. Wong, Taylor series expansion of the intermediate coupling energy levels of Nd3+ and Er3+, *J. Chem. Phys.* **35** (1961) 544. https://doi.org/10.1063/1.1731965.

[8] R.D. Peacock, The intensities of lanthanide f ↔ f transitions, in: E. Nieboer, C.K. Jørgensen, R.D. Peacock, R. Reisfeld (Eds.), Rare Earths, 1st ed., Springer Berlin Heidelberg, Berlin, 2007: pp. 83–122. https://doi.org/10.1007/bfb0116556.

[9] C.K. Jørgensen, B.R. Judd, Hypersensitive pseudoquadrupole transitions in lanthanides, *Mol. Phys.* **8** (1964) 281–290. https://doi.org/10.1080/00268976400100321.

[10] D.E. Henrie, R.L. Fellows, G.R. Choppin, Hypersensitivity in the electronic transitions of lanthanide and actinide complexes, *Coord. Chem. Rev.* **18** (1976) 199–224. https://doi.org/10.1016/S0010-8545(00)82044-5.

[11] S.P. Sinha, H.-H. Schmidtke, The nephelauxetic effect in rare earth complexes illustrated for praseodymium (III), *Mol. Phys.* **10** (1965) 7–11. https://doi.org/10.1080/00268976600100021.

[12] S.P. Sinha, Spectroscopic investigations of some neodymium complexes, *Spectrochim. Acta.* **22** (1966) 57–62. https://doi.org/10.1016/0371-1951(66)80008-5.

[13] S.P. Sinha, P.C. Mehta, S.S.L. Surana, Spectral intensities of lanthanide complexes, *Mol. Phys.* **23** (1972) 807–813. https://doi.org/10.1080/00268977200100781.

[14] E.U. Condon, E.U. Condon, G.H. Shortley, The theory of atomic spectra, Cambridge University Press, Cambridge, 1935.

[15] J.-C.G. Bünzli, S. V Eliseeva, Basics of Lanthanide Photophysics BT - Lanthanide Luminescence: Photophysical, Analytical and Biological Aspects, in: Lanthan. Lumin. Photophysical, Anal. Biol. Asp., Berlin Heidelberg, Springer-Verlag, 2010: pp. 1–45.

[16] C. Görller-Walrand, K. Binnemans, Chapter 167 Spectral intensities of f-f transitions, *Handb. Phys. Chem. Rare Earths.* **25** (1998) 101–264. https://doi.org/10.1016/S0168-1273(98)25006-9.

[17] C.V. Devi, 4f-4f absorption spectral study for the interaction of Pr(III) and Nd(III) with uracil in presence and absence of Ca(II): A Model on the use of Ln(III) as probes at Ca(II) binding sites in biological systems, *Int. J. Chem. Biochem. Sci.* **7** (2015) 68–78.

[18] R.S. Naorem, N.P. Singh, N.M. Singh, 4f–4f Spectral Analysis and Solvent Effect for the Interaction of Pr(III) with l-Tryptophan Using Different Aquated Solvents in the Presence and Absence of Zn(II), *Chem. Africa.* **3** (2020) 171–180. https://doi.org/10.1007/s42250-019-00111-9.

[19] S.N. Misra, Lanthanoid (III) ions as structural probe in biochemical reactions, *Proc. - Indian Natl. Sci. Acad. Part A, Phys. Sci.* **60** (1994) 637–655.

Table 3.2: Computed values of the energy interaction parameters: Slater-Condon factor F_k (cm^{-1}), Lande's Spin-orbit interactions ξ_{4f} (cm^{-1}), Racah parameters (E^k), Nephelauxetic ratio (β), Bonding ($b^{1/2}$) and Percent covalency (δ) of Nd(III) with L-Glutamine in absence and presence of Mg(II) in 50% (v/v) aquated solvents (Methanol, 1,4-Dioxane, Acetonitrile and Dimethylformamide)

.

System	F$_2$	F$_4$	F$_6$	ξ_{4f}	E^1	E^2	E^3	β	b$^{1/2}$	δ
Methanol:Water										
Nd(III)	332.3578	45.8820	5.0186	904.0346	3773.8067	25.5380	660.7495	0.9836	0.0904	1.6626
Nd(III): L-Gln	332.2749	45.8705	5.0174	903.2520	3772.8650	25.5316	660.5846	0.9831	0.0919	1.7198
Nd(III): L-Gln:Mg(II)	331.9873	45.8308	5.0130	901.6364	3769.5992	25.5095	660.01281	0.9818	0.0954	1.8557
1,4-Dioxane:Water										
Nd(III)	332.2808	45.8714	5.0174	904.0265	3772.9322	25.5321	660.5964	0.9835	0.0908	1.6747
Nd(III): L-Gln	331.6439	45.7834	5.0078	901.6082	3765.7002	25.4831	659.3301	0.9813	0.0968	1.9093
Nd(III): L-Gln:Mg(II)	331.4242	45.7531	5.0045	901.2112	3763.2057	25.4663	658.8934	0.9807	0.0982	1.9653
Acetonitrile:Water										
Nd(III)	332.6322	45.9438	5.0925	910.7169	3784.2126	25.5654	660.6188	0.9848	0.0871	1.4418
Nd(III): L-Gln	331.0217	45.6975	4.9984	899.6475	3758.6352	25.4353	658.0931	0.9793	0.1018	2.1163
Nd(III): L-Gln:Mg(II)	330.9200	45.6835	4.9969	894.3980	3757.4814	25.4275	657.8911	0.9762	0.1090	2.4348
DMF:Water										
Nd(III)	332.5350	45.9065	5.0213	908.1243	3775.8190	25.5516	661.1018	0.9862	0.0832	1.4033
Nd(III): L-Gln	331.2466	45.7286	5.0018	898.6042	3761.1891	25.4526	658.5403	0.9790	0.1044	2.1421
Nd(III): L-Gln:Mg(II)	330.9982	45.6943	4.9981	820.2622	3758.3685	25.4335	658.0464	0.9354	0.1797	2.9027

Table 3.3: Computed values of the energy interaction parameters: Slater-Condon factor F_k (cm^{-1}), Lande's Spin-orbit interactions ξ_{4f} (cm^{-1}), Racah parameters (E^k), Nephelauxetic ratio (β), Bonding ($b^{1/2}$) and Percent covalency (δ) of Nd(III) with L-Threonine in absence and presence of Mg(II) in 50% (v/v) aquated solvents (Methanol, 1,4-Dioxane, Acetonitrile and Dimethylformamide)

System	F_2	F_4	F_6	ξ_{4f}	E^1	E^2	E^3	β	$b^{1/2}$	δ
Methanol:Water										
Nd(III)	331.3885	45.7482	5.0040	901.8069	3762.8006	25.4635	658.8224	0.9810	0.0954	1.8525
Nd(III): L-Thr	331.3284	45.7399	5.0031	899.5703	3762.1185	25.4589	658.7030	0.9797	0.0978	1.9486
Nd(III): L-Thr:Mg(II)	331.2447	45.7283	5.0018	899.0934	3761.1682	25.4525	658.5366	0.9793	0.0988	1.9809
1,4-Dioxane:Water										
Nd(III)	332.0036	45.8331	5.0133	901.5840	3769.7844	25.5108	660.0452	0.9818	0.0955	1.8662
Nd(III): L-Thr	331.8272	45.8087	5.0106	900.4339	3767.7818	25.4972	659.6946	0.9809	0.0978	1.9588
Nd(III): L-Thr:Mg(II)	331.7958	45.8044	5.0101	899.8346	3767.4256	25.4948	659.6322	0.9805	0.0987	1.9880
Acetonitrile:Water										
Nd(III)	331.9617	45.8273	5.0126	901.7590	3769.3093	25.5076	659.9620	0.9818	0.0975	1.9366
Nd(III): L-Thr	331.8306	45.8092	5.0106	900.4282	3767.8204	25.4975	659.7014	0.9809	0.1008	2.0741
Nd(III): L-Thr:Mg(II)	331.7775	45.8019	5.0098	899.8325	3767.2175	25.4934	659.5958	0.9805	0.1017	2.1143
DMF:Water										
Nd(III)	330.7827	45.6646	4.9948	895.9892	3755.9221	25.4170	657.6181	0.9769	0.1075	2.3638
Nd(III): L-Thr	330.5342	45.6302	4.9911	894.6682	3753.0998	25.3979	657.1239	0.9758	0.1100	2.4783
Nd(III): L-Thr:Mg(II)	330.7252	45.6566	4.9939	891.3555	3755.2684	25.4126	657.5036	0.9743	0.1134	2.6413

Table 3.4: Computed values of the energy interaction parameters: Slater-Condon factor F_k (cm^{-1}), Lande's Spin-orbit interactions ξ_{4f} (cm^{-1}), Racah parameters (E^k), Nephelauxetic ratio (β), Bonding ($b^{1/2}$) and Percent covalency (δ) of Nd(III) with L-Tryptophan in absence and presence of Mg(II) in 50% (v/v) aquated solvents (Methanol, 1,4-Dioxane, Acetonitrile and Dimethylformamide)

System	F_2	F_4	F_6	ξ_{4f}	E^1	E^2	E^3	β	$b^{1/2}$	δ
Methanol:Water										
Nd(III)	332.3578	45.8820	5.0186	904.0346	3773.8067	25.5380	660.7495	0.9836	0.0904	1.6626
Nd(III): L-Trp	331.9674	45.8281	5.0127	900.5182	3769.3743	25.5080	659.9734	0.9811	0.0971	1.9227
Nd(III): L-Trp:Mg(II)	331.7901	45.8036	5.0100	901.8274	3767.3603	25.4944	659.6208	0.9810	0.0989	1.9546
1,4-Dioxane:Water										
Nd(III)	332.2808	45.8714	5.0174	904.0265	3772.9322	25.5321	660.5964	0.9835	0.0908	1.6747
Nd(III): L-Trp	331.1914	45.7210	5.0010	902.6973	3760.5629	25.4484	658.4307	0.9812	0.0969	1.9154
Nd(III): L-Trp:Mg(II)	331.674	45.8281	5.0127	900.5182	3769.3743	25.5080	659.9734	0.9811	0.0971	1.9227
Acetonitrile:Water										
Nd(III)	332.6322	45.9438	5.0925	910.7169	3784.2126	25.5654	660.6188	0.9848	0.0871	1.4418
Nd(III): L-Trp	331.9896	45.8312	5.0130	901.3413	3769.6255	25.5097	660.0174	0.9816	0.0959	1.8722
Nd(III): L-Trp:Mg(II)	331.6863	45.7893	5.0085	899.9380	3766.1816	25.4864	659.4144	0.9804	0.0990	1.9986
DMF:Water										
Nd(III)	332.5350	45.9065	5.0213	908.1243	3775.8190	25.5516	661.1018	0.9862	0.0832	1.4033
Nd(III): L-Trp	331.1718	45.7183	5.0007	898.5755	3760.3400	25.4469	658.3916	0.9789	0.1027	2.1552
Nd(III): L-Trp:Mg(II)	330.5354	45.6304	4.9911	893.3401	3753.1143	25.3980	657.1265	0.9751	0.1116	2.5551

Table 3.5: Computed values of the energy interaction parameters: Slater-Condon factor F_k (cm^{-1}), Lande's Spin-orbit interactions ξ_{4f} (cm^{-1}), Racah parameters (E^k), Nephelauxetic ratio (β), Bonding ($b^{1/2}$) and Percent covalency (δ) of Nd(III) with L-Isoleucine in absence and presence of Mg(II) in 50% (v/v) aquated solvents (Methanol, 1,4-Dioxane, Acetonitrile and Dimethylformamide)

System	F_2	F_4	F_6	ξ_{4f}	E^1	E^2	E^3	β	$b^{1/2}$	δ
Methanol:Water										
Nd(III)	332.3578	45.8820	5.0186	904.0346	3773.8067	25.5380	660.7494	0.9836	0.0904	1.6626
Nd(III): L-Ile	331.9890	45.8311	5.0130	902.8934	3769.6190	25.5097	660.0163	0.9825	0.0936	1.7835
Nd(III): L-Ile:Mg(II)	331.8128	45.8068	5.0104	902.2215	3767.6187	25.4961	659.6660	0.9818	0.0953	1.8486
1,4-Dioxane:Water										
Nd(III)	332.2808	45.8714	5.0174	904.0265	3772.9322	25.5321	660.5964	0.9835	0.0908	1.6747
Nd(III): L-Ile	331.6051	45.7781	5.0072	902.3056	3765.2599	25.4802	659.2530	0.9816	0.0959	1.8752
Nd(III): L-Ile:Mg(II)	331.3650	45.7449	5.0036	901.9641	3762.5339	25.4617	658.7758	0.9811	0.0973	1.9311
Acetonitrile:Water										
Nd(III)	332.6322	45.9438	5.0925	910.7169	3784.2126	25.5654	660.6188	0.9848	0.0871	1.4418
Nd(III): L-Ile	331.8618	45.8135	5.0111	901.0042	3768.1746	25.4999	659.7634	0.9812	0.0968	1.9109
Nd(III): L-Ile:Mg(II)	331.6725	45.7874	5.0083	898.5182	3766.0249	25.4853	659.3870	0.9796	0.1010	2.0823
DMF:Water										
Nd(III)	332.5350	45.9065	5.0213	908.1243	3775.8190	25.5516	661.1018	0.9862	0.0832	1.4033
Nd(III): L-Ile	330.9806	45.6919	4.9978	899.2026	3758.1686	25.4322	658.0114	0.9790	0.1025	2.1482
Nd(III): L-Ile:Mg(II)	330.5282	45.6294	4.9910	895.0738	3753.0322	25.3974	657.1121	0.9760	0.1095	2.4557

Table 3.6: Observed and computed values of energies (cm^{-1}) and R.M.S values of Nd(III) with L-Glutamine in absence and presence of Mg(II) systems in 50% (v/v) aquated solvents (Methanol, 1,4-Dioxane, Acetonitrile and Dimethylformamide)

System	$^4I_{9/2} \to \, ^4G_{7/2}$ E$_{obs}$ (E$_{cal}$)	$^4I_{9/2} \to$ $^4G_{5/2}$ E$_{obs}$ (E$_{cal}$)	$^4I_{9/2} \to \, ^4F_{7/2}$ E$_{obs}$ (E$_{cal}$)	$^4I_{9/2} \to \, ^4F_{5/2}$ E$_{obs}$ (E$_{cal}$)	$^4I_{9/2} \to \, ^4F_{3/2}$ E$_{obs}$ (E$_{cal}$)	RMS
Methanol:Water						
Nd(III)	19206.60 (19313.99)	17401.38 (17398.50)	13524.23 (13475.06)	12609.58 (12629.32)	11565.88 (11598.03)	55.46
Nd(III):L-Gln	19206.60 (19307.28)	17396.06 (17392.93)	13511.14 (13469.62)	12596.62 (12624.41)	11565.88 (11595.09)	51.95
Nd(III):L-Gln:Mg(II)	19176.41 (19288.54)	17370.41 (17375.04)	13498.07 (13454.31)	12591.66 (12610.19)	11558.66 (11584.91)	55.75
1,4-Dioxane:Water						
Nd(III)	19136.26 (19263.16)	17315.16 (17343.53)	13491.73 (13433.21)	12594.77 (12589.43)	11546.64 (11564.97)	64.34
Nd(III):L-Gln	19122.62 (19239.82)	17277.38 (17319.38)	13484.04 (13414.05)	12580.03 (12571.33)	11534.25 (11550.72)	64.41
Nd(III):L-Gln:Mg(II)	19121.06 (18910.97)	17267.11 (17215.68)	13467.14 (13156.02)	12573.22 (12365.70)	11143.23 (11549.89)	65.33
Acetonitrile:Water						
Nd(III)	19245.07 (19338.31)	17414.49 (17413.52)	13535.16 (13494.51)	12621.11 (12646.06)	11579.08 (11604.31)	48.18
Nd(III):L-Gln	19203.91 (19310.72)	17396.41 (17394.26)	13511.14 (13472.33)	12600.21 (12626.61)	11569.48 (11595.30)	53.45
Nd(III):L-Gln:Mg(II)	19181.91 (19274.02)	17335.67 (17356.12)	13487.19 (13442.19)	12590.74 (12598.12)	11549.25 (11572.75)	48.03
DMF:Water						
Nd(III)	19243.63 (19269.19)	17241.93 (17312.25)	13424.48 (13436.27)	12539.83 (12586.29)	11579.08 (11536.93)	43.98
Nd(III):L-Gln	19217.13 (19244.94)	17310.08 (17330.40)	13400.85 (13418.55)	12528.57 (12576.50)	11551.92 (11558.68)	27.72
Nd(III):L-Gln:Mg(II)	19162.12 (19213.87)	17285.65 (17307.02)	13375.16 (13393.48)	12507.98 (12554.24)	11542.37 (11547.12)	33.57

Table 3.7: Observed and computed values of energies (cm^{-1}) and R.M.S values of Nd(III) with L-Threonine in absence and presence of Mg(II) systems in 50% (v/v) aquated solvents (Methanol, 1,4-Dioxane, Acetonitrile and Dimethylformamide)

System	$^4I_{9/2} \rightarrow {}^4G_{7/2}$ E_{obs} (E_{cal})	$^4I_{9/2} \rightarrow {}^4G_{5/2}$ E_{obs} (E_{cal})	$^4I_{9/2} \rightarrow {}^4F_{7/2}$ E_{obs} (E_{cal})	$^4I_{9/2} \rightarrow {}^4F_{5/2}$ E_{obs} (E_{cal})	$^4I_{9/2} \rightarrow {}^4F_{3/2}$ E_{obs} (E_{cal})	RMS
Methanol:Water						
Nd(III)	19137.52 (19264.12)	17314.10 (17342.34)	13504.25 (13433.89)	12570.12 (12589.72)	11551.94 (11563.71)	66.78
Nd(III):L-Thr	19126.62 (19252.37)	17309.78 (17336.15)	13497.22 (13424.54)	12565.82 (12581.85)	11543.71 (11561.58)	66.88
Nd(III):L-Thr:Mg(II)	19121.09 (19246.89)	17302.21 (17330.93)	13493.86 (13420.07)	12563.23 (12577.69)	11541.17 (11558.62)	67.25
1,4-Dioxane:Water						
Nd(III)	19174.2 (19289)	17371.8 (17375.9)	13497 (13454.7)	12595 (12610.6)	11558.68 (11585.49)	56.45
Nd(III):L-Thr	19159.6 (19276.9)	17355.9 (17364.7)	13490.3 (13444.8)	12590.2 (12601.5)	11552.90 (11579.24)	57.83
Nd(III):L-Thr:Mg(II)	19156.1 (19273.1)	17354 (17362.2)	13488.7 (13441.8)	12583.8 (12598.9)	11551.66 (11578.13)	58.12
Acetonitrile:Water						
Nd(III)	19173.44 (19287.97)	17367.32 (17373.79)	13501.75 (13453.81)	12593.59 (12609.62)	11557.62 (11584.01)	57.29
Nd(III):L-Thr	19160.75 (19276.98)	17356.20 (17364.87)	13493.56 (13444.91)	12588.08 (12601.60)	11552.56 (11579.36)	58.06
Nd(III):L-Thr:Mg(II)	19148.99 (19272.29)	17351.98 (17361.18)	13491.37 (13441.12)	12586.47 (12598.21)	11551.05 (11577.48)	61.07
DMF:Water						
Nd(III)	19156.92 (19214.69)	17270.82 (17301.53)	13375.42 (13393.83)	12515.42 (12553.55)	11544.81 (11542.26)	34.87
Nd(III):L-Thr	19131.45 (19198.80)	17249.03 (17286.16)	13368.82 (13380.84)	12505.49 (12541.46)	11539.24 (11533.45)	38.43
Nd(III):L-Thr:Mg(II)	19121.79 (19193.13)	17270.89 (17292.38)	13359.43 (13376.80)	12500.08 (12539.58)	11534.33 (11540.22)	38.60

Table 3.8: Observed and computed values of energies (cm^{-1}) and R.M.S values of Nd(III) with L-Tryptophan in absence and presence of Mg(II) systems in 50% (v/v) aquated solvents (Methanol, 1,4-Dioxane, Acetonitrile and Dimethylformamide)

System	$^4I_{9/2}\rightarrow\,^4G_{7/2}$ E_{obs} (E_{cal})	$^4I_{9/2}\rightarrow\,^4G_{5/2}$ E_{obs} (E_{cal})	$^4I_{9/2}\rightarrow\,^4F_{7/2}$ E_{obs} (E_{cal})	$^4I_{9/2}\rightarrow\,^4F_{5/2}$ E_{obs} (E_{cal})	$^4I_{9/2}\rightarrow\,^4F_{3/2}$ E_{obs} (E_{cal})	RMS
Methanol:Water						
Nd(III)	19206.60 (19313.99)	17401.38 (17398.50)	13524.23 (13475.06)	12609.58 (12629.32)	11565.88 (11598.03)	55.46
Nd(III):L-Trp	19181.60 (19283.09)	17367.68 (17372.51)	13487.20 (13449.99)	12599.39 (12606.61)	11551.93 (11584.21)	50.60
Nd(III):L-Trp:Mg(II)	19166.93 (19281.06)	17353.16 (17364.44)	13487.20 (13448.02)	12583.17 (12603.80)	11559.91 (11577.93)	55.56
1,4-Dioxane:Water						
Nd(III)	19136.26 (19263.16)	17315.16 (17343.53)	13491.73 (13433.21)	12594.77 (12589.43)	11546.64 (11564.97)	64.34
Nd(III):L-Trp	19126.34 (19259.54)	17294.22 (17332.65)	13501.75 (13429.88)	12574.38 (12585.13)	11551.60 (11556.73)	70.03
Nd(III):L-Trp:Mg(II)	19181.60 (19283.09)	17367.68 (17372.51)	13487.20 (13449.99)	12599.39 (12606.61)	11551.93 (11584.21)	50.60
Acetonitrile:Water						
Nd(III)	19245.07 (19338.31)	17414.49 (17413.52)	13535.16 (13494.51)	12621.11 (12646.06)	11579.08 (11604.31)	48.18
Nd(III):L-Trp	19161.74 (19287.42)	17371.13 (17374.78)	13498.07 (13453.43)	12595.21 (12609.51)	11559.06 (11584.99)	61.12
Nd(III):L-Trp:Mg(II)	19142.44 (19268.90)	17344.10 (17356.30)	13481.74 (13438.27)	12585.83 (12595.30)	11552.31 (11574.25)	60.99
DMF:Water						
Nd(III)	19243.63 (19269.19)	17241.93 (17312.25)	13424.48 (13436.27)	12539.83 (12586.29)	11579.08 (11536.93)	43.98
Nd(III):L-Trp	19190.70 (19241.69)	17307.08 (17326.25)	13387.99 (13415.83)	12519.20 (12573.81)	11559.90 (11556.03)	36.71
Nd(III):L-Trp:Mg(II)	19135.11 (19193.37)	17249.45 (17284.51)	13375.16 (13376.59)	12496.78 (12538.08)	11532.83 (11533.50)	35.58

Table 3.9: Observed and computed values of energies (cm^{-1}) and R.M.S values of Nd(III) with L-Isoleucine in absence and presence of Mg(II) systems in 50% (v/v) aquated solvents (Methanol, 1,4-Dioxane, Acetonitrile and Dimethylformamide)

System	$^4I_{9/2} \to {}^4G_{7/2}$ E_{obs} (E_{cal})	$^4I_{9/2} \to {}^4G_{5/2}$ E_{obs} (E_{cal})	$^4I_{9/2} \to {}^4F_{7/2}$ E_{obs} (E_{cal})	$^4I_{9/2} \to {}^4F_{5/2}$ E_{obs} (E_{cal})	$^4I_{9/2} \to {}^4F_{3/2}$ E_{obs} (E_{cal})	RMS
Methanol:Water						
Nd(III)	19206.60 (19313.99)	17401.38 (17398.50)	13524.23 (13475.06)	12609.58 (12629.32)	11565.88 (11598.03)	55.46
Nd(III):L-Ile	19168.73 (19293.80)	17369.46 (17376.75)	13505.85 (13458.44)	12598.44 (12613.50)	11562.78 (11584.97)	61.09
Nd(III):L-Ile:Mg(II)	19163.51 (19283.64)	17353.16 (17366.20)	13500.52 (13450.10)	12591.48 (12605.61)	11557.87 (11578.73)	59.63
1,4-Dioxane:Water						
Nd(III)	19136.26 (19263.16)	17315.16 (17343.53)	13491.73 (13433.21)	12594.77 (12589.43)	11546.64 (11564.97)	64.34
Nd(III):L-Ile	19167.66 (19275.27)	17334.15 (17354.89)	13489.54 (13443.09)	12580.80 (12598.57)	11556.30 (11571.38)	54.24
Nd(III):L-Ile:Mg(II)	19154.63 (19263.79)	17311.85 (17341.25)	13489.47 (13433.58)	12570.47 (12589.30)	11552.13 (11562.88)	57.22
Acetonitrile:Water						
Nd(III)	19245.07 (19338.31)	17414.49 (17413.52)	13535.16 (13494.51)	12621.11 (12646.06)	11579.08 (11604.31)	48.18
Nd(III):L-Ile	19168.77 (19280.66)	17357.37 (17367.32)	13499.59 (13447.87)	12593.95 (12604.18)	11551.93 (11580.47)	56.95
Nd(III):L-Ile:Mg(II)	19142.46 (19262.45)	17342.20 (17353.71)	13487.20 (13433.18)	12584.09 (12591.15)	11543.96 (11573.76)	60.64
DMF:Water						
Nd(III)	19243.63 (19269.19)	17241.93 (17312.25)	13424.48 (13436.27)	12539.83 (12586.29)	11579.08 (11536.93)	43.98
Nd(III):L-Ile	19190.69 (19236.26)	17288.65 (17316.55)	13375.17 (13411.17)	12519.20 (12568.75)	11559.90 (11549.26)	36.66
Nd(III):L-Ile:Mg(II)	19142.46 (19200.23)	17249.47 (17286.35)	13364.50 (13381.95)	12496.78 (12542.30)	11542.37 (11533.24)	37.83

Table 3.10: Computed values of the energy interaction parameters: Slater-Condon factor F_k (cm^{-1}), Lande's Spin-orbit interactions ξ_{4f} (cm^{-1}), Racah (E^k), Nephelauxetic ratio (β), Bonding ($b^{1/2}$) and Percent covalency (δ) for the different Nd(III) systems with L-Glutamine in absence and presence of Mg(II) in 50% (v/v) aquated DMF solvent at pH 2, 4 and 6

System	F_2	F_4	F_6	ξ_{4f}	E^1	E^2	E^3	β	$b^{1/2}$	δ
pH = 2										
Nd(III)	331.7303	45.7954	5.0091	902.6434	3766.6819	25.4898	659.5020	0.9820	0.0950	1.8369
Nd(III): L-Gln	331.2714	45.7320	5.0022	899.9656	3761.4707	25.4545	658.5896	0.9798	0.1005	2.0600
Nd(III): L-Gln:Mg(II)	330.8363	45.6720	4.9956	896.7061	3756.5305	25.4211	657.7246	0.9774	0.1063	2.3141
pH = 4										
Nd(III)	331.2405	45.7278	5.0017	900.2354	3761.1202	25.4522	658.5282	0.9799	0.1002	2.0492
Nd(III): L-Gln	331.0370	45.6997	4.9987	898.4762	3758.8097	25.4365	658.1237	0.9787	0.1033	2.1814
Nd(III): L-Gln:Mg(II)	330.5812	45.6367	4.9918	895.9162	3753.6337	25.4015	657.2174	0.9766	0.1082	2.3988
pH = 6										
Nd(III)	330.9604	45.6891	4.9975	896.8080	3757.9392	25.4306	657.9713	0.9776	0.1058	2.2893
Nd(III): L-Gln	330.7478	45.6597	4.9943	892.5707	3755.5257	25.4143	657.5487	0.9750	0.1119	2.5672
Nd(III): L-Gln:Mg(II)	330.1061	45.5712	4.9846	890.2894	3748.2397	25.3650	656.2730	0.9728	0.1167	2.7986

Table 3.11: Computed values of the energy interaction parameters: Slater-Condon factor F_k (cm^{-1}), Lande's Spin-orbit interactions ξ_{4f} (cm^{-1}), Racah (E^k), Nephelauxetic ratio (β), Bonding ($b^{1/2}$) and Percent covalency (δ) for the different Nd(III) systems with L-Threonine in absence and presence of Mg(II) in 50% (v/v) aquated DMF solvent at pH 2, 4 and 6

System	F_2	F_4	F_6	ξ_{4f}	E^1	E^2	E^3	β	$b^{1/2}$	δ
pH = 2										
Nd(III)	330.7514	45.6602	4.9943	896.3936	3755.5661	25.4146	657.5558	0.9771	0.1070	2.3452
Nd(III): L-Thr	330.7004	45.6532	4.9936	895.8108	3754.9871	25.4106	657.4544	0.9767	0.1080	2.3867
Nd(III): L-Thr:Mg(II)	330.6478	45.6459	4.9928	895.3156	3754.3905	25.4066	657.3499	0.9763	0.1088	2.4234
pH = 4										
Nd(III)	330.7352	45.6580	4.9941	895.3749	3755.3821	25.4133	657.5236	0.9765	0.1084	2.4066
Nd(III): L-Thr	330.6574	45.6473	4.9929	894.7144	3754.4997	25.4074	657.3691	0.9760	0.1095	2.4567
Nd(III): L-Thr:Mg(II)	330.6225	45.6424	4.9924	894.1354	3754.1023	25.4047	657.2995	0.9757	0.1103	2.4956
pH = 6										
Nd(III)	330.5910	45.6381	4.9919	896.1296	3753.7449	25.4022	657.2369	0.9767	0.1079	2.3850
Nd(III): L-Thr	330.5191	45.6282	4.9908	894.8046	3752.9285	25.3967	657.0940	0.9759	0.1098	2.4727
Nd(III): L-Thr:Mg(II)	330.4396	45.6172	4.9896	893.8842	3752.0257	25.3906	656.9359	0.9752	0.1113	2.5382

Table 3.12: Computed values of the energy interaction parameters: Slater-Condon factor F_k (cm^{-1}), Lande's Spin-orbit interactions ξ_{4f} (cm^{-1}), Racah (E^k), Nephelauxetic ratio (β), Bonding ($b^{1/2}$) and Percent covalency (δ) for the different Nd(III) systems with L-Tryptophan in absence and presence of Mg(II) in 50% (v/v) aquated DMF solvent at pH 2, 4 and 6

System	F_2	F_4	F_6	ξ_{4f}	E^1	E^2	E^3	β	$b^{1/2}$	δ
pH = 2										
Nd(III)	331.3150	45.7380	5.0029	901.9381	3761.9662	25.4579	658.6763	0.9810	0.0976	1.9402
Nd(III): L-Trp	331.0568	45.7024	4.9990	899.4058	3759.0342	25.4380	658.1630	0.9792	0.1020	2.1249
Nd(III): L-Trp:Mg(II)	330.5976	45.6390	4.9920	892.9057	3753.8199	25.4028	657.2500	0.9749	0.1119	2.5708
pH = 4										
Nd(III)	330.8880	45.6791	4.9964	899.7173	3757.1170	25.4251	657.8273	0.9791	0.1022	2.1326
Nd(III): L-Trp	330.6590	45.6475	4.9930	897.5792	3754.5176	25.4075	657.3722	0.9776	0.1058	2.2908
Nd(III): L-Trp:Mg(II)	330.6275	45.6431	4.9925	896.2200	3754.1593	25.4050	657.3094	0.9768	0.1077	2.3741
pH = 6										
Nd(III)	330.5959	45.6388	4.9920	896.2906	3753.8007	25.4026	657.2467	0.9768	0.1077	2.3749
Nd(III): L-Trp	330.4845	45.6234	4.9903	893.1318	3752.5354	25.3941	657.0251	0.9749	0.1120	2.5750
Nd(III): L-Trp:Mg(II)	330.0892	45.5688	4.9843	886.2640	3748.0477	25.3637	656.2394	0.9705	0.1214	3.0365

Table 3.13: Computed values of the energy interaction parameters: Slater-Condon factor F_k (cm^{-1}), Lande's Spin-orbit interactions ξ_{4f} (cm^{-1}), Racah (E^k), Nephelauxetic ratio (β), Bonding ($b^{1/2}$) and Percent covalency (δ) for the different Nd(III) systems with L-Isoleucine in absence and presence of Mg(II) in 50% (v/v) aquated DMF solvent at pH 2, 4 and 6

System	F_2	F_4	F_6	ξ_{4f}	E^1	E^2	E^3	β	$b^{1/2}$	δ
pH = 2										
Nd(III)	331.0916	45.7072	4.9995	903.1195	3759.4294	25.4407	658.2322	0.9813	0.0967	1.9063
Nd(III): L-Ile	330.7921	45.6658	4.9950	899.5873	3756.0286	25.4177	657.6367	0.9789	0.1027	2.1547
Nd(III): L-Ile:Mg	330.4551	45.6193	4.9899	895.4064	3752.2019	25.3918	656.9667	0.9761	0.1093	2.3476
pH = 4										
Nd(III)	330.7608	45.6615	4.9945	895.5086	3755.6731	25.4153	657.5745	0.9766	0.1081	2.3949
Nd(III): L-Ile	330.5943	45.6385	4.9920	894.3124	3753.7823	25.4025	657.2434	0.9757	0.1102	2.4197
Nd(III): L-Ile:Mg	330.3112	45.5995	4.9877	895.8930	3750.5687	25.3807	656.6808	0.9762	0.1092	2.4414
pH = 6										
Nd(III)	330.7598	45.6614	4.9945	896.6060	3755.6613	25.4152	657.5724	0.9772	0.1067	2.3316
Nd(III): L-Ile	330.5045	45.6261	4.9906	895.4113	3752.7625	25.3956	657.0649	0.9762	0.1091	2.4398
Nd(III): L-Ile:Mg	330.2275	45.5879	4.9864	888.7902	3749.6173	25.3743	656.5142	0.9721	0.1181	2.8674

Table 3.14: Computed and observed values of energy (cm^{-1}) and R.M.S values for the different Nd(III) systems with L-Glutamine in absence and presence of Mg(II) in 50% (v/v) aquated DMF solvent at pH 2, 4 and 6

System	$^4I_{9/2} \rightarrow {}^4G_{7/2}$ E_{obs} (E_{cal})	$^4I_{9/2} \rightarrow {}^4G_{5/2}$ E_{obs} (E_{cal})	$^4I_{9/2} \rightarrow {}^4F_{7/2}$ E_{obs} (E_{cal})	$^4I_{9/2} \rightarrow {}^4F_{5/2}$ E_{obs} (E_{cal})	$^4I_{9/2} \rightarrow {}^4F_{3/2}$ E_{obs} (E_{cal})	R.M.S
pH = 2						
Nd(III)	19168.77 (19225.52)	17288.65 (17312.35)	13387.99 (13402.70)	12506.11 (12561.87)	11551.93 (11548.55)	37.73
Nd(III): L-Gln	19142.46 (19199.10)	17270.80 (17295.20)	13375.17 (13381.53)	12496.78 (12543.51)	11534.42 (11541.02)	34.85
Nd(III): L-Gln:Mg(II)	19094.43 (19162.76)	17210.45 (17256.97)	13364.50 (13351.67)	12485.61 (12515.21)	11516.97 (11518.30)	39.69
pH = 4						
Nd(III)	19185.48 (19251.43)	17313.68 (17332.17)	13387.44 (13423.62)	12526.70 (12580.49)	11569.48 (11558.47)	42.46
Nd(III): L-Gln	19167.22 (19235.62)	17295.80 (17318.72)	13381.58 (13410.79)	12517.34 (12568.85)	11561.50 (11551.26)	41.99
Nd(III): L-Gln:Mg(II)	19133.70 (19205.93)	17256.58 (17290.35)	13355.97 (13386.54)	12496.78 (12546.32)	11551.93 (11535.12)	44.78
pH = 6						
Nd(III)	19230.33 (19281.92)	17356.74 (17362.21)	13415.89 (13448.57)	12537.96 (12603.82)	11579.09 (11575.81)	40.27
Nd(III): L-Gln	19203.92 (19251.61)	17313.68 (17333.52)	13405.15 (13423.83)	12526.70 (12580.88)	11561.50 (11559.56)	34.51
Nd(III): L-Gln:Mg(II)	19181.91 (19219.89)	17274.38 (17305.40)	13392.28 (13398.03)	12506.11 (12557.27)	11543.96 (11544.15)	31.80

Table 3.15: Computed and observed values of energy (cm^{-1}) and R.M.S values for the different Nd(III) systems with L-Threonine in absence and presence of Mg(II) in 50% (v/v) aquated DMF solvent at pH 2, 4 and 6

System	$^4I_{9/2} \rightarrow {}^4G_{7/2}$ E$_{obs}$ (E$_{cal}$)	$^4I_{9/2} \rightarrow {}^4G_{5/2}$ E$_{obs}$ (E$_{cal}$)	$^4I_{9/2} \rightarrow {}^4F_{7/2}$ E$_{obs}$ (E$_{cal}$)	$^4I_{9/2} \rightarrow {}^4F_{5/2}$ E$_{obs}$ (E$_{cal}$)	$^4I_{9/2} \rightarrow {}^4F_{3/2}$ E$_{obs}$ (E$_{cal}$)	R.M.S
pH = 2						
Nd(III)	19119.41 (19215.04)	17270.97 (17300.32)	13380.29 (13394.04)	12508.85 (12553.5)	11553.50 (11541.15)	49.68
Nd(III): L-Thr	19112.46 (19210.49)	17266.7 (17296.77)	13378.24 (13390.37)	12506.5 (12550.21)	11551.38 (11539.34)	50.43
Nd(III): L-Thr:Mg(II)	19107.8 (19206.24)	17262.22 (17293.24)	13375.28 (13386.92)	12504.13 (12547.1)	11549.43 (11537.48)	50.55
pH = 4						
Nd(III)	19142.16 (19207.22)	17253.46 (17291.17)	13374.81 (13387.57)	12507.07 (12547.21)	11544.52 (11535.47)	38.76
Nd(III): L-Thr	19133.38 (19198.73)	17248.68 (17285.5)	13362.62 (13380.76)	12501.04 (12541.28)	11541.74 (11532.92)	39.12
Nd(III): L-Thr:Mg(II)	19127.5 (19191.6)	17242.24 (17279.94)	13358.08 (13374.99)	12494.55 (12536.13)	11538.51 (11530.1)	39.03
pH = 6						
Nd(III)	19150.09 (19210.15)	17267.76 (17298.12)	13374.06 (13390.17)	12507.18 (12550.3)	11544.04 (11540.57)	36.50
Nd(III): L-Thr	19142.65 (19204.16)	17261.14 (17292.99)	13369.95 (13385.31)	12503.72 (12545.88)	11541.54 (11537.82)	36.95
Nd(III): L-Thr:Mg(II)	19138.57 (19200.31)	17258.39 (17290.3)	13365.89 (13382.21)	12502.18 (12543.17)	11539.66 (11536.58)	36.84

Table 3.16: Computed and observed values of energy (cm^{-1}) and R.M.S values for the different Nd(III) systems with L-Tryptophan in absence and presence of Mg(II) in 50% (v/v) aquated DMF solvent at pH 2, 4 and 6

System	$^4I_{9/2} \rightarrow {}^4G_{7/2}$ E_{obs} (E_{cal})	$^4I_{9/2} \rightarrow {}^4G_{5/2}$ E_{obs} (E_{cal})	$^4I_{9/2} \rightarrow {}^4F_{7/2}$ E_{obs} (E_{cal})	$^4I_{9/2} \rightarrow {}^4F_{5/2}$ E_{obs} (E_{cal})	$^4I_{9/2} \rightarrow {}^4F_{3/2}$ E_{obs} (E_{cal})	R.M.S
pH = 2						
Nd(III)	19203.92 (19261.58)	17316.68 (17338.47)	13405.15 (13431.75)	12537.96 (12587.49)	11569.71 (11561.11)	37.51
Nd(III): L-Trp	19181.91 (19240.29)	17295.80 (17321.00)	13392.28 (13414.50)	12517.34 (12571.94)	11561.50 (11551.96)	39.01
Nd(III): L-Trp:Mg(II)	19133.70 (19194.18)	17256.58 (17287.37)	13368.75 (13377.36)	12496.78 (12539.12)	11534.42 (11535.70)	35.98
pH = 4						
Nd(III)	19162.15 (19234.50)	17278.89 (17312.12)	13389.78 (13409.59)	12524.83 (12566.84)	11559.91 (11545.98)	41.69
Nd(III): L-Trp	19155.58 (19216.06)	17260.13 (17296.78)	13378.00 (13394.65)	12502.39 (12553.33)	11551.93 (11537.88)	40.18
Nd(III): L-Trp:Mg(II)	19133.70 (19209.13)	17260.13 (17293.29)	13368.75 (13389.14)	12496.78 (12548.72)	11551.93 (11536.76)	45.01
pH = 6						
Nd(III)	19107.49 (19208.09)	17256.58 (17291.64)	13376.21 (13388.26)	12506.11 (12547.80)	11551.93 (11535.64)	51.96
Nd(III): L-Trp	19085.72 (19190.37)	17250.24 (17281.44)	13368.75 (13374.13)	12485.61 (12535.76)	11543.96 (11531.69)	54.07
Nd(III): L-Trp:Mg(II)	19037.97 (19145.43)	17217.54 (17250.85)	13345.33 (13338.03)	12465.16 (12504.23)	11516.97 (11517.70)	53.36

Table 3.17: Computed and observed values of energy (cm^{-1}) and R.M.S values for the different Nd(III) systems with L-Isoleucine in absence and presence of Mg(II) in 50% (v/v) aquated DMF solvent at pH 2, 4 and 6

System	$^4I_{9/2} \rightarrow {}^4G_{7/2}$ E_{obs} (E_{cal})	$^4I_{9/2} \rightarrow {}^4G_{5/2}$ E_{obs} (E_{cal})	$^4I_{9/2} \rightarrow {}^4F_{7/2}$ E_{obs} (E_{cal})	$^4I_{9/2} \rightarrow {}^4F_{5/2}$ E_{obs} (E_{cal})	$^4I_{9/2} \rightarrow {}^4F_{3/2}$ E_{obs} (E_{cal})	R.M.S
pH = 2						
Nd(III)	19217.13 (19257.09)	17294.63 (17327.71)	13400.86 (13427.75)	12528.58 (12582.73)	11569.48 (11553.19)	36.36
Nd(III): L-Ile	19168.77 (19229.94)	17270.83 (17306.68)	13375.17 (13405.82)	12519.12 (12563.16)	11559.91 (11542.59)	40.51
Nd(III): L-Ile:Mg(II)	19138.79 (19198.53)	17242.21 (17282.76)	13364.50 (13380.47)	12496.78 (12540.60)	11542.37 (11530.65)	38.80
pH = 4						
Nd(III)	19124.15 (19211.78)	17270.83 (17299.70)	13387.99 (13391.50)	12507.99 (12551.54)	11546.92 (11541.48)	45.72
Nd(III): L-Ile	19116.22 (19199.85)	17256.64 (17289.00)	13375.17 (13381.80)	12499.56 (12542.64)	11542.37 (11535.58)	44.69
Nd(III): L-Ile:Mg(II)	19113.81 (19194.51)	17228.16 (17275.48)	13375.17 (13377.01)	12496.78 (12536.83)	11542.37 (11525.56)	46.13
pH = 6						
Nd(III)	19142.46 (19216.27)	17270.80 (17301.06)	13375.17 (13395.02)	12507.99 (12554.34)	11551.93 (11541.44)	42.46
Nd(III): L-Ile	19129.90 (19200.63)	17249.47 (17285.48)	13364.50 (13382.21)	12487.47 (12542.34)	11548.17 (11532.40)	44.44
Nd(III): L-Ile:Mg(II)	19094.43 (19161.66)	17228.16 (17261.71)	13326.21 (13351.06)	12476.30 (12515.58)	11524.89 (11522.59)	39.53

Comparative UV-Vis. absorption spectra of Nd(III) with the selected amino acids in different aquated solvents

1. L-Glutamine
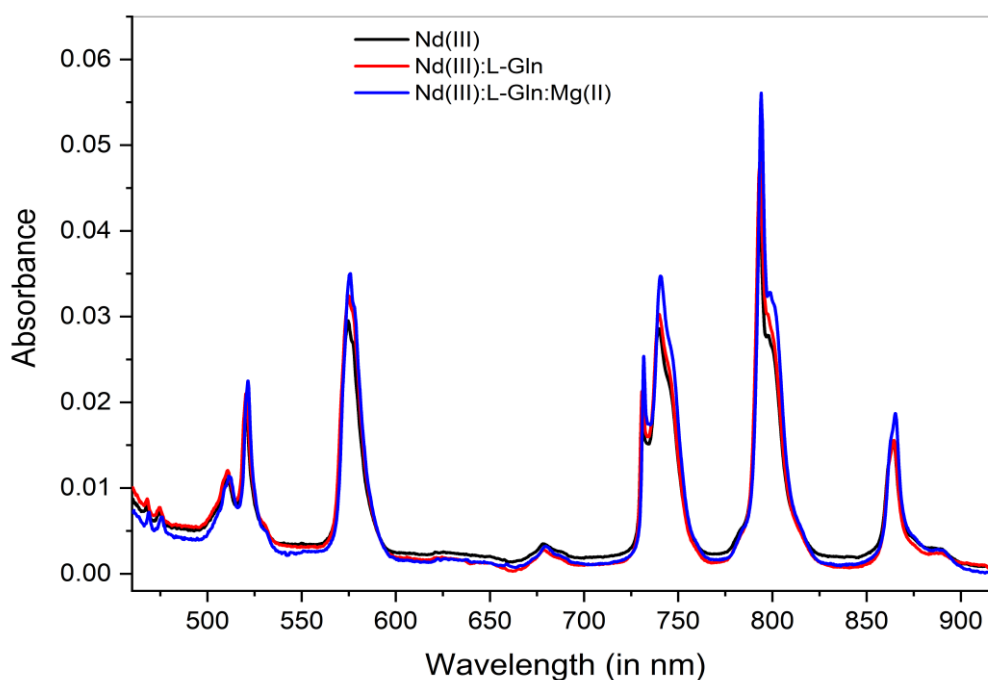
Fig. 3.4: Comparative UV-Vis. absorption spectra of Nd(III), Nd(III):L-Gln and Nd(III):L-Gln:Mg(II) in methanol: water (50% v/v) solvent

Fig. 3.5: Comparative UV-Vis. absorption spectra of Nd(III), Nd(III):L-Gln and Nd(III):L-Gln:Mg(II) in 1,4-dioxane: water (50% v/v) solvent

Fig. 3.6: Comparative UV-Vis. absorption spectra of Nd(III), Nd(III):L-Gln and
Nd(III):L-Gln:Mg(II) in acetonitrile: water (50% v/v) solvent

Fig. 3.7: Comparative UV-Vis. absorption spectra of Nd(III), Nd(III):L-Gln and
Nd(III):L-Gln:Mg(II) in DMF: water (50% v/v) solvent

Fig. 3.8: Comparative UV-Vis. absorption spectra of Nd(III):L-Gln in different aquated solvents

2. **L-Threonine**
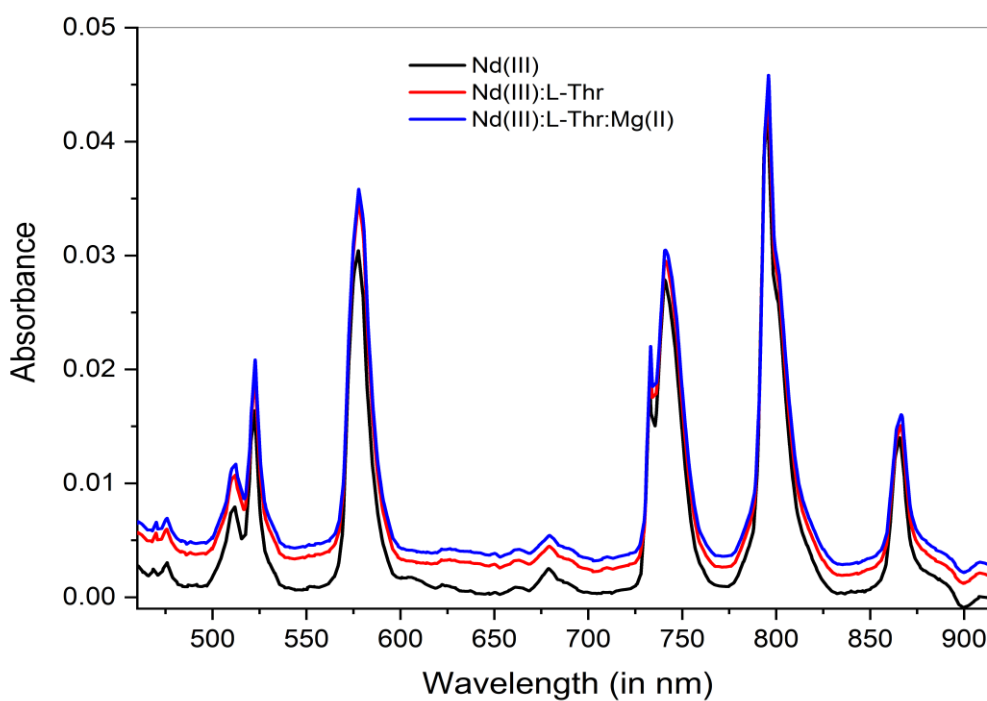
Fig. 3.9: Comparative UV-Vis. absorption spectra of Nd(III), Nd(III):L-Thr and
Nd(III):L-Thr:Mg(II) in methanol: water (50% v/v) solvent
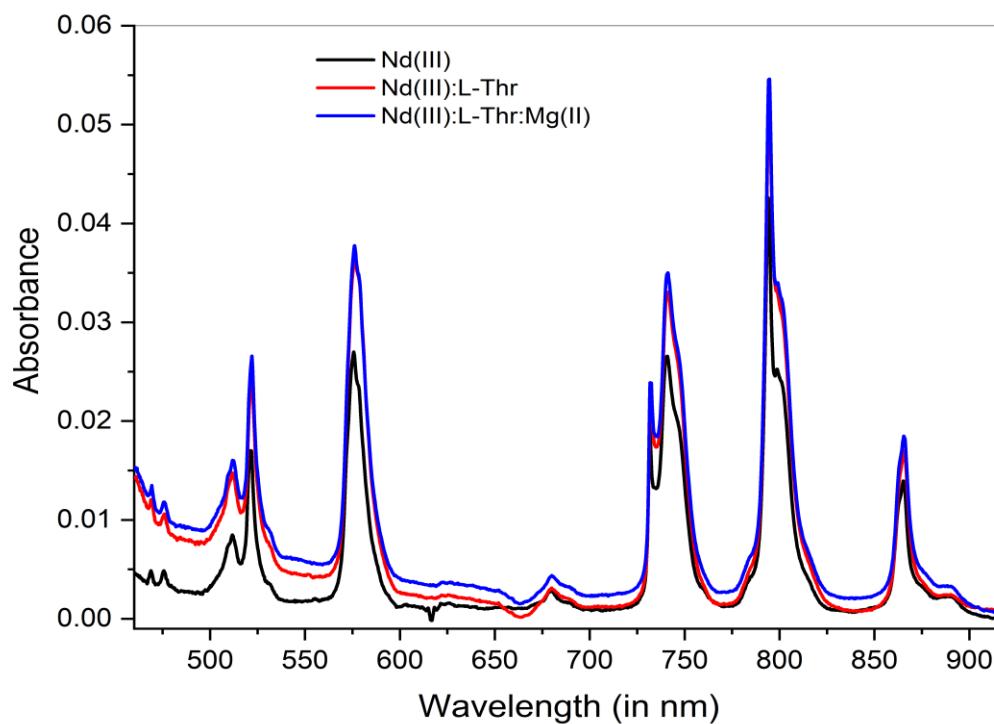
Fig. 3.10: Comparative UV-Vis. absorption spectra of Nd(III), Nd(III):L-Thr and
Nd(III):L-Thr:Mg(II) in 1,4-dioxane: water (50% v/v) solvent
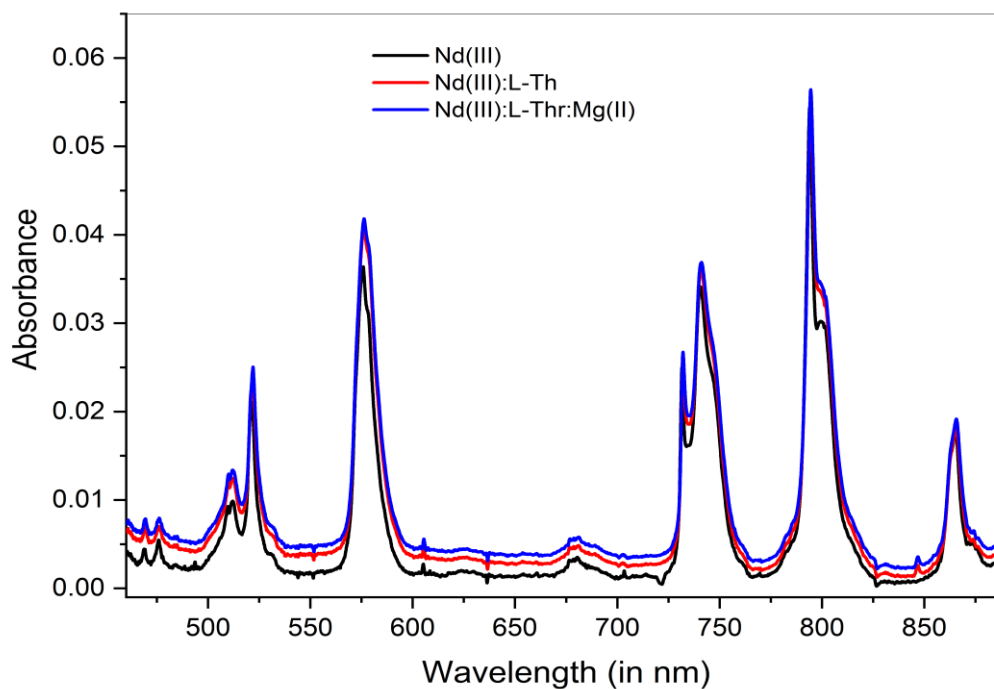
Fig. 3.11: Comparative UV-Vis. absorption spectra of Nd(III), Nd(III):L-Thr and
Nd(III):L-Thr:Mg(II) in acetonitrile: water (50% v/v) solvent

Fig. 3.12: Comparative UV-Vis. absorption spectra of Nd(III), Nd(III):L-Thr and Nd(III):L-Thr:Mg(II) in DMF: water (50% v/v) solvent

Fig. 3.13: Comparative UV-Vis. absorption spectra of Nd(III):L-Thr in different aquated solvents

3. L-Tryptophan
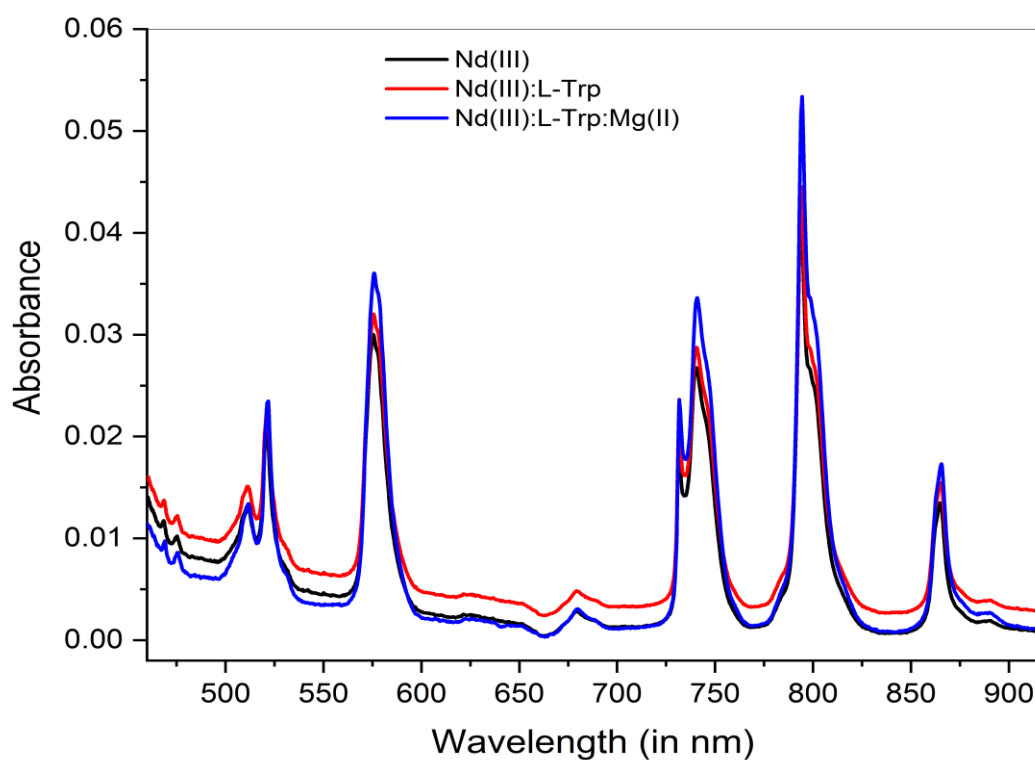
Fig. 3.14: Comparative UV-Vis. absorption spectra of Nd(III), Nd(III):L-Trp and
Nd(III):L-Trp:Mg(II) in methanol: water (50% v/v) solvent
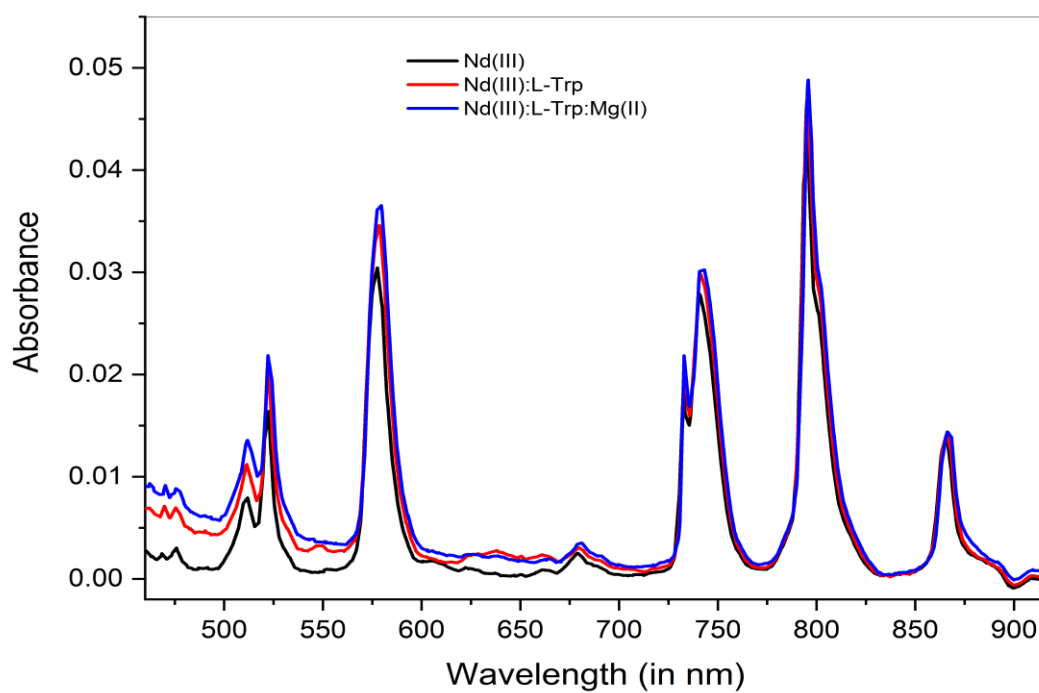
Fig. 3.15: Comparative UV-Vis. absorption spectra of Nd(III), Nd(III):L-Trp and
Nd(III):L-Trp:Mg(II) in 1,4-dioxane: water (50% v/v) solvent
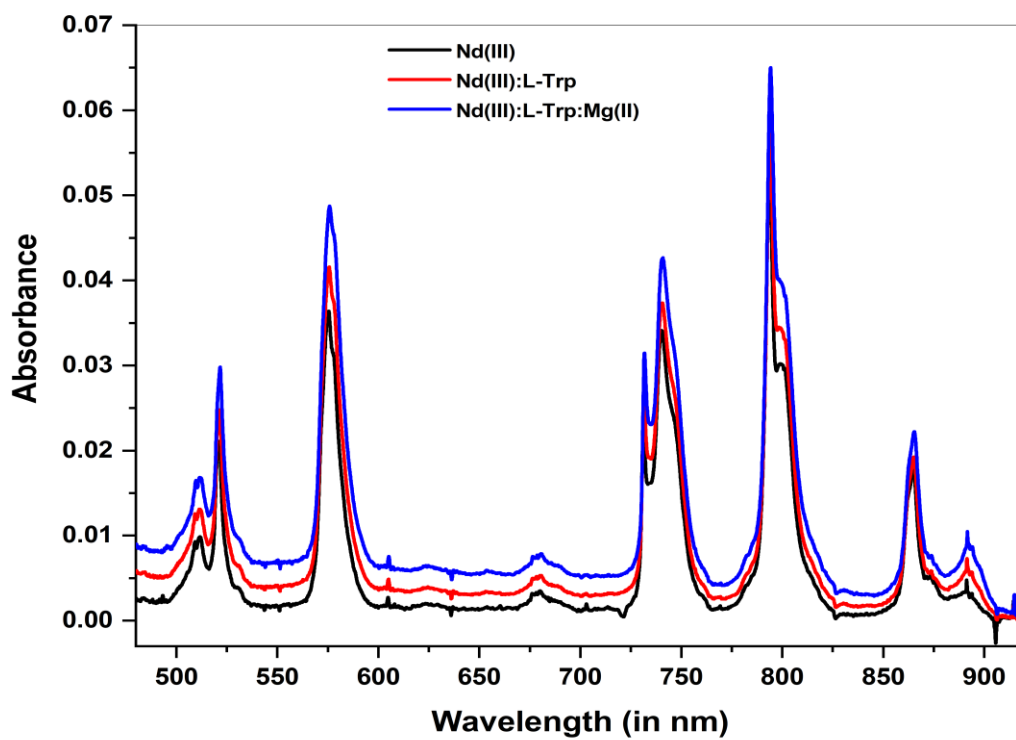
Fig. 3.16: Comparative UV-Vis. absorption spectra of Nd(III), Nd(III):L-Trp and
Nd(III):L-Trp:Mg(II) in acetonitrile: water (50% v/v) solvent
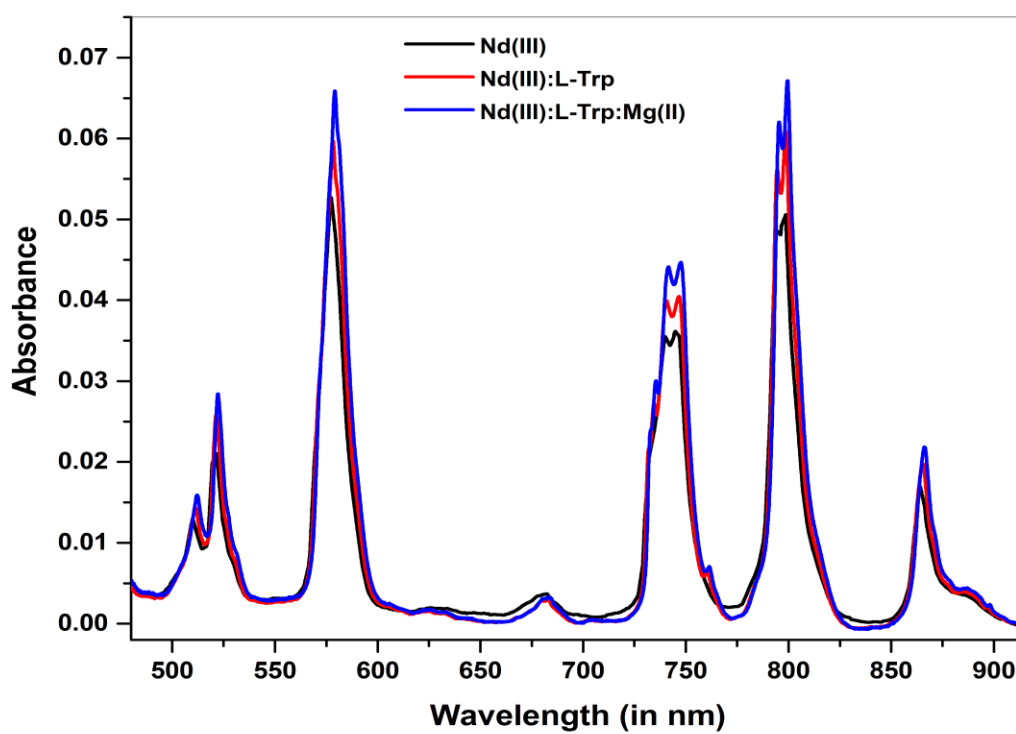
Fig. 3.17: Comparative UV-Vis. absorption spectra of Nd(III), Nd(III):L-Trp and
Nd(III):L-Trp:Mg(II) in DMF: water (50% v/v) solvent
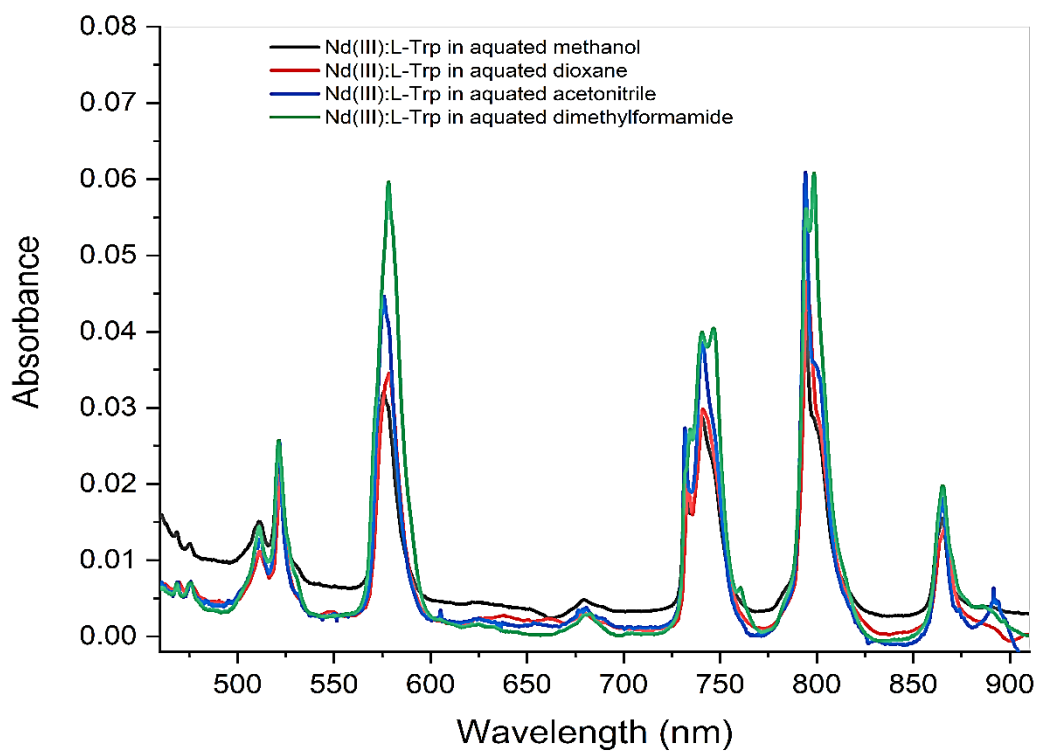
Fig. 3.18: Comparative UV-Vis. absorption spectra of Nd(III):L-Trp in different aquated solvents

4. L-Isoleucine
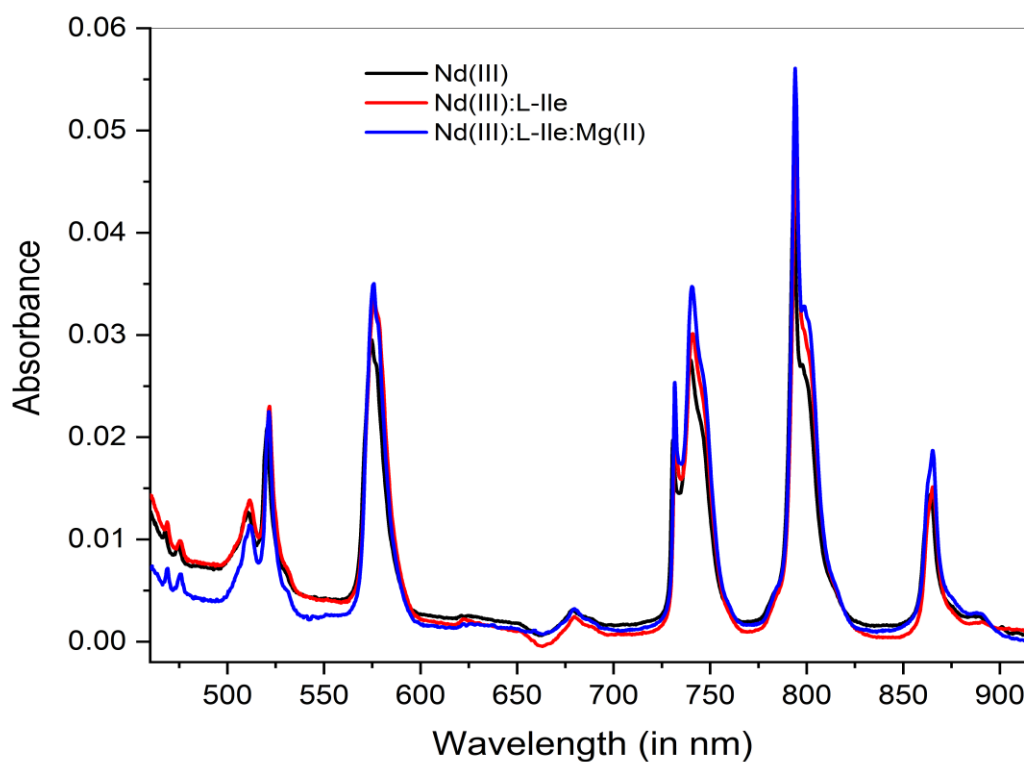
Fig. 3.19: Comparative UV-Vis. absorption spectra of Nd(III), Nd(III):L-Ile and
Nd(III):L-Ile:Mg(II) in methanol: water (50% v/v) solvent
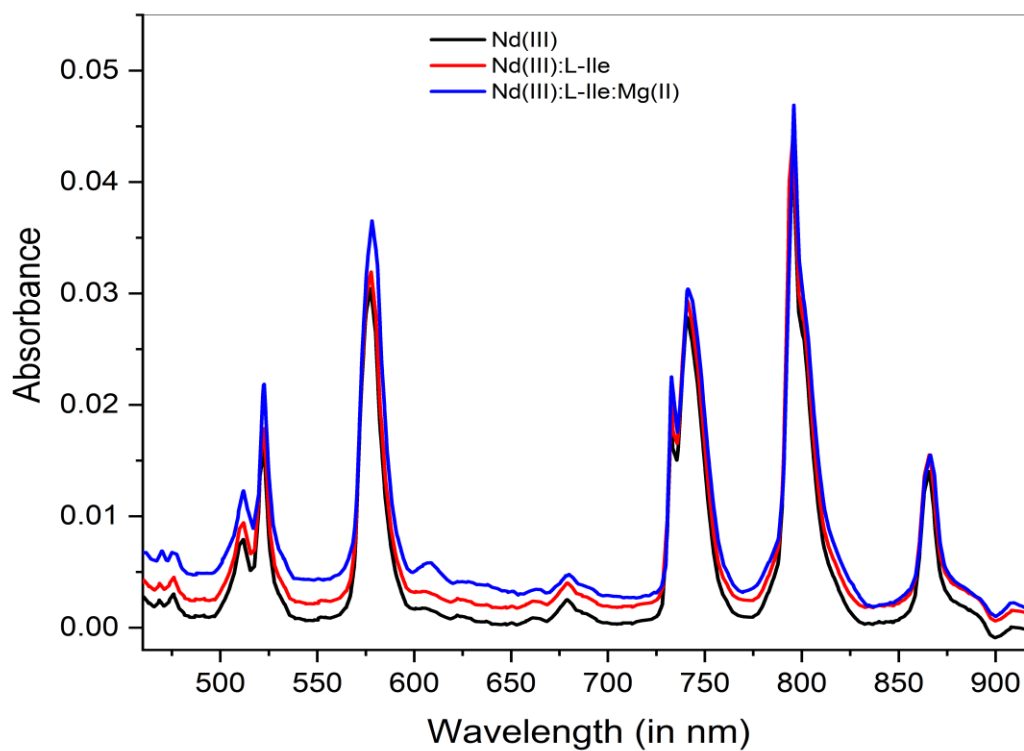
Fig. 3.20: Comparative UV-Vis. absorption spectra of Nd(III), Nd(III):L-Ile and
Nd(III):L-Ile:Mg(II) in 1,4-dioxane: water (50% v/v) solvent
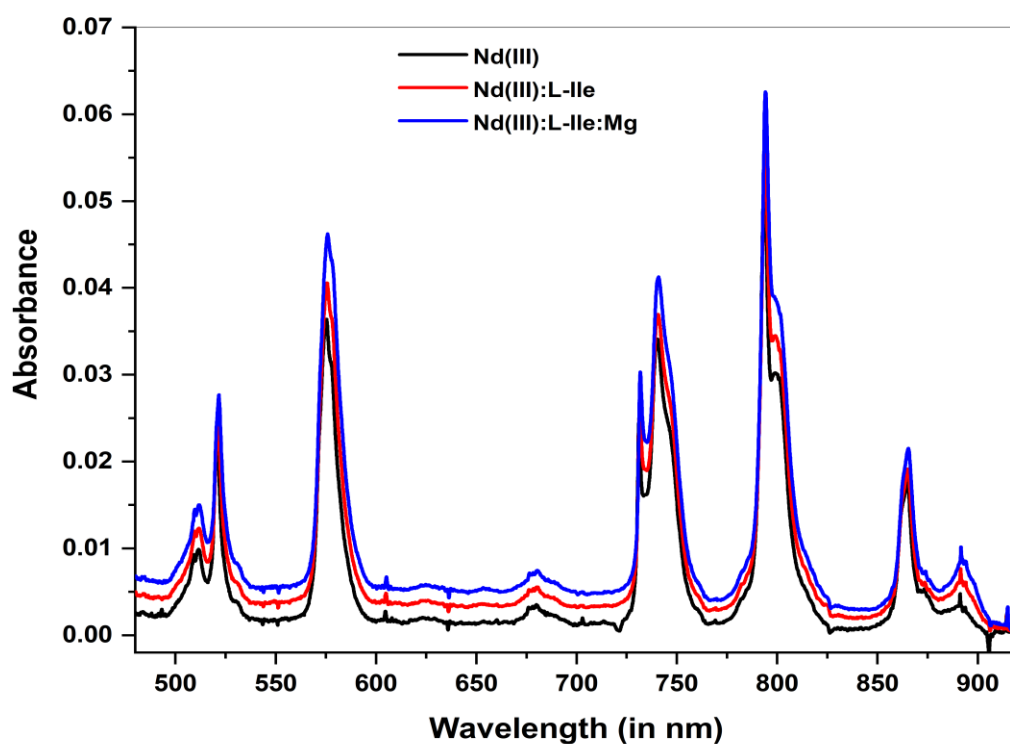
Fig. 3.21: Comparative UV-Vis. absorption spectra of Nd(III), Nd(III):L-Ile and
Nd(III):L-Ile:Mg(II) in acetonitrile: water (50% v/v) solvent
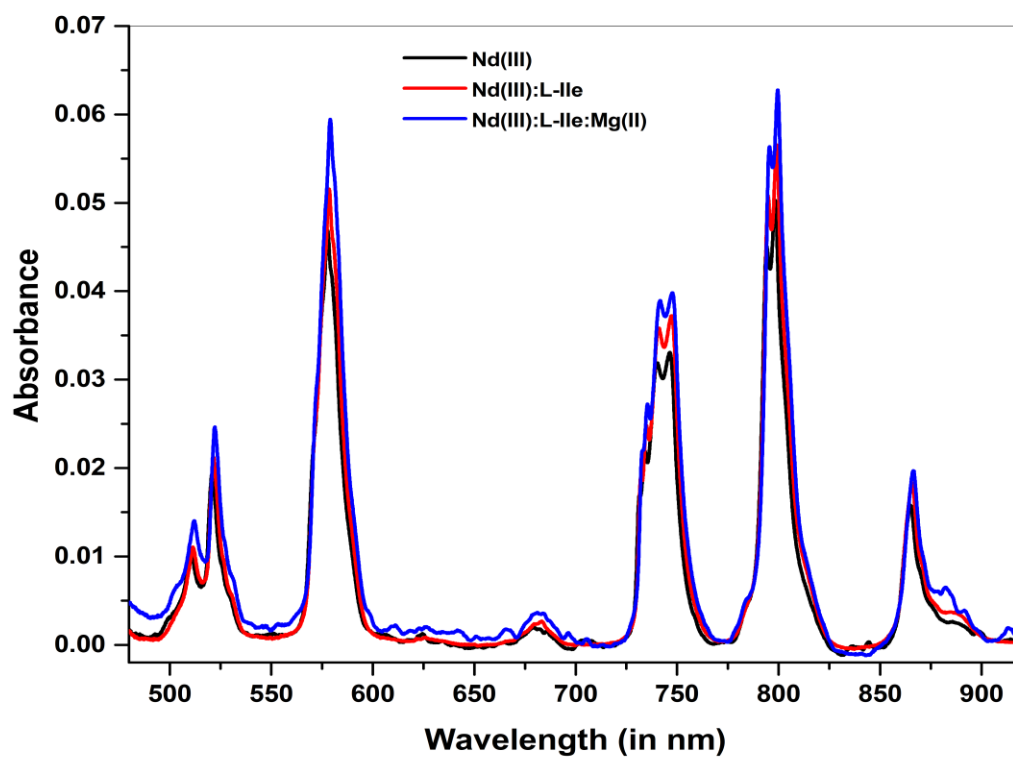
Fig. 3.22: Comparative UV-Vis. absorption spectra of Nd(III), Nd(III):L-Ile and Nd(III):L-Ile:Mg(II) in DMF: water (50% v/v) solvent
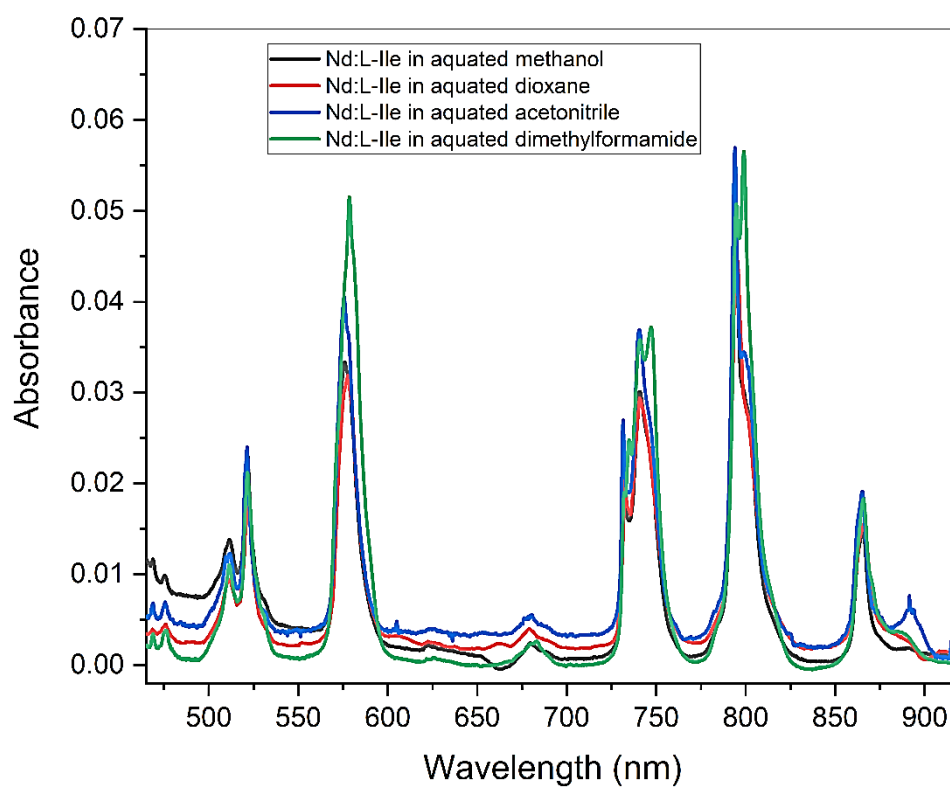
Fig. 3.23: Comparative UV-Vis. absorption spectra of Nd(III):L-Ile in different aquated solvents

Comparative UV-Vis. absorption spectra of Nd(III) with the selected amino acids at different pH levels in aquated DMF solvent

1. **L-Glutamine**
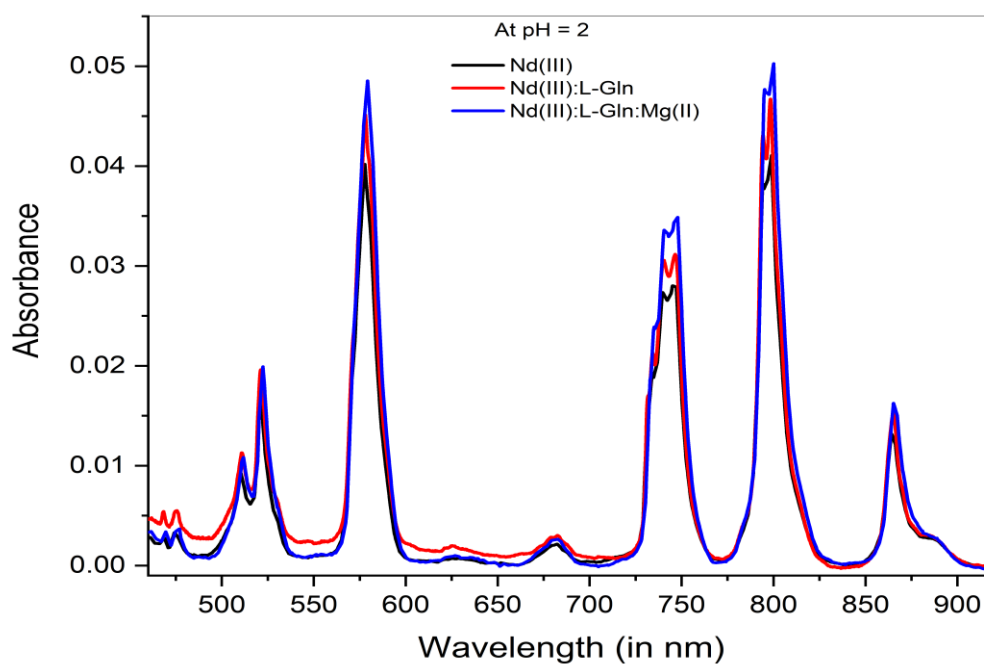
Fig. 3.24: Comparative UV-Vis. absorption spectra of Nd(III), Nd(III):L-Gln and Nd(III):L-Gln:Mg(II) at pH = 2 in DMF: water (50% v/v) solvent
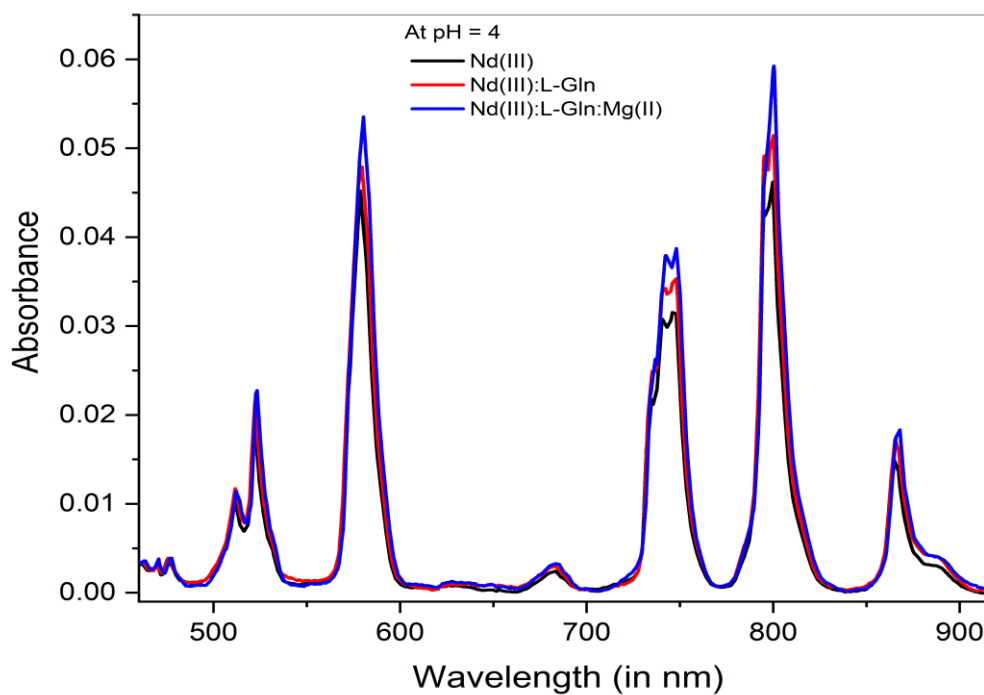
Fig. 3.25: Comparative UV-Vis. absorption spectra of Nd(III), Nd(III):L-Gln and Nd(III):L-Gln:Mg(II) at pH = 4 in DMF: water (50% v/v) solvent
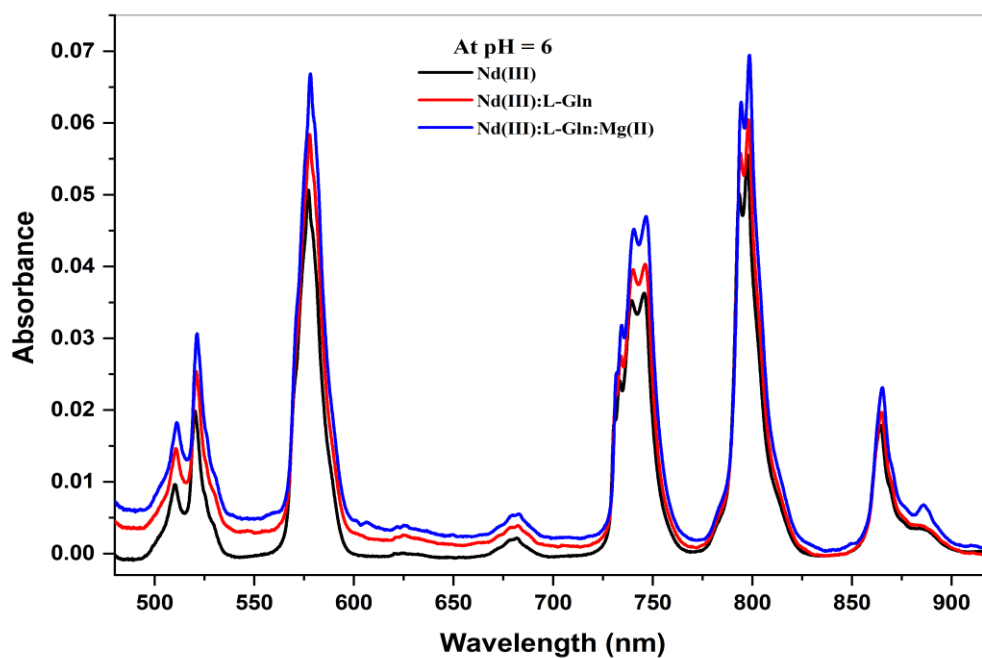
Fig. 3.26: Comparative UV-Vis. absorption spectra of Nd(III), Nd(III):L-Gln and Nd(III):L-Gln:Mg(II) at pH = 6 in DMF: water (50% v/v) solvent
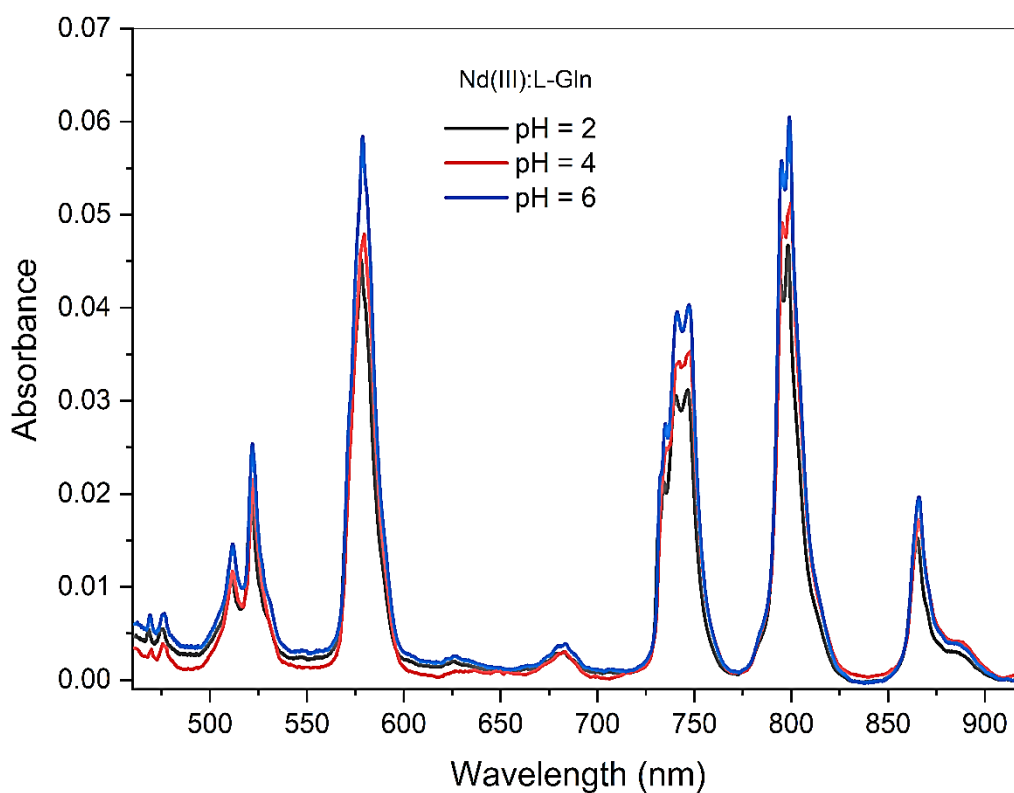
Fig. 3.27: Comparative UV-Vis. absorption spectra of Nd(III):L-Gln at pH = 2, 4 and 6 in DMF: water (50% v/v) solvent

2. L-Threonine
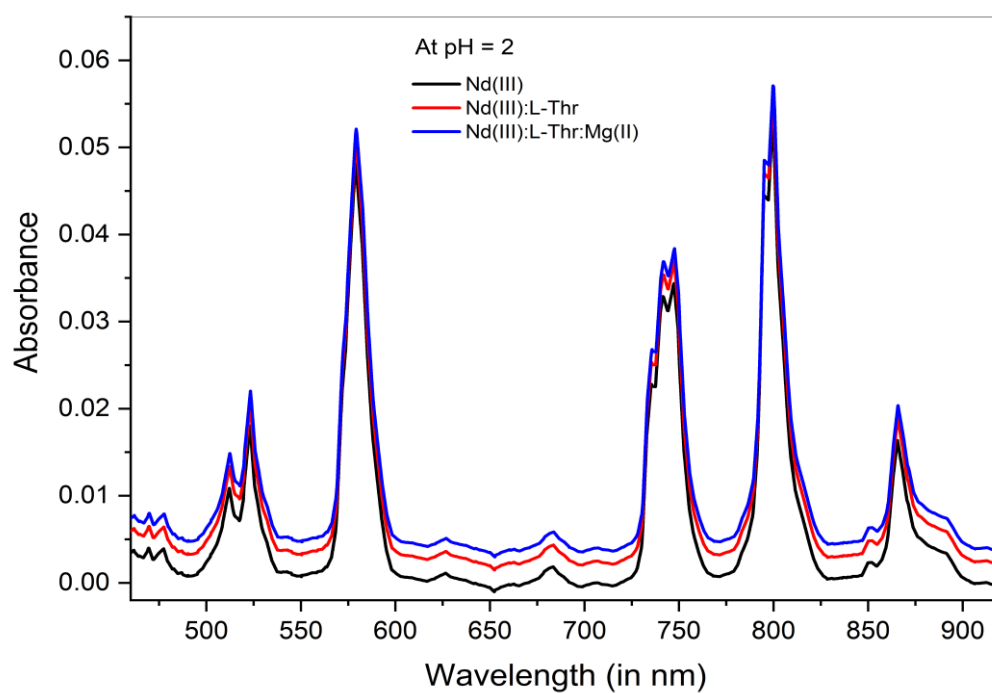
Fig. 3.28: Comparative UV-Vis. absorption spectra of Nd(III), Nd(III):L-Thr and Nd(III):L-Thr:Mg(II) at pH = 2 in DMF: water (50% v/v) solvent
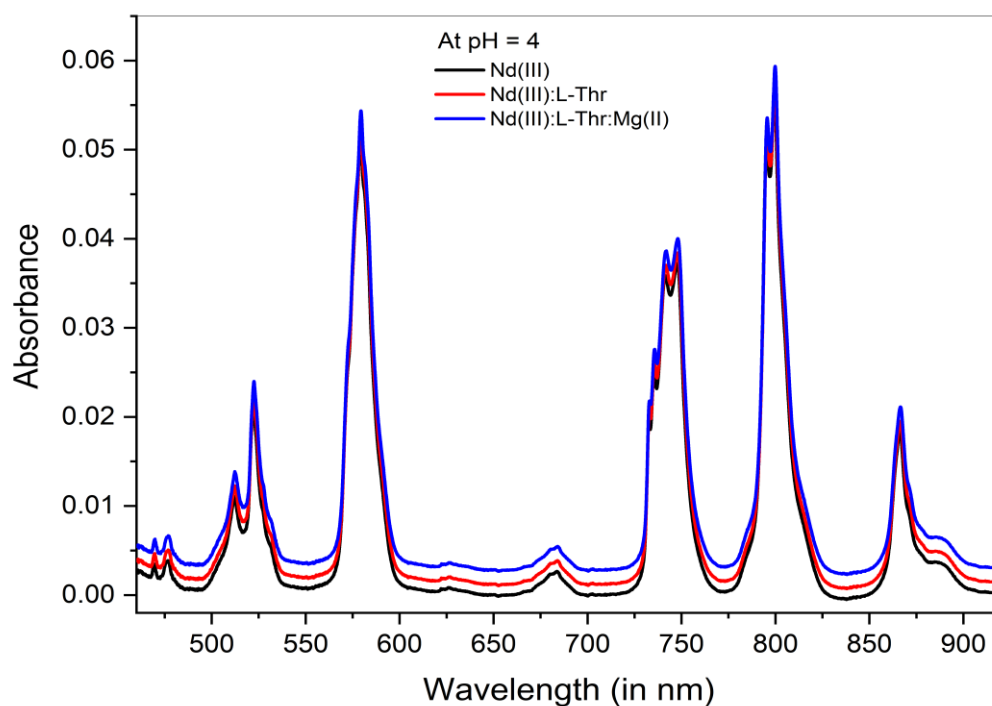
Fig. 3.29: Comparative UV-Vis. absorption spectra of Nd(III), Nd(III):L-Thr and Nd(III):L-Thr:Mg(II) at pH = 4 in DMF: water (50% v/v) solvent
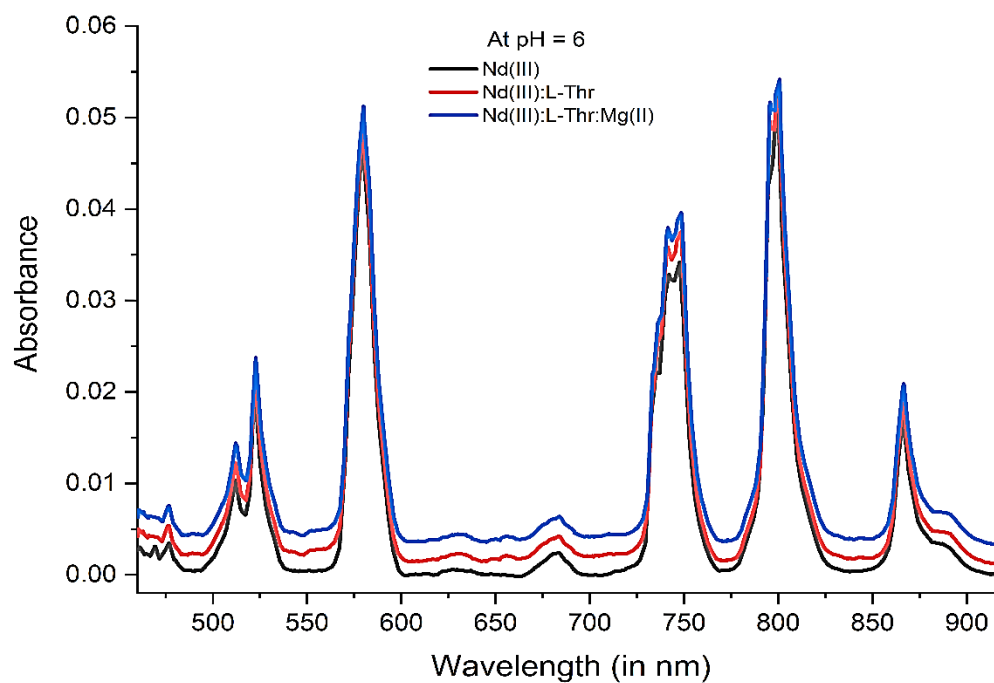
Fig. 3.30: Comparative UV-Vis. absorption spectra of Nd(III), Nd(III):L-Thr and Nd(III):L-Thr:Mg(II) at pH = 6 in DMF: water (50% v/v) solvent
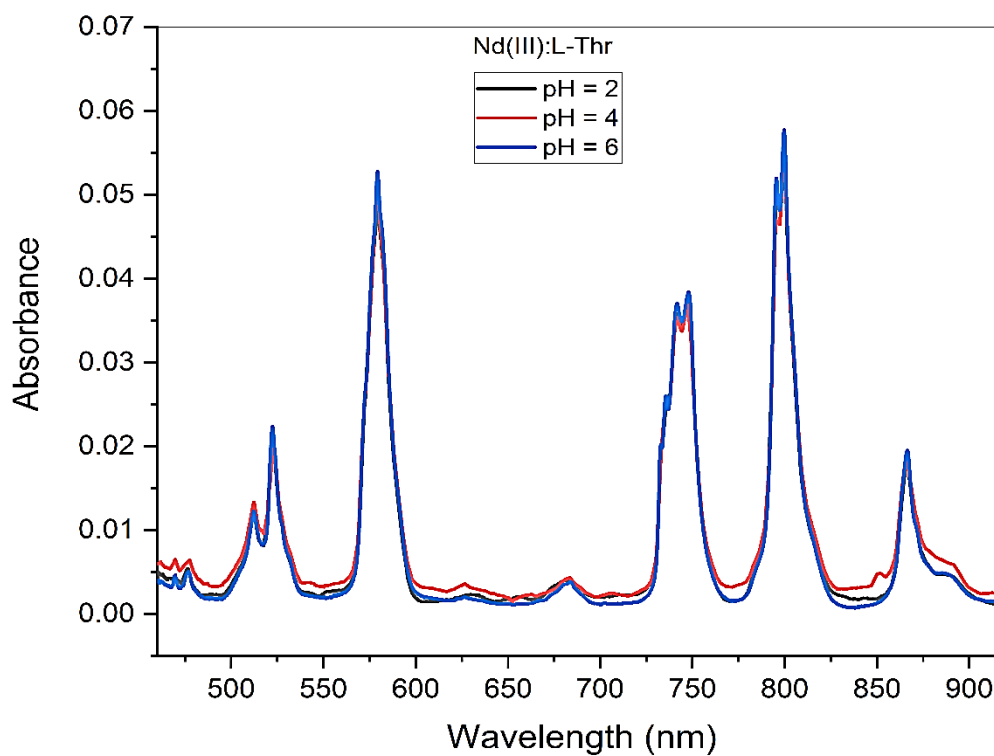
Fig. 3.31: Comparative UV-Vis. absorption spectra of Nd(III):L-Thr at pH = 2, 4 and 6 in DMF: water (50% v/v) solvent

3. **L-Tryptophan**
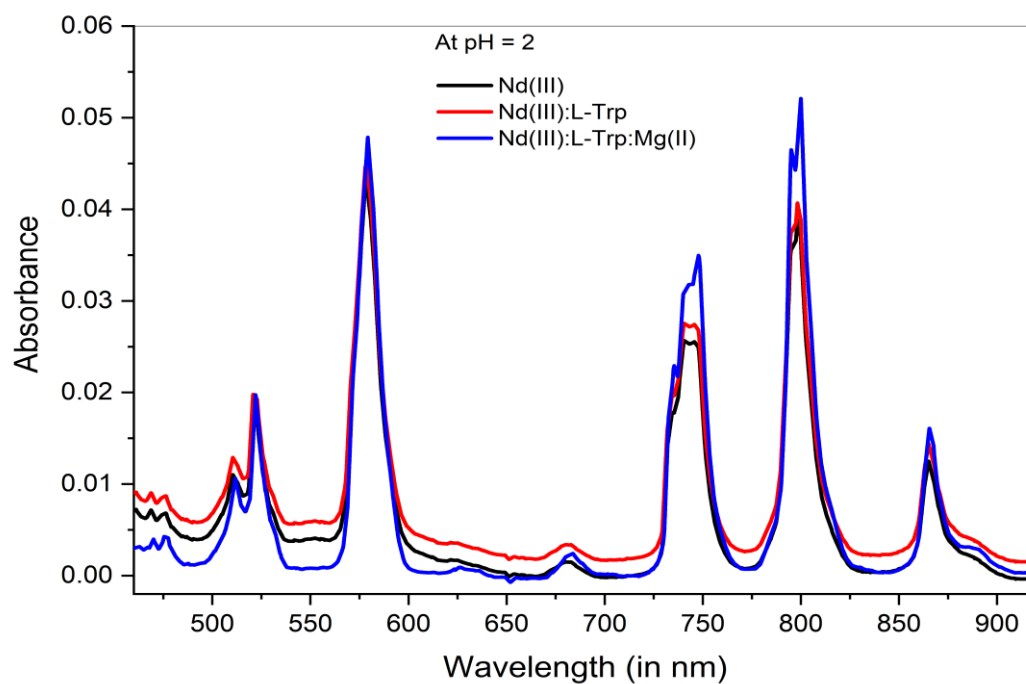
Fig. 3.32: Comparative UV-Vis. absorption spectra of Nd(III), Nd(III):L-Trp and Nd(III):L-Trp:Mg(II) at pH = 2 in DMF: water (50% v/v) solvent
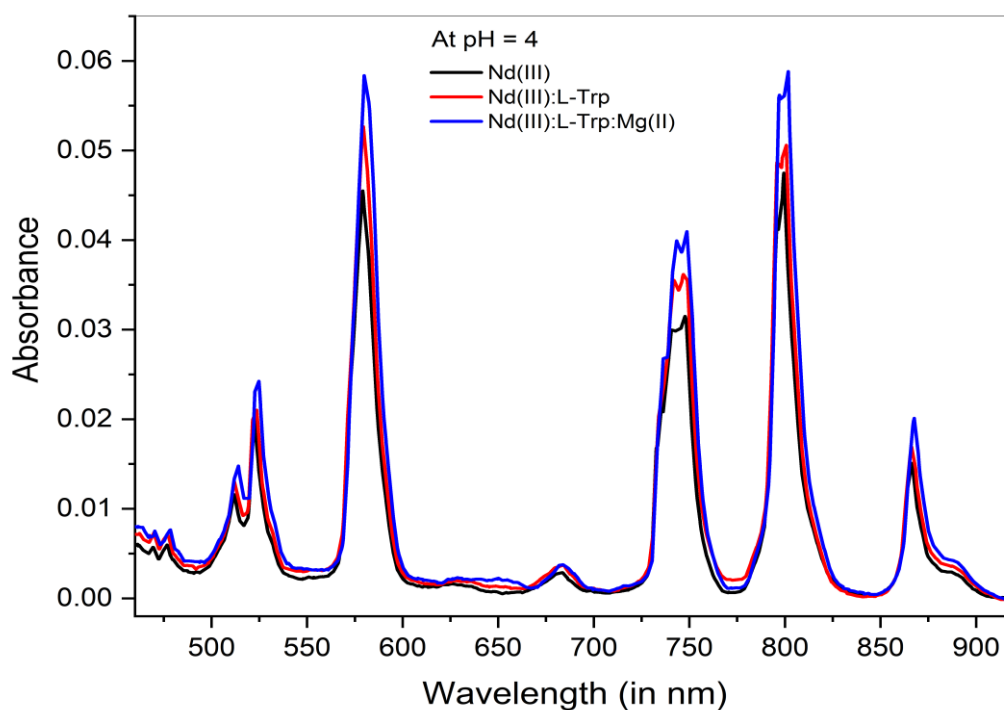
Fig. 3.33: Comparative UV-Vis. absorption spectra of Nd(III), Nd(III):L-Trp and Nd(III):L-Trp:Mg(II) at pH = 4 in DMF: water (50% v/v) solvent
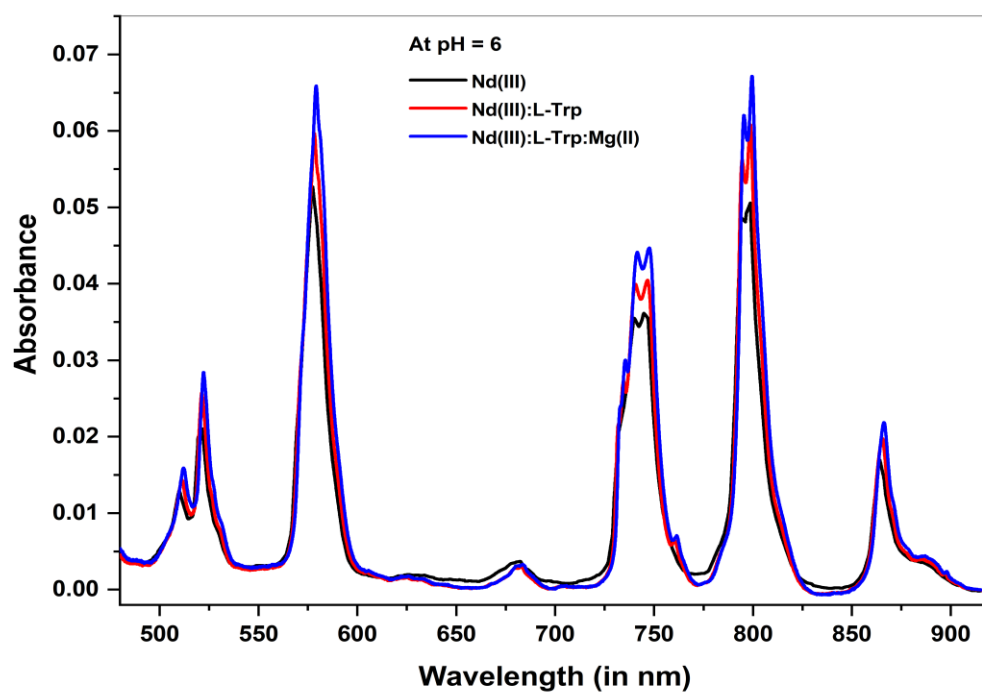
Fig. 3.34: Comparative UV-Vis. absorption spectra of Nd(III), Nd(III):L-Trp and Nd(III):L-Trp:Mg(II) at pH = 6 in DMF: water (50% v/v) solvent
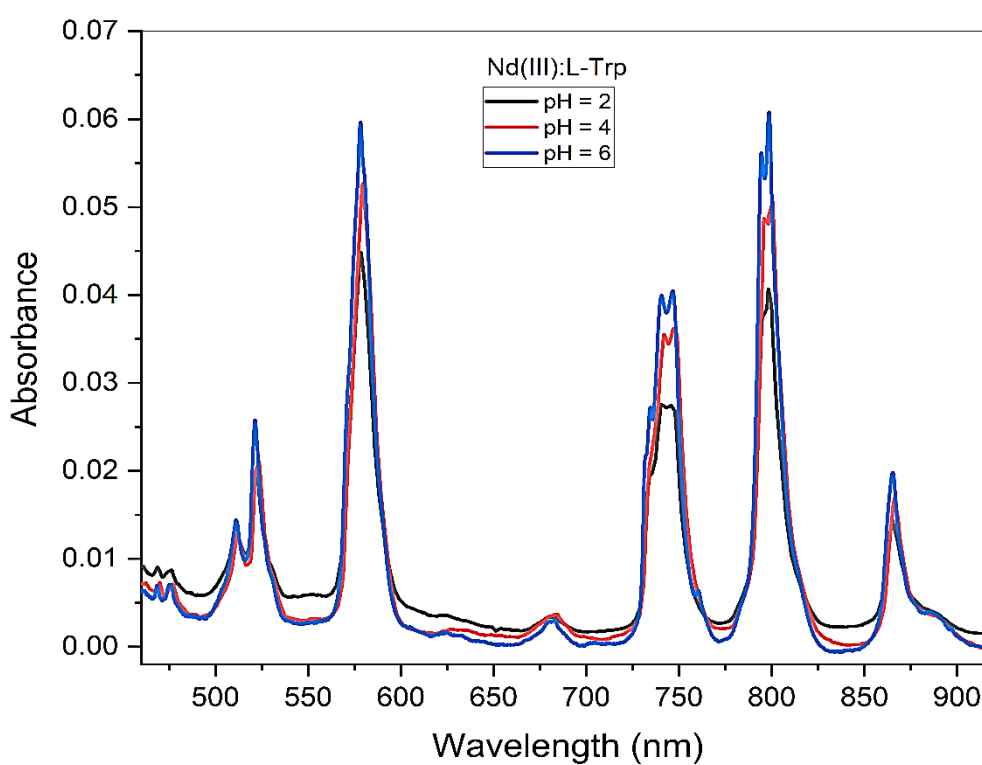
Fig. 3.35: Comparative UV-Vis. absorption spectra of Nd(III):L-Trp at pH = 2, 4 and 6 in DMF: water (50% v/v) solvent
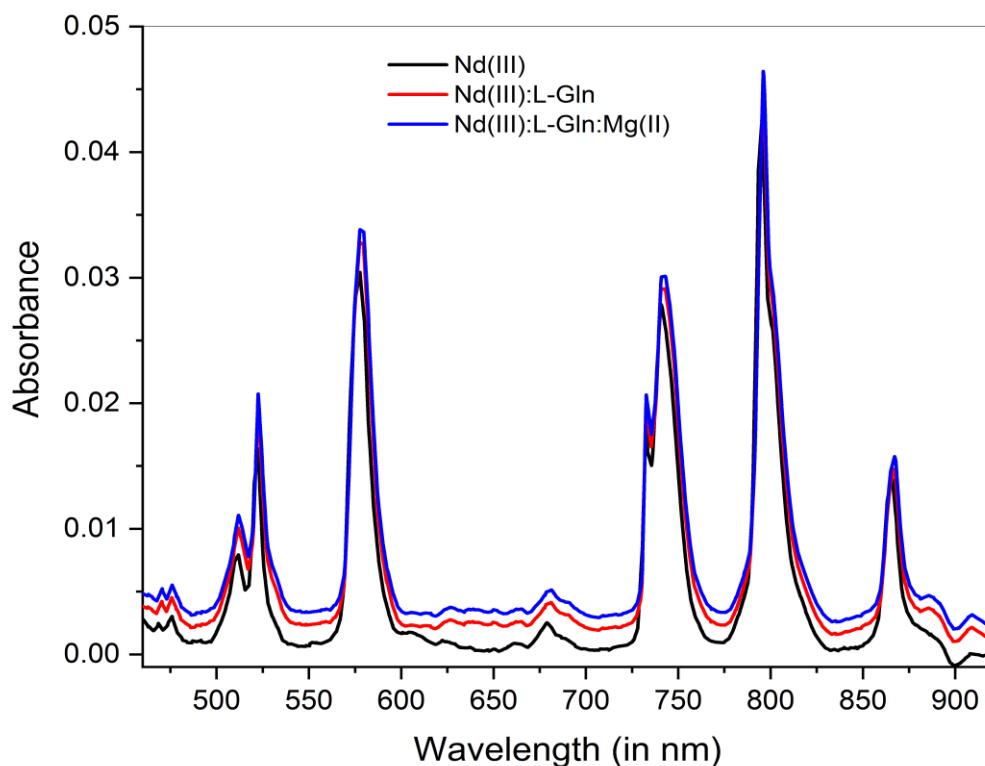
4. L-Isoleucine
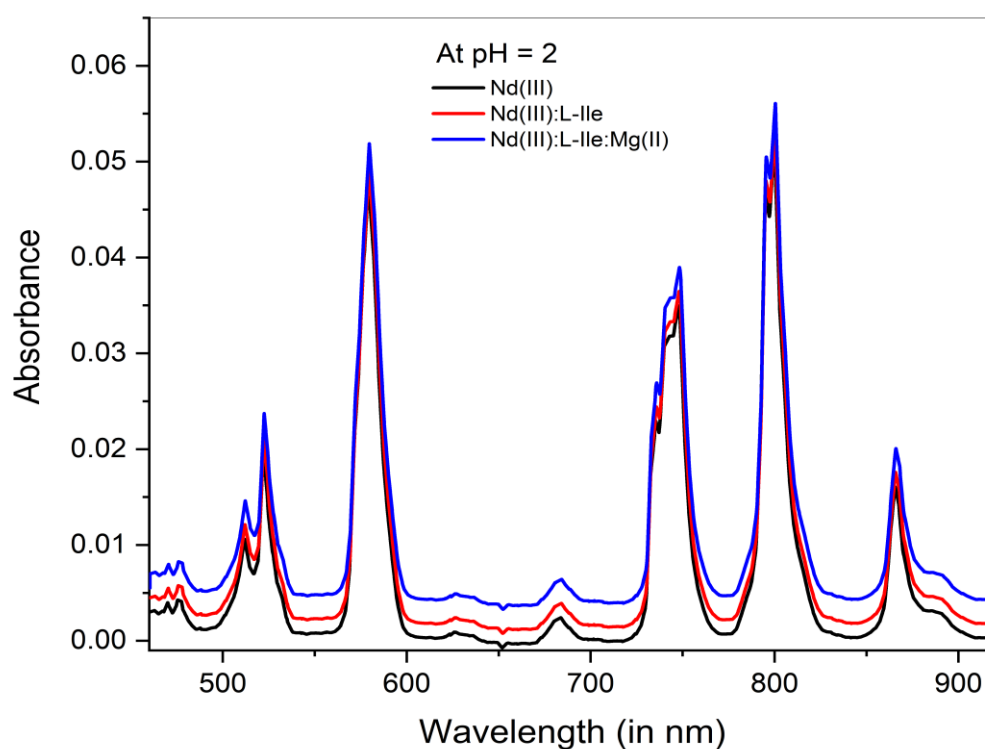
Fig. 3.36: Comparative UV-Vis. absorption spectra of Nd(III), Nd(III):L-Ile and Nd(III):L-Ile:Mg(II) at pH = 2 in DMF: water (50% v/v) solvent
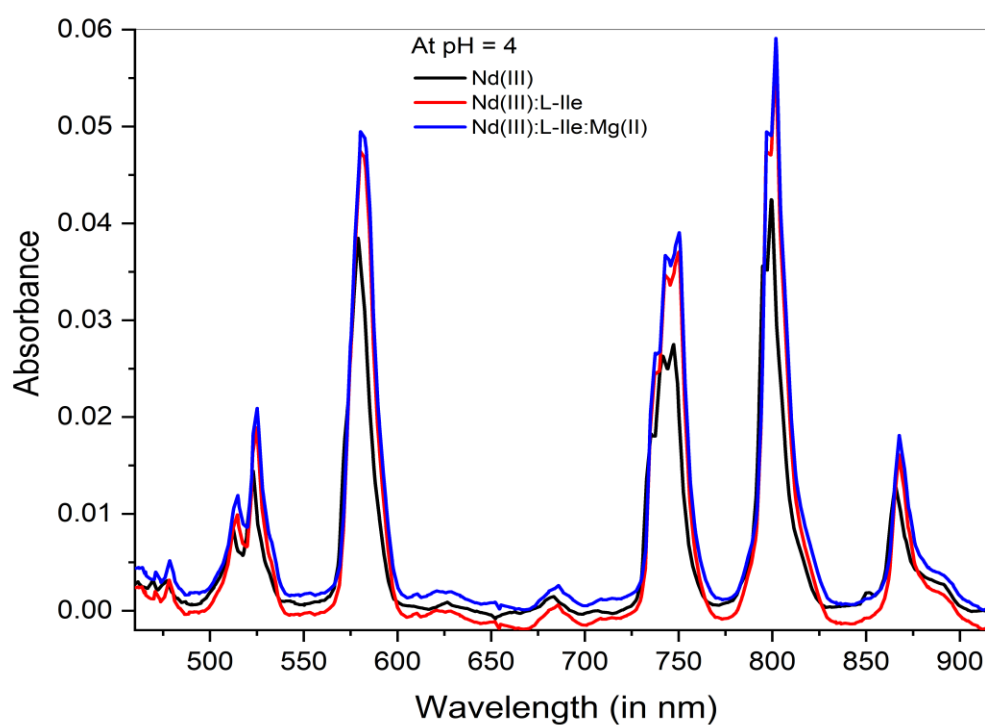
Fig. 3.37: Comparative UV-Vis. absorption spectra of Nd(III), Nd(III):L-Ile and Nd(III):L-Ile:Mg(II) at pH = 4 in DMF: water (50% v/v) solvent
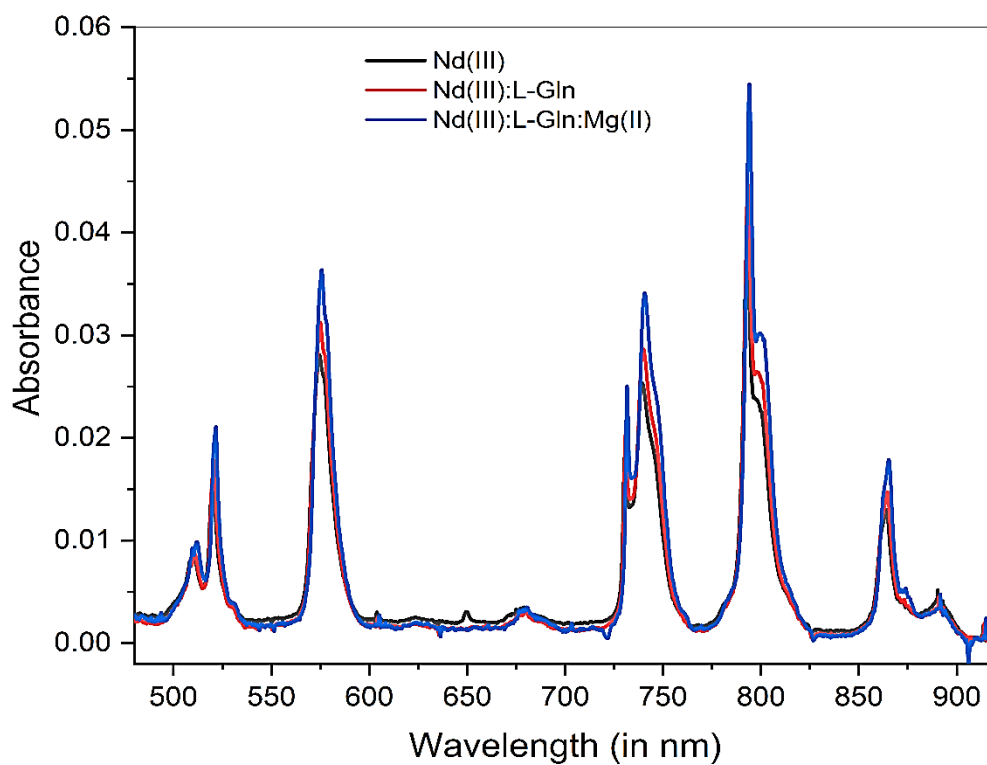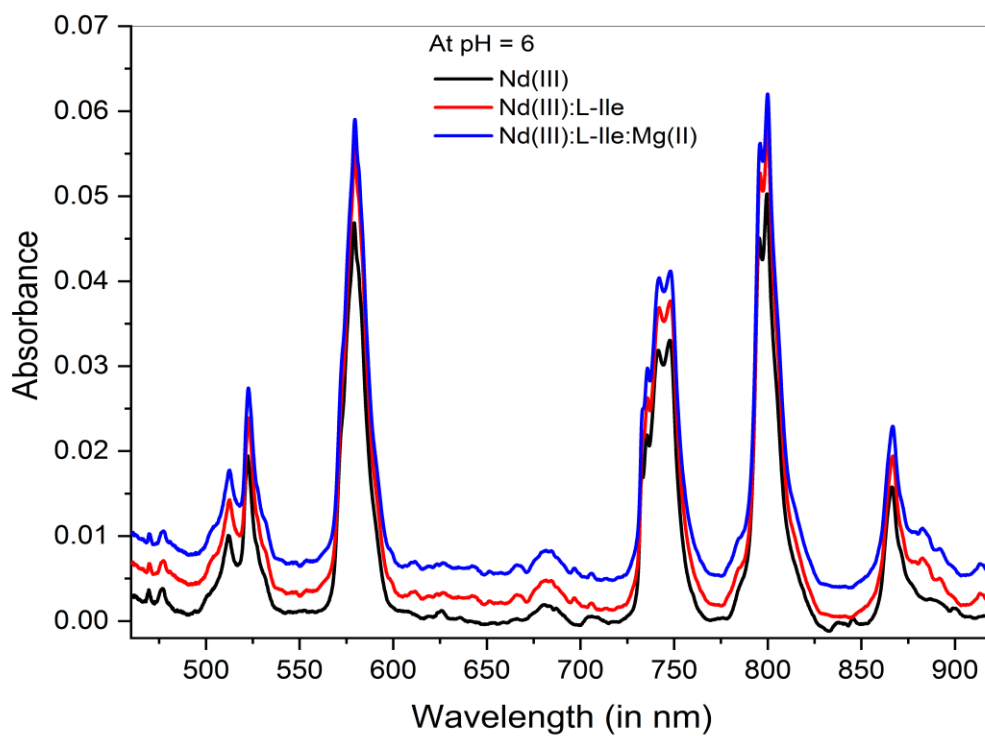
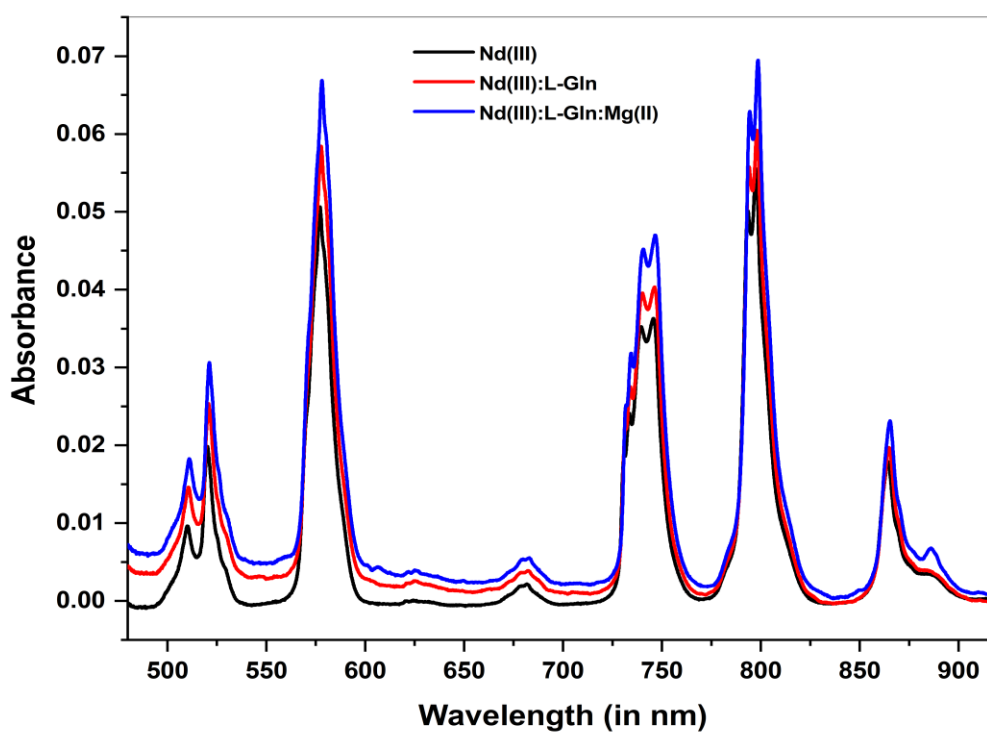**Fig. 3.38**: Comparative UV-Vis. absorption spectra of Nd(III), Nd(III):L-Ile and Nd(III):L-Ile:Mg(II) at pH = 6 in DMF: water (50% v/v) solvent
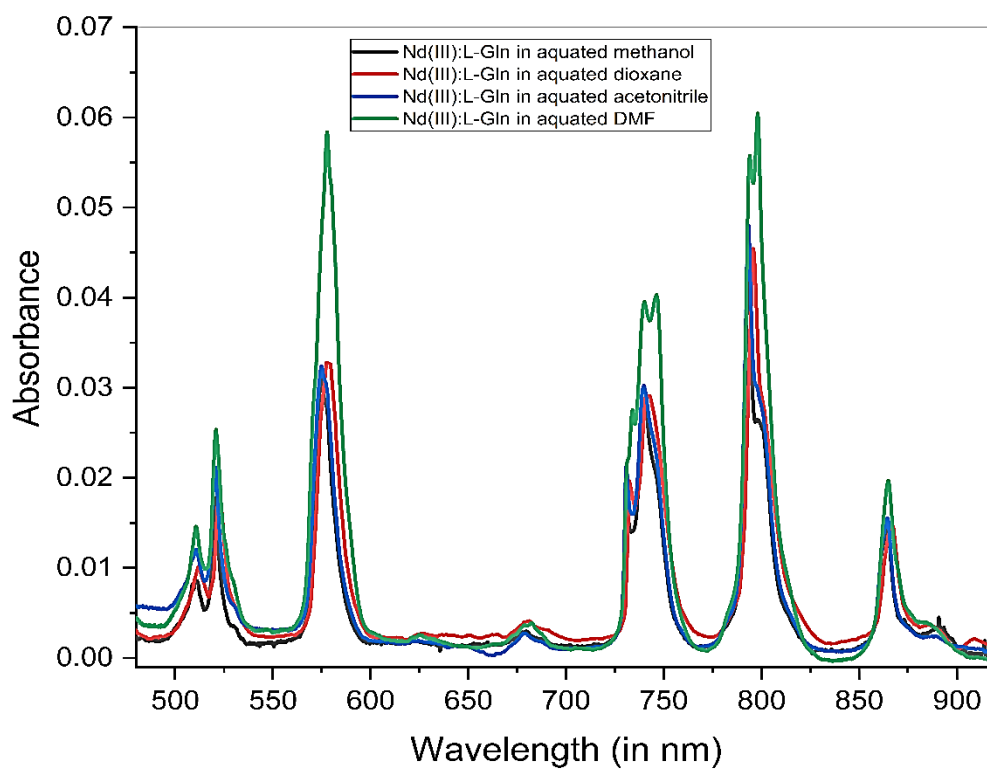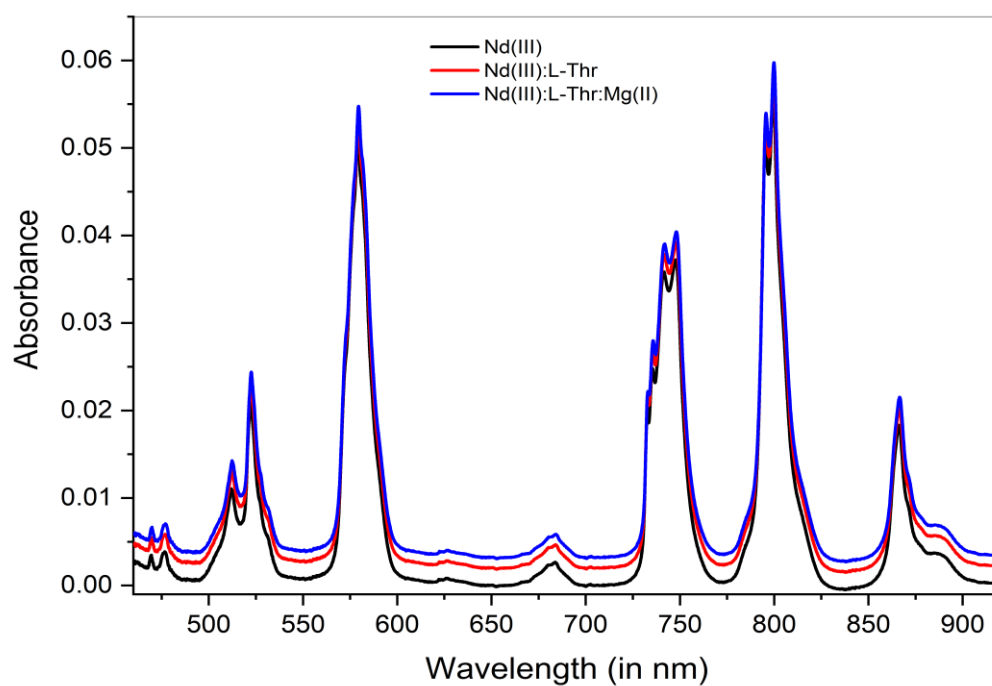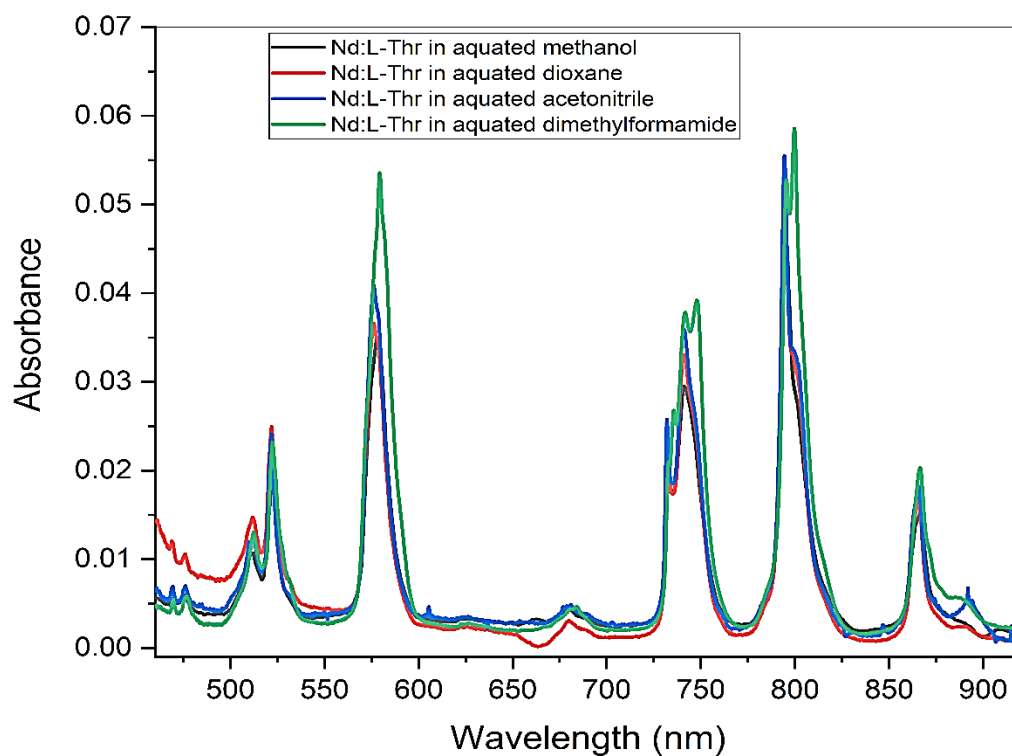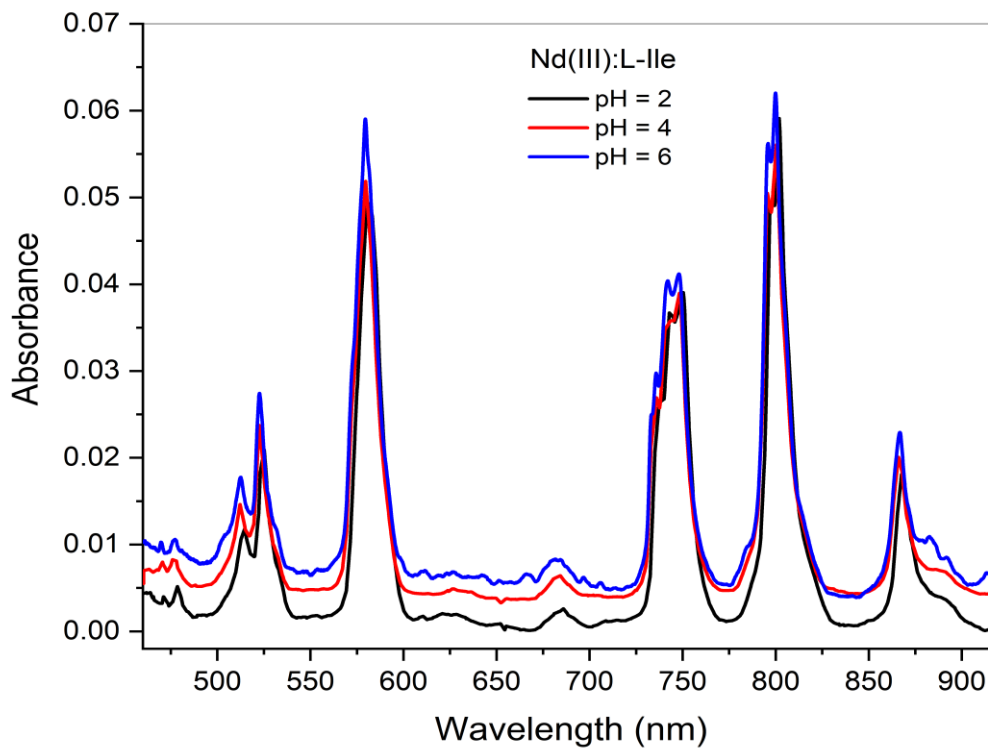

Fig. 3.39: Comparative UV-Vis. absorption spectra of Nd(III):L-Ile at pH = 2, 4 and 6 in DMF: water (50% v/v) solvent

Chapter 4

Kinetics for the complexation of Pr(III) with amino acids ligands in presence of Mg(II) in DMF solvent

4.1 Introduction

Absorption spectra in transition metal ions containing d-d transitions have been utilised for the purpose of monitoring the kinetics of chemical reactions, which has resulted in the development of mechanisms for chemical reactions. In lanthanide, however, mechanistic investigations for the kinetic processes involving lanthanide ions and coordination ligands, including biomolecules, rarely make use of absorption spectra containing the 4f-4f transition. The kinetics of the complexation of Pr(III):Amino acids with Mg(II) in DMF medium will be investigated in this chapter at different temperatures, viz., 298K (25° C), 303K (30° C), 308K (35° C), 313K (40° C), and 318K (45° C). The following three amino acids, L-Glutamine, L-Tryptophan and L-Isoleucine, were selected out of the four amino acids which were earlier used for the quantitative absorption spectral analysis in the previous chapter, and were utilized to follow the trend of the complexation reaction involved. The complexation rates of Pr(III):Ligands with Mg(II) have been measured using comparative absorption spectroscopy by monitoring the changes in absorbance and oscillator strengths of the 4f-4f electronic transitions of Pr(III) ion, $^3H_4{\rightarrow}^3P_2$, $^3H_4{\rightarrow}^3P_1$, $^3H_4{\rightarrow}^3P_0$ and $^3H_4{\rightarrow}^1D_2$. The reaction dynamics and thermodynamic properties for the complexation of Pr(III) with amino acids and Mg(II) have been investigated using different computed parameters like rate constant (k), activation energy (E_a), A (pre-exponential factor) and thermodynamic parameters, ΔH^0, ΔG^0 and ΔS^0 in different temperatures.

4.2 Experimental

Analytical grade chemicals viz., L-Glutamine, L-Tryptophan, L-Isoleucine, Magnesium nitrate hexahydrate (99.0%) from HiMedia and Praseodymium nitrate hexahydrate (99.9%) from Sigma-Aldrich were used for the kinetic studies. The solvent Dimethylformamide (99.5%) from HiMedia was used for the present study. UV-Vis spectra in the region of 460-620 nm were recorded using a conventional 1cm path length quartz cuvette on a Shimadzu UV- 2600i spectrophotometer.

For the kinetic studies, Pr(III), amino acid ligands and Mg(II) concentrations are kept constant at 0.005 M for absorption spectral studies and were prepared in aquated dimethylformamide solvent (50 % v/v). The complex Pr(III):Amino acid:Mg(II) was prepared by mixing all the solutions thoroughly and the molar ratio for the Pr(III):Amino acid:Mg(II) multimetal complexation kinetic investigation was maintained at 1:1:1.

For kinetics and thermodynamic investigations, the UV-Vis spectra of the Pr(III):Ligands:Mg(II) complex are recorded in DMF-water solvent at five different temperatures of 298K, 303K, 308K, 313K and 318K.

4.3 Methods

The calculation of the band intensities is based upon the theoretical treatment derived by Judd and Ofelt [1,2]. They considered the transitions are essentially electric dipole in character and the oscillator strength corresponding to the induced electric dipole transition $\Psi J \rightarrow \Psi`J`$ as given by

$$P_{cal} = \sum_{\lambda=2,4,6} T_\lambda \sigma (f^N \psi J \| U^\lambda \| f^N \psi' J')^2 \qquad (4.1)$$

where $U^{(\lambda)}$ (λ=2,4,6) are Carnall's reduced matrix elements for Pr^{3+} [3]. The Judd-Ofelt intensity parameters, T_λ (λ=2,4,6) are phenomenological parameters that describe the intensity of the 4f electron transitions of lanthanides.

153

The three quantities T_2, T_4 and T_6 connects the ground and final states ($f^N\psi J$ and $f^N\psi'J'$) through the squared reduced matrix elements U^λ.

The oscillatory strength is defined as the area under the absorption curve. This is given as

$$P = 4.6 \text{ x } 10^{-9}\left[\frac{9\eta}{(\eta^2+\eta)^2}\right]\int \varepsilon_{max}\bar{v}d\bar{v} \tag{4.2}$$

Where $\bar{v}$, ε_{max} and η are wave number, molar extinction coefficient and refractive index respectively.

Using the following expression, the experimental oscillator Strength (P_{obs}) values of the absorption bands are calculated

$$P_{obs} = 4.6 \text{ x } 10^{-9}\text{x } \varepsilon_{max}\bar{v}_{\frac{1}{2}} \tag{4.3}$$

Where $\bar{v}_{\frac{1}{2}}$ is the half bandwidth

Using the value of P_{obs} and reduced matrix elements $U^{(\lambda}$[3], the Judd-Ofelt intensity parameters T_2, T_4 and T_6 can be calculated from the following expression,

$$\frac{P_{obs}}{v} = [(U^2)]^2.T_2 + [U^4]^2.T_4 + [U^6]^2.T_6 \tag{4.4}$$

Where, v = energy transition and U = matrix element

The activation energy (Ea) for the complexation of Pr(III) with the selected amino acids and Mg(II) in DMF:water was calculated by plotting log k (k= rate constant) against 1/T using the Arrhenius reaction rate equation.

$$\log k \;=\; \log A - \frac{E_a}{2.303R}\frac{1}{T} \tag{4.5}$$

Here the pre-exponential factor is represented by '*A*' which is related to the frequency of collisions and orientation probability of collisions for the reaction. The reaction rate (k) can be calculated from the Activation energy (E_a).

The activation energy (E_a) is calculated using the slope as,

$$E_a = slope \times 2.303 \times R \tag{4.6}$$

The thermodynamic parameters (ΔH^0, ΔG^0, ΔS^0) for the complexation are calculated using the Van't Hoff plot of log k vs $1/T \times 10^3$

$$log\ k = -\frac{\Delta H°}{R}\left[\frac{1}{T}\right] + \frac{\Delta S°}{R} \tag{4.7}$$

$$\text{Or} \quad log\ k = -\frac{\Delta G°}{RT}$$

4.4 Results and discussion

Figures 4.1-4.5 depict the UV-Vis absorption spectra of the complexation of Pr(III):L-Glutamine with Mg(II) at 298K ($25°$ C), 303K ($30°$ C), 308K ($35°$ C), 313K ($40°$ C), and 318K ($45°$ C) with respect to time (hours). It is observed that with time, there is an increase in absorbance and intensity of the 4f-4f transition bands of Pr(III). A similar trend was seen for Pr(III):L-Tryptophan:Mg(II) and Pr(III):L-Isoleucine:Mg(II) at various temperatures, viz., 298K, 303K, 308K, 313K, and 318K. Table 4.1 to 4.15 gives the observed and calculated Oscillator strengths ($Px10^6$) and Judd-Ofelt parameters [T_λ, (λ = 2, 4, 6) x 10^{10} cm^{-1}] for Pr(III):L-Glutamine:Mg(II), Pr(III):L-Tryptophan:Mg(II) and Pr(III):L-Isoleucine:Mg(II) complex in DMF at five different temperatures, 298K, 303K, 308K, 313K and 318K at different time interval of two hours. From Tables 4.1 to 4.15 it can be clearly observed that the complexation rate of Pr(III):Amino acids with Mg(II) increases linearly with time. The complexation rate constants of Pr(III):Amino acids with Mg(II) at different temperatures were calculated using oscillator strength (P_{obs}) versus time (hr) plots (Figures 4.11, 4.13 and 4.15). The observed rate (k) values were evaluated in terms of the complex created during the reaction's progress, and were determined from plots of oscillator strength of $^3H_4 \rightarrow ^3P_2$ transitions of Pr(III):Amino acid:Mg(II) complex vs time for the different temperatures.

155

Tables 4.16, 4.17, 4.18, 4.19, 4.20 and 4.21 give the evaluated values of rate constants (k), activation energy E_a and the thermodynamic parameters, ΔH^0, ΔG^0 and ΔS^0 at different temperatures (298K, 303K, 308K, 313K and 318K) for Pr(III):L-Glutamine:Mg(II), Pr(III):L-Tryptophan:Mg(II) and Pr(III):L-Isoleucine:Mg(II) complexes. The Van't Hoff plot of log k vs 1/T is used to calculate the activation energy (E_a) and thermodynamic parameters (Figures 4.12, 4.14 and 4.16). This technique enables us to examine the thermodynamics of the complexation of Pr(III):Amino acids with Mg(II) through the determination of the various thermodynamic parameters. It was evident from the evaluated values that the rate of complexation increases as the temperature increases and is in the tune with Arrhenius prediction. We can see from the thermodynamic parameter values given in Tables 4.17, 4.19 and 4.21 that the values of enthalpy (ΔH^0) and entropy (ΔS^0) are positive, indicating that the complexation reaction is endothermic and entropy increasing. The reaction is found to be an entropy driven process since $\Delta S^0 > \Delta H^0$. Negative ΔG^0 values indicate that the complex formation is favourable in solution and also spontaneous, and was observed for all the complexation systems [Pr(III): L-Glutamine:Mg(II), Pr(III):L-Tryptophan:Mg(II) and Pr(III):L-Isoleucine:Mg(II)]. As a result, we can further justify that the simultaneous complexation reaction of Pr(III) ions with amino acids and Mg(II), proceeds at a spontaneously pace as following the randomness of the system (increased entropy values) as it approaches higher temperatures.

References

[1]   B.R. Judd, Optical absorption intensities of rare-earth ions, *Phys. Rev.* **127** (1962) 750–761. https://doi.org/10.1103/PhysRev.127.750.

[2]   G.S. Ofelt, Intensities of Crystal Spectra of Rare-Earth Ions, *J. Chem. Phys.* **37** (1962) 511–520. https://doi.org/10.1063/1.1701366.

[3]   W.T. Carnall, P.R. Fields, B.G. Wybourne, Spectral intensities of the trivalent lanthanides and actinides in solution. I. Pr3+, Nd3+, Er3+, Tm3+, and Yb3+, *J. Chem. Phys.* **42** (1965) 3797–3806. https://doi.org/10.1063/1.1695840.

Table 4.1: Observed and Calculated Oscillator strengths (Px10^6) and Judd Ofelt parameter [T$_\lambda$, (λ = 2, 4, 6) x 10^{10} cm^{-1}] for Pr(III):L-Glutamine:Mg(II) complex at 298K (25^{0}C) at different time (hrs)

Time (hr)	$^3H_4 \to {}^3P_2$		$^3H_4 \to {}^3P_1$		$^3H_4 \to {}^3P_0$		$^3H_4 \to {}^1D_2$		T$_2$	T$_4$	T$_6$
	Pobs	Pcal	Pobs	Pcal	Pobs	Pcal	Pobs	Pcal			
0	6.2938	6.2938	2.2921	1.6780	1.0478	1.6526	1.9180	1.9180	-17.5712	4.6097	19.4152
2	6.4782	6.4782	2.4006	1.7487	1.0801	1.7222	2.0462	2.0462	34.3703	4.8039	19.9683
4	6.7090	6.7090	2.5356	1.8520	1.1507	1.8240	2.1910	2.1910	-51.8031	5.0877	20.6496
6	6.7693	6.7693	2.5944	1.8943	1.1760	1.8656	2.2677	2.2677	65.1554	5.2038	20.8162
8	6.8404	6.8404	2.6587	1.9407	1.2043	1.9113	2.3698	2.3698	83.5423	5.3315	21.0154
10	6.9145	6.9145	2.7234	1.9910	1.2394	1.9608	2.4639	2.4639	99.9088	5.4695	21.2217
12	7.0001	7.0001	2.7906	2.0402	1.2703	2.0094	2.6340	2.6340	132.8075	5.6049	21.4662
14	7.1242	7.1242	2.8938	2.1162	1.3184	2.0842	2.8216	2.8216	167.0379	5.8136	21.8177
16	7.2695	7.2695	3.0252	2.2127	1.3789	2.1792	3.0011	3.0011	198.0069	6.0786	22.2233
18	7.3834	7.3834	3.1254	2.2892	1.4311	2.2546	3.1843	3.1843	231.9201	6.2889	22.5407
20	7.4822	7.4822	3.2339	2.3664	1.4761	2.3305	3.3377	3.3377	260.0723	6.5008	22.8083
22	7.5605	7.5605	3.3042	2.4179	1.5084	2.3813	3.4398	3.4398	277.9682	6.6423	23.0275
24	7.6991	7.6991	3.4158	2.5023	1.5649	2.4645	3.6490	3.6490	316.1591	6.8743	23.4202
26	7.7913	7.7913	3.5034	2.5655	1.6029	2.5266	3.7895	3.7895	341.8298	7.0478	23.6763
28	7.8799	7.8799	3.5741	2.6187	1.6381	2.5791	3.9133	3.9133	363.9852	7.1940	23.9278
30	7.9685	7.9685	3.6563	2.6784	1.6747	2.6378	4.0581	4.0581	390.8919	7.3580	24.1746
32	8.1071	8.1071	3.7764	2.7671	1.7312	2.7252	4.2586	4.2586	427.0940	7.6016	24.5642
34	8.1818	8.1818	3.8466	2.8208	1.7678	2.7781	4.3694	4.3694	447.1948	7.7491	24.7699

Table 4.2: Observed and Calculated Oscillator strengths (Px10^6) and Judd Ofelt parameter [T$_\lambda$, (λ = 2, 4, 6) x 10^{10} cm^{-1}] for Pr(III):L-Glutamine:Mg(II) complex at 303K (30^{0}C) at different time (hrs)

Time (hr)	$^3H_4 \to {}^3P_2$		$^3H_4 \to {}^3P_1$		$^3H_4 \to {}^3P_0$		$^3H_4 \to {}^1D_2$		T$_2$	T$_4$	T$_6$
	Pobs	Pcal	Pobs	Pcal	Pobs	Pcal	Pobs	Pcal			
0	7.1248	7.1248	2.5501	1.8634	1.1591	1.8355	1.9865	1.9865	-22.025	5.120	22.005
2	7.2880	7.2880	2.6634	1.9411	1.2004	1.9119	2.1799	2.1799	-10.973	5.333	22.483
4	7.3981	7.3981	2.7261	1.9926	1.2403	1.9627	2.3201	2.3201	35.461	5.475	22.806
6	7.4954	7.4954	2.7767	2.0288	1.2617	1.9983	2.4197	2.4197	51.580	5.574	23.099
8	7.7066	7.7066	2.9441	2.1528	1.3411	2.1205	2.6527	2.6527	90.280	5.915	23.701
10	7.8481	7.8481	3.0873	2.2583	1.4078	2.2244	2.8461	2.8461	124.611	6.205	24.088
12	7.9844	7.9844	3.1877	2.3332	1.4566	2.2982	3.0191	3.0191	154.7582	6.4107	24.4797
14	8.0907	8.0907	3.2803	2.3998	1.4964	2.3637	3.2193	3.2193	193.0686	6.5935	24.7797
16	8.1431	8.1431	3.3808	2.4766	1.5488	2.4394	3.5383	3.5383	261.8767	6.8045	24.8952
18	8.2539	8.2539	3.4812	2.5478	1.5901	2.5095	3.6989	3.6989	290.879	7.000	25.206
20	8.3550	8.3550	3.5567	2.6065	1.6315	2.5674	3.8719	3.8719	323.389	7.162	25.495
22	8.4920	8.4920	3.6949	2.7032	1.6857	2.6626	4.0642	4.0642	357.786	7.427	25.874
24	8.6987	8.6987	3.8630	2.8322	1.7743	2.7897	4.3978	4.3978	419.6453	7.7816	26.4568
26	8.8844	8.8844	4.0311	2.9592	1.8588	2.9147	4.6704	4.6704	469.0035	8.1305	26.9727
28	9.1225	9.1225	4.2278	3.0977	1.9382	3.0512	4.9837	4.9837	524.1401	8.5113	27.6521
30	9.2236	9.2236	4.3075	3.1633	1.9887	3.1158	5.1567	5.1567	556.6274	8.6914	27.9356
32	9.4130	9.4130	4.5049	3.3050	2.0736	3.2554	5.4836	5.4836	618.0318	9.0808	28.4530
34	9.5545	9.5545	4.6139	3.3861	2.1260	3.3353	5.6431	5.6431	644.7303	9.3036	28.8577

Table 4.3: Observed and Calculated Oscillator strengths (Px10^6) and Judd Ofelt parameter [T$_\lambda$, (λ = 2, 4, 6) x 10^{10} cm^{-1}] for Pr(III):L-Glutamine:Mg(II) complex at 308K (35^{0}C) at different time (hrs)

Time (hr)	$^3H_4 \to {}^3P_2$		$^3H_4 \to {}^3P_1$		$^3H_4 \to {}^3P_0$		$^3H_4 \to {}^1D_2$		T$_2$	T$_4$	T$_6$
	Pobs	Pcal	Pobs	Pcal	Pobs	Pcal	Pobs	Pcal			
0	7.1412	7.1412	2.7054	1.9554	1.1873	1.9259	2.1332	2.1332	9.9722	5.3721	21.9914
2	7.2657	7.2657	2.8157	2.0314	1.2282	2.0007	2.3332	2.3332	47.0209	5.5807	22.3442
4	7.5832	7.5832	3.0504	2.2079	1.3449	2.1746	2.6910	2.6910	106.9593	6.0658	23.2560
6	7.7413	7.7413	3.1905	2.3128	1.4134	2.2779	2.9003	2.9003	143.8087	6.3538	23.6980
8	7.9792	7.9792	3.3844	2.4548	1.5021	2.4177	3.2707	3.2707	211.9406	6.7439	24.3739
10	8.2641	8.2641	3.6648	2.6542	1.6188	2.6141	3.7018	3.7018	290.5883	7.2918	25.1623
12	8.4481	8.4481	3.8228	2.7769	1.7049	2.7350	3.9843	3.9843	342.3360	7.6290	25.6757
14	8.6264	8.6264	3.9928	2.9004	1.7807	2.8567	4.2438	4.2438	389.2166	7.9683	26.1702
16	8.7521	8.7521	4.0863	2.9730	1.8316	2.9281	4.4405	4.4405	425.4523	8.1675	26.5292
18	8.9372	8.9372	4.2623	3.1023	1.9130	3.0554	4.7251	4.7251	477.5807	8.5228	27.0415
20	9.2087	9.2087	4.5198	3.2863	2.0219	3.2367	5.1687	5.1687	560.0164	9.0284	27.7969
22	9.4465	9.4465	4.7186	3.4295	2.1081	3.3777	5.4763	5.4763	613.8730	9.4217	28.4720
24	9.6776	9.6776	4.9294	3.5786	2.1942	3.5246	5.8090	5.8090	673.8602	9.8313	29.1207
26	9.9154	9.9154	5.1580	3.7482	2.3032	3.6917	6.2276	6.2276	752.8426	10.2974	29.7763
28	10.0074	10.0074	5.2395	3.8085	2.3415	3.7510	6.3887	6.3887	783.2396	10.4629	30.0339
30	10.1072	10.1072	5.3161	3.8647	2.3768	3.8063	6.5226	6.5226	806.9503	10.6173	30.3202
32	10.1992	10.1992	5.4215	3.9431	2.4276	3.8836	6.6335	6.6335	825.8702	10.8329	30.5643
34	10.3641	10.3641	5.5388	4.0289	2.4810	3.9681	6.8805	6.8805	870.9035	11.0685	31.0423

Table 4.4: Observed and Calculated Oscillator strengths (Px10^6) and Judd Ofelt parameter [T$_\lambda$, (λ = 2, 4, 6) x 10^{10} cm^{-1}] for Pr(III):L-Glutamine:Mg(II) complex at 313K (40^{0}C) at different time (hrs)

Time (hr)	$^3H_4 \to {}^3P_2$		$^3H_4 \to {}^3P_1$		$^3H_4 \to {}^3P_0$		$^3H_4 \to {}^1D_2$		T$_2$	T$_4$	T$_6$
	Pobs	Pcal	Pobs	Pcal	Pobs	Pcal	Pobs	Pcal			
0	7.5551	7.5551	2.7212	1.9785	1.2171	1.9486	2.2904	2.2904	18.6402	5.4357	23.3319
2	7.9325	7.9325	2.9608	2.1840	1.3860	2.1510	2.6484	2.6484	-74.6054	6.0002	24.4192
4	8.0650	8.0650	3.1035	2.2829	1.4403	2.2485	2.8963	2.8963	121.9480	6.2721	24.7813
6	8.2042	8.2042	3.2150	2.3582	1.4786	2.3226	3.0583	3.0583	149.4121	6.4788	25.1825
8	8.3038	8.3038	3.3024	2.4407	1.5552	2.4039	3.2300	3.2300	181.6529	6.7056	25.4488
10	8.4975	8.4975	3.4598	2.5468	1.6092	2.5084	3.5168	3.5168	233.8044	6.9971	26.0062
12	8.6244	8.6244	3.5766	2.6384	1.6746	2.5986	3.6885	3.6885	264.2268	7.2488	26.3552
14	8.8124	8.8124	3.7141	2.7484	1.7558	2.7069	3.9542	3.9542	311.9467	7.5509	26.8913
16	9.0060	9.0060	3.8931	2.8609	1.8010	2.8177	4.2604	4.2604	368.4981	7.8598	27.4440
18	9.1226	9.1226	3.9848	2.9456	1.8775	2.9011	4.4516	4.4516	404.0423	8.0926	27.7642
20	9.3331	9.3331	3.9848	2.9638	1.9135	2.9191	4.7367	4.7367	455.0037	8.1428	28.4416
22	9.4601	9.4601	4.2495	3.1350	1.9901	3.0877	4.8517	4.8517	472.2711	8.6131	28.7322
24	9.6377	9.6377	4.4069	3.2619	2.0850	3.2127	5.1482	5.1482	527.6132	8.9618	29.2219
26	9.8586	9.8586	4.5851	3.3946	2.1708	3.3433	5.4722	5.4722	586.3621	9.3261	29.8492
28	10.0805	10.0805	4.7788	3.5142	2.2156	3.4611	5.8351	5.8351	653.9334	9.6547	30.4892
30	10.1961	10.1961	4.8808	3.5984	2.2810	3.5441	5.9874	5.9874	680.6994	9.8862	30.8067
32	10.3456	10.3456	5.0080	3.6906	2.3373	3.6349	6.2158	6.2158	722.5335	10.1394	31.2294
34	10.5176	10.5176	5.1663	3.8173	2.4312	3.7597	6.4443	6.4443	762.7736	10.4877	31.7006

Table 4.5: Observed and Calculated Oscillator strengths (Px10^6) and Judd Ofelt parameter [T$_\lambda$, (λ = 2, 4, 6) x 10^{10} cm^{-1}] for Pr(III):L-Glutamine:Mg(II) complex at 318K (45^{0}C) at different time (hrs)

Time (hr)	$^3H_4 \rightarrow\ ^3P_2$		$^3H_4\ \rightarrow\ ^3P_1$		$^3H_4\ \rightarrow\ ^3P_0$		$^3H_4 \rightarrow\ ^1D_2$		T$_2$	T$_4$	T$_6$
	Pobs	Pcal	Pobs	Pcal	Pobs	Pcal	Pobs	Pcal			
0	7.8466	7.8466	3.1389	2.2286	1.2998	2.1975	2.2771	2.2771	-4.2033	6.1302	24.1029
2	8.0048	8.0048	3.3045	2.3403	1.3570	2.3077	2.4688	2.4688	-28.6360	6.4377	24.5399
4	8.1462	8.1462	3.4127	2.4173	1.4020	2.3835	2.6497	2.6497	60.2572	6.6492	24.9469
6	8.2959	8.2959	3.5598	2.5212	1.4620	2.4861	2.8848	2.8848	103.5767	6.9352	25.3619
8	8.4542	8.4542	3.7383	2.6455	1.5311	2.6086	3.1399	3.1399	150.7991	7.2772	25.7897
10	8.6944	8.6944	3.9223	2.7833	1.6214	2.7445	3.4908	3.4908	214.4069	7.6561	26.4765
12	8.8696	8.8696	4.1138	2.9195	1.7011	2.8788	3.7785	3.7785	267.8838	8.0307	26.9513
14	9.0533	9.0533	4.2858	3.0383	1.7659	2.9959	4.0028	4.0028	306.4607	8.3576	27.4666
16	9.2271	9.2271	4.4708	3.1668	1.8368	3.1226	4.3429	4.3429	371.9878	8.7110	27.9423
18	9.4857	9.4857	4.7132	3.3394	1.9381	3.2928	4.6522	4.6522	424.8126	9.1857	28.6638
20	9.7189	9.7189	4.9231	3.4957	2.0394	3.4469	5.0465	5.0465	498.6979	9.6156	29.3138
22	9.8927	9.8927	5.0886	3.6079	2.0975	3.5576	5.2709	5.2709	537.9454	9.9244	29.8015
24	10.0269	10.0269	5.2228	3.7045	2.1557	3.6528	5.4825	5.4825	576.9602	10.1901	30.1709
26	10.2177	10.2177	5.3818	3.8155	2.2179	3.7623	5.7177	5.7177	617.5678	10.4955	30.7151
28	10.3265	10.3265	5.5030	3.9045	2.2738	3.8500	5.7177	5.7177	610.1366	10.7402	31.0067
30	10.4678	10.4678	5.6177	3.9795	2.3086	3.9240	6.1229	6.1229	692.7842	10.9464	31.4151
32	10.6416	10.6416	5.7897	4.1059	2.3883	4.0486	6.3454	6.3454	731.5736	11.2942	31.8924
34	10.8084	10.8084	5.9228	4.2040	2.4504	4.1453	6.5914	6.5914	776.2688	11.5640	32.3673

Table 4.6: Observed and Calculated Oscillator strengths (Px10^6) and Judd Ofelt parameter [T$_\lambda$, (λ = 2, 4, 6) x 10^{10} cm^{-1}] for Pr(III):L-Tryptophan:Mg(II) complex at 298K (25^{0}C) at different time (hrs)

Time (hr)	$^3H_4 \rightarrow\ ^3P_2$		$^3H_4\ \rightarrow\ ^3P_1$		$^3H_4\ \rightarrow\ ^3P_0$		$^3H_4 \rightarrow\ ^1D_2$		T$_2$	T$_4$	T$_6$
	Pobs	Pcal	Pobs	Pcal	Pobs	Pcal	Pobs	Pcal			
0	6.9537	6.9537	2.6324	1.9203	1.1916	1.8940	2.2644	2.2644	52.3473	5.2795	21.4009
2	7.2992	7.2992	2.8915	2.1078	1.3059	2.0789	2.7510	2.7510	139.6991	5.7949	22.3967
4	7.4649	7.4649	3.0579	2.2333	1.3893	2.2027	3.0398	3.0398	194.0962	6.1400	22.8481
6	7.5956	7.5956	3.1827	2.3225	1.4423	2.2907	3.2305	3.2305	228.5912	6.3854	23.2112
8	7.7716	7.7716	3.3311	2.4310	1.5098	2.3976	3.5194	3.5194	282.3720	6.6835	23.7088
10	7.8476	7.8476	3.4371	2.5045	1.5504	2.4702	3.6592	3.6592	308.9299	6.8857	23.9041
12	7.9979	7.9979	3.5619	2.5959	1.6075	2.5603	3.8551	3.8551	343.3282	7.1369	24.3301
14	8.2046	8.2046	3.7095	2.7069	1.6809	2.6698	4.1556	4.1556	397.7295	7.4421	24.9267
16	8.3199	8.3199	3.8256	2.7857	1.7218	2.7475	4.3320	4.3320	430.0105	7.6587	25.2470
18	8.5463	8.5463	4.0242	2.9347	1.8198	2.8944	4.6939	4.6939	496.9606	8.0683	25.8801
20	8.6470	8.6470	4.1302	3.0092	1.8624	2.9680	4.8402	4.8402	523.3754	8.2734	26.1559
22	8.7828	8.7828	4.2048	3.0704	1.9095	3.0283	5.0480	5.0480	561.4993	8.4415	26.5565
24	8.8930	8.8930	4.3249	3.1531	1.9541	3.1099	5.1943	5.1943	587.2711	8.6689	26.8572
26	9.0092	9.0092	4.4544	3.2428	2.0033	3.1983	5.4020	5.4020	626.5901	8.9155	27.1724
28	9.1048	9.1048	4.5416	3.3058	2.0418	3.2605	5.5405	5.5405	651.5966	9.0889	27.4399
30	9.2552	9.2552	4.6577	3.3940	2.1010	3.3474	5.8097	5.8097	702.6418	9.3311	27.8683
32	9.3508	9.3508	4.7315	3.4537	2.1460	3.4063	5.9181	5.9181	720.8265	9.4953	28.1383
34	9.4516	9.4516	4.8611	3.5381	2.1848	3.4896	6.0945	6.0945	754.0417	9.7274	28.4069

Table 4.7: Observed and Calculated Oscillator strengths (P$\times 10^6$) and Judd Ofelt parameter [T_λ, (λ = 2, 4, 6) x 10^{10} cm^{-1}] for Pr(III):L-Tryptophan:Mg(II) complex at 303K (30^{0}C) at different time (hrs)

Time (hr)	$^3H_4 \to {}^3P_2$		$^3H_4 \to {}^3P_1$		$^3H_4 \to {}^3P_0$		$^3H_4 \to {}^1D_2$		T_2	T_4	T_6
	Pobs	Pcal	Pobs	Pcal	Pobs	Pcal	Pobs	Pcal			
0	6.7792	6.7792	2.7451	1.9980	1.2338	1.9707	2.3559	2.3559	84.3509	5.4929	20.7722
2	6.9694	6.9694	2.9380	2.1396	1.3227	2.1103	2.7206	2.7206	154.3373	5.8821	21.2921
4	7.1434	7.1434	3.1208	2.2662	1.3923	2.2352	2.9618	2.9618	197.3428	6.2304	21.7700
6	7.2439	7.2439	3.2097	2.3321	1.4346	2.3002	3.1441	3.1441	231.9988	6.4115	22.0513
8	7.4709	7.4709	3.4269	2.4922	1.5361	2.4581	3.5074	3.5074	299.1766	6.8516	22.6783
10	7.5929	7.5929	3.5360	2.5702	1.5824	2.5350	3.7074	3.7074	336.3930	7.0659	23.0213
12	7.7355	7.7355	3.6693	2.6690	1.6459	2.6325	3.9147	3.9147	373.8589	7.3377	23.4166
14	7.8306	7.8306	3.7532	2.7281	1.6796	2.6907	4.0530	4.0530	398.8589	7.5000	23.6853
16	8.0208	8.0208	3.9402	2.8698	1.7747	2.8305	4.3735	4.3735	458.8128	7.8895	24.2051
18	8.1949	8.1949	4.0987	2.9832	1.8421	2.9423	4.6338	4.6338	506.2090	8.2014	24.6928
20	8.3689	8.3689	4.2614	3.1000	1.9120	3.0575	4.9191	4.9191	559.2788	8.5225	25.1779
22	8.4963	8.4963	4.3704	3.1769	1.9562	3.1334	5.1015	5.1015	592.1329	8.7339	25.5394
24	8.6120	8.6120	4.4987	3.2721	2.0175	3.2273	5.2912	5.2912	627.3638	8.9957	25.8491
26	8.7394	8.7394	4.6170	3.3569	2.0681	3.3109	5.5000	5.5000	666.2111	9.2288	26.2047
28	8.8973	8.8973	4.7503	3.4547	2.1294	3.4074	5.7074	5.7074	702.6800	9.4976	26.6509
30	9.0032	9.0032	4.8644	3.5395	2.1843	3.4910	5.8985	5.8985	738.9269	9.7308	26.9359
32	9.1673	9.1673	5.0271	3.6541	2.2499	3.6041	6.1927	6.1927	794.6578	10.0459	27.3903
34	9.2885	9.2885	5.1403	3.7396	2.3070	3.6884	6.3824	6.3824	829.5675	10.2811	27.7248

Table 4.8: Observed and Calculated Oscillator strengths (P$\times 10^6$) and Judd Ofelt parameter [T_λ, (λ = 2, 4, 6) x 10^{10} cm^{-1}] for Pr(III):L-Tryptophan:Mg(II) complex at 308K (35^{0}C) at different time (hrs)

Time (hr)	$^3H_4 \to {}^3P_2$		$^3H_4 \to {}^3P_1$		$^3H_4 \to {}^3P_0$		$^3H_4 \to {}^1D_2$		T_2	T_4	T_6
	Pobs	Pcal	Pobs	Pcal	Pobs	Pcal	Pobs	Pcal			
0	7.0873	7.0873	2.7597	2.0300	1.2824	2.0022	2.6340	2.6340	127.1468	5.5810	21.7593
2	7.2984	7.2984	2.9293	2.1619	1.3753	2.1322	2.9738	2.9738	190.1290	5.9436	22.3549
4	7.4940	7.4940	3.1142	2.2895	1.4446	2.2581	3.2540	3.2540	240.5627	6.2943	22.9029
6	7.6705	7.6705	3.2593	2.4009	1.5214	2.3680	3.4826	3.4826	280.5945	6.6007	23.4001
8	7.8315	7.8315	3.4340	2.5258	1.5954	2.4911	3.8101	3.8101	344.0766	6.9439	23.8366
10	7.9866	7.9866	3.5739	2.6322	1.6674	2.5961	4.0531	4.0531	388.8110	7.2367	24.2670
12	8.1762	8.1762	3.7282	2.7445	1.7367	2.7069	4.3559	4.3559	444.8371	7.5454	24.8066
14	8.3789	8.3789	3.9080	2.8803	1.8272	2.8408	4.6484	4.6484	497.5839	7.9188	25.3720
16	8.5268	8.5268	4.0132	2.9553	1.8713	2.9147	4.8297	4.8297	528.8432	8.1248	25.8021
18	8.6747	8.6747	4.1430	3.0495	1.9292	3.0076	5.0727	5.0727	574.0874	8.3838	26.2180
20	8.8643	8.8643	4.3279	3.1818	2.0079	3.1382	5.3631	5.3631	627.2379	8.7476	26.7429
22	8.9621	8.9621	4.4076	3.2476	2.0591	3.2031	5.5568	5.5568	664.6233	8.9286	27.0154
24	9.1100	9.1100	4.5127	3.3248	2.1075	3.2791	5.7524	5.7524	699.1533	9.1406	27.4439
26	9.2639	9.2639	4.6629	3.4351	2.1771	3.3880	5.9811	5.9811	740.6753	9.4440	27.8675
28	9.3628	9.3628	4.7527	3.4988	2.2141	3.4508	6.1397	6.1397	770.0286	9.6192	28.1455
30	9.5167	9.5167	4.8969	3.6027	2.2767	3.5532	6.3951	6.3951	817.6597	9.9046	28.5739
32	9.7349	9.7349	5.0716	3.7347	2.3649	3.6835	6.6731	6.6731	866.1236	10.2676	29.1929
34	9.8888	9.8888	5.2167	3.8437	2.4369	3.7910	6.9409	6.9409	916.5472	10.5674	29.6175

Table 4.9: Observed and Calculated Oscillator strengths (Px10^6) and Judd Ofelt parameter [T$_\lambda$, (λ = 2, 4, 6) x 10^{10} cm^{-1}] for Pr(III):L-Tryptophan:Mg(II) complex at 313K (40^{0}C) at different time (hrs)

Time (hr)	$^3H_4 \to {}^3P_2$		$^3H_4 \to {}^3P_1$		$^3H_4 \to {}^3P_0$		$^3H_4 \to {}^1D_2$		T$_2$	T$_4$	T$_6$
	Pobs	Pcal	Pobs	Pcal	Pobs	Pcal	Pobs	Pcal			
0	7.7052	7.7052	2.9931	2.1592	1.3067	2.1290	2.1872	2.1872	-15.2424	5.9393	23.6906
2	7.9928	7.9928	3.1444	2.2664	1.3690	2.2347	2.4313	2.4313	21.0617	6.2342	24.5551
4	8.1121	8.1121	3.2324	2.3332	1.4140	2.3006	2.5864	2.5864	48.2801	6.4180	24.8974
6	8.2452	8.2452	3.3462	2.4114	1.4561	2.3778	2.7513	2.7513	76.8055	6.6332	25.2765
8	8.4963	8.4963	3.5554	2.5646	1.5518	2.5288	3.1307	3.1307	146.1106	7.0545	25.9879
10	8.6885	8.6885	3.7131	2.6850	1.6337	2.6475	3.3831	3.3831	190.5087	7.3856	26.5297
12	8.8956	8.8956	3.9084	2.8270	1.7213	2.7876	3.9457	3.9457	304.3763	7.7764	27.1050
14	9.0802	9.0802	4.0790	2.9524	1.8002	2.9112	4.3152	4.3152	375.8884	8.1212	27.6184
16	9.3690	9.3690	4.3452	3.1410	1.9098	3.0972	4.5478	4.5478	409.2163	8.6401	28.4272
18	9.5097	9.5097	4.4653	3.2312	1.9692	3.1861	4.8596	4.8596	470.5971	8.8882	28.8223
20	9.7232	9.7232	4.6478	3.3639	2.0511	3.3170	5.2868	5.2868	553.3206	9.2532	29.4251
22	10.0195	10.0195	4.9010	3.5447	2.1578	3.4952	5.5590	5.5590	595.1839	9.7504	30.2644
24	10.2192	10.2192	5.1220	3.7040	2.2540	3.6523	5.9764	5.9764	676.4753	10.1886	30.8023
26	10.4778	10.4778	5.3495	3.8663	2.3497	3.8123	6.2287	6.2287	716.3690	10.6350	31.5316
28	10.5978	10.5978	5.5137	3.9884	2.4287	3.9327	6.6758	6.6758	809.7617	10.9710	31.8355
30	10.9512	10.9512	5.7852	4.1870	2.5527	4.1286	6.9480	6.9480	847.8230	11.5173	32.8489
32	11.1433	11.1433	5.9558	4.3109	2.6288	4.2507	7.1201	7.1201	873.9637	11.8581	33.3881
34	11.4096	11.4096	6.1768	4.4714	2.7274	4.4090	7.2977	7.2977	896.3498	12.2996	34.1435

Table 4.10: Observed and Calculated Oscillator strengths (Px10^6) and Judd Ofelt parameter [T$_\lambda$, (λ = 2, 4, 6) x 10^{10} cm^{-1}] for Pr(III):L-Tryptophan:Mg(II) complex at 318K (45^{0}C) at different time (hrs)

Time (hr)	$^3H_4 \to {}^3P_2$		$^3H_4 \to {}^3P_1$		$^3H_4 \to {}^3P_0$		$^3H_4 \to {}^1D_2$		T$_2$	T$_4$	T$_6$
	Pobs	Pcal	Pobs	Pcal	Pobs	Pcal	Pobs	Pcal			
0	7.8565	7.8565	2.9689	2.1618	1.3358	2.1316	2.2164	2.2164	-18.4864	5.9464	24.1844
2	8.0533	8.0533	3.1607	2.2905	1.4006	2.2586	2.5054	2.5054	33.8975	6.3005	24.7355
4	8.1708	8.1708	3.2885	2.3891	1.4688	2.3557	2.6902	2.6902	67.8909	6.5716	25.0485
6	8.4317	8.4317	3.2885	2.4374	1.5643	2.4034	3.0617	3.0617	135.1118	6.7047	25.8689
8	8.5843	8.5843	3.6576	2.6563	1.6319	2.6192	3.2701	3.2701	171.7722	7.3067	26.2086
10	8.8269	8.8269	3.8771	2.8095	1.7175	2.7703	3.6043	3.6043	231.3554	7.7280	26.8919
12	9.1412	9.1412	4.1195	2.9961	1.8465	2.9543	4.0328	4.0328	307.5834	8.2414	27.7858
14	9.2663	9.2663	4.2474	3.0893	1.9044	3.0462	4.2412	4.2412	346.4587	8.4979	28.1277
16	9.4021	9.4021	4.3535	3.1703	1.9593	3.1260	4.4378	4.4378	381.9912	8.7205	28.5137
18	9.6081	9.6081	4.5525	3.3111	2.0409	3.2649	4.6815	4.6815	423.4516	9.1080	29.0859
20	9.9133	9.9133	4.8154	3.5013	2.1566	3.4524	5.1454	5.1454	508.3163	9.6310	29.9473
22	10.1742	10.1742	5.0567	3.6791	2.2694	3.6277	5.5268	5.5268	577.3471	10.1200	30.6725
24	10.4977	10.4977	5.3690	3.9145	2.4255	3.8598	6.0595	6.0595	676.5095	10.7675	31.5607
26	10.7845	10.7845	5.6320	4.0961	2.5245	4.0389	6.4645	6.4645	749.1910	11.2671	32.3682
28	11.1354	11.1354	5.9444	4.3265	2.6708	4.2661	6.9048	6.9048	825.5550	11.9009	33.3501
30	11.3597	11.3597	6.1072	4.4460	2.7460	4.3840	7.2174	7.2174	881.5322	12.2297	33.9981
32	11.6573	11.6573	6.4135	4.6716	2.8889	4.6065	7.7029	7.7029	971.6985	12.8503	34.8083
34	11.8281	11.8281	6.5691	4.7823	2.9537	4.7156	7.9467	7.9467	1015.5608	13.1547	35.2876

Table 4.11: Observed and Calculated Oscillator strengths (Px10^6) and Judd Ofelt parameter [T$_\lambda$, (λ = 2, 4, 6) x 10^{10} cm^{-1}] for Pr(III):L-Isoleucine:Mg(II) complex at 298K (25^{0}C) at different time (hrs)

Time (hr)	$^3H_4 \rightarrow {}^3P_2$		$^3H_4 \rightarrow {}^3P_1$		$^3H_4 \rightarrow {}^3P_0$		$^3H_4 \rightarrow {}^1D_2$		T$_2$	T$_4$	T$_6$
	Pobs	Pcal	Pobs	Pcal	Pobs	Pcal	Pobs	Pcal			
0	6.1562	6.1562	2.4385	1.7480	1.0418	1.7220	1.9489	1.9489	-33.4445	4.8035	18.9120
2	6.2678	6.2678	2.5189	1.8021	1.0692	1.7753	2.1047	2.1047	-61.3545	4.9522	19.2383
4	6.3962	6.3962	2.6395	1.8882	1.1199	1.8600	2.2783	2.2783	92.1217	5.1886	19.5964
6	6.4993	6.4993	2.7233	1.9508	1.1609	1.9218	2.4330	2.4330	120.3168	5.3608	19.8887
8	6.6439	6.6439	2.8561	2.0474	1.2203	2.0169	2.6498	2.6498	159.7995	5.6262	20.2920
10	6.7393	6.7393	2.9644	2.1248	1.2661	2.0932	2.8045	2.8045	188.4525	5.8390	20.5483
12	6.9498	6.9498	3.1484	2.2538	1.3390	2.2203	3.0959	3.0959	240.4873	6.1934	21.1441
14	7.1147	7.1147	3.2928	2.3562	1.3984	2.3211	3.3317	3.3317	282.9222	6.4747	21.6099
16	7.2558	7.2558	3.4257	2.4545	1.4613	2.4180	3.5421	3.5421	321.1939	6.7449	22.0004
18	7.4291	7.4291	3.5742	2.5632	1.5290	2.5250	3.8147	3.8147	371.4292	7.0434	22.4893
20	7.5203	7.5203	3.6702	2.6362	1.5783	2.5969	3.9054	3.9054	385.8247	7.2442	22.7349
22	7.6319	7.6319	3.7867	2.7195	1.6276	2.6790	3.9567	3.9567	389.9083	7.4730	23.0397
24	7.7350	7.7350	3.8746	2.7867	1.6735	2.7452	4.1304	4.1304	422.3948	7.6577	23.3288
26	7.8754	7.8754	3.9829	2.8606	1.7124	2.8180	4.2608	4.2608	442.6104	7.8608	23.7349
28	7.9869	7.9869	4.0831	2.9323	1.7550	2.8887	4.4587	4.4587	480.0321	8.0579	24.0482
30	8.0901	8.0901	4.2037	3.0141	1.7974	2.9692	4.7996	4.7996	550.5101	8.2827	24.3266
32	8.2143	8.2143	4.3242	3.0986	1.8450	3.0524	4.9859	4.9859	584.4297	8.5147	24.6720
34	8.4206	8.4206	4.5129	3.2395	1.9367	3.1912	5.2647	5.2647	633.8308	8.9019	25.2454

Table 4.12: Observed and Calculated Oscillator strengths (Px10^6) and Judd Ofelt parameter [T$_\lambda$, (λ = 2, 4, 6) x 10^{10} cm^{-1}] for Pr(III):L-Isoleucine:Mg(II) complex at 303K (30^{0}C) at different time (hrs)

Time (hr)	$^3H_4 \rightarrow {}^3P_2$		$^3H_4 \rightarrow {}^3P_1$		$^3H_4 \rightarrow {}^3P_0$		$^3H_4 \rightarrow {}^1D_2$		T$_2$	T$_4$	T$_6$
	Pobs	Pcal	Pobs	Pcal	Pobs	Pcal	Pobs	Pcal			
0	6.7790	6.7790	2.5914	1.8667	1.1251	1.8391	1.8590	1.8590	-28.3079	5.1298	20.8679
2	7.0688	7.0688	2.7219	1.9616	1.1835	1.9325	2.1279	2.1279	-13.4862	5.3905	21.7488
4	7.2636	7.2636	2.8938	2.0869	1.2609	2.0559	2.3905	2.3905	-59.9902	5.7348	22.2961
6	7.4432	7.4432	3.0658	2.2131	1.3402	2.1803	2.6479	2.6479	106.3119	6.0815	22.7926
8	7.5873	7.5873	3.2762	2.3620	1.4263	2.3270	2.8804	2.8804	149.2302	6.4908	23.1557
10	7.7575	7.7575	3.3646	2.4206	1.4548	2.3848	3.1005	3.1005	187.8903	6.6520	23.6713
12	7.8372	7.8372	3.5030	2.5282	1.5304	2.4908	3.2469	3.2469	215.5834	6.9477	23.8536
14	8.0812	8.0812	3.6664	2.6439	1.5974	2.6047	3.5396	3.5396	265.7381	7.2656	24.5691
16	8.2159	8.2159	3.8518	2.7786	1.6800	2.7374	3.7545	3.7545	305.3033	7.6356	24.9121
18	8.4658	8.4658	3.9945	2.8804	1.7401	2.8377	4.0721	4.0721	360.7776	7.9154	25.6572
20	8.5802	8.5802	4.1579	3.0040	1.8227	2.9595	4.2922	4.2922	402.8930	8.2550	25.9417
22	8.6903	8.6903	4.2171	3.0425	1.8403	2.9974	4.3773	4.3773	414.8897	8.3610	26.2747
24	8.8149	8.8149	4.3305	3.1199	1.8810	3.0737	4.5610	4.5610	448.2310	8.5736	26.6264
26	8.8792	8.8792	4.3811	3.1630	1.9160	3.1161	4.6586	4.6586	466.0461	8.6920	26.8060
28	8.9945	8.9945	4.4981	3.2412	1.9549	3.1932	4.8050	4.8050	491.5011	8.9069	27.1266
30	9.1038	9.1038	4.5951	3.3102	1.9953	3.2611	4.9825	4.9825	524.4546	9.0966	27.4344
32	9.2139	9.2139	4.6836	3.3786	2.0428	3.3285	5.1112	5.1112	546.2641	9.2844	27.7456
34	9.3283	9.3283	4.8049	3.4661	2.0958	3.4147	5.3064	5.3064	582.8348	9.5249	28.0565

Table 4.13: Observed and Calculated Oscillator strengths (Px10^6) and Judd Ofelt parameter [T$_\lambda$, (λ = 2, 4, 6) x 10^{10} cm^{-1}] for Pr(III):L-Isoleucine:Mg(II) complex at 308K (35^{0}C) at different time (hrs)

Time (hr)	$^3H_4 \to {}^3P_2$		$^3H_4 \to {}^3P_1$		$^3H_4 \to {}^3P_0$		$^3H_4 \to {}^1D_2$		T$_2$	T$_4$	T$_6$
	Pobs	Pcal	Pobs	Pcal	Pobs	Pcal	Pobs	Pcal			
0	6.7719	6.7719	2.4695	1.8439	1.2002	1.8165	1.9566	1.9566	-5.3717	5.0670	20.8624
2	6.9553	6.9553	2.7605	2.0598	1.3389	2.0292	2.2867	2.2867	-56.9658	5.6603	21.3056
4	7.1196	7.1196	2.8796	2.2038	1.5052	2.1710	2.5738	2.5738	110.9942	6.0559	21.7391
6	7.3026	7.3026	3.0423	2.3196	1.5732	2.2851	2.8436	2.8436	159.9767	6.3743	22.2544
8	7.4784	7.4784	3.1958	2.4283	1.6360	2.3921	3.1149	3.1149	209.7842	6.6728	22.7512
10	7.6314	7.6314	3.3434	2.5431	1.7168	2.5052	3.3258	3.3258	247.3536	6.9883	23.1688
12	7.7037	7.7037	3.4919	2.6594	1.7997	2.6198	3.5454	3.5454	292.1674	7.3079	23.3208
14	7.9353	7.9353	3.6839	2.7899	1.8677	2.7484	3.8842	3.8842	353.5824	7.6666	23.9847
16	8.0749	8.0749	3.7930	2.8763	1.9306	2.8335	4.0951	4.0951	392.1268	7.9041	24.3791
18	8.1968	8.1968	3.9313	2.9685	1.9759	2.9243	4.2803	4.2803	425.9296	8.1574	24.7116
20	8.3064	8.3064	4.0202	3.0347	2.0186	2.9895	4.4583	4.4583	458.9998	8.3392	25.0226
22	8.4036	8.4036	4.1091	3.1227	2.1046	3.0763	4.6865	4.6865	504.2370	8.5812	25.2767
24	8.5566	8.5566	4.2618	3.2323	2.1700	3.1842	4.9491	4.9491	553.5753	8.8821	25.6983
26	8.7210	8.7210	4.3951	3.3538	2.2781	3.3039	5.1773	5.1773	594.2935	9.2162	26.1483
28	8.9639	8.9639	4.3951	3.3922	2.3538	3.3417	5.5060	5.5060	652.9800	9.3218	26.9171
30	9.1221	9.1221	4.7507	3.5892	2.3916	3.5358	5.7687	5.7687	701.6918	9.8631	27.2913
32	9.3412	9.3412	4.9436	3.7188	2.4568	3.6634	6.0643	6.0643	754.1310	10.2191	27.9152
34	9.5490	9.5490	5.1164	3.8473	2.5398	3.7900	6.3772	6.3772	811.2371	10.5721	28.5026

Table 4.14: Observed and Calculated Oscillator strengths (Px10^6) and Judd Ofelt parameter [T$_\lambda$, (λ = 2, 4, 6) x 10^{10} cm^{-1}] for Pr(III):L-Isoleucine:Mg(II) complex at 313K (40^{0}C) at different time (hrs)

Time (hr)	$^3H_4 \to {}^3P_2$		$^3H_4 \to {}^3P_1$		$^3H_4 \to {}^3P_0$		$^3H_4 \to {}^1D_2$		T$_2$	T$_4$	T$_6$
	Pobs	Pcal	Pobs	Pcal	Pobs	Pcal	Pobs	Pcal			
0	6.7161	6.7161	2.4171	1.7678	1.1015	1.7410	1.8585	1.8585	-23.9885	4.8565	20.7353
2	6.7812	6.7812	2.6955	1.9536	1.1934	1.9241	1.8773	1.8773	-24.6045	5.3671	20.8125
4	7.0867	7.0867	3.0969	2.2348	1.3519	2.2010	2.0697	2.0697	-1.8361	6.1396	21.6081
6	7.1639	7.1639	3.3325	2.3891	1.4238	2.3529	2.2448	2.2448	-32.4094	6.5634	21.7483
8	7.3602	7.3602	3.4928	2.5079	1.5000	2.4700	2.4654	2.4654	69.2726	6.8898	22.3050
10	7.8680	7.8680	3.6018	2.5883	1.5510	2.5491	2.6499	2.6499	77.6446	7.1107	23.9119
12	8.1278	8.1278	3.7243	2.6806	1.6121	2.6401	2.7891	2.7891	91.9386	7.3643	24.6965
14	8.3660	8.3660	3.8942	2.8086	1.6969	2.7661	3.1020	3.1020	147.0027	7.7160	25.3838
16	8.5923	8.5923	4.0216	2.9024	1.7562	2.8585	3.2771	3.2771	171.6670	7.9737	26.0574
18	8.8087	8.8087	4.1771	3.0188	1.8324	2.9732	3.5618	3.5618	221.7956	8.2935	26.6818
20	8.9529	8.9529	4.2716	3.0854	1.8705	3.0388	3.7088	3.7088	245.5344	8.4765	27.1061
22	9.3760	9.3760	4.3518	3.1481	1.9151	3.1005	3.8574	3.8574	251.3447	8.6487	28.4481
24	9.5986	9.5986	4.4463	3.2200	1.9636	3.1713	4.0044	4.0044	269.9288	8.8463	29.1254
26	9.8212	9.8212	4.5497	3.2933	2.0060	3.2434	4.1702	4.1702	292.7667	9.0474	29.8021
28	9.9465	9.9465	4.6490	3.3634	2.0463	3.3125	4.3079	4.3079	315.6056	9.2401	30.1616
30	10.0556	10.0556	4.7484	3.4399	2.0991	3.3878	4.4283	4.4283	335.5705	9.4502	30.4635
32	10.1722	10.1722	4.8469	3.5127	2.1455	3.4595	4.6207	4.6207	371.4142	9.6503	30.7925
34	10.2510	10.2510	4.9743	3.6076	2.2069	3.5530	4.7505	4.7505	395.4435	9.9110	30.9813

Table 4.15: Observed and Calculated Oscillator strengths (P$\times 10^6$) and Judd Ofelt parameter [T$_\lambda$, (λ = 2, 4, 6) x 10^{10} cm^{-1}] for Pr(III):L-Isoleucine:Mg(II) complex at 318K (45^0C) at different   time (hrs)

| Time (hr)	$^3H_4 \to {}^3P_2$		$^3H_4 \to {}^3P_1$		$^3H_4 \to {}^3P_0$		$^3H_4 \to {}^1D_2$		T$_2$	T$_4$	T$_6$
	Pobs	Pcal	Pobs	Pcal	Pobs	Pcal	Pobs	Pcal			
0	8.0245	8.0245	2.5119	1.8668	1.2033	1.8387	1.9206	1.9206	-96.0935	5.1288	24.9549
2	8.4679	8.4679	2.7372	2.0348	1.3123	2.0042	2.1412	2.1412	-75.5957	5.5904	26.2861
4	9.1119	9.1119	2.9960	2.2204	1.4230	2.1870	2.3565	2.3565	-69.5285	6.1003	28.2627
6	9.6052	9.6052	3.1780	2.3495	1.4983	2.3142	2.4587	2.4587	-79.0829	6.4552	29.7864
8	9.9079	9.9079	3.2824	2.4246	1.5432	2.3881	2.5077	2.5077	-88.0431	6.6614	30.7243
10	10.4541	10.4541	3.5110	2.5866	1.6373	2.5478	2.6889	2.6889	-83.2218	7.1066	32.3971
12	10.9101	10.9101	3.6850	2.7098	1.7085	2.6690	2.8161	2.8161	-84.6374	7.4449	33.8026
14	11.0543	11.0543	3.8046	2.8029	1.7742	2.7608	3.0364	3.0364	-44.3415	7.7008	34.2075
16	11.2669	11.2669	3.9668	2.9193	1.8437	2.8754	3.3057	3.3057	2.5457	8.0206	34.8193
18	11.3863	11.3863	4.0640	2.9966	1.9001	2.9515	3.4670	3.4670	31.1096	8.2329	35.1544
20	11.4980	11.4980	4.1448	3.0617	1.9489	3.0157	3.6241	3.6241	59.2778	8.4119	35.4729
22	11.6434	11.6434	4.2532	3.1465	2.0092	3.0992	3.8393	3.8393	98.3891	8.6449	35.8878
24	11.7038	11.7038	4.2880	3.1725	2.0261	3.1248	3.9374	3.9374	116.6357	8.7163	36.0668
26	11.7038	11.7038	4.3425	3.2178	2.0615	3.1694	3.9915	3.9915	128.7678	8.8405	36.0336
28	11.8648	11.8648	4.4082	3.2687	2.0972	3.2196	4.1186	4.1186	146.9415	8.9806	36.5245
30	11.9541	11.9541	4.4890	3.3263	2.1310	3.2763	4.2508	4.2508	170.9369	9.1387	36.7751
32	12.0346	12.0346	4.5553	3.3756	2.1629	3.3249	4.3580	4.3580	189.8644	9.2743	37.0030
34	12.1109	12.1109	4.6250	3.4276	2.1967	3.3761	4.4802	4.4802	212.4581	9.4171	37.2153
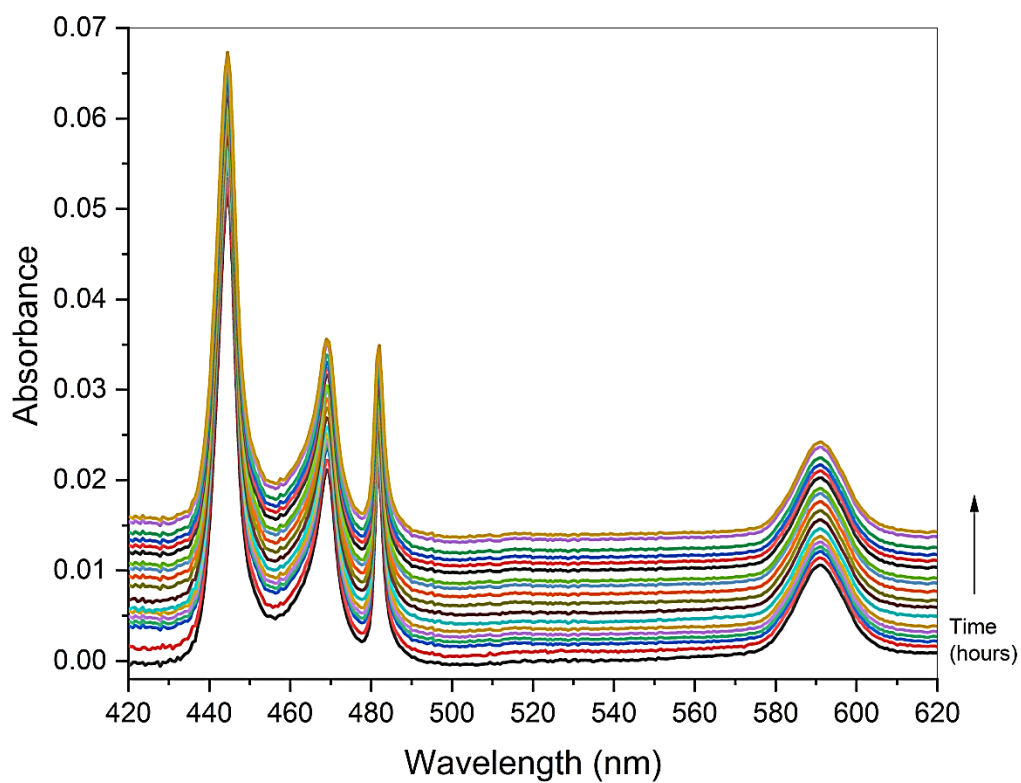
Fig 4.1: Comparative absorption spectra of Pr(III):L-Glutamine complexation with Mg(II) in DMF at 298 K (25^0C) and at different time (hour)
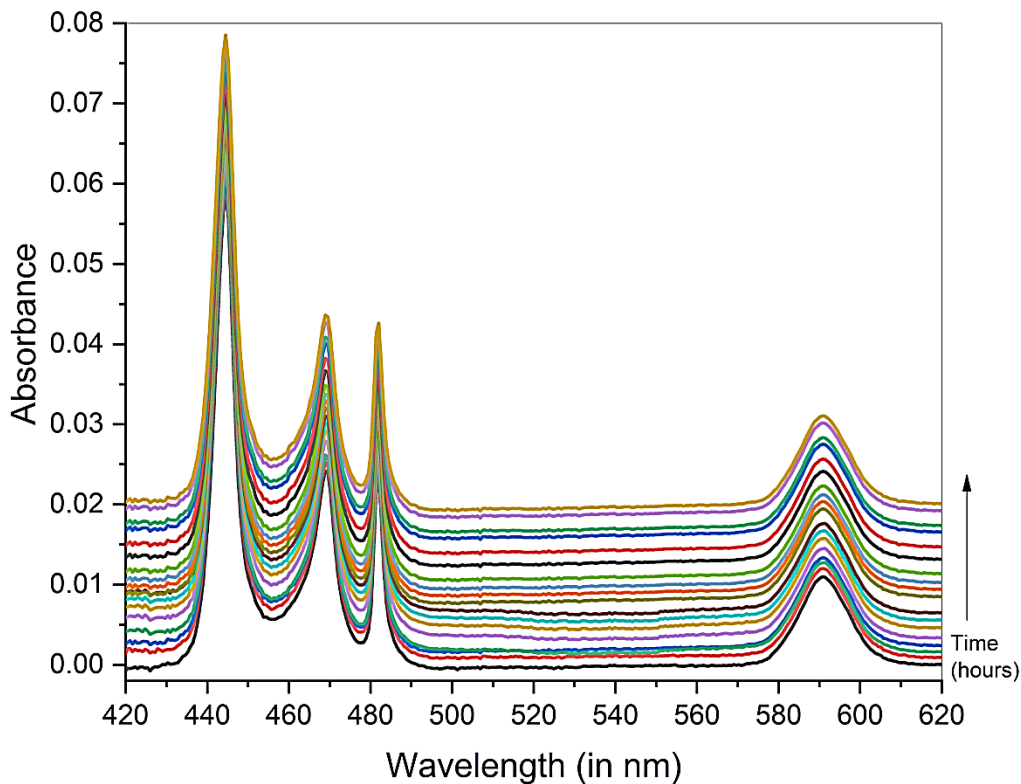

Fig 4.2: Comparative absorption spectra of Pr(III):L-Glutamine complexation with Mg(II) in DMF at 303 K (30^0C) and at different time (hour)
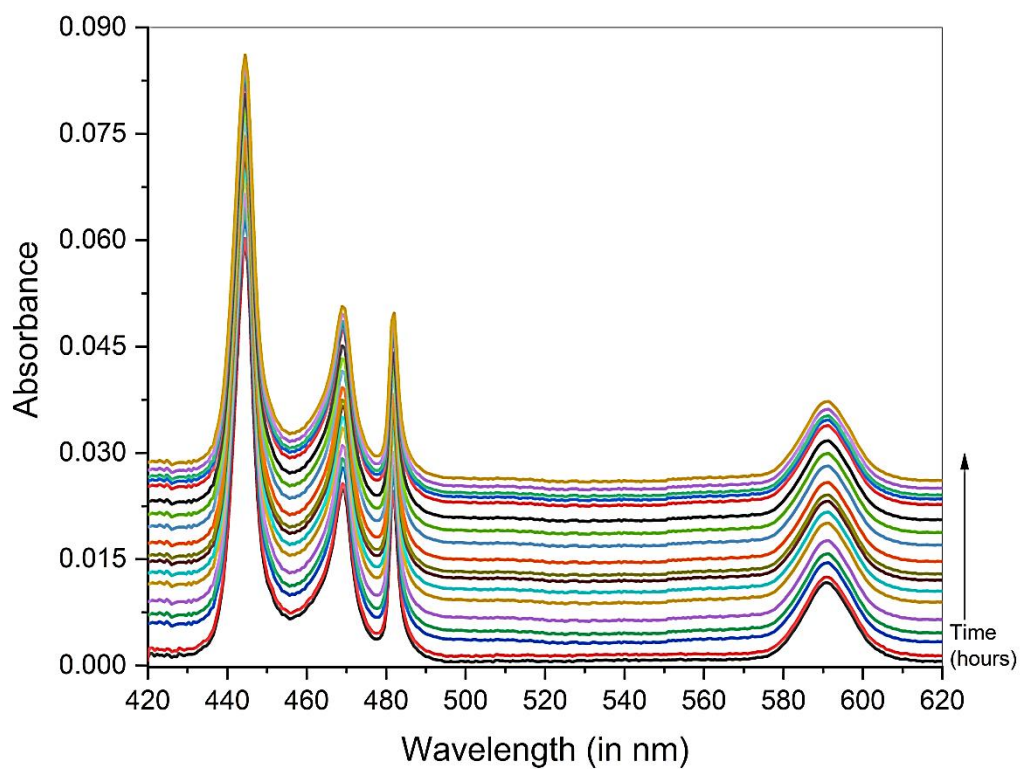
Fig 4.3: Comparative absorption spectra of Pr(III):L-Glutamine complexation with Mg(II) in DMF at 308 K (35^0C) and at different time (hour)
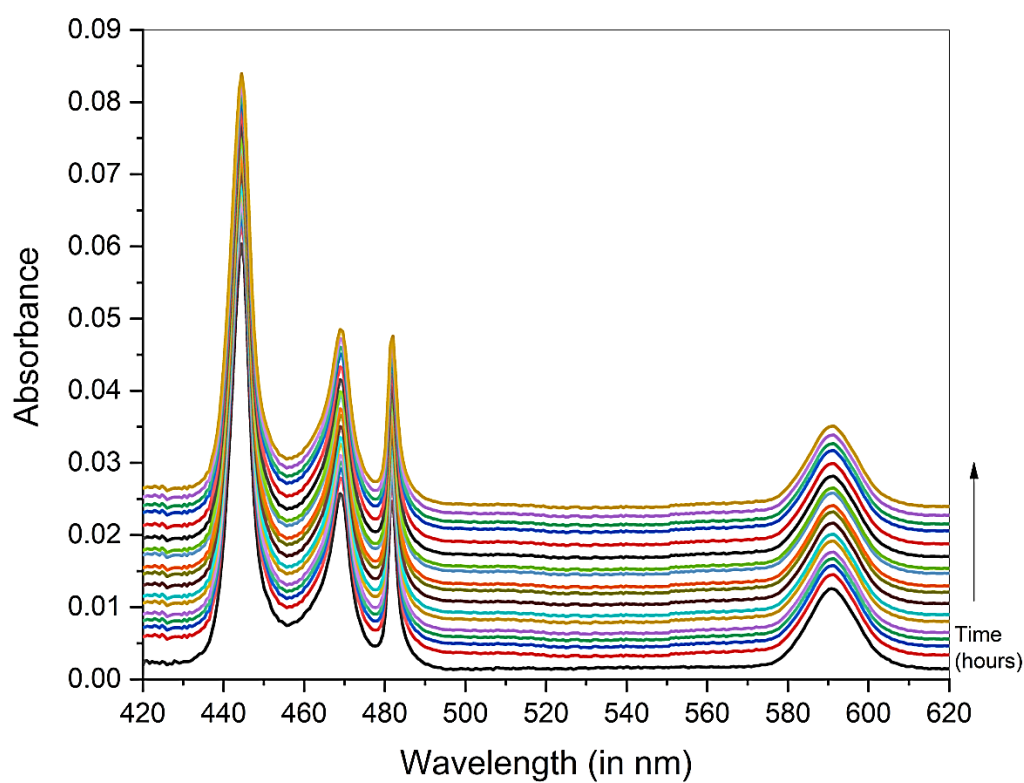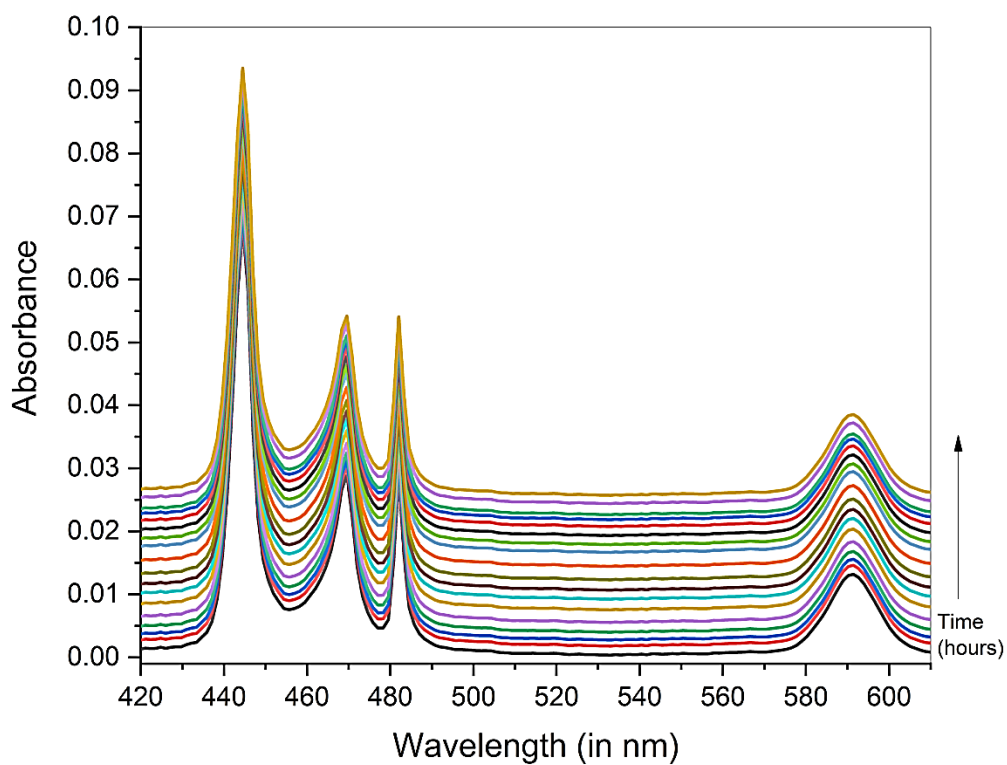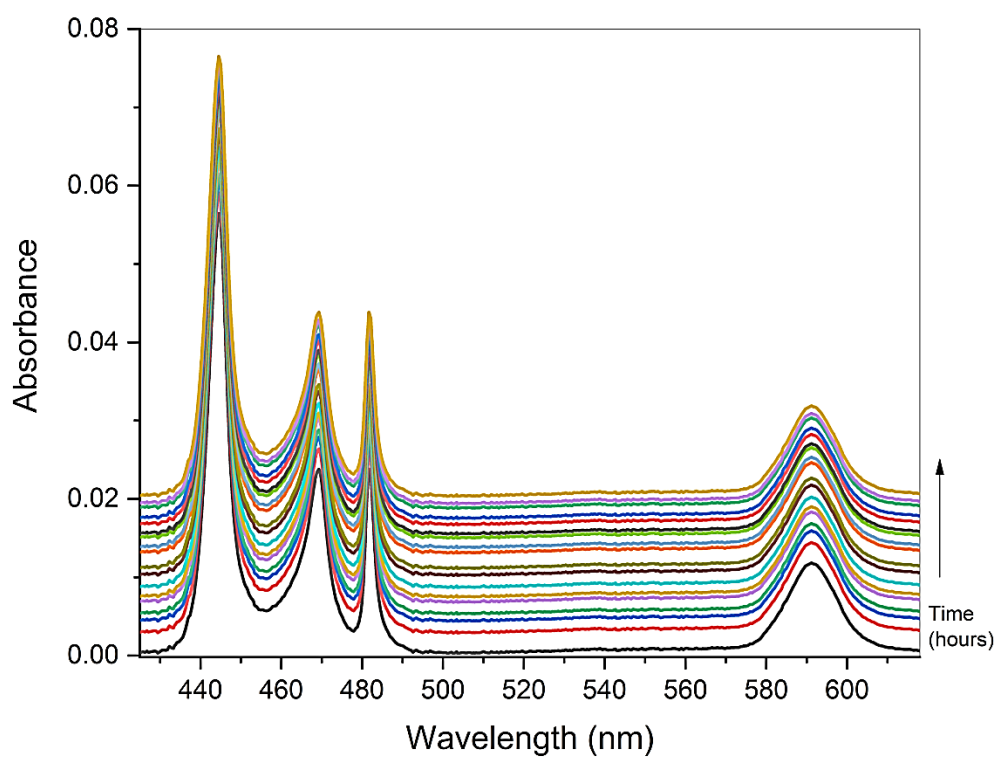

Fig 4.4: Comparative absorption spectra of Pr(III):L-Glutamine complexation with Mg(II) in DMF at 313 K (40^0C) and at different time (hour)

Fig 4.5: Comparative absorption spectra of Pr(III):L-Glutamine complexation with Mg(II) in DMF at 318 K (45^0C) and at different time (hour)

Fig 4.6: Comparative absorption spectra of Pr(III):L-Tryptophan complexation with Mg(II) in DMF at 298 K (25^0C) and at different time (hour)
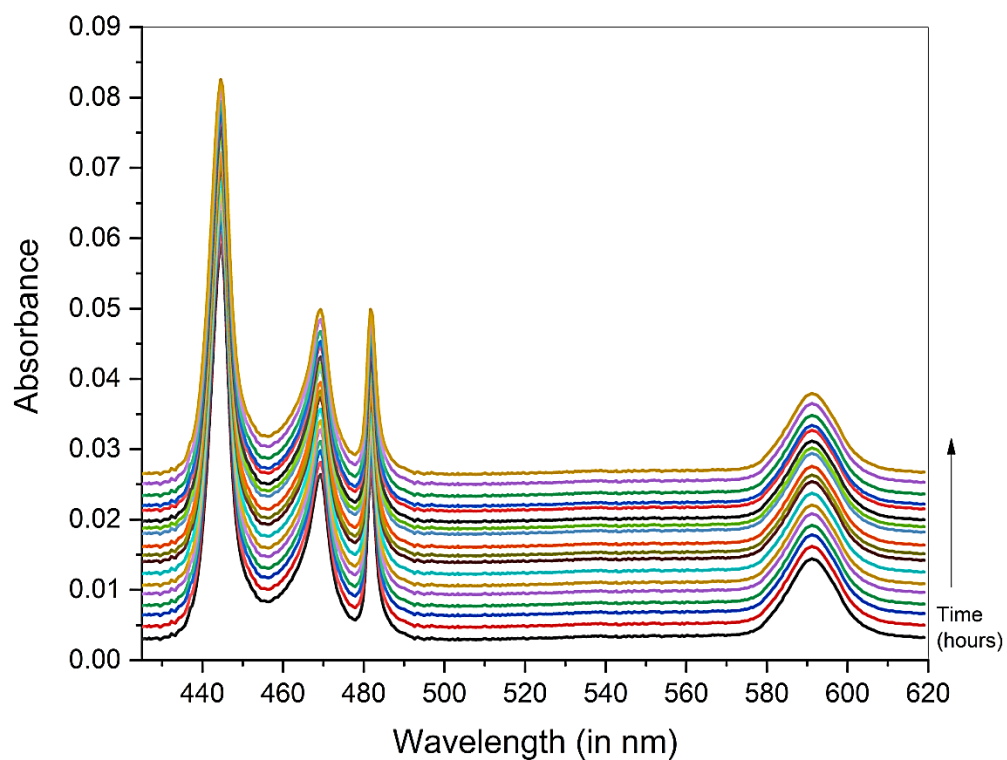
Fig 4.7: Comparative absorption spectra of Pr(III):L-Tryptophan complexation with Mg(II) in DMF at 308 K (35^0C) and at different time (hour)
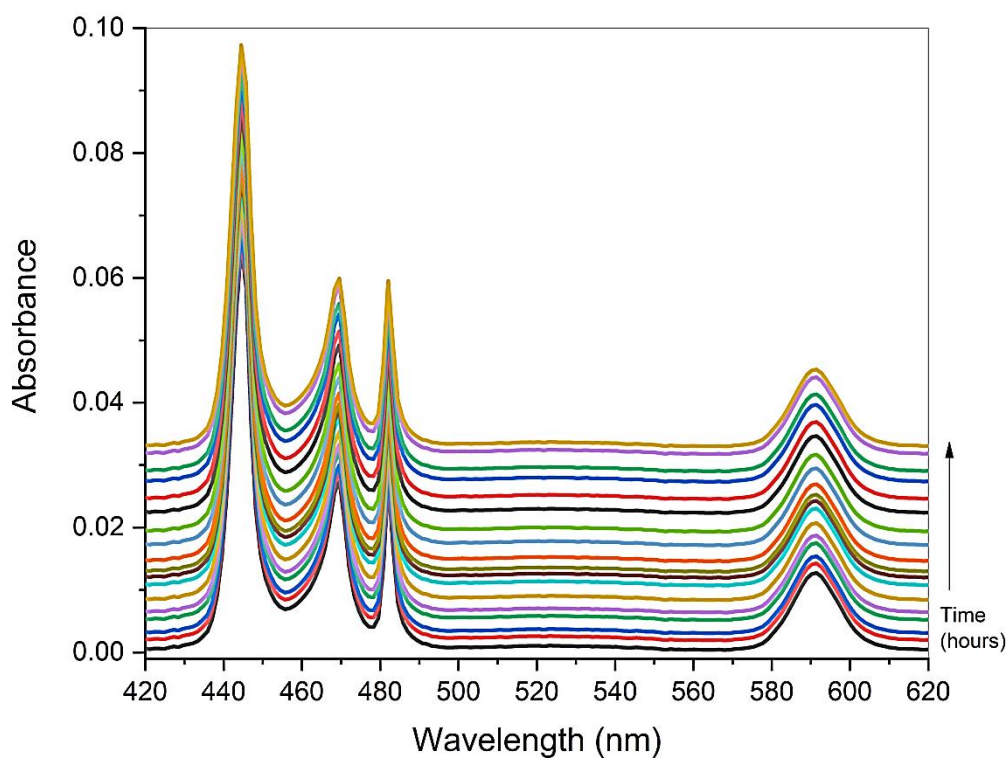

Fig 4.8: Comparative absorption spectra of Pr(III):L-Tryptophan complexation with Mg(II) in DMF at 318 K (45^0C) and at different time (hour)
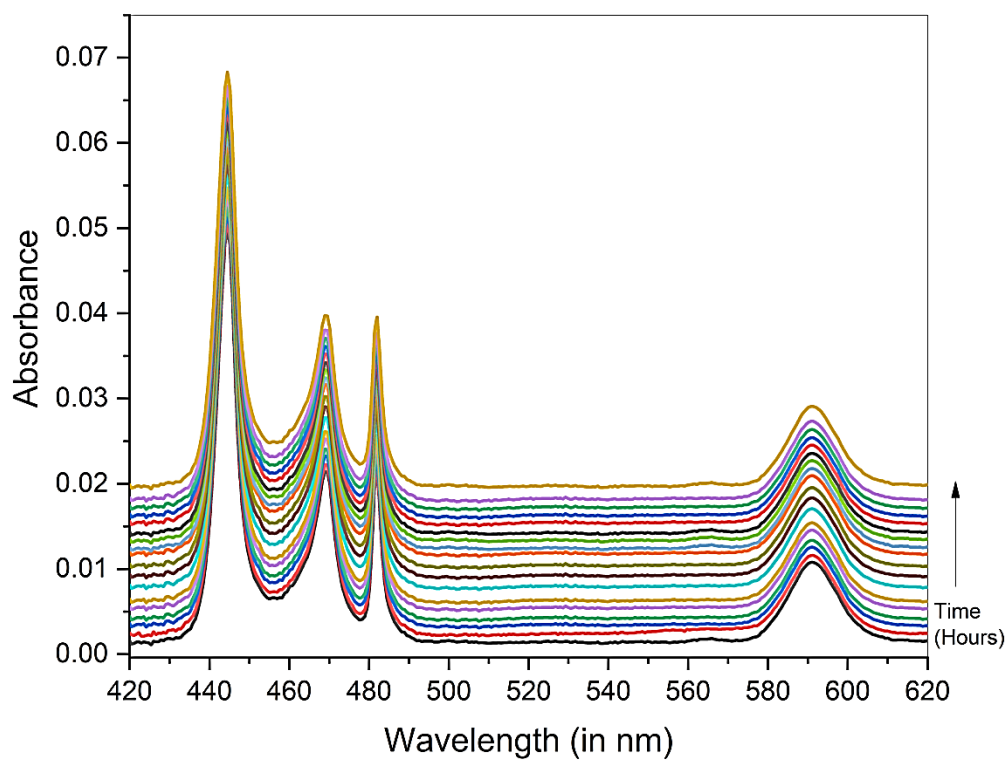
Fig 4.9: Comparative absorption spectra of Pr(III):L-Isoleucine complexation with Mg(II) in DMF at 298 K (25^0C) and at different time (hour)
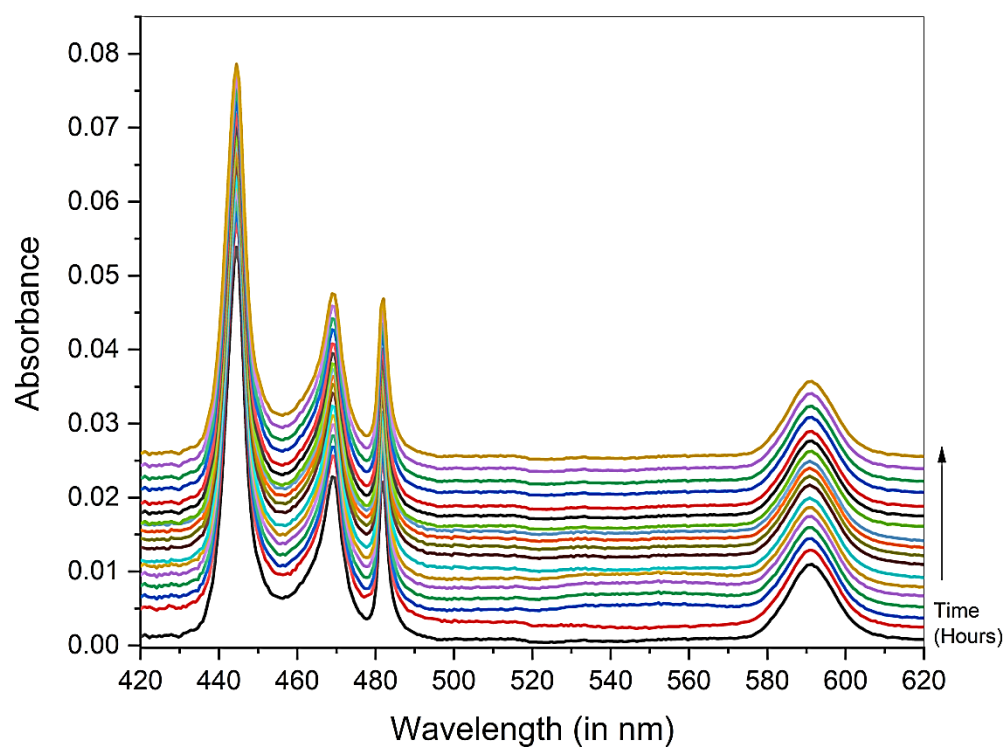

Fig 4.10: Comparative absorption spectra of Pr(III):L-Isoleucine complexation with Mg(II) in DMF at 308 K (35^0C) and at different time (hour)
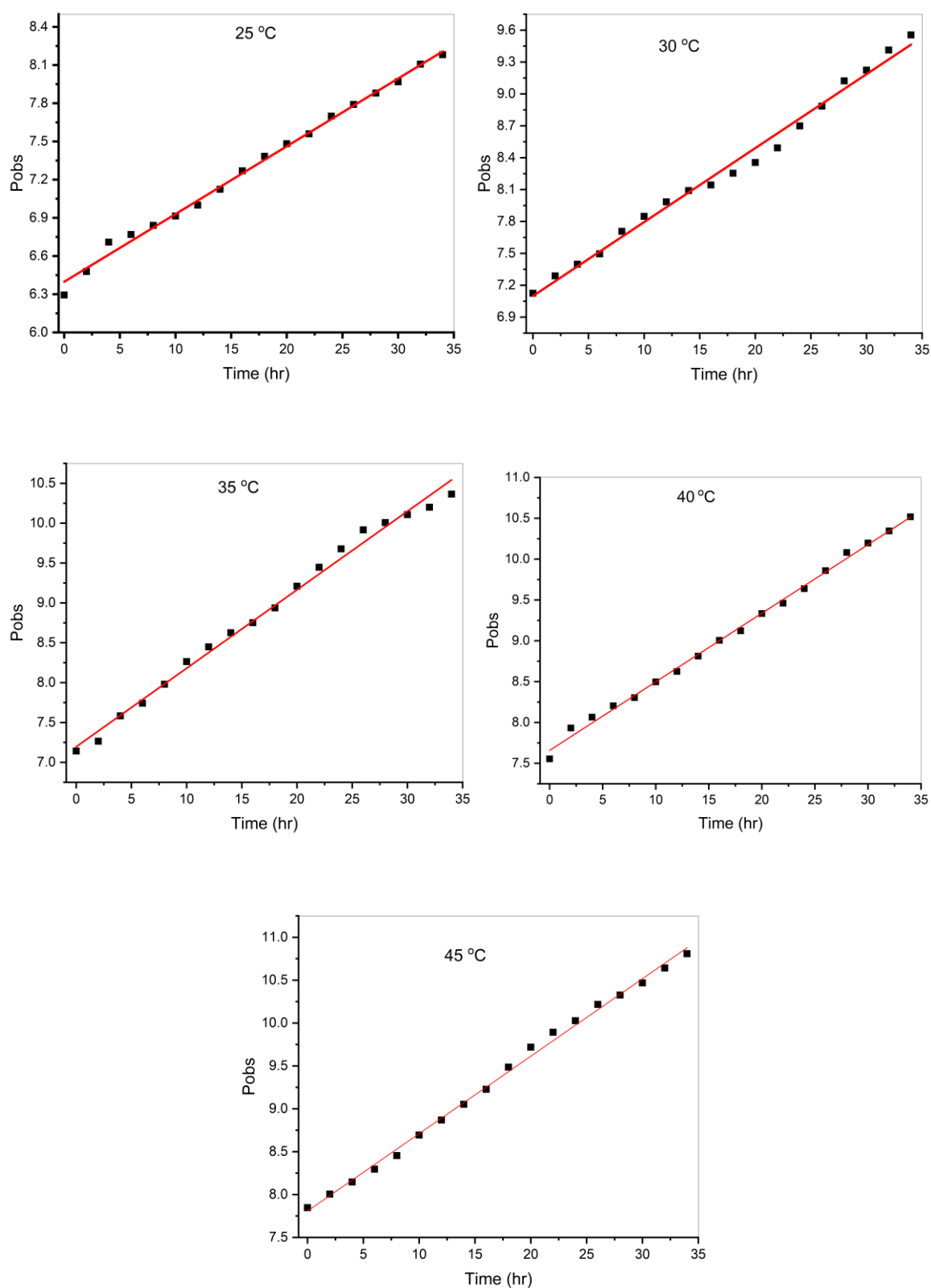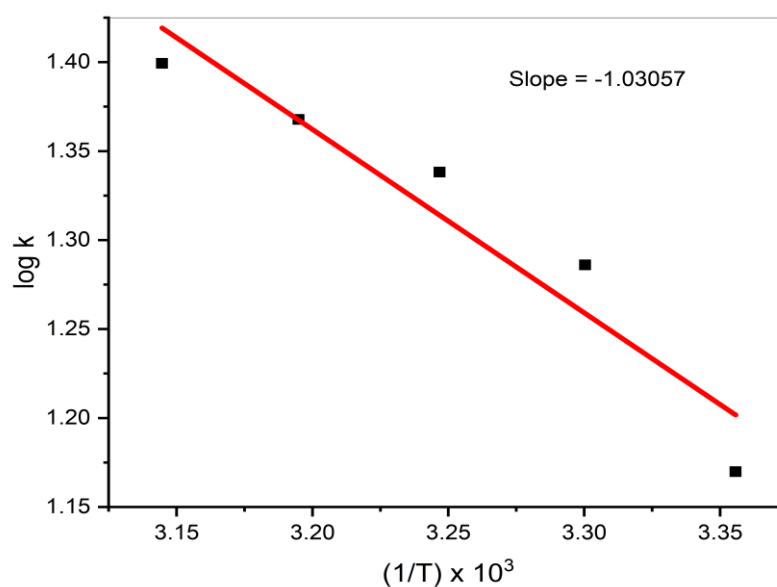
Pr(III):L-Glutamine:Mg(II) Complex

Fig 4.11: Plot of Pobs versus Time (hr) for the $^3H_4 \rightarrow ^3P_2$ transition of Pr(III):L-Glutamine:Mg(II) at different temperatures

Table 4.16: Rate Constants at different temperatures (298K, 303K, 308K, 313K and 318K) and activation energy E_a for Pr(III):L-Gln:Mg(II) complex

Temperature (K)	$1/T^3 K^{-1}$	Rate Constant (k) $Mol\ L^{-1}h^{-1}$	Rate Constant (k) $Mol\ L^{-1}S^{-1}\times 10^{-6}$	log k	Pre-exponential factor (A)	Activation Energy $\Delta Ea(kJ/mol)$
298	3.36	0.05323	14.79	1.17	6.39805	
303	3.30	0.06956	19.32	1.29	7.09953	
308	3.25	0.07844	21.79	1.34	7.19678	0.020
313	3.19	0.08397	23.33	1.37	7.65875	
318	3.14	0.09029	25.08	1.40	7.80825	

Fig. 4.12: Plot of log k versus $(1/T) \times 10^3$ for the complexation of Pr(III):L-Gln:Mg(II) in aquated DMF medium

Table 4.17: Rate constants and thermodynamic parameters for Pr(III):L-Gln:Mg(II) complex at different temperatures

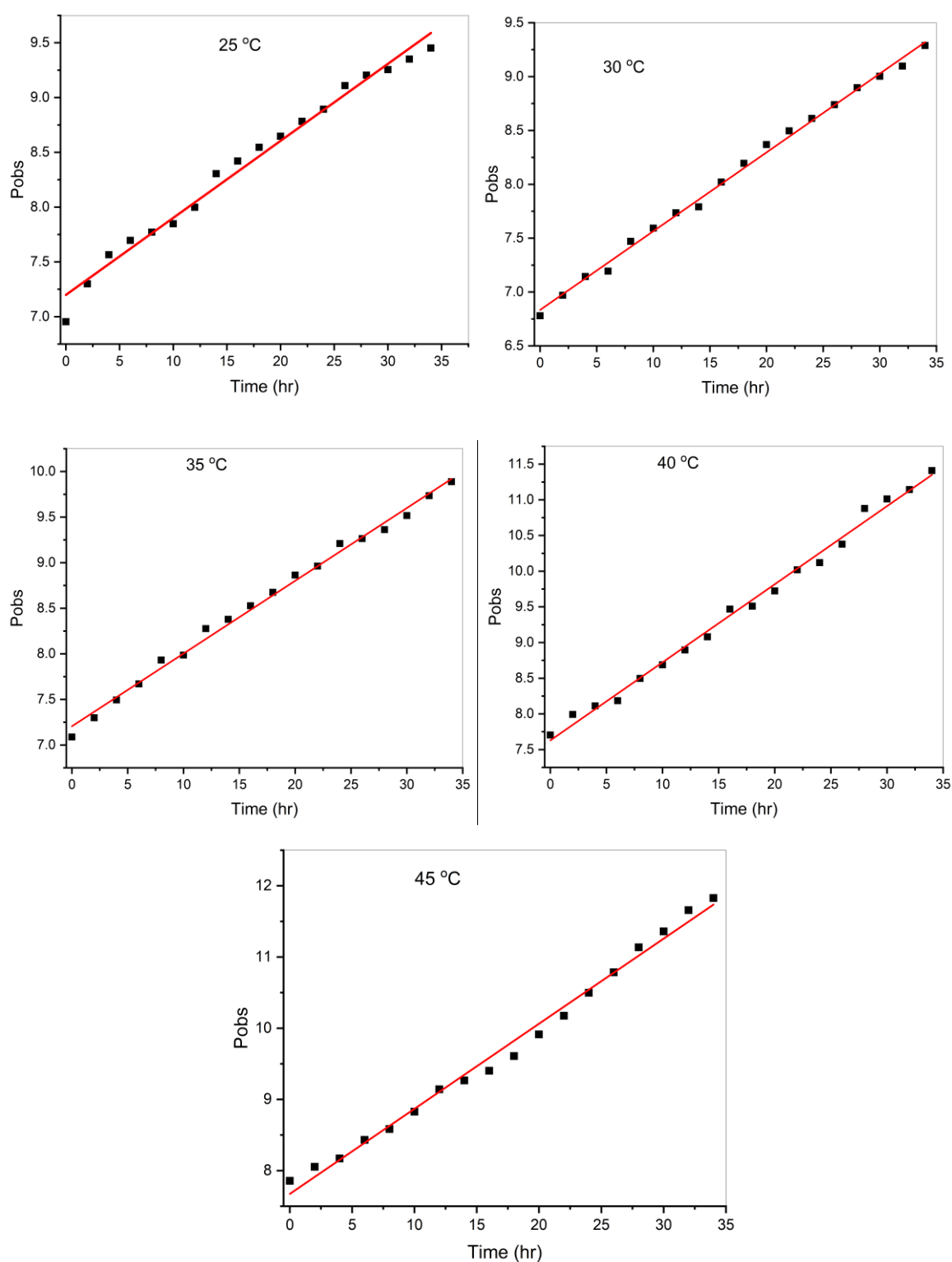| Temperature (K)	Rate (k) $Mol\ L^{-1}S^{-1}\times 10^{-6}$	ΔH^0 $(kJmol^{-1})$	ΔG^0 $(kJmol^{-1})$	ΔS^0 $(JK^{-1}mol^{-1})$
298	14.79		-6.675	0.042
303	19.32		-7.461	0.044
308	21.79	0.020	-7.892	0.045
313	23.33		-8.197	0.046
318	25.08		-8.520	0.047

Pr(III):L-Tryptophan:Mg(II) Complex

Fig 4.13: Plot of Pobs versus Time (hr) for the $^3H_4 \rightarrow {}^3P_2$ transition of Pr(III):L-Tryptophan:Mg(II) at different temperatures

Table 4.18: Rate Constants at different temperatures (298K, 303K, 308K, 313K and 318K) and activation energy E_a for Pr(III):L-Trp:Mg(II) complex

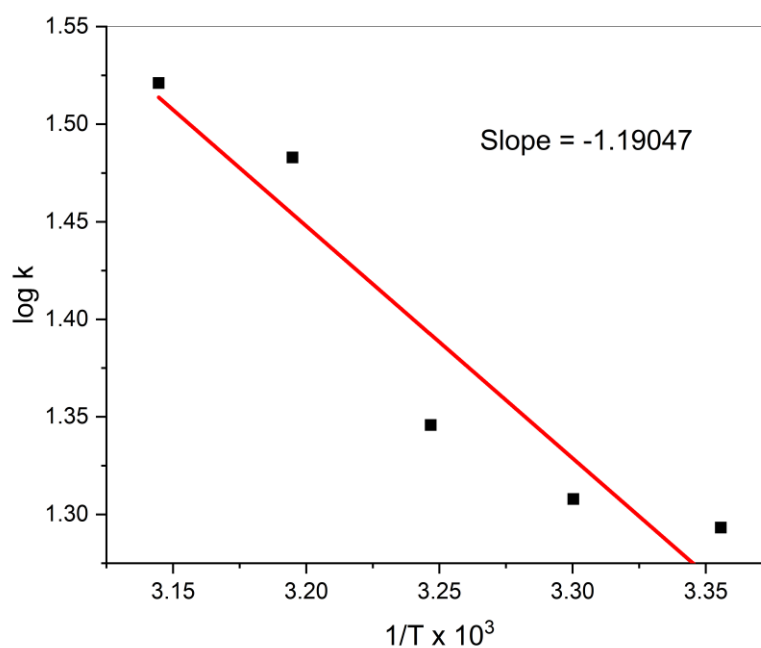| Temperature (K)	$1/T^3 K^{-1}$	Rate Constant (k) Mol $L^{-1} h^{-1}$	Rate Constant (k) Mol $L^{-1} S^{-1} \times 10^{-6}$	log k	Pre-exponential factor (A)	Activation Energy ΔEa(kJ/mol)
298	3.36	0.07072	19.64	1.29	7.15871	
303	3.30	0.07314	20.32	1.31	6.83401	
308	3.25	0.07981	22.17	1.35	7.20592	0.023
313	3.19	0.10944	30.40	1.48	7.6294	
318	3.14	0.1195	33.19	1.52	7.67366	

Fig. 4.14: Plot of log k versus $(1/T) \times 10^3$ for the complexation of Pr(III):L-Trp:Mg(II) in aquated DMF medium

Table 4.19: Rate constants and thermodynamic parameters for Pr(III):L-Trp:Mg(II) complex at different temperatures

Temperature (K)	Rate (k) Mol $L^{-1}S^{-1} \times 10^{-6}$	ΔH^0 (kJmol^{-1})	ΔG^0 (kJmol^{-1})	ΔS^0 (JK^{-1}mol^{-1})
298	19.64		-7.379	0.048
303	20.32		-7.588	0.048
308	22.17	0.023	-7.936	0.049
313	30.40		-8.887	0.051
318	33.19		-9.261	0.052

174

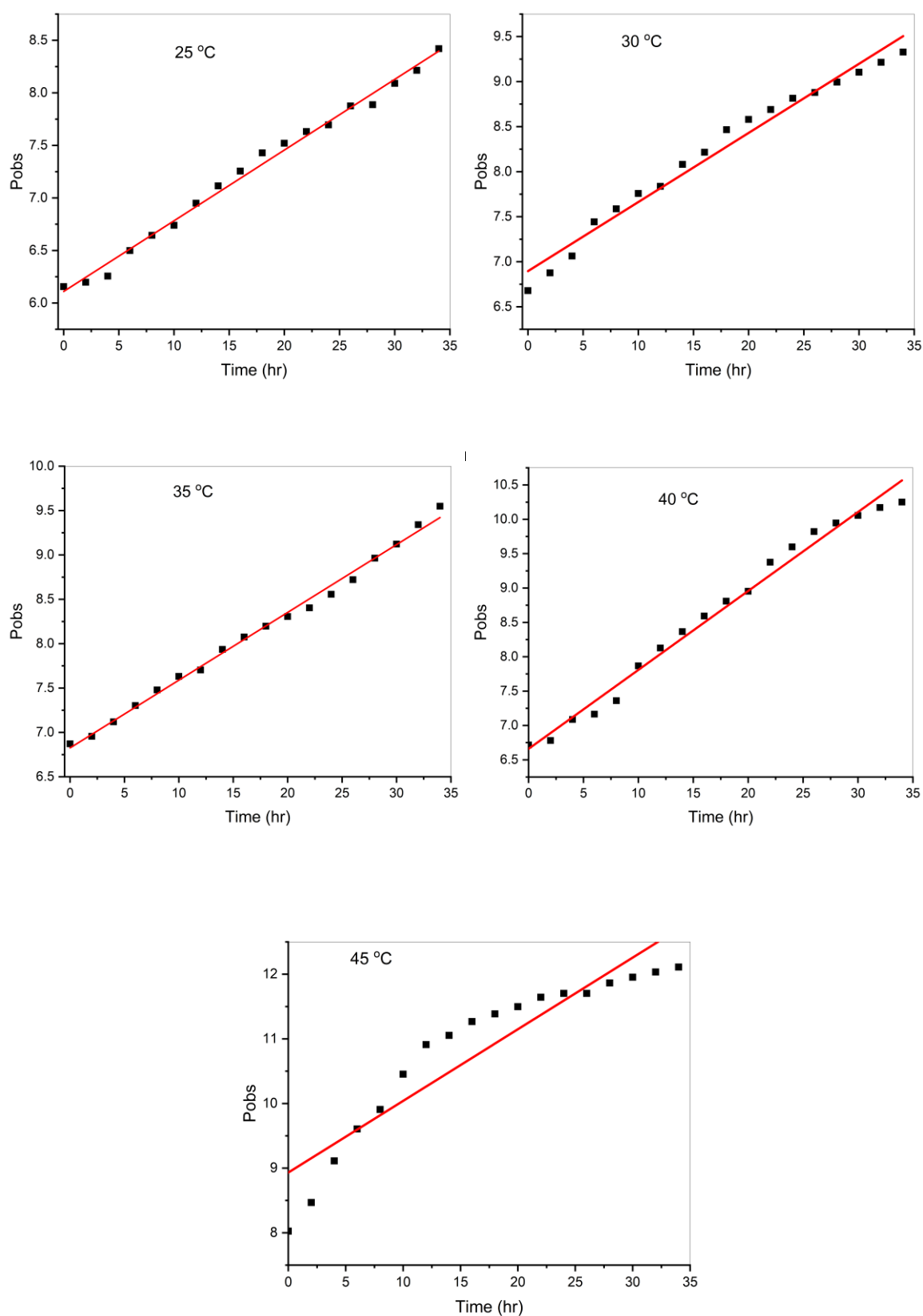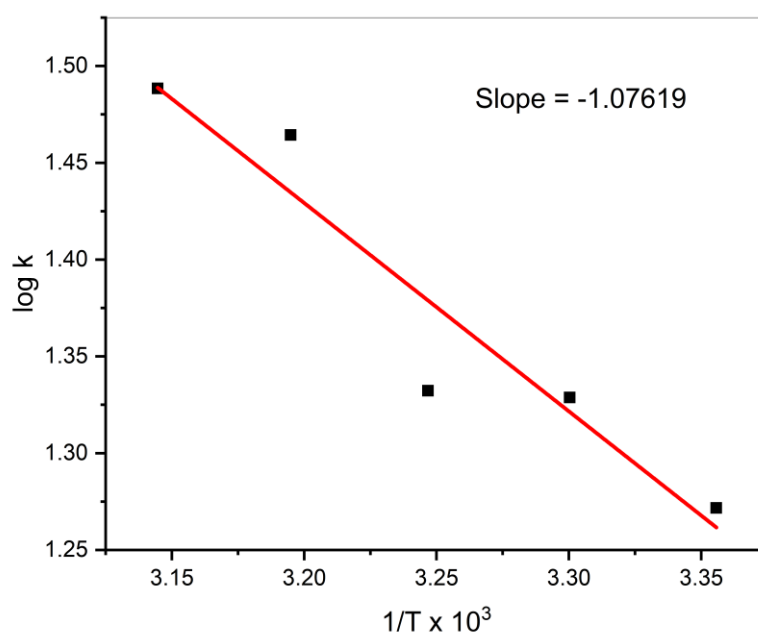**Pr(III):L-Isoleucine:Mg(II) Complex**

Fig 4.15: Plot of Pobs versus Time (hr) for the $^3H_4 \rightarrow {}^3P_2$ transition of
Pr(III):L-Isoleucine:Mg(II) at different temperatures

Table 4.20: Rate Constants at different temperatures (298K, 303K, 308K, 313K and 318K) and activation energy E_a for Pr(III):L-Ile:Mg(II) complex

Temperature (K)	$1/T^3 K^{-1}$	Rate Constant (k) Mol $L^{-1} h^{-1}$	Rate Constant (k) Mol $L^{-1} S^{-1} \times 10^{-6}$	log k	Pre-exponential factor (A)	Activation Energy ΔE_a(kJ/mol)
298	3.36	0.0673	18.69	1.27	6.11023	
303	3.30	0.07675	21.32	1.33	6.89596	
308	3.25	0.07737	21.49	1.33	6.82582	0.021
313	3.19	0.10488	29.13	1.46	6.66062	
318	3.14	0.11084	30.79	1.49	8.93258	

Fig. 4.16: Plot of log k versus $(1/T) \times 10^3$ for the complexation of Pr(III):L-Ile:Mg(II) in aquated DMF medium

Table 4.21: Rate constants and thermodynamic parameters for Pr(III):L-Ile:Mg(II) complex at different temperatures

Temperature (K)	Rate (k) Mol $L^{-1}S^{-1} \times 10^{-6}$	ΔH^0 (kJmol^{-1})	ΔG^0 (kJmol^{-1})	ΔS^0 (JK^{-1}mol^{-1})
298	18.69		-7.256	0.045
303	21.32		-7.709	0.046
308	21.49	0.021	-7.857	0.046
313	29.13		-8.776	0.049
318	30.79		-9.063	0.049

Chapter 5

Summary and Conclusion

As proteins are made of amino acids, their structure and reactivity depend on the specific properties of the amino acids they contain. Nevertheless, the effect of water on the geometric and electrical structures of amino acids is crucial for understanding biological activity. The behaviour of proteins in water is greatly influenced by the side chains of amino acids. In fact, water participates in a variety of cellular processes and is an essential component of all proteins in variable quantities. Moreover, the structure of the solvated amino acid is particularly sensitive to the pH of the solution; this is one of the reasons why pH management is essential in living organisms. The extraordinarily important biological fluids are essentially multimetal-multiligand systems. In these systems, a number of endogenous metal ions compete with the coordinating sites of multidentate macromolecular metabolites, and multidonor sites also experience strong competition for different metal sites. Therefore, the process of metal binding to a specific donor site on a biomolecule is determined by a number of factors including the capability of the donor site, the structure, the conformation, the orientation, the physiological pH, the presence of similar types of metal ions, and the relative abundance of those ions. Because of this, it is thought to be worthwhile to investigate the simultaneous coordination of two or three distinct metal ions with a multidentate biological molecule that has a significant amount of biological significance.

In the present study, we investigated the simultaneous co-ordination of Pr(III)/Nd(III) and Mg(II) with amino acids: L-Glutamine, L-Threonine, L-Typtophan and L-Isoleucine in a variety of solvents by using absorption difference and comparative absorption spectrophotometry as a PROBE. It has been found that important information that can be of direct chemical relevance can be obtained, such as the co-ordination number, structure, geometry, and nature of complex species, as well as in the process of following a number of biological reactions. The results obtained from solution spectral analysis are helpful for structural determination and the study of mechanistic processes. It has been used in biochemical reactions, or while monitoring the behaviour of contrast enhancing biological drugs, or in following the kinetics of complexation of two or more chemically different metal ions to biomolecular polydentate ligand, or while following the controlled hydrolysis of multimetal alkoxide precursor for synthesis of industrially important high valued ceramics, thereby broadening the investigation in these fields, and it can prove to be an important tool on mechanistic and in diagnosing the biological and medicinal activities of lanthanide co-ordination compounds.

In the present thesis, the pseudohypersensitive transitions, $^3H_4 \rightarrow {}^3P_2$, $^3H_4 \rightarrow {}^3P_1$, $^3H_4 \rightarrow {}^3P_0$ and $^3H_4 \rightarrow {}^1D_2$ for Pr(III) and $^4I_{9/2} \rightarrow {}^4G_{7/2}$, $^4I_{9/2} \rightarrow {}^4F_{7/2}$, $^4I_{9/2} \rightarrow {}^4F_{5/2}$, and $^4I_{9/2} \rightarrow {}^4F_{3/2}$ for Nd(III) have been employed for studying the complexation of L-Glutamine, L-Threonine, L-Tryptophan and L-Isoleucine with Ln(III) and Mg(II) via quantitative absorption spectroscopy. Ln(III) complexation with selected amino acids in the presence and absence of Mg(II) was investigated in different aquated organic solvents (DMF, dioxane, acetonitrile and methanol) and pH levels (2, 4, 6). Further, kinetics for the complexation of Pr(III):amino acids with Mg(II) at five different temperatures viz., 298K, 303K, 308K, 313K and 318K was also studied. Using the spectral data, various energy interaction parameters such as Slater-Condon (F_k, $k = 2, 4, 6$), Lande spin-orbit interaction (ξ_{4f}), Racah (E^k), nephelauxetic ratio (β), bonding parameter ($b^{1/2}$) and percent covalency

(δ) and intensity parameters [(Oscillator strength (P) and Judd-Ofelt T_λ, (λ=2,4,6)] were computed to analyse the interaction between Ln(III) and the ligands. Several variations in the computed energy and intensity parameter values as well as enhancement of the 4f-4f transition band intensities from the comparative UV-Vis spectra could be observed which indicated the formation of Ln(III):amino acids complex with Mg(II). The lowered values of the interelectronic repulsion parameters such as Slator-Condon (F_k), Racah parameters (E^k), Lande (ζ_{4f}) parameters on the complexation of Pr(III) with the amino acids ligands and Mg(II) could indicate the possibility of expansion of metal orbital on the addition of the ligands thereby, shortening of the metal-ligand bond distance leading to the formation of the complex Pr(III):L:Mg(II). The increase in $b^{1/2}$ and δ values could indicate the covalent character and a stronger binding in the complexation of Ln(III) with the ligands. The increased value of Judd-Ofelt intensity parameters could play a significant role in the formation of Pr(III) complexes with the amino acid ligands and Mg(II), substantiating the information obtained through the energy interaction parameters and leading to a coherent conclusion. Moreover, the significant variation in the Judd-Ofelt parameters and oscillator strength values, on the addition of the amino acids and Mg(II), could convey inner-sphere coordination in the present study of the multi-metal complexation. Out of the four solvents, maximum intensities were observed in DMF solvent. pH studies showed that pH 6 is the optimum pH for complexation where deprotonation of the binding sites of the amino acids was more favourable. Kinetics of the formation of Pr(III):L:Mg(II) at different temperatures was explored and it was found that the rate of complexation increases with increasing temperature and time. The rate constants (k), Activation energy (E_a), $\Delta H°$, $\Delta S°$ and $\Delta G°$ for Ln(III):GSH:Mg(II) were also evaluated. The lower E_a value predicts that the reaction is a fast reaction.The positive enthalpy and entropy values indicates that the complexation is an endothermic and entropy increasing process. Negative $\Delta G°$ value indicates that the reaction is spontaneous and favourable in solution.

APPENDIX

PLAGIARISM REPORT

WORKSHOP AND SEMINARS ATTENDED

LIST OF PUBLICATIONS

नागालैण्ड विश्वविद्यालय
NAGALAND UNIVERSITY
(केंद्रीय विश्वविद्यालय) / (A Central University)

मुख्यालय : लुमामी, जिला : जुन्हेबोटो (नागालैण्ड) – 798 627
Hqrs: Lumami, Dist: Zunheboto, Nagaland – 798 627

Ph.D Thesis Certificate on Plagiarism check

Name of the research scholar	Chubazenba Imsong
Ph.D registration number	808/2018
Title of Ph.D thesis	Spectral studies of the complexation of lanthanides with selected amino acids: Evaluation of thermodynamic parameters
Name & institutional address of the supervisor	Prof. M. Indira Devi Department of Chemistry Nagaland University, Lumami
Name of the department and school	Department of Chemistry, School of Sciences
Date of submission	15/02/2023
Date of plagiarism check	15/02/2023
Percentage of similarity detected by the **URKUND** software	4%

I hereby declare that/certify that the Ph.D thesis submitted by me is complete in all respect as per the guidelines of Nagaland University (NU) for this purpose. I also certify that the thesis (soft copy) has been checked for plagiarism using **URKUND** similarity check software. It is also certified that the contents of the electronic version of the thesis are the same as the final hard copy of the thesis. Copy of the report generated by the **URKUND** software is also enclosed.

CHUBAZENBA IMSONG
(Name & signature of the Scholar)

Place: Lumami

Date: 23/02/'23

Name & signature of the Supervisor
Prof. M. Indira Devi
Professor
Dept. of Chemistry
Nagaland University
Lumami-798627

Document Information

Analyzed document	Chubazenba Imsong PhD Thesis.docx (D158355553)
Submitted	2/10/2023 4:08:00 PM
Submitted by	Indira Devi
Submitter email	indira@nagalanduniversity.ac.in
Similarity	4%
Analysis address	indira.naga@analysis.urkund.com

Sources included in the report

W URL: https://www.mdpi.com/1996-1944/15/19/6518/pdf?version=1663679781
Fetched: 2/10/2023 3:54:28 PM — 2

W URL: https://apps.dtic.mil/sti/pdfs/ADP011904.pdf
Fetched: 2/10/2023 3:54:30 PM — 1

W URL: https://www.scielo.br/j/jbchs/a/gHMZTs4FmPYqCg7wLmwZKCK/?lang=en
Fetched: 12/24/2022 2:40:17 PM — 4

W URL: https://www.hindawi.com/journals/ijs/2009/784305/
Fetched: 9/30/2019 9:50:20 AM — 4

J **09_chapter_2.pdf**
URL: c2e532b4-ed5a-42b9-8b73-47834102efce
Fetched: 8/18/2022 2:50:48 PM — 1

W URL: https://www.pnrjournal.com/index.php/home/article/download/866/673/1030
Fetched: 12/15/2022 7:31:04 AM — 2

W URL: https://www.mdpi.com/1996-1944/15/24/9042/pdf
Fetched: 2/10/2023 3:47:20 PM — 1

Entire Document

Workshop and Seminars attended

➢ UGC sponsored National Seminar on Interdisciplinary Research in Chemical Sciences, NSIRCS-2016, Department of Chemistry, Kohima Science College, Jotsoma, 28th - 29th September 2016.

➢ National seminar on Chemistry in interdisciplinary research organised by Department of Chemistry, Nagaland University, March 16th -17th 2017.

➢ DBT sponsored National seminar on Bio-resource exploration and utilization: Application in modern biology organised by BIF, Nagaland University, October 9th - 10th 2018.

➢ National Seminar on Chemistry in Interdisciplinary Research (NSCIR-2018), Department of Chemistry, Nagaland University, 9th – 10th November 2018.

➢ DBT sponsored national workshop on "Newer frontiers in bioinformatics and research methodology", organised by BIF centre, Nagaland University, Lumami, October 13th to 19th 2018.

➢ National e-Seminar on "Chemistry in emerging trends of interdisciplinary research" (NeSCETIR- 2020), organised by Department of Chemistry, Nagaland University, November 18th-20th 2020.

➢ Oral presentation Global Web Conference on Impact of Engineering, Science & Management on Digital Transformation, Centre for Research & Training, National Foundation for Entrepreneurship, Tamil Nadu, 29th – 30th January 2021.

➢ One day Workshop on Research Publications, RDC, Fazl Ali College, Mokokchung, Nagaland, 21st September 2021.

➢ IP Awareness program under National Intellectual Property Awareness Mission, organized by Intellectual Property Office, India, 04th March 2022.

Lists of Publications

- "**Absorption spectral and thermodynamic analysis for the complexation of Pr^{3+} with L-Phenylalanine in the presence/absence of Mg^{2+} using 4f-4f transitions spectra as probe**", Zevivonü Thakro, T. Moaienla Ao, Juliana Sanchu, **Chubazenba Imsong**, Mhasiriekho Ziekhrü, M. Indira Devi has been published in The *European Physical Journal Plus*, Springer.

- "**Complexation of Pr^{3+} with L-methionine in the presence/absence of Mg^{2+}: their reaction dynamics and thermodynamic properties**", Zevivonü Thakro, Juliana Sanchu, **Chubazenba Imsong,** M. Indira Devi was pusblished in the journal of *Chemical Physics Impact,* Elsevier.

- "**Computation of energy interaction and intensity parameters for the complexation of Pr(III) with glutathione at different pH in the presence/absence of Mg^{2+}: 4f-4f transition spectra as a probe**", Mhasiriekho Ziekhrü, Zevivonü Thakro, **Chubazenba Imsong**, Juliana Sanchu and M. Indira Devi was pusblished in the journal of *Polyhedron*, Elsevier.

- "**Computation of spectral parameters for the complexation of Pr(III) with L-Histidine through 4f-4f transition spectra: Further analysis of its kinetic and thermodynamic parameters**", Juliana Sanchu, Zevivonü Thakro, **Chubazenba Imsong** and M. indira Devi was published in the jounal of *Chemical Physics Impact,* Elsevier.

- "**Computational study of multimetal complexation of Nd(III) with GSH and Mg(II) in solution at different pH through 4f-4f transition spectra**", Mhasiriekho Ziekhrü, Juliana Sanchu, Zevivonü Thakro, **Chubazenba Imsong** and M. Indira Devi was pusblished in the journal of *Chemical Physics Impact,* Elsevier.

- "**Theoretical study of the heterometal complexation of Pr(III) with L-isoleucine in the presence/absence of Mg(II) in solution: 4f-4f transition spectra as probe**", Chubazenba Imsong, Mhasiriekho Ziekhrü, Zevivonü Thakro, Juliana Sanchu and M. Indira Devi was pusblished in the journal of *Chemical Physics Impact,* Elsevier.

- "**Absorption spectral study for the interaction of Pr (III) with L-Aspartic acid in various aquated organic solvents through 4f-4f transition spectra: Analysis of reaction pathways and thermodynamic parameters.**" Juliana Sanchu, **Chubazenba Imsong**, Zevivonü Thakro, Mhasiriekho Ziekhrü, and M. Indira Devi was published in the journal of *Journal of Pharmaceutical Negative Results*.

Papers Communicated:

- "**Spectral Analysis for the Complexation of Nd(III) with L-Tryptophan and L-Isoleucine in the presence/absence of Mg^{2+}: 4f-4f transition spectra as probe**" has been communicated and is under review.